Dear Brent,

With best regards!

Sandip Shah

MARCH 26, 1992

A STUDY OF THE BEHAVIOUR OF JOINTED ROCK MASSES

by

Sandip Shah

A Thesis submitted in conformity with the requirements
for the Degree of Doctor of Philosophy in the
University of Toronto

Dedicated
to
my parents

ABSTRACT

This thesis dwells on three principal issues in rock mechanics: firstly, statistical analysis of laboratory strength data; secondly, failure criteria for rock mass and rockfill materials; and finally, constitutive relations for rock mass.

In the first segment, the Linear Regression Analysis, Simplex and LOWESS statistical techniques are used for fitting nonlinear failure envelopes to triaxial and shear test data for rock masses. The Simplex technique was found to be the most appropriate procedure for fitting strength data to nonlinear failure criteria, e.g. the Hoek–Brown criterion.

A discussion on existing failure criteria for rock masses is presented in the second part of this thesis with emphasis on the strength predictions from the Hoek–Brown criterion. The limitations of this criterion in the estimation of strength of rock masses in the range of low confining stresses is eliminated by the development of the *Modified Hoek–Brown criterion.* A numerical solution procedure is developed to generate the nonlinear Mohr envelope for this criterion. A methodology for estimating the parameters of this criterion from rock mass classification schemes is also presented. A set of non–dimensional, nonlinear shear and triaxial strength criteria are developed for estimating the strength of rockfill materials and the procedure for estimating these strength parameters from triaxial or shear test data is given.

The final aspect of this thesis deals with the development of constitutive relations for rock masses and their implementation into the finite element analysis program ABAQUS. These constitutive relations are developed on the basis of the incremental theory of plasticity with the Hoek–Brown surface adopted as the yield surface for the rock mass. This constitutive model is an elastic–perfectly plastic one involving six parameters and incorporates the *associated* as well as *nonassociated* flow rules.

ACKNOWLEDGEMENTS

I wish to express my profound gratitude to my supervisor, Prof. Evert Hoek, for his invaluable guidance, encouragement, support and inspiration during the course of this project.

I am also thankful to Profs. J. H. Curran and S. Pantazopoulou, and Mr. David Wood for their advice and support during various stages of this work. Thanks are also due to every member of the Rock Engineering Group and the Data Visualization Laboratory at the University of Toronto for their help, constructive discussions and moral support.

I am extremely grateful to my parents for the colossal sacrifices they have made for providing me with the best possible education and for the immense efforts they have made for the betterment of my life and career. I thank all the members of my family for providing me with continuous support and encouragement. To my brother, Sanjiv, I am especially grateful, for being a constant source of inspiration and for guiding me through difficult times and anxious moments during the span of my research. To my niece, Tanvi, a special thanks for proving to be a constant source of joy especially after a hard and demanding days work. Last, but not the least, I warmly acknowledge and appreciate the encouragement and assistance provided by my wife, Devika, over the years required to complete this work. Her patience and love during these years have been a great source of inspiration to me.

This project was jointly funded by the Mining Research Directorate of Ontario and by the Universities Research Incentive Fund (URIF) of the Ministry of Colleges and Universities of Ontario.

Table of Contents

List of Figures

List of Tables

Chapter 1

Introduction

The prediction of the behaviour of a rock mass under the conditions of imposed or induced stresses and deformations is of prime importance to a geotechnical engineer involved in the design and construction of any structure on the surface or in subsurface regions. Underground excavations are designed to accommodate specific requirements, such as transport of people and materials, provision of safe and secure work places for mine staff, location of turbines, generators and transformers for power generation, storage of oil, disposal of nuclear and other types of wastes, transfer of water for irrigation as well as power generation, and in recent years, for shelters and for recreational purposes. Surface excavations are carried out for purposes of open–pit mining operations, construction of highways in hilly and mountainous regions, and construction of dams, spillways, abutments, and canals for water resources development purposes. In all circumstances, the main goal of the excavation designer is to ensure that the deformation of the rock mass in the vicinity of the excavation is within safe and allowable limits and is harmonious with the performance of the specified activities within it. The ability of the engineer to analyze and design the structure to satisfy these requirements is dependent on his knowledge and understanding of the behaviour or response of the rock mass subjected to the stress conditions which it will encounter in the altered stress state.

The construction of an excavation in a rock mass results in significant changes in the stress field in the surrounding domain. In order to understand the response of the rock mass

to the excavation and subsequent excavations, an analysis or several parametric analyses have to be performed, with the parameters of the rock mass which define its strength and deformation characteristics, to evaluate the stresses and deformations induced in it. In an underground mining environment, a large number of stopes are excavated, and it is essential to assess the influence of one opening on neighbouring, previously mined stopes or on stopes to be mined in the future. The assessment of deformation and failure modes is important in these situations because the requirement and design of support systems is made on the basis of ensuring the safety of the men and machines during the life of the mine while maximizing the extraction of the ore. In an underground civil engineering environment, the construction of pressure tunnels, power and transformer caverns, portals and adits necessitates the analysis of stress and deformation in the rock mass since these type of projects have longer design lives and are deemed to be permanent in nature along with the fact that they are capital intensive. The design of this category of excavations and their support systems has to be carried out keeping these specific, long–term requirements in perspective. When excavations are conducted on the surface for civil or mining engineering purposes, it is the foremost responsibility of the geotechnical engineer to assess the strength of the rock mass which is required in the analysis of the stability of the rock mass exposed to the excavation process, and its deformation characteristics for analyzing the response of bridge piers, dams and high–rise structures on rock foundations.

A study of the behaviour of a jointed rock mass involves two aspects: firstly, the estimation of its strength, i.e., its ability to sustain loads in a multi–axial, complex state of stress, and, secondly, its deformation characteristics in the elastic range of stresses as well as in the post–yield range of stresses. These two characteristics are the fundamental properties which determine the response of the rock mass to the stresses to which it is subjected. The stability of the excavation in this rock mass depends not only on the structural features present in it but also upon the relationship between the stress in the rock and its strength, and its deformation characteristics which are essential for estimating the displacement and stress distributions from numerical modelling tools or analytical techniques.

The engineering mechanics based approach to the solution of a rock mechanics problem requires the prior definition of the stress–strain behaviour of the rock mass. Important aspects of this approach are the constants relating the stresses and strains in the elastic range, the stress levels at which yield, fracturing or slip occurs within the rock mass, and the

post–peak constitutive behaviour of the fractured or "failed" rock mass. It is not uncommon in rock mechanics investigation to assume that the rock mass can be modelled as a linear elastic material. Some of the earliest stress analysis techniques utilized closed form mathematical solution or photoelastic models. These solutions are valid mainly for homogeneous, elastic materials with defined mathematical cross–sectional shapes, e.g., circle, ellipse, etc.. However, the shapes of excavations are more complex in practice and the rock mass is not always homogeneous and elastic. Ground conditions have a lot of variation, and it is vital that more sophisticated constitutive models be used in order to model the behaviour of the rock mass and to analyze the effects of the support systems such as cable bolts, rock bolts, steels sets, shotcrete, etc.. The advent of high–powered, efficient and easily accessible computers has encouraged the development of numerical tools capable of modelling situations involving complicated geometry and sophisticated constitutive relations. The selection of a suitable constitutive model and the appropriate numerical modelling technique is a function of the quality of the rock mass and the stress conditions in which the excavations are to be made.

The main aim of the present research program is to investigate the behaviour of jointed rock masses. An attempt has been made in this thesis to address these fundamental properties of, first of all, the rock mass strength, and secondly, the deformation characteristics in the post–peak region of deformations for the design and analysis of structures in the rock mass. The latter is based on the development of constitutive relations generated on the basis of a yield criterion and the rules of the theory of plasticity.

The estimation of the strength of a rock mass from an empirical strength criterion involves the determination of parameters which define the correlation between the variables measured in laboratory tests. The tests carried out in laboratories to ascertain the strength of rock masses are, in most cases, the triaxial tests and direct shear tests. Linear regression analysis is used extensively in soil and rock mechanics to fit laboratory data to linear and nonlinear strength envelopes and to obtain the material strength parameters. As a first step in this study, an investigation was carried out to assess the statistical techniques used for the analysis of laboratory data. A curve fitting procedure involving the Simplex Reflection technique, which is a function minimization technique, and a data smoothing procedure, LOWESS (Locally Weighted Regression Scatterplot Smoothing) were employed to determine a suitable curve fitting technique for laboratory strength data. The values of

the strength parameters obtained from these techniques were compared to those obtained from Linear Regression Analysis for linear and nonlinear envelopes. A discussion on the applicability and suitability of these techniques for assessing the strength parameters is presented in Chapter 2, with special emphasis on assessing the parameters of the nonlinear Hoek–Brown failure criterion (Hoek, 1983) for rock masses.

During the research process, several linear and nonlinear failure or strength criteria for rock masses, as suggested by various researchers, were examined with emphasis on their ability to predict the rock mass strength at low confining stresses. The assumptions, strengths and weaknesses of these criteria have been appraised, and their results compared with the nonlinear Hoek–Brown failure criterion. The Hoek–Brown failure criterion has been widely accepted by the rock engineering community as the most suitable failure criterion for estimating the strength of jointed rock masses. The fact that a rock mass classification scheme, such as the Norwegian Geotechnical Institute's (NGI) Q system as proposed by Barton, Lien & Lunde (1974) or the Geomechanics Classification Rock Mass Rating RMR scheme as suggested by Bieniawski (1983), can be utilized to estimate the strength parameters of this failure criterion, has proved to be a definite advantage in using this criterion for assessing the strength of a rock mass in a multi–axial state of stress.

In recent applications of the Hoek–Brown failure criterion, it has been found that the strength predicted by this criterion is adequate for the range of stresses which are associated with the brittle failure of rock masses. However, the restriction on the curvature of the failure envelope imposes an artificial restraint on it, especially in the low confining range of stresses. It also predicts a uniaxial tensile and compressive strength for a broken rock mass which should be *zero* as observed in practice. These limitations have been overcome by the development of the *Modified Hoek–Brown Failure Criterion* which has proven to give a better fit to the available triaxial test data. By removing the restraint on the curvature of the strength envelope and neglecting the uniaxial tensile and compressive strength of the rock mass, this curve is found to be highly nonlinear in the region near the origin showing the fact that the strength of the rock mass increases rapidly with the application of a confining pressure. Several other equations were also tried to obtain a failure criterion which would overcome the limitations mentioned above, and a discussion on these along with the properties of the *Modified Hoek–Brown Failure Criterion* and the reason why it was ultimately selected is presented in Chapter 3. The application of the

Simplex Reflection technique for assessing the strength parameters of this criterion is also shown in this chapter. The non-linear relation for the Mohr envelope for this criterion does not have a closed-form solution. Therefore, a numerical equation solution technique was used to solve this equation to calculate the instantaneous values of cohesion and friction angles of the rock mass.

The relationships between the material strength parameters of the Hoek–Brown criterion and rock mass classifications systems are well established. These relations have been developed on the bases of analysis of several sets of broken rock data and actual practical experience. The strength parameters are assigned values depending on the type of rock, degree of weathering and size of blocks. In a similar fashion, a table relating the parameters of the *Modified Hoek–Brown failure criterion* with rock mass classification systems was developed. The methodology involved in the development of these relationships is discussed in Chapter 3.

The applicability of the Hoek-Brown failure criterion for intact rocks was also investigated. A three–parameter equation which involved a variable exponent for the Hoek-Brown equation was tried for fitting the laboratory triaxial test data on intact rock specimens. However, it was found that the three-parameter equation did not give any better results than the original Hoek-Brown criterion. Therefore, it was decided to use the original criterion for estimating the strength of intact rocks.

As a corollary to the development of a failure criterion for rock masses, the strength of rockfills was also investigated. The failure criterion for rockfills as proposed by Charles & Watts (1980) was studied, and a non–dimensional form of the criterion was proposed. A two–step process was developed for determining the shear strength parameters of the rockfill from the results of large–scale triaxial tests on rockfill samples. This method, as explained in Chapter 4, involves the fitting of the laboratory data to a nonlinear, non–dimensional triaxial strength envelope in the first step, and then generating a set of shear and normal stress values using Balmer's solution (1952) for nonlinear Mohr envelopes. The generated data set is then fitted to the non–dimensional Mohr envelope to obtain the shear strength parameters which are used in slope stability analysis of rockfills. This process was generalized so that the data from either triaxial tests or shear tests could be used to obtain the shear strength parameters or the triaxial strength parameters.

The response of the rock mass to the induced stress changes due to a change in the stress field has to be determined from a knowledge of the properties of the rock mass. The linear stress–strain relationship for the elastic analysis of structures has been extensively applied in practice to estimate stress or strain under the induced stresses at various locations in the rock mass. However, the actual rock mass is a very complex structure with an extremely complicated state of stress. The combination of unknown initial stress, secondary stresses, and stress concentrations and redistribution due to discontinuities defy an idealized calculation based on the theory of elasticity. The *theory of plasticity* represents a necessary extension of the theory of elasticity and is concerned with the analysis of stresses and strains in the plastic as well as elastic ranges. It furnishes more realistic estimates of the load–carrying capacity of the rock mass and provides a better understanding of the reaction of the structural elements to the forces induced in the material.

As outlined in Chen and Han (1988), a complete account of the theory and application of plasticity to the behaviour of rock mass must deal with two equally important aspects: firstly, the technique used in the development of stress-strain relationships for an elastic-plastic material with work hardening as well as strain softening; and secondly, the numerical solution procedure for solving an elastic-plastic problem under the action of loads or displacements. The first task for the plasticity theory is to set up *constitutive* or stress–strain laws under a complex stress state that can describe adequately the observed plastic deformation. The deformation rules for metals have been well established and successfully used in engineering applications. In recent years, the methods of plasticity have also been extended and applied to study the deformational behaviour of geological materials, such as rocks, soils and concretes. The second task of the theory is to develop numerical techniques for implementing these stress-strain relationships in actual analysis. Because of the nonlinear nature of the plastic deformation rules, solutions of the basic equations of solid mechanics inevitably present considerable difficulty. However, in recent years, the rapid development of high-speed computers and techniques of finite element, finite difference, and boundary integral equation methods of analysis has provided the engineer with a powerful tool for the solution of virtually any nonlinear problem. It has now been realized that the advances and sophistication in the solution techniques have far exceeded our knowledge of the behaviour of materials defined by constitutive laws. As a consequence, very often,

results from a numerical procedure that may have used less appropriate constitutive laws can be of limited or doubtful validity.

The foregoing realization has spurred active research and interest in the theoretical formulation of constitutive laws and determination of their parameters. The former involves the use of the principles of continuum mechanics and the theory of plasticity, whereas the latter hinges on accurate identification and determination of parameters that define the constitutive model. The objective of the research in this area was to develop the constitutive relations for the rock mass based on the Hoek–Brown failure criterion and the rules of the classical theory of plasticity. This approach was chosen as it is a practical one since the behaviour of the rock mass depends on the geological type, origin, condition of joints, degree of interlocking, etc., and hence cannot be generalized by determining the parameters of the model from a series of tests on one particular type of rock mass. It should be stressed here that testing of rock mass in the laboratory is in itself a difficult and extremely expensive task. The parameters of the Hoek-Brown criterion are related to the type of rock and the geological conditions of the site, and hence, an estimate can be made of the failure strength of the rock mass.

In order to use the Hoek–Brown failure criterion as the yield function, it has been extended to a three-dimensional form which involves the major, minor and intermediate principal stresses to define the limit of elasticity in a multi-axial state of stress. The *flow rule* which defines the direction of flow of the material in the plastic state has been derived on the basis of the *normality condition* which assumes that the direction of the incremental plastic strain vector is always normal to the yield surface. The development of these constitutive relations are discussed in Chapter 5. The application of the *associated flow rule* (AFR), which assumes that the incremental plastic strain vector is normal to the yield surface, results in a finite value of the plastic volumetric strains indicating that there is a dilation in the material after failure. However, as observed in laboratory tests for geologic materials like rocks, soils and concrete, the volumetric dilation is negligible after failure. In order to model this behaviour, a *non-associated flow rule* (NAFR) has to be used according to which the incremental plastic strain vector is normal to a *plastic potential surface* which models the volume dilation behaviour. A *plastic potential surface* was developed for the constitutive model which is nonlinear in nature along the meridians of the surface, similar

to the Hoek–Brown yield surface, and has a circular cross-section. The affect of using an AFR or a NAFR has been studied for the case of simple and complex stress states.

In the first step, the constitutive model has been developed as an elastic, perfectly plastic model, and this model has been implemented into the non-linear finite element stress analysis program ABAQUS. The details of the implementation are discussed in Chapter 6 along with the presentation of the results of the test cases of uniaxial and triaxial compression tests, plane strain analysis of a circular opening in an infinite rock mass under a hydrostatic *in situ* stress field. As a final test for the applicability of this constitutive model, an actual excavation of the Underground Research Laboratory at Pinawa, Manitoba, was analyzed and the results are compared with observations made at the site.

In Chapter 7, the conclusions of the research program are presented, and the recommendations for the future enhancements of the failure criterion and the constitutive model for jointed rock masses are discussed.

Appendix A includes the pseudocode for the Simplex Reflection technique as applied to the determination of the parameters of the Hoek–Brown and Modified Hoek–Brown failure criteria for implementation into a computer program.

The subroutine which was developed for the computation of the constitutive matrix of rock mass and incorporated into ABAQUS is presented in Appendix B along with a sample input data file for ABAQUS.

Chapter 2

Statistical Analysis of Laboratory Strength Data

2.1 Introduction

It is a truism to say that an improvement in the knowledge of the world around us requires an ever–increasing use of statistical methods and inferences. The need for some knowledge of statistics has become universal in order to have a better understanding of the processes happening around us. However, because of the width and depth of the subject, a selection has to be made regarding the field of knowledge and methods relevant to a particular purpose. This chapter is primarily concerned with the application of statistical procedures in geotechnical engineering with emphasis on the extraction of information from the results of strength tests in the laboratory.

As stated in Kennedy and Neville (1968 & 1976) , "Statistics can be defined as the science that deals with the collection, tabulation, analysis, and interpretation of quantitative and qualitative data; this process includes determining the actual attributes or qualities as well as making estimates and the testing of hypotheses by which *probable* or expected values are determined". In the field of engineering the use of statistics is almost invariably required in routine testing in the laboratory, in research work, and in production and construction. In the laboratory, we may want to know whether our testing is "precise", or whether the variability of our results is greater than expected, or greater than in some other test. In research, we may want to know whether a change in an ingredient affects

the properties of the resulting material; to compare the efficiency of processes of testing machines; to determine whether the results fit a suspected or postulated form; or to design an experiment that will enable us to separate out the variation due to different causes.

In geotechnical engineering statistical methods have mainly been used in the analysis of laboratory strength data. Several types of tests, including the triaxial test and the direct shear test, are commonly used to ascertain the strength of a sample of soil or rock mass. The strength of a soil or a rock sample is expressed in the form of a failure envelope which can be linear or nonlinear. The estimation of their strength from an empirical strength criterion involves, firstly, the determination of the parameters which define the correlation between the variables measured in the laboratory, and secondly, the estimation of the coefficient of correlation which enables us to obtain the goodness of fit of the data to a suspected or theorized form of the curve.

Statistical techniques such as Linear Regression analysis have been used extensively for fitting laboratory strength data to the proposed failure envelopes. The Simplex Reflection technique, which is a unique technique for minimizing a function, has been implemented as a curve–fitting tool for fitting a set of data points from laboratory strength tests for the determination of the parameters of failure envelopes. The LOWESS (Locally Weighted Regression Scatterplot Smoothing) technique, which is a data smoothing technique, has also been investigated for the generation of a smoothed data set from the experimental data set, which can then be analyzed by a suitable curve-fitting technique to determine the parameters of the failure criteria. A description of these techniques with their relative merits and demerits is presented in this chapter with their application towards the fitting of laboratory data to linear and nonlinear failure envelopes.

2.2 Failure Criteria for Soil and Rock Masses

A variety of failure criteria is used for the determination of the strength of soil or rock masses. These range from simple, linear relations using two parameters to define the failure envelope, e.g. Mohr–Coulomb Failure criterion, Drucker–Prager criterion, etc., to complex, non-linear mathematical relations using two or several parameters, e.g. Griffith's criterion (1921), Hoek–Brown failure criterion (Hoek and Brown (1980, 1983)), Bieniawski's criterion

(1974), the failure criterion proposed by Ramamurthy (1985), etc.. The discussion in this section will be limited to the linear Mohr-Coulomb failure criterion for soil and rock masses, and the nonlinear Hoek–Brown failure criterion for jointed rock masses.

2.2.1 Mohr–Coulomb Failure Criterion

The most commonly used failure criterion in soil and rock mechanics is the Mohr–Coulomb failure criterion which relates the shear and normal stresses in the material at failure. This is a linear failure criterion, as shown in Figure 2.1, which is determined by carrying out direct shear tests or triaxial tests on soil or rock samples. The parameters of this criterion are c', the cohesion of the material, and ϕ', the friction angle, and it is expressed as

$$\tau = c' + \sigma'_n \tan \phi' \tag{2.1}$$

where,

τ = shear stress at failure,

σ'_n = effective normal stress at failure,

c' and ϕ' are material parameters.

This failure criterion can also be expressed as a relation between the major and minor principal stresses at failure in the form

$$\sigma'_1 = \sigma'_3 \frac{1 + \sin \phi'}{1 - \sin \phi'} + \frac{2c' \cos \phi'}{1 - \sin \phi'} \tag{2.2}$$

where,

σ'_1 = major principal stress at failure,

σ'_3 = minor principal stress at failure.

Laboratory strength data from either triaxial tests or shear tests can be analyzed to determine the material strength parameters, c' and ϕ'. Linear regression analysis has been used traditionally in order to determine these parameters, and it has been found to produce excellent results generally.

2.2.2 Hoek–Brown Failure Criterion

The Hoek–Brown criterion for the strength of jointed rock masses as proposed by Hoek and Brown ((Hoek and Brown, (1980) and Hoek (1983)), as shown in Figure 2.2, is expressed

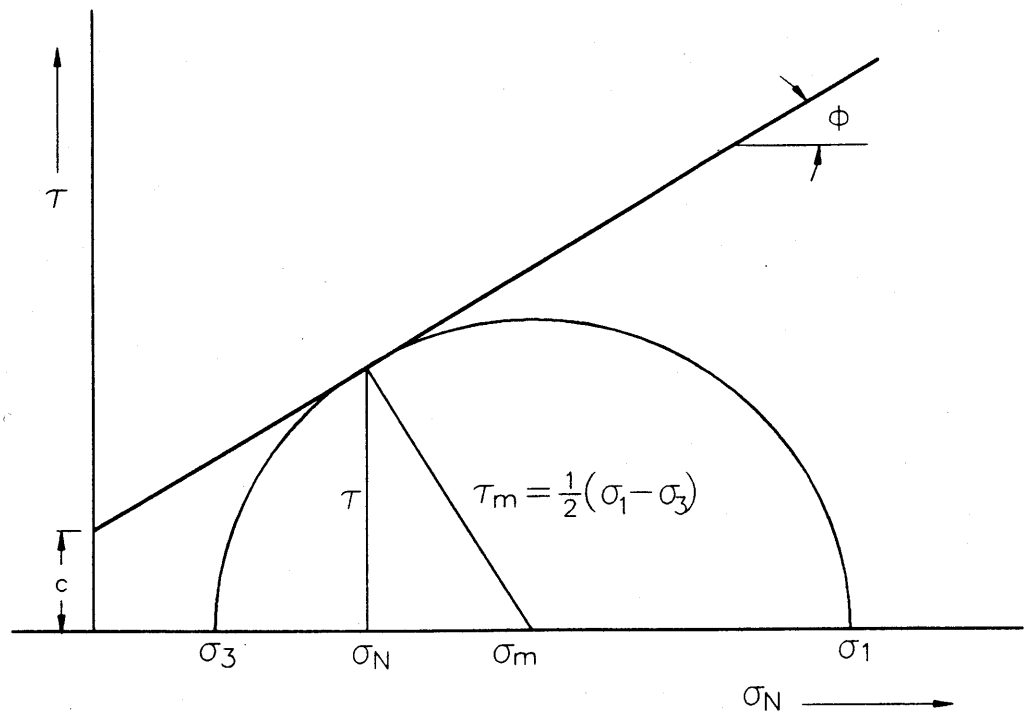

Figure 2.1: Mohr–Coulomb Failure Criterion

as

$$\sigma_1' = \sigma_3' + \sqrt{m\sigma_3'\sigma_c + s\sigma_c^2} \tag{2.3}$$

where,

σ_1' = major principal stress at failure,

σ_3' = minor principal stress at failure,

σ_c = unconfined compressive strength of intact rock,

m and s are material parameters.

The corresponding nonlinear Mohr failure envelope, as outlined in Hoek (1983), is given by:

$$\tau = \frac{1}{8}\left(\cot\phi_i' - \cos\phi_i'\right) m\sigma_c \tag{2.4}$$

where,

τ = shear stress at failure, and

ϕ_i' = instantaneous friction angle at the given values of σ_n' and τ, i.e., it is the inclination of the tangent to the Mohr failure envelope at the point (σ_n', τ).

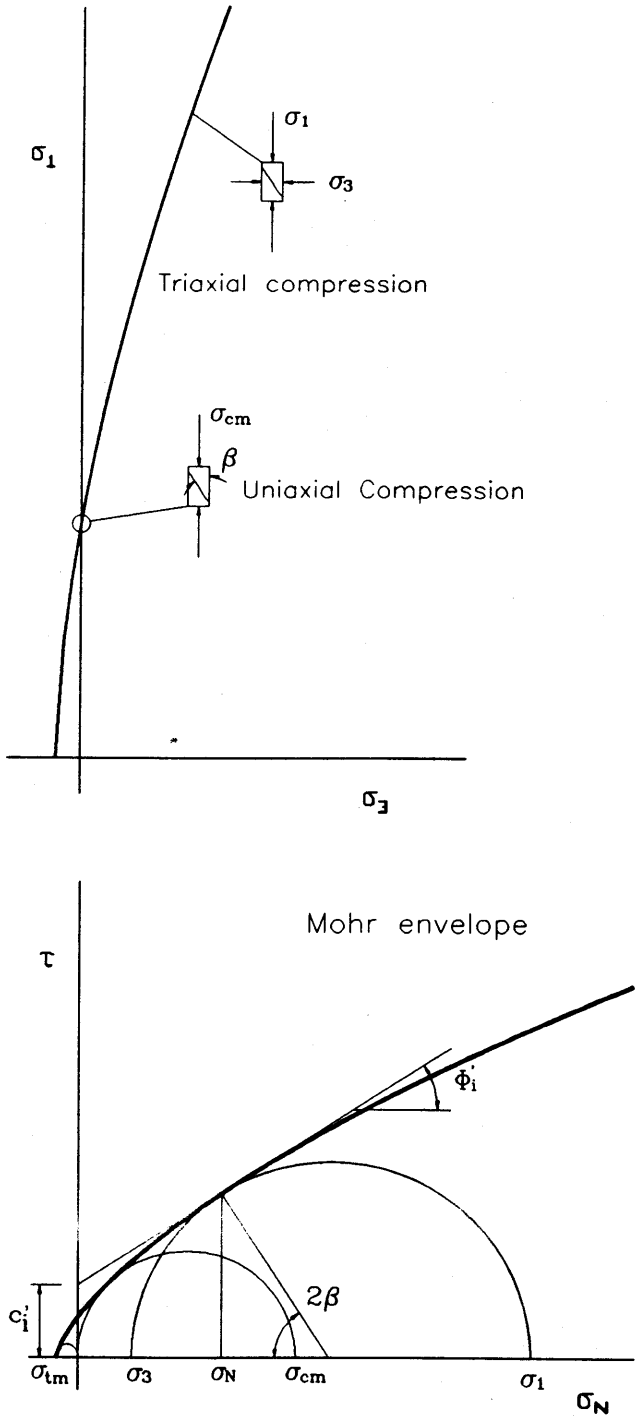

Figure 2.2: Hoek–Brown Failure Criterion

The value of ϕ'_i is given by

$$\phi'_i = \tan^{-1}\left(4h\cos^2\left(\frac{\pi}{3} + \sin^{-1}\frac{1}{\sqrt{h^3}}\right) - 1\right)^{-1/2} \tag{2.5}$$

where,

$$h = 1 + \frac{16\left(m\sigma'_n + s\sigma_c\right)}{3m^2\sigma_c} \tag{2.6}$$

and

$$c'_i = \tau - \sigma'_n \tan\phi'_i \tag{2.7}$$

where,

c'_i = instantaneous value of cohesion at the given values of σ'_n and τ.

This failure criterion is applicable to intact rocks as well as to broken rock masses. The parameters to be obtained from statistical analysis of experimental data are m and σ_c for intact rock as $s = 1$, and m and s for broken rock masses. The value of σ_c obtained from the analysis of the data for intact rocks is taken as an input for the analysis of the broken rock data.

The unconfined compressive strength σ_{cmass} and tensile strength σ_{tmass} of the rock mass are given by

$$\sigma_{cmass} = \sqrt{s}\sigma_c \tag{2.8}$$

$$\sigma_{tmass} = -\frac{s\sigma_c}{m} \tag{2.9}$$

2.3 Linear Regression Analysis and the Method of Least Squares

Statistical methods, for example, Linear Regression Analysis, help us to fit the "best" line to a given set of data, instead of simply drawing a line or a curve "by eye". In elementary work we often establish numerical relations by determining the values of the variables at a number of points equal to the total number of variables. For example, if a linear relation $y = a + bx$ is postulated, two pairs of values (x_1, y_1) and (x_2, y_2) determine the constants in the equation. This is satisfactory, provided that the observed quantities are free from error. In practice, however, errors enter all our observations, and if we take further observations,

say (x_3, y_3), we may obtain a point that does not fit exactly on the straight line through the original two points. This also applies, of course, to nonlinear curves involving powers of x and y.

The Linear Regression method of fitting the "best" curve through a set of n data points is based on the principle of Least Squares (Kennedy and Neville, 1976), according to which if y is a linear function of an independent variable x, the most probable position of a line

$$y = a + bx \tag{2.10}$$

is such that the sum of the squares of the residuals or the deviations of the n data points (x_i, y_i) from the line is a minimum, i.e.,

$$\sum \epsilon^2 = \sum_{i=1}^{n} [y_i - (a + bx_i)]^2 = \text{minimum} \tag{2.11}$$

the deviations being measured *in the direction of the y-axis.* It should be stressed that the underlying assumption of this procedure is that x_i are either free from error as they are assigned values or are subject to negligible error only, while y_i are the observed or measured quantity which are subject to errors that have to be "eliminated" by the method of least squares. The observed y is thus a random value from the population of values of y corresponding to a given x. Such a situation exists in *controlled* experiments, where the interest is to find a mean value of y_i for each given value of x_i. It is also necessary that the values of y_i corresponding to a given x_i be normally distributed, with the mean of the distribution satisfying the regression equation. The correlation obtained from this analysis is concerned with the degree of association between the variables, and not with their dependence or independence.

By applying the condition of equation (2.11), and solving the resulting *normal equations*, we obtain

$$a = \frac{\sum x^2 \sum y - \sum x \sum xy}{n \sum x^2 - (\sum x)^2} \tag{2.12}$$

and

$$b = \frac{n \sum xy - \sum x \sum y}{n \sum x^2 - (\sum x)^2} \tag{2.13}$$

and the coefficient of correlation r^2 is given by

$$r^2 = \frac{(\sum xy - \sum x \sum y/n)^2}{\left(\sum x^2 - (\sum x)^2/n\right)\left(\sum y^2 - (\sum y)^2/n\right)} \tag{2.14}$$

2.3.1 Application to Mohr–Coulomb Criterion

The Mohr–Coulomb failure criterion is a linear criterion, and therefore, the method of linear regression described in section 2.3 can be used directly. The parameters c' and ϕ' can be obtained from a set of (σ_n, τ) data set from shear test results as follows:

$$c' = \frac{\sum \sigma_n'^2 \sum \tau - \sum \sigma_n' \sum \sigma_n' \tau}{n \sum \sigma_n'^2 - \left(\sum \sigma_n'\right)^2} \tag{2.15}$$

and

$$\phi' = \tan^{-1}\left(\frac{n \sum \sigma_n' \tau - \sum \sigma_n' \sum \tau}{n \sum \sigma_n'^2 - \left(\sum \sigma_n'\right)^2}\right) \tag{2.16}$$

and the coefficient of correlation r^2 is given by

$$r^2 = \frac{\left(\sum \sigma_n' \tau - \sum \sigma_n' \sum \tau / n\right)^2}{\left(\sum \sigma_n'^2 - \left(\sum \sigma_n'\right)^2 / n\right)\left(\sum \tau^2 - \left(\sum \tau\right)^2 / n\right)} \tag{2.17}$$

Example 1 An example of linear regression analysis of direct shear test data to obtain the parameters of the Mohr–Coulomb criterion is given in Tables 2.1 and 2.2, and the results are shown in Figure 2.3.

σ_n' (kPa)	τ (kPa)
6.21	8.21
17.70	18.61
41.75	39.00
62.90	52.62

Table 2.1: Shear Test Data for Mohr–Coulomb Criterion (from Hoek, 1980)

c'	4.296 kPa
ϕ'	38.22°
r^2	0.995

Table 2.2: Results of Analysis of Shear Test Data for Mohr–Coulomb Criterion

In the case when the data is obtained from a series of triaxial tests, the values of c' and ϕ' can be obtained as follows:

$$\phi = \sin^{-1}\left(\frac{B-1}{B+1}\right) \tag{2.18}$$

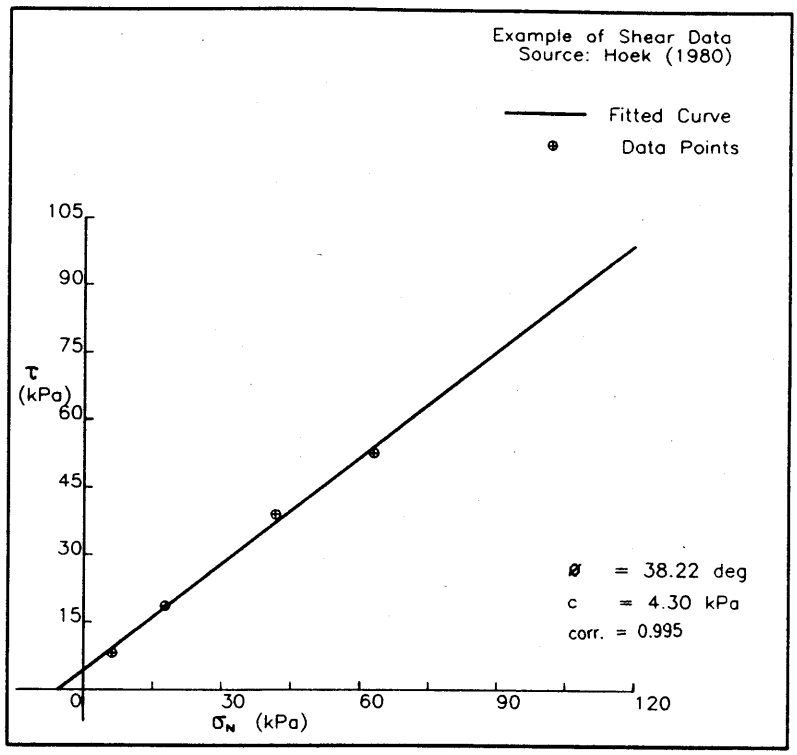

Figure 2.3: Results of analysis of shear data for Mohr–Coulomb Criterion

$$c = A\frac{(1-\sin\phi)}{2\cos\phi} \tag{2.19}$$

where,

$$B = \frac{\sum \sigma_3'\sigma_1' - \sum \sigma_3' \sum \sigma_1'/n}{\sum \sigma_3'^2 - \left(\sum \sigma_3'\right)^2/n} \tag{2.20}$$

$$A = \frac{\left(\sum \sigma_1' - B\sum \sigma_3'\right)}{n} \tag{2.21}$$

and the coefficient of correlation is given by

$$r^2 = \frac{\left(\sum \sigma_3'\sigma_1' - \sum \sigma_3' \sum \sigma_1'/n\right)^2}{\left(\sum \sigma_3'^2 - \left(\sum \sigma_3'\right)^2/n\right)\left(\sum \sigma_1'^2 - \left(\sum \sigma_1'\right)^2/n\right)} \tag{2.22}$$

Example 2 An example of linear regression analysis of triaxial test data to obtain the material parameters of the Mohr–Coulomb criterion is given in Tables 2.3 and 2.4, and the results are shown in Figure 2.4.

σ_3' (kPa)	σ_1' (kPa)
3.85	31.85
9.93	62.26
21.24	115.90
32.26	154.52

Table 2.3: Triaxial Test Data for Mohr–Coulomb Criterion (from Hoek, 1980)

c'	4.348 kPa
ϕ'	38.72°
r^2	0.995

Table 2.4: Results of Analysis of Triaxial Test Data for Mohr–Coulomb Criterion

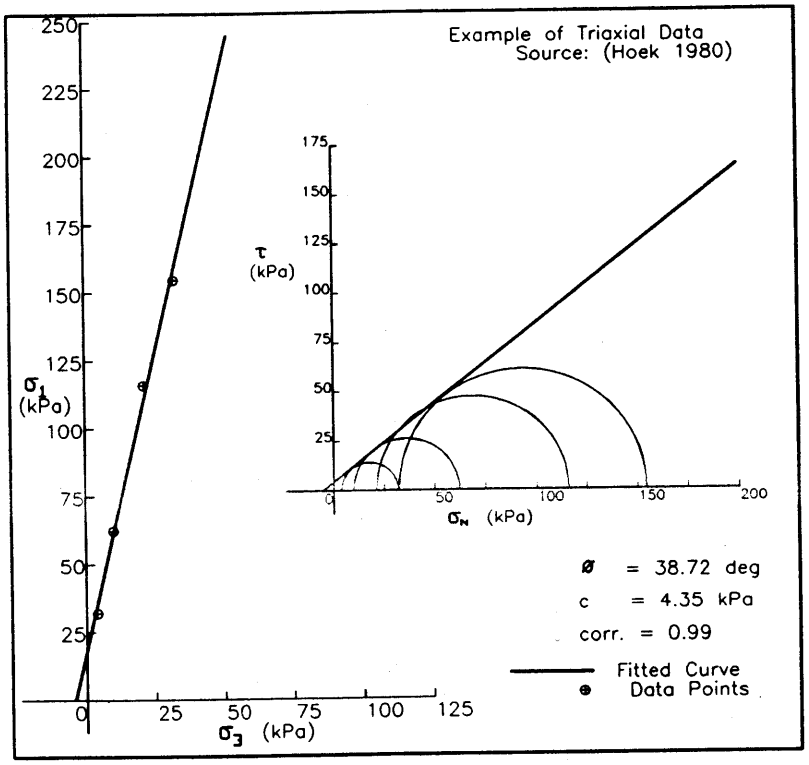

Figure 2.4: Plot of results of analysis of Triaxial test data for Mohr–Coulomb Criterion

2.3.2 Application to Nonlinear Relations

The method of fitting a regression line can be extended to the case where the known or expected relation is not in the form of a straight line. The procedure for nonlinear relations is to write the equation of the curve in its general form, tabulate the deviations of y from the assumed curve, and to find the constants in the equation which satisfy the condition that the sum of the square of the deviations is a minimum. This procedure requires a great deal of computational effort for curves with a high order of nonlinearity. However, in many cases, a nonlinear relation can be transformed to a straight–line relation, i.e., it can be rectified. This not only simplifies the handling of the data, but also results in a graphical presentation that is more revealing as far as the assessment of the scatter is concerned. Extrapolation of the curve is also easier, and so is the calculation of various statistics, such as standard deviation and confidence limits. The process of rectification for three simple cases is illustrated below:

1. The *power function* $y = ax^b$ can be rectified by taking logarithm of both sides of the equation to obtain:

$$\log y = \log a + b \log x \tag{2.23}$$

   This rectified equation will plot as a straight line if the ordinates are given as $\log y$ and the abscissae $\log x$, or if x and y are plotted to a logarithmic scale. The fitting constants are now $\log a$ and b, and the new variables $\log x$ and $\log y$ are linearly related, and hence, the principle of least squares can be applied.

2. The *exponential function* $y = ab^x$ can also be rectified by log transformation, i.e.,

$$\log y = \log a + x \log b \tag{2.24}$$

   The fitting parameters are $\log a$ and $\log b$, and $\log y$ and x are treated as the linear variables. This rectified equation will plot as a straight line on a semi–log graph in which the ordinate is $\log y$ and the abscissae is x.

3. The *hyperbola* $y = a + b/x$ can be rectified by treating $1/x = u$ as the new variable. Then y and u are linearly related. If the equation is in the form

$$y = \frac{x}{a + bx} \tag{2.25}$$

it can be inverted to the form

$$\frac{1}{y} = \frac{a}{x} + b \tag{2.26}$$

Then $1/x$ and $1/y$ are linearly related.

2.3.3 Application to Hoek–Brown Failure Criterion

The Hoek–Brown failure criterion, as expressed by equation (2.3) is a nonlinear relation, and therefore, the equation has to be rectified or modified into a linearized form as

$$(\sigma_1' - \sigma_3')^2 = m\sigma_c\sigma_3' + s\sigma_c^2 \tag{2.27}$$

or,

$$y = m\sigma_c x + s\sigma_c^2 \tag{2.28}$$

where,

$$y = (\sigma_1' - \sigma_3')^2 \tag{2.29}$$

and

$$x = \sigma_3' \tag{2.30}$$

The linear variables are now $y = (\sigma_1' - \sigma_3')^2$ and $x = \sigma_3'$. Thus, the application of the method of Least Squares to the linearized equation will minimize the deviations of the transformed dependent variable, i.e. $y = (\sigma_1' - \sigma_3')^2$. The determination of the material constants σ_c, m and s for intact rock and broken rock mass are outlined as below:

- *Intact rock*

  For intact rocks, $s = 1$ and the uniaxial compressive strength σ_c and the material constant m are obtained from linear regression analysis as

$$\sigma_c^2 = \frac{\sum y}{n} - \left[\frac{\sum xy - \sum x \sum y/n}{\sum x^2 - (\sum x)^2/n}\right]\frac{\sum x}{n} \tag{2.31}$$

$$m = \frac{1}{\sigma_c}\left[\frac{\sum xy - \sum x \sum y/n}{\sum x^2 - (\sum x)^2/n}\right] \tag{2.32}$$

  where n is the number of data pairs.

  The coefficient of correlation is given by

$$r^2 = \frac{(\sum xy - \sum x \sum y/n)^2}{\left(\sum x^2 - (\sum x)^2/n\right)\left(\sum y^2 - (\sum y)^2/n\right)} \tag{2.33}$$

Example 3 An example of linear regression analysis of triaxial test data of *intact* Panguna Andesite from Bougainville in order to determine the parameters of the Hoek–Brown criterion is given in Tables 2.5 and 2.6, and the results are shown in Figure 2.5.

σ_3' (MPa)	σ_1' (MPa)
0.00	269.00
6.90	206.70
27.60	503.50
31.00	586.50
69.00	683.30

Table 2.5: Triaxial Data of *intact* rock for Hoek–Brown Criterion (from Hoek, 1980)

σ_c	265.42 MPa
m	18.837
s	1.000
σ_{tmass}	-14.05 MPa
$\sum \epsilon^2$	23227.4
r^2	0.849

Table 2.6: Results of Linear Regression Analysis of Triaxial Test Data *intact* rock for Hoek–Brown Criterion

- *Broken rock*

  For broken or heavily jointed rock, the strength of the intact rock pieces is determined by the analysis given above. The value of the constant m for the rock mass is found from equation (2.32). The value of the constant s is given by

$$s = \frac{1}{\sigma_c^2}\left[\frac{\sum y}{n} - m\sigma_c\frac{\sum x}{n}\right] \tag{2.34}$$

  The coefficient of correlation is found from equation (2.33).

  As discussed in Hoek (1983), when the value of s is very close to zero, equation (2.34) will sometimes give a small negative value. In such cases, s is taken as 0 and the constant m is calculated as

$$m = \frac{\sum y}{\sigma_c \sum x} \tag{2.35}$$

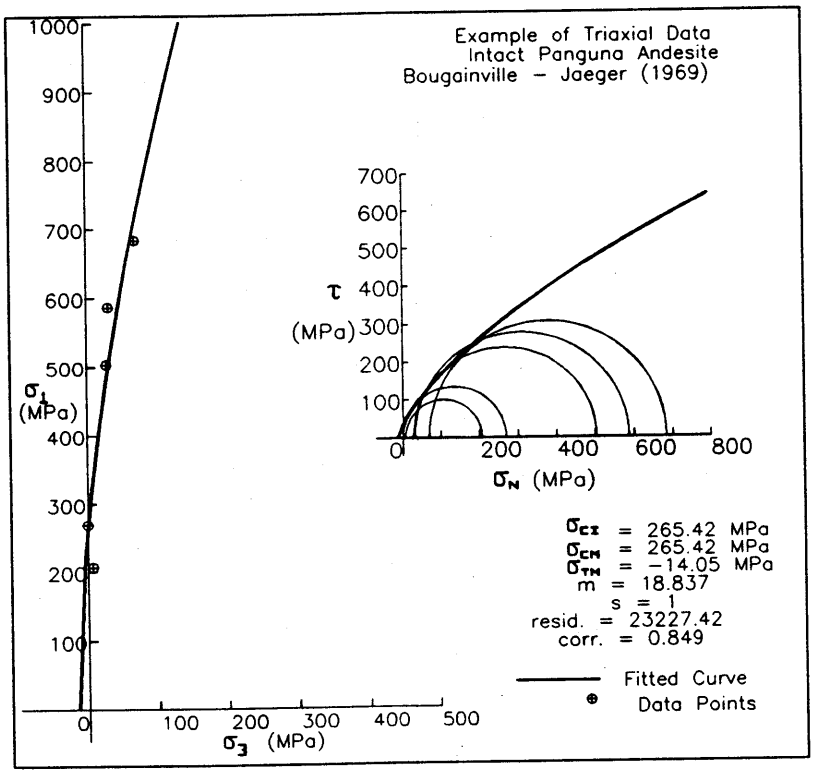

Figure 2.5: Plot of results of linear regression analysis of Triaxial test data of *intact* rock for Hoek–Brown Criterion

When equation (2.35) is used, equation (2.33) is not valid.

Example 4 An example of linear regression analysis of triaxial test data for jointed Panguna Andesite from Bougainville in order to determine the strength parameters of the Hoek–Brown criterion is given in Tables 2.7 and 2.8, and the results are shown in Figure 2.6.

σ_3' (MPa)	σ_1' (MPa)
0.00	1.24
0.35	6.07
0.69	8.96
1.24	12.07
1.38	12.82
3.45	19.31
3.45	20.00

Table 2.7: Triaxial Data of *broken* rock for Hoek–Brown Criterion (from Hoek, 1980)

σ_c	265.42 MPa
m	0.277
s	0.000203
σ_{cmass}	3.78 MPa
σ_{tmass}	-0.19 MPa
$\sum \epsilon^2$	7.96
r^2	0.986

Table 2.8: Results of Linear Regression Analysis of Triaxial Test Data *broken* rock for Hoek–Brown Criterion

The sum of the square of the residuals for σ_1' is calculated as

$$\sum \epsilon^2 = \sum \left(\sigma'_{1experimental} - \sigma'_{1calculated}\right)^2 \tag{2.36}$$

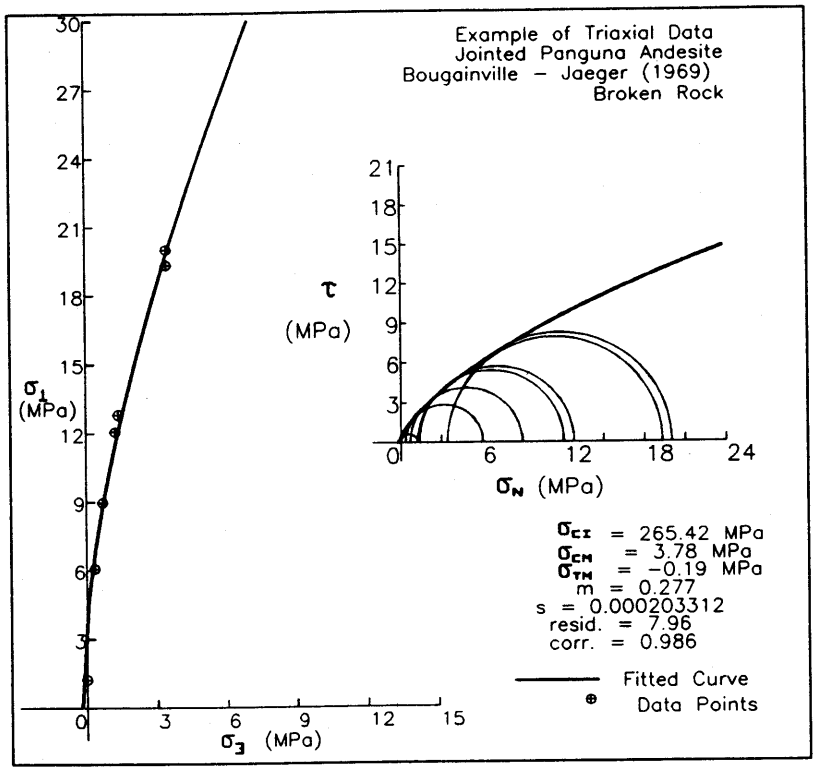

Figure 2.6: Plot of results of linear regression analysis of Triaxial test data of *broken* rock for Hoek–Brown Criterion

2.3.4 Determination of m and s from direct shear test data

As outlined in Hoek (1983), the method for determining the material constants m and s from direct shear test data is as follows.

The major and minor principal stresses corresponding to each τ , σ_n' pair can be calculated as

$$\sigma_1' = \frac{\left(\sigma_n'^2 + (\tau - c')\,\tau\right) + \tau\sqrt{\sigma_n'^2 + (\tau - c')^2}}{\sigma_n'} \tag{2.37}$$

$$\sigma_3' = \frac{\left(\sigma_n'^2 + (\tau - c')\,\tau\right) - \tau\sqrt{\sigma_n'^2 + (\tau - c')^2}}{\sigma_n'} \tag{2.38}$$

where, c' = is an estimate of the cohesion intercept for the entire τ , σ_n' data set. This estimate can be assumed a value greater than or equal to zero or it can be determined by linear regression analysis of the shear test data according to equation (2.15).

After the calculation of the values of σ_1' and σ_3' by means of equations (2.37 and 2.38), the determination of the material constants m and s is carried out as for broken rock. An estimate of the uniaxial compressive strength σ_c of the intact rock is required in order to complete the analysis.

Example 5 An example of linear regression analysis of shear test data for weathered Greywacke joints (Martin & Miller, 1974) in order to compute the strength parameters of the Hoek–Brown criterion is given in Tables 2.9 and 2.10, and the results are shown in Figure 2.7.

The above-mentioned method assumes that the relation between σ_n' and τ in the entire data set can be approximated by a linear relation. However, if it is assumed that a nonlinear relationship exists between σ_n' and τ, then σ_1' and σ_3' can be calculated as follows. If the assumed nonlinear relation between σ_n' and τ is

$$\tau = \alpha\left(\sigma_n' - k\right)^{\beta} \tag{2.39}$$

where, α, β and k are constants of the assumed curve, then

σ_n' (MPa)	τ (MPa)
0.29	0.45
0.65	0.75
1.36	1.23
2.55	1.84
4.87	2.79

Table 2.9: Shear Test Data of *broken* rock for Hoek–Brown Criterion (source: Hoek, 1980)

σ_c	80.00 MPa
m	0.147
s	0.000181
σ_{cmass}	1.08 MPa
σ_{tmass}	-0.1 MPa
$\sum \epsilon^2$	0.855
r^2	0.996

Table 2.10: Results of Analysis of Shear Test Data of *broken* rock for Hoek–Brown Criterion

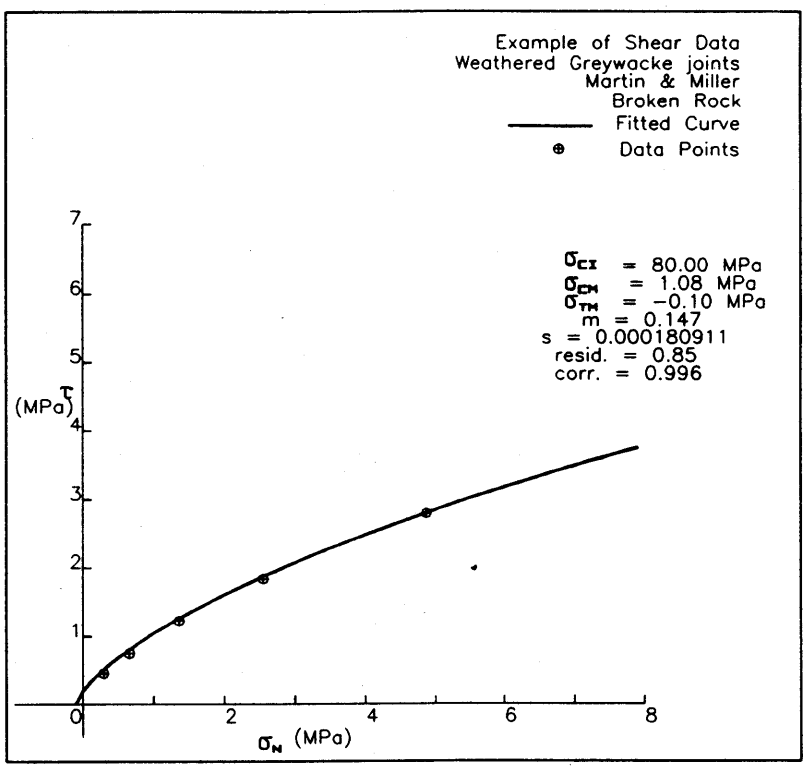

Figure 2.7: Plot of results of linear regression analysis of Direct Shear test data for Hoek–Brown Criterion

$$\sigma_1' = \sigma_n' + \tau \left[\alpha\beta \left(\sigma_n' - k\right)^{\beta-1} + \sqrt{1 + \alpha^2\beta^2 \left(\sigma_n' - k\right)^{2(\beta-1)}} \right] \tag{2.40}$$

$$\sigma_3' = \sigma_n' - \tau \left[\frac{\alpha\beta \left(\sigma_n' - k\right)^{\beta-1} - 1 - \sqrt{1 + \alpha^2\beta^2 \left(\sigma_n' - k\right)^{2(\beta-1)}}}{\alpha\beta \left(\sigma_n' - k\right)^{\beta-1} + 1 + \sqrt{1 + \alpha^2\beta^2 \left(\sigma_n' - k\right)^{2(\beta-1)}}} \right] \tag{2.41}$$

The derivation of equations (2.40 and 2.41) and the procedure to obtain α, β and k are similar to that given in Chapter 4 for conversion of shear test data to triaxial test data for rockfill materials. Once these values of σ_1' and σ_3' are calculated, the material parameters m and s can be obtained as for broken rock.

2.3.5 Limitations of Linear Regression Analysis

The limitations of the linear regression analysis (Kennedy and Neville, 1976, Crow, Davis and Maxfield, 1960) as applied to the determination of parameters of a nonlinear criterion such as the Hoek–Brown criterion are as follows:

1. nonlinear relations such as the Hoek-Brown failure criterion have to be modified to a linear form in order to apply the method of linear regression analysis. The method of Least Squares when applied to this linearized equation minimizes the sum of the square of the residuals of the transformed dependent variable, i.e. $y = (\sigma_1' - \sigma_3')^2$, and not the sum of the square of the residuals of the original dependent variable σ_1'. Therefore, the process of transformation results in the minimization of a function other than the one which involves the sum of the square of the residuals of σ_1';

2. the method of least squares assumes that the observed values y_i correspond to assigned or error-free values of x_i, and that the error in y is independent of the level of x. This is not true for the case of the experimental measurements of σ_1' and σ_3' as both variables are subjected to measurement error. Besides this, the process of rectification, i.e., by taking $y = (\sigma_1' - \sigma_3')^2$ and $x = \sigma_3'$, causes the errors in the measurement of σ_1' and σ_3' to be combined. Furthermore, the variance of the values of y for a given value of x should be independent of the magnitude of x. This is not always true in experimental measurements as has been established in the case of concrete for which the scatter of

values of the strength of concrete is greater the higher the confining stress. This is also a major determining factor in the measurement of σ_1' and σ_3' for rock samples;

3. for inferences and estimates to be made using linear regression, the values of y_i corresponding to x_i must be normally distributed, with the mean of the distribution satisfying the regression equation. Most of the data sets available for the triaxial testing of rock specimens show that for any value of σ_3', there is usually one value of σ_1' or at most two or three values. For these data sets, it has to be assumed that the value of σ_1' corresponds to the mean of the assumed normal distribution for σ_1'. However, it is possible that the value of σ_1', corresponding to the σ_3' value, being considered in the analysis may lie anywhere in the normal distribution curve for σ_1', and the values of σ_1' for successive values of σ_3' may not lie at the same location of the distribution. Therefore, a serious error is introduced in the analysis process;

4. linear regression analysis is found to be adequate when the data set contains relatively evenly spaced points with very little scatter about a general trend line. Where the data points are clustered, unevenly spaced or widely scattered, this method gives poor results. The experimental data obtained corresponding to σ_1' and σ_3' are generally unevenly spaced as very few data points are available in practice, with more uniaxial compression tests and few triaxial test data points. This can result in a strong bias in the data being analyzed. If the number of observations (σ_3', σ_1') is small, not even the mean will be estimated very precisely by the fitted regression equation;

5. the statistics, e.g. coefficient of determination or goodness of fit, calculated for the modified variables apply to the transformed data only and not to the original data. Therefore, the coefficient of correlation calculated by equation (2.33) estimates the goodness of fit of the linear equation corresponding to equation (2.27) and not to the nonlinear relation given by equation (2.3);

6. extrapolation of the data should be done with caution because in regression analysis, the assumption is made that the mean of y is a linear function of the x's. If the resulting equation is used for predicting beyond the range of x's for which this assumption holds true, errors not accounted for in the confidence intervals for the regression will occur; and

7. from physical considerations, the deviations of the original variable, σ_1', and not the transformed variable should be minimized by the method of Least Squares, and for

this the transformed variables should be weighted as a function of the error, i.e.,

$$\text{weight} \propto \frac{1}{\mathcal{F}(\text{error})} \tag{2.42}$$

However, it is difficult to ascertain the value of these weights in practice.

It should be noted here that methods are available to calculate regression when both variables are subject to error, but they are beyond the scope of this work.

2.4 Simplex Reflection Technique

The Simplex Reflection Technique (Nash, 1979) is a procedure for the minimization of a function of n parameters, and was developed by Nelder and Mead in 1965. It is a search procedure based largely on heuristic ideas and an intuitive conception of the minimisation problem. Among numerous applications of this technique, it has been found to be appropriate for fitting a nonlinear curve through a non-uniform distribution of data in statistical applications. It has proved to be effective in the determination of the Hoek-Brown strength parameters as the data available does not follow a uniform distribution in most cases.

The strengths of this method lie in the fact that it does not require the computation of any derivatives, and therefore, it can cope with functions which are not easily written as analytic expressions, e.g., the results of simulations. It always increases the information available concerning the function by reporting its value at a number of points. However, its weakness is that it does not use this information very effectively since it is a technique based on heuristics, and requires a large number of function evaluations to locate a solution. The procedure has been found to be inefficient for functions with more than five parameters.

2.4.1 The Simplex Algorithm

A *simplex* is a structure formed by $(n+1)$ points, not in the same plane, in an n-dimensional space. The main features of the algorithm are as follows:

- The function is evaluated at each vertex of the simplex and the vertex having the highest function value is replaced by a new point with a lower function value. This

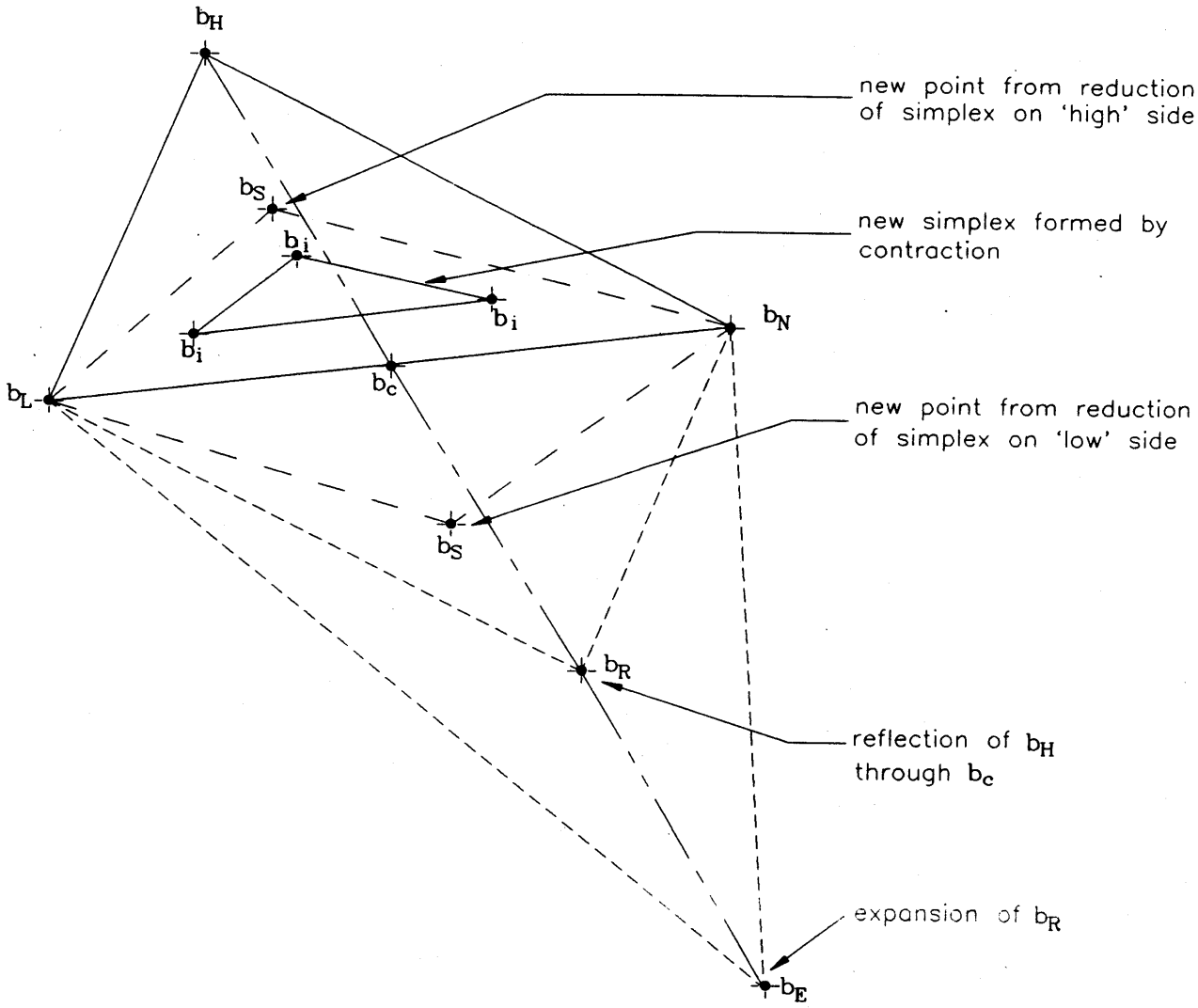

Figure 2.8: Operations of the Simplex Technique

is performed in such a way that the *simplex* adapts itself to the local landscape, and contracts to the final minimum. There are four main operations which are made on the simplex: *reflection*, *expansion*, *reduction* and *contraction*. In order to operate on the simplex, it is essential to order the points so that the highest is b_H, the next-to-highest b_N, and the lowest b_L. Hence, the associated function values obey

$$\mathcal{S}(b_H) \geq \mathcal{S}(b_N) \geq \mathcal{S}(b_i) \geq \mathcal{S}(b_L) \tag{2.43}$$

for all $i \neq H, N$, or L. Figure 2.8 depicts this situation and the other operations of the simplex method.

The centroid of all points other than b_H is defined by

$$b_C = \frac{1}{n} \sum_{\substack{j=1 \\ j \neq H}}^{n+1} b_j \tag{2.44}$$

- **Reflection:**

  The operation of *reflection* then reflects b_H through b_C using a reflection coefficient α, that is

$$\begin{aligned} b_R &= b_C + \alpha (b_C - b_H) \\ &= (1+\alpha) b_C - \alpha b_H \end{aligned} \tag{2.45}$$

- **Expansion:**

  If $\mathcal{S}(b_R)$ is less than $\mathcal{S}(b_L)$, a new low point has been found, and the *simplex* can be expanded by extending the line $(b_R - b_C)$ to give the point

$$\begin{aligned} b_E &= b_R + (\gamma - 1)(b_R - b_C) \\ &= \gamma b_R + (1-\gamma) b_C \\ &= (1+\alpha\gamma) b_C - \alpha\gamma b_H \end{aligned} \tag{2.46}$$

  where γ is the expansion factor having a value greater than unity.

  If $\mathcal{S}(b_E) < \mathcal{S}(b_R)$, then b_H is replaced by b_E and the procedure is repeated by finding a new centroid of n points b_C. Otherwise b_R is the new lowest point and it replaces b_H.

In the situation where b_R is not a new lowest point, but is less than b_N, i.e.,

$$\mathcal{S}(b_L) \leq \mathcal{S}(b_R) < \mathcal{S}(b_N) \tag{2.47}$$

b_H is replaced by b_R and the procedure repeated.

- **Reduction:**

In the remaining situation, $\mathcal{S}(b_R)$ is at least as great as $\mathcal{S}(b_N)$, and should reduce the simplex.

There are two possibilities:

(i) If

$$\mathcal{S}(b_N) \leq \mathcal{S}(b_R) < \mathcal{S}(b_H) \tag{2.48}$$

then the reduction is made by replacing b_H by b_R and finding a new vertex between b_C and b_R (now b_H). This is a reduction on the side of the reflection, i.e., on the 'low' side.

(ii) If

$$\mathcal{S}(b_R) > \mathcal{S}(b_H) \tag{2.49}$$

the reduction is made by finding a new vertex between b_C and b_H, i.e., the 'high' side. In either of these cases, the reduction is controlled by a factor β, where $0 < \beta < 1$. Since case (i) above replaces b_H by b_R, the same formula applies for the new point b_S ('S' denotes that the simplex is smaller) in both cases. b_H is used to denote both b_R and b_H since in case (i) b_R has become the new highest point in the simplex. Hence,

$$\begin{aligned} b_S &= b_C + \beta(b_H - b_C) \\ &= \beta b_H + (1-\beta) b_C \end{aligned} \tag{2.50}$$

The new point b_S then replaces the current b_H which in case (i) is b_R, unless

$$\mathcal{S}(b_S) > \min(\mathcal{S}(b_H), \mathcal{S}(b_R)) \tag{2.51}$$

The replacement of b_H by b_R in case (i) will mean that this minimum has already been saved with its associated point.

- **Contraction:**

  When the previous equation is satisfied, a reduction has given a point higher than $\mathcal{S}(b_N)$, so a general contraction of the simplex about the lowest point so far, b_L, is suggested. That is

$$\begin{aligned} b_i' &= b_L + \beta'(b_i - b_L) \\ &= \beta' b_i + (1-\beta') b_L \end{aligned} \tag{2.52}$$

  for all $i \neq L$.

The rate of convergence of the procedure depends upon the *reflection*, *expansion*, *reduction* and *contraction* factors, and on the basis of extensive tests conducted by Nelder and Mead (1965), Nash (1979) and other researchers, the values that have been found to be effective are:

$$\alpha = 1, \quad \gamma = 2, \quad \beta = \beta' = 0.5 \tag{2.53}$$

The *simplex* algorithm is very robust, and, if permitted to continue long enough, almost always finds the minimum. In order to determine the point where the minimum has been achieved, Nelder and Mead (1965) suggest using the 'standard error' of the function values, i.e.,

$$\text{test} = \left[\left(\sum_{j=1}^{n+1} \left[\mathcal{S}(b_j) - \bar{\mathcal{S}} \right]^2 \right) \Big/ n \right]^{\frac{1}{2}} \tag{2.54}$$

where

$$\bar{\mathcal{S}} = \sum_{j=1}^{n+1} \mathcal{S}(b_j) \Big/ (n+1) \tag{2.55}$$

The procedure is taken to have converged when the test value falls below some pre-assigned tolerance. Another logical way of checking for convergence is by the equality between $\mathcal{S}(b_L)$ and $\mathcal{S}(b_H)$, that is a test for equal height of all points in the simplex. This test is more suitable for problems with fairly flat areas of the function surface.

A pseudocode for the Simplex Reflection Technique is presented in Appendix A for application in determining of the parameters of any nonlinear failure criteria.

2.4.2 Application of Simplex Reflection Technique for Calculation of Hoek-Brown Failure Criterion Parameters

The Hoek-Brown failure criterion parameters for *intact* rocks are m and σ_c, and for *broken* rocks are m and s. Since the number of parameters are two in both the cases, the *simplex* formed will have three vertices, i.e., it is a triangle. The procedure presented here is adapted from Caceci and Cacheris (1984) and Lee (1987). The Simplex technique, along with Linear Regression analysis, has been incorporated into a computer program ROCK-DATA, developed by the author at the Department of Civil Engineering in the University of Toronto, and the pseudocode for this algorithm is given in Appendix A. Figure 2.9 shows the travel of the coordinates (m, s) during the minimization process, and Figure 2.10 shows the variation of the sum of the square of the residuals, $\sum \epsilon^2$, with m and s as the minimum of the function is being searched for. The procedures for using the Simplex technique for evaluating the parameters for *intact* rocks and *broken* rock mass are outlined below:

- **Intact Rocks:**

  The Simplex procedure can be started with any value within the limits of applicability of the parameters, i.e. $m > 0$ and $\sigma_c > 0$, in order to determine the initial coordinates of the *simplex*. However, as a matter of convenience and to reduce the number of iterations, the parameters obtained from Linear Regression analysis are selected as the coordinates of the initial point. Hence, as a first step, linear regression analysis is performed on the data pairs to obtain the coordinates (m,σ_c) of the initial point of the *simplex*. In order to set up the initial *simplex* triangle, two more coordinates are required which are obtained by providing appropriate step sizes for the values of m and σ_c. These coordinates of the *simplex* are calculated by the operations outlined in Appendix A in such a way to obtain a stable triangle.

  The function $S(b)$ that is to be evaluated is the sum of the square of the residuals, i.e.,

$$S(b_i) = \sum \epsilon^2 = \sum_{j=1}^{n} (\sigma_{1experimental} - \sigma_{1calculated})^2 \tag{2.56}$$

  at each vertex of the triangle for the coordinates (m_i,σ_{c_i}) to ascertain the highest b_H, next-to-highest b_N, and lowest b_L points of the triangle. There are three test

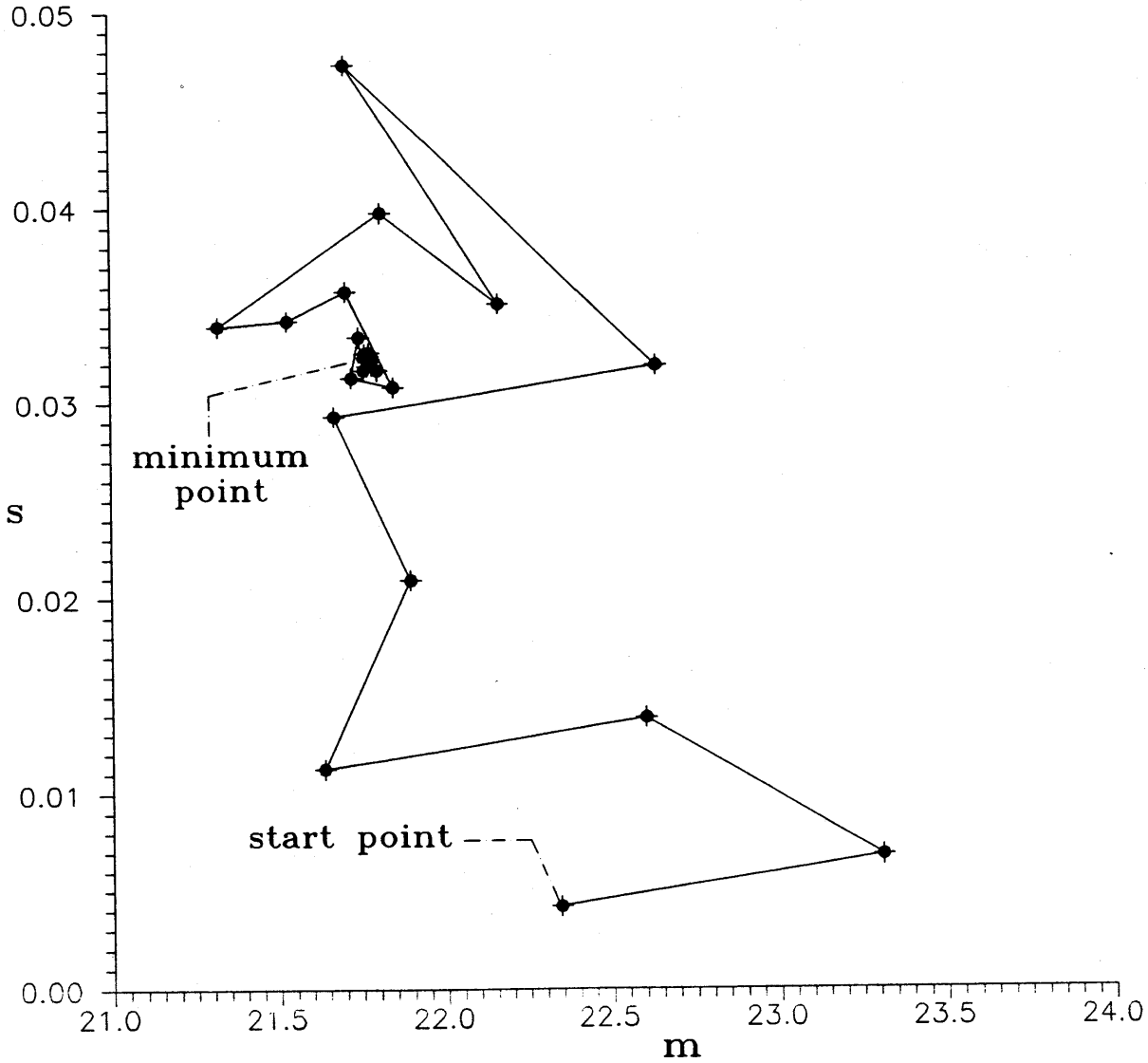

Figure 2.9: Example of Simplex Technique with travel of coordinates (m, s) during various operations

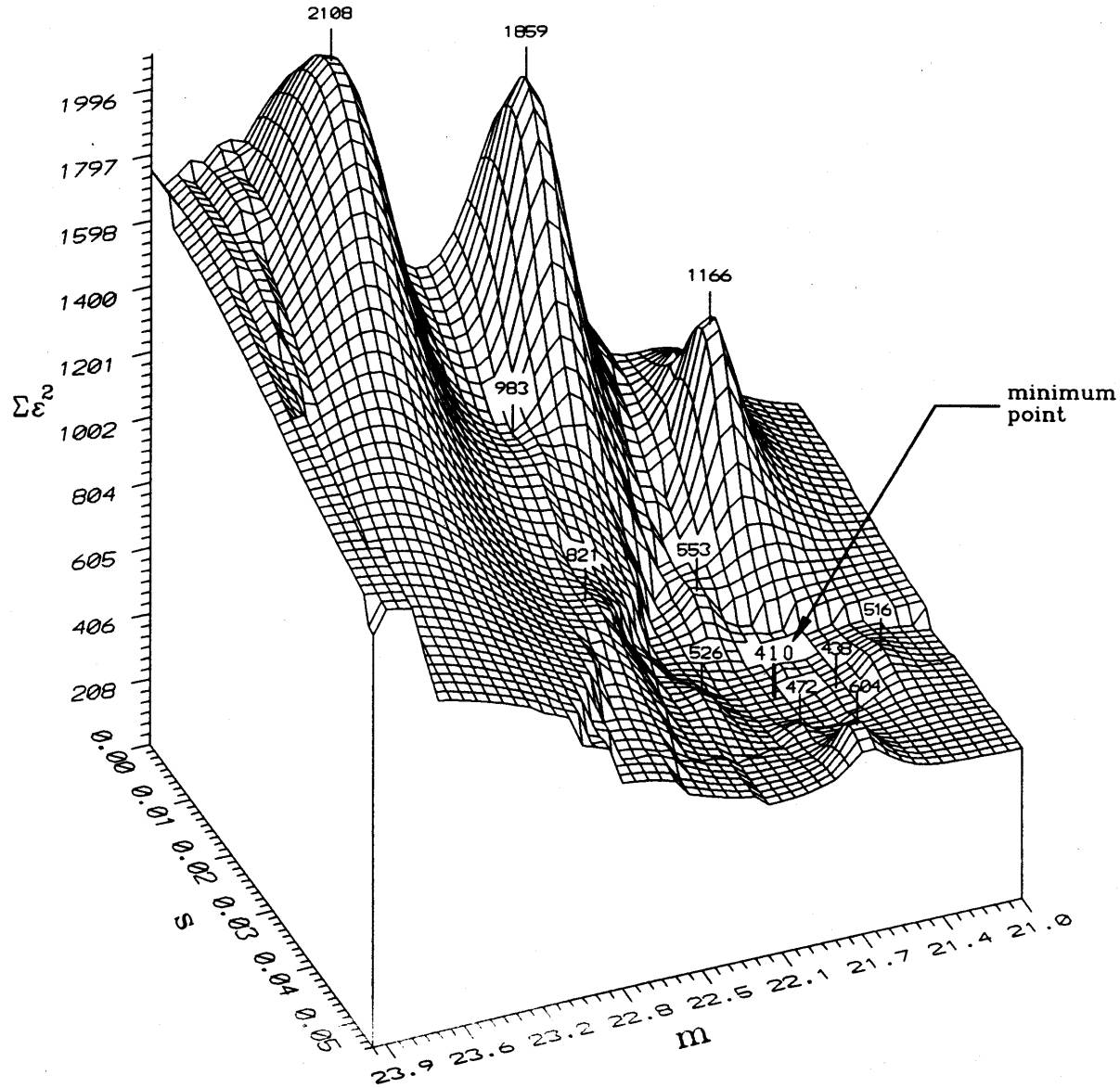

Figure 2.10: Plot of variation of $\sum \epsilon^2$ with m and s during Simplex procedure

conditions used in these calculations to obtain the minimum of the function. They are:

$$\begin{aligned} \left(\mathcal{S}\left(b_H\right)-\mathcal{S}\left(b_L\right)\right)/\mathcal{S}\left(b_H\right) &\leq \text{tolerance for residuals} \\ \left(m_H-m_L\right)/m_H &\leq \text{tolerance for } m \\ \left(\sigma_{c_H}-\sigma_{c_L}\right)/\sigma_{c_H} &\leq \text{tolerance for } \sigma_c \end{aligned} \tag{2.57}$$

The values of the tolerance are given in Tables A.1, A.2 and A.3.

Example 6 An example of Simplex Reflection analysis of triaxial test data for *intact* Carrara marble (Gerogiannopoulous, 1977) for calculating the parameters of the Hoek–Brown criterion is given in Tables 2.11 and 2.12, and the results are shown in Figure 2.11.

σ_3' (MPa)	σ_1' (MPa)
1.72	78.60
3.44	89.33
5.17	99.81
6.89	123.78
6.89	125.23
10.34	125.64
10.34	138.36
13.79	137.37
13.79	146.60
17.24	150.77
17.24	160.75
20.68	173.79
27.58	187.89
34.48	205.98
34.48	213.57

Table 2.11: Triaxial Test Data of intact Carrara marble (Gerogiannopoulous, 1977) for Hoek–Brown Criterion

- **Broken Rocks:**

  In the case of broken rocks, the coordinate pair of the *simplex* will correspond to m and s. The initial coordinates (m,s) of the *simplex* can be taken as any value within

σ_c	78.3 MPa
m	9.63
s	1.000
σ_{cmass}	78.3 MPa
σ_{tmass}	-8.04 MPa
$\sum \epsilon^2$	730.7

Table 2.12: Results of Simplex Reflection Analysis of Triaxial Test Data of intact Carrara marble for Hoek–Brown Criterion

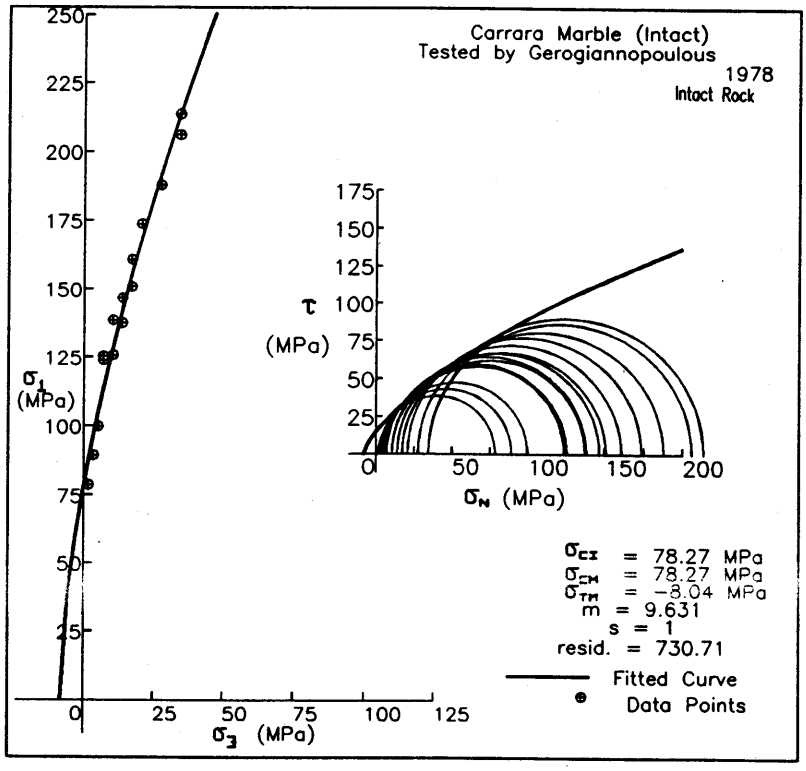

Figure 2.11: Plot of results of Simplex Reflection analysis of Triaxial test data of *intact* rock for Hoek–Brown Criterion

the range of applicability of these parameters, i.e. $m > 0$ and $0 < s \leq 1$. However, as stated for *intact* rock, these initial values can be obtained from linear regression analysis of the broken rock data. The other calculation steps are similar to the ones outlined for the intact rocks except that σ_c is replaced by s. The test conditions are:

$$\begin{aligned} (\mathcal{S}(b_H) - \mathcal{S}(b_L))/\mathcal{S}(b_H) &\leq \text{tolerance for residuals} \\ (m_H - m_L)/m_H &\leq \text{tolerance for } m \\ (s_H - s_L)/s_H &\leq \text{tolerance for } s \end{aligned} \tag{2.58}$$

The four simplex operations for a broken rock mass are shown in Figure 2.9, and the value of the residuals are plotted for various combinations of m and s in Figure 2.10. It can be observed from Figure 2.9 that the the simplex method converges to a minimum very rapidly and efficiently. The values of the tolerance are given in Tables A.1 and A.3.

Example 7 An example of simplex reflection analysis of triaxial test data for *broken* rock (Granulated Carrara marble - tested by Gerogiannopoulous, 1977) is given in Tables 2.13 and 2.14, and the results are shown in Figure 2.12.

A penalty function is used during the evaluation of the sum of the square of the residuals, $\sum \epsilon^2$, for the new values of the coordinates of the *simplex* to ensure that these values are always within the range or limits of their applicability. As explained earlier, the range of applicability of s is between 0 and 1, and for m and σ_c is greater than 0, and if at any iteration, the value of any of these parameters is outside of their respective limits, the value of $\sum \epsilon^2$ is set to a high value (10^{30}). This causes the point to become the highest point in the *simplex*, and thus, is reflected such that a new value of the coordinates is obtained. The *simplex* procedure is continued from here onwards in the usual manner.

The minimization process of the Simplex technique may result in a *global* minimum or a *local* minimum for the function being minimized. In order to be certain that the *global* minimum of the residuals is achieved during the *simplex* process, a series of tests were carried out in which the value of the variables, viz. (m, σ_c) or (m, s), were shifted to a new set once the minimum was obtained, and the *simplex* procedure was reapplied with these values as the initial vertex of the *simplex*. This process was performed in an iterative

σ_3' (MPa)	σ_1' (MPa)
1.72	45.17
3.44	77.78
3.44	90.95
5.17	95.77
6.89	104.52
10.34	109.58
13.79	129.60
17.24	141.76
20.68	158.93
24.13	169.64
27.58	171.54
27.58	180.00
34.48	178.97

Table 2.13: Triaxial Test Data of broken Carrara marble (Gerogiannopoulous, 1977) for Hoek–Brown Criterion

σ_c	78.3 MPa
m	8.548
s	0.550553
σ_{cmass}	58.1 MPa
σ_{tmass}	-5.0 MPa
$\sum \epsilon^2$	1316.1

Table 2.14: Results of Simplex Reflection Analysis of Triaxial Test Data of broken Carrara marble for Hoek–Brown Criterion

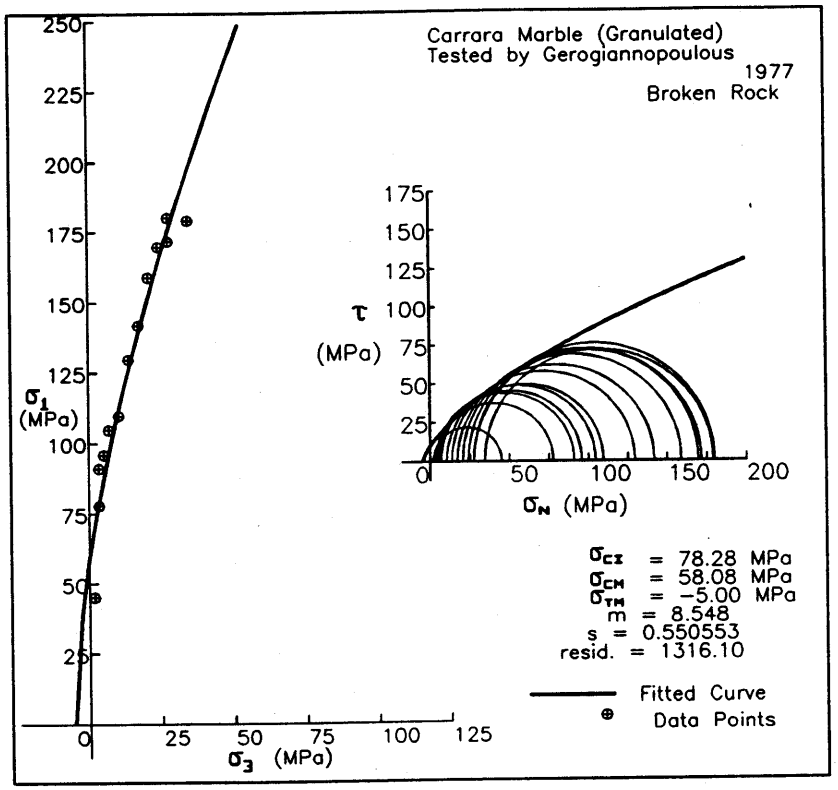

Figure 2.12: Plot of results of Simplex Reflection analysis of Triaxial test data of *broken* rock for Hoek–Brown Criterion

manner till successive values of the variables differed only by a value smaller than a specified tolerance value. During the course of analyzing a large number of data sets, it was found that the Simplex procedure invariably located the *global* minimum in the first cycle. This was confirmed by the values obtained from the successive iterations with initial points that were shifted from the first minimum point.

2.4.3 Advantages of Simplex Reflection Technique

The advantages of the Simplex Reflection technique over linear regression analysis with regards to fitting a nonlinear curve through a set of data points are as outlined below:

1. The minimization process does not require any rectification of the variables, and the function to be minimized is the sum of the square of the residuals of the original dependent variable, i.e. σ_1'. Besides this, the errors in the measurement of σ_1' and σ_3' are not combined;
2. The Simplex technique does not assume any distribution for the data. The process of searching for the minimum of the function is based on the physical interpretation of the minimization problem, and as such, any distribution or statistical relation between the variables does not have to be assumed;
3. The derivatives of the function do not have to be calculated. Therefore, a curve with any degree of complexity can be fitted to the data set;
4. The introduction of a penalty function during the *simplex* procedure for the calculation of the parameters of the Hoek-Brown criterion ensures that these parameters are always within their limits of applicability. This procedure overcomes the problem encountered in linear regression analysis in which, at times, s has a small negative value when calculated from equation (2.34). In such cases s was set to zero and m was calculated from equation (2.35) and not from equation (2.32);
5. It provides more information regarding the function at a number of locations;
6. It is a simple, iterative process and can be easily programmed on a computer.

2.5 LOWESS Technique

LOWESS is the acronym for locally weighted regression scatter plot smoothing, and it is an algorithm for smoothing a data set. This technique was first published by W.S. Cleveland (1979) at the Bell Telephone Laboratories. The computer program LOWESS was developed by Golder Associates (LOWESS, 1987) for the Basalt Waste Isolation Project in Richland, Washington, U.S.A.. This program applies the robust locally weighted regression technique to a set of data points containing large scatter to obtain a set of smoothed data points. This set of smoothed points can be linked together to show the major trend and form in the original data that was obscured by the presence of the scatter. Once the trend and form of the data are revealed, conventional regression analysis can be used to fit the data to a function that best follows the trend and form. This procedure is a powerful alternative, as well as, a companion technique, to conventional regression and smoothing techniques. The LOWESS program has been designed to assist the user in exploring the trend and form followed by a set of geomechanics data using the LOWESS algorithm. Golder Associates used this program to study the Geomechanics data in their site characterization study for a candidate high level nuclear waste repository at the Hanford Site in U.S.A.. LOWESS was used in this study to obtain a set of smoothed data points from a data set from the experimental measurement of the strength of rock mass.

2.5.1 The LOWESS Algorithm

LOWESS is a data smoothing technique and statistical procedure that can assist in identifying the trend and variability of a set of data that contains a large degree of scatter. Its primary application is to identify the trend in data which exhibits scatter. The results will also provide some indication of the magnitude of the scatter which may be useful for subsequent statistical analysis. The assumptions involved in the development of the LOWESS technique are as follows:

1. The analysis assumes that each data point is made up of two components:
   (a) one representing the smooth trend of the data as a result of the underlying physical or other processes that produced the data; and

(b) another corresponding to some noise or scatter superimposed on the underlying trend;

2. The trend and form followed by a data point is influenced by the points obtained from adjacent measurements; and

3. The source and magnitude of error will be similar in adjacent measurements.

The introduction of *scatter* in a data set can be caused by the following reasons:

1. measurement error;

2. application of inconsistent procedures in obtaining the data;

3. natural variability of samples collected; and

4. other factors not known at the time of conducting the analysis.

The difference between **Conventional** Regression Analysis and the **LOWESS** technique is that the former assumes that the data will follow some pre-determined form and attempts to fit the data within the "mould". It also involves prior assumptions regarding the trend and form of the data and the statistical distribution of the scatter. In this way it imposes a restriction on the data. However, the latter technique works on the data to explore any relationship that may exist without assigning any pre-determined form. It is functionally similar to image processing in that it allows the "true" form of the data to be reconstructed. It is used as a pre-processor for regression or other statistical analysis because of its ability to reveal the underlying trend and form of the data.

The basic operation in the LOWESS procedure is weighted local regression, e.g. linear or simple polynomial regression, performed on each point of the data set, with the result taken as the smoothed value of that point. The steps involved in the procedure are as outlined below:

1. "Local" regression analysis is conducted with a fixed proportion of the total number of data points surrounding the point of interest. The fraction of the total number of points to be used in "local" regression is calculated as:

$$f = \frac{\text{no. of points used in local regression}}{\text{total no. of points}} = \frac{m}{n} \tag{2.59}$$

$$0 \leq f \leq 1, \quad \text{usually } 0.2 \leq f \leq 0.8 \tag{2.60}$$

2. The distance, d_i, between the point to be smoothed, x_i, and the most distant of the m adjacent points in the local group, x_j, is determined as

$$d_i = | (x_i - x_j) | \tag{2.61}$$

3. Each point within the "local" region is assigned a weight for regression analysis depending on the relative distance of the point and the point currently being smoothed. The value of the weight $t_{i,k}$ (weight for point k when regressing point i) is calculated as follows:

$$\text{Let} \qquad X_{i,k} = \frac{| (x_i - x_k) |}{d_i} \tag{2.62}$$

$$\text{then} \qquad t_{i,k} = \begin{cases} \left(1 - X_{i,k}^3\right)^3 & \text{if } X_{i,k} < 1 \\ 0 & \text{if } X_{i,k} \geq 1 \end{cases} \tag{2.63}$$

Thus points outside the local group are assigned zero weights and play no part in the weighted regression for the point being smoothed. This weighting function indicates that points further away from the point that is currently being smoothed will carry a small weight to reduce their effect on the smoothed value.

4. Locally weighted regression analysis is then conducted for point i using the weights $t_{i,k}$. If $y = A + Bx$ defines the best locally fitted line at point x_i, then the function to be minimized in order to get A and B is

$$F = \sum_{k=1}^{m} t_{i,k} \left(y_k - (A + Bx_k)\right)^2 \tag{2.64}$$

and A and B are evaluated as

$$B = \frac{\sum t_{i,k} x_i y_i - \left(\sum x_i \sum t_{i,k} y_i\right) / \sum t_{i,k}}{\sum t_{i,k} x_i^2 - \left(\sum t_{i,k} x_i\right)^2 / \sum t_{i,k}} \tag{2.65}$$

$$A = \frac{\sum t_{i,k} y_i - B \sum t_{i,k} x_i}{\sum t_{i,k}} \tag{2.66}$$

From this analysis a set of smoothed value of y is obtained as y_{si} for each point corresponding to x_i. Linear regression analysis has been used here as rapid change in trend over a local area is not expected in geotechnical applications.

5. Steps 2 to 4 are repeated till all the points are covered. The LOWESS technique is then terminated if the *robust* procedure is not included.

6. **Robust** procedure: If the *scatter* follows a distribution other than *normal*, then the *robust* procedure should be used. After the smoothed values have been obtained from the initial locally weighted regression analysis, a *robust* procedure may be applied to reduce the influence of *outliers* on the regression analysis. *Outliers* are those points that do not conform to the overall trend and form depicted by the smoothed points. The reduction in the influence of the outliers is achieved by calculating the residuals r_i for each data point as

$$r_i = y_i - y_{si} \tag{2.67}$$

7. The median r_m of the absolute value of the residuals is calculated.

8. A weight is assigned to each data point according to the magnitude of its residual relative to the median value. This robust weight w_i for each point is calculated as below:

$$\text{Let} \qquad R_i = \left|\left(\frac{r_i}{6r_m}\right)\right| \tag{2.68}$$

$$\text{then} \qquad w_i = \begin{cases} \left(1 - R_i^2\right)^2 & \text{if } R_i < 1 \\ 0 & \text{if } R_i \geq 1 \end{cases} \tag{2.69}$$

9. The weighted local regression analysis is repeated for each point with the robust weight attached according to

$$G = \sum_{k=1}^{m} w_k t_{i,k} \left(y_k - (A + Bx_k)\right)^2 \tag{2.70}$$

The modified weights, $w_i t_{i,k}$, are used in place of $t_{i,k}$ in the formulation of regression parameters A and B given in equations (2.65 and 2.66) to compute new robust smoothed values, y_{si}.

10. The robust procedure is applied iteratively until convergence of the smoothed values y_{si} has been achieved in successive iterations.

2.5.1.1 Assessing Goodness of Fit

The resulting set of smoothed values is affected by the selected f value and also by the application of the *robust* procedure. There is no universally applicable method of judging the goodness of fit to the original data. However, Cleveland (1979) has suggested that firstly, the residuals should be plotted, and secondly, the residuals should be subjected to

the LOWESS procedure. If the residuals are evenly distributed around 0, and the smoothed points of residuals are reasonably close to 0, then the results should be considered acceptable. Another method is to compare successive values of residuals, but this may not always yield satisfactory results. It may be misleading at times due to the presence of a few *outliers* in the database which will exaggerate the residuals. The visual examination of residuals is better and is more reliable for judging the goodness of fit.

2.5.1.2 Selection of f values

A large value of f will result in a smoother trend, although the smoothed values may be further apart from the original values, and therefore, will increase the residuals. In order to optimize the selection of f the values of the residuals can be minimized, but experience indicates that this often results in lower values of f. The resulting trend curve may not be sufficiently smooth to be useful for any practical purpose.

2.5.1.3 Assessing the Quality of Results

1. In applications where the main purpose is to gain some general idea of the trend of the data, the use of a larger value of f will generally yield a smooth curve, from which it is easier to identify the trend.

2. In applications involving the development of a model or the establishment of some empirical correlations, the choice of f value and whether to use the *robust* procedure will depend on the data being studied. If there is a considerable degree of scatter in the data, two separate analyses, with and without the *robust* procedure, should be conducted. Any difference in result should be noted, and the data points causing the difference should be identified. The *outliers* should be reexamined to decide whether they should be discarded if they are affected by factors which are not present in other data points, or whether they should be included and the *robust* procedure should be used to reduce their influence.

3. If there is a scatter in both x and y, the LOWESS technique should be applied such that regression of x is conducted on y as well.

2.5.2 Advantages and Disadvantages of LOWESS Technique

The advantages of the LOWESS technique are that, first of all, the data points need not be equally spaced; secondly, data sets containing multiple values can be handled; thirdly, a prior assumption regarding trend and form of the data is not required; and finally, if required, the influence of *outliers* can be reduced.

The disadvantages of this technique are that it does not produce a functional form of the curve, i.e., it does not calculate any descriptive parameters that quantify a functional form. It also lacks a practical method that can be used to estimate the goodness of fit of smoothed values. The properties of errors cannot be easily estimated because the scatter does not follow the same statistical distribution from point to point. It also requires at least 10 data points for the procedure to work efficiently.

2.5.3 Application of LOWESS technique to Hoek–Brown Criterion

The experimental data for the strength of a Basalt Rock mass (Lee, 1987) was used to apply the LOWESS technique for obtaining a set of smoothed data through which the Hoek–Brown criterion could be fitted either by linear regression or Simplex reflection analysis.

Tables 2.15 and 2.16 show the LOWESS technique applied to the data set for $f = 1.0$ with and without the *robust* procedure, respectively. It can be seen that the application of the *robust* procedure does not reduce the residuals from lowessing the data and the residuals from lowessing the residuals. Thus, for this data set, the *robust* procedure does not help the smoothing process. Figure 2.13 shows the experimental and smoothed values of σ_1' for $f = 1.0$. It can be observed from this figure that the smoothed values are close to the experimental values away from the origin, however, there is a significant difference in the values close to the origin. This can be attributed to the fact that by taking $f = 1.0$, the entire data set is used in "local" regression. Therefore, a smoother curve is obtained, but the higher curvature near the origin is not adequately modelled.

Tables 2.17 and 2.18 show the LOWESS technique applied to the same data set for $f = 0.575$ with and without the *robust* procedure, respectively. It can be deduced from these tables that the application of the robust procedure does not reduce the residuals from

σ_3' (MPa)	σ_1' (MPa)	σ_{1s}' (MPa) smoothed value	$r = \sigma_1' - \sigma_{1s}'$ residuals	r_s smoothed value of r
0	61	116.0273	-55.02734	-8.228123
3.05	146.1	160.223	-14.12303	-4.686673
6.1	200.9	203.6832	-2.783188	-1.554875
9.15	257.2	246.4638	10.73621	1.249237
12.2	304.8	288.807	15.99304	3.928405
15.26	335.6	331.095	4.504974	6.644368
18.31	371.5	365.0074	6.492584	5.083011
21.36	408.2	398.0795	10.12054	2.992203
24.41	434.1	430.7829	3.317139	.7354698
27.46	460	463.0405	-3.040527	-1.706808
30.51	485.5	494.8132	-9.313232	-4.368292

$\sum \epsilon^2$ (lowessing data) = 3878.116; $\sum \epsilon^2$ (lowessing residuals) = 2606.551

Table 2.15: LOWESS analysis of Basalt data: f=1.0, with *robust* procedure

σ_3' (MPa)	σ_1' (MPa)	σ_{1s}' (MPa) smoothed value	$r = \sigma_1' - \sigma_{1s}'$ residuals	r_s smoothed value of r
0	61	91.39015	-30.39015	-6.87004
3.05	146.1	141.0671	5.032913	-2.510702
6.1	200.9	189.8338	11.06616	1.35573
9.15	257.2	237.9362	19.26386	4.961322
12.2	304.8	285.5999	19.20007	8.443401
15.26	335.6	331.3667	4.233307	10.42453
18.31	371.5	365.1644	6.335632	7.47385
21.36	408.2	398.1451	10.05493	4.18726
24.41	434.1	430.7962	3.303803	.8841667
27.46	460	463.0217	-3.021668	-2.459282
30.51	485.5	494.7727	-9.272736	-5.890823

$\sum \epsilon^2$ (lowessing data) = 2076.283; $\sum \epsilon^2$ (lowessing residuals) = 1116.327

Table 2.16: LOWESS analysis of Basalt data: f=1.0, without *robust* procedure

σ_3' (MPa)	σ_1' (MPa)	σ_{1s}' (MPa) smoothed value	$r = \sigma_1' - \sigma_{1s}'$ residuals	r_s smoothed value of r
0	61	67.75246	-6.752457	-6.307138
3.05	146.1	132.5149	13.58508	-1.913142
6.1	200.9	196.919	3.981018	2.453105
9.15	257.2	251.7101	5.48996	4.926156
12.2	304.8	295.9664	8.833618	3.631807
15.26	335.6	336.069	-.4690247	2.72812
18.31	371.5	371.1851	.3148804	1.807053
21.36	408.2	403.2106	4.98938	1.60621
24.41	434.1	432.9065	1.193481	1.491128
27.46	460	459.7679	.2321167	.3846655
30.51	485.5	486.2809	-.7809448	-.8403473

$\sum \epsilon^2$ (lowessing data) = 381.4723; $\sum \epsilon^2$ (lowessing residuals) = 294.1141

Table 2.17: LOWESS analysis of Basalt data: f=0.575, with *robust* procedure

σ_3' (MPa)	σ_1' (MPa)	σ_{1s}' (MPa) smoothed value	$r = \sigma_1' - \sigma_{1s}'$ residuals	r_s smoothed value of r
0	61	70.36516	-9.365158	-2.789931
3.05	146.1	134.3769	11.72307	1.196195
6.1	200.9	197.6711	3.228851	5.211572
9.15	257.2	251.6908	5.509247	5.577828
12.2	304.8	296.7284	8.071625	3.877696
15.26	335.6	336.3724	-.7723999	2.932028
18.31	371.5	371.3039	.196106	2.017886
21.36	408.2	403.3492	4.85083	1.674775
24.41	434.1	432.9792	1.120819	1.564142
27.46	460	459.7837	.2163391	.4053316
30.51	485.5	486.2639	-.763916	-.8628759

$\sum \epsilon^2$ (lowessing data) = 357.1171; $\sum \epsilon^2$ (lowessing residuals) = 202.9446

Table 2.18: LOWESS analysis of Basalt data: f=0.575, without *robust* procedure

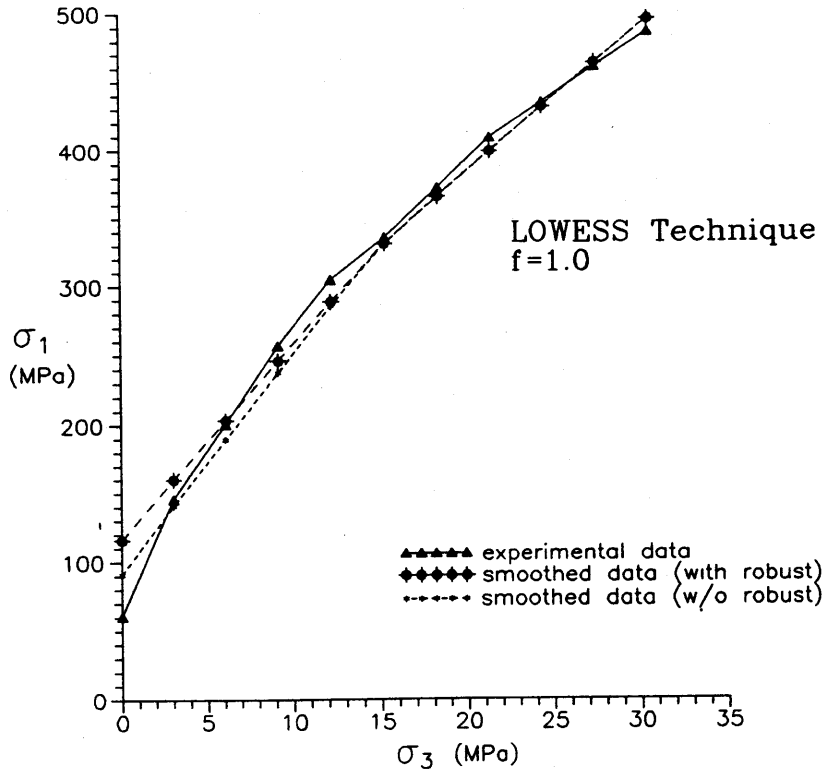

Figure 2.13: LOWESS Analysis of Basalt Rock Data with $f = 1.0$

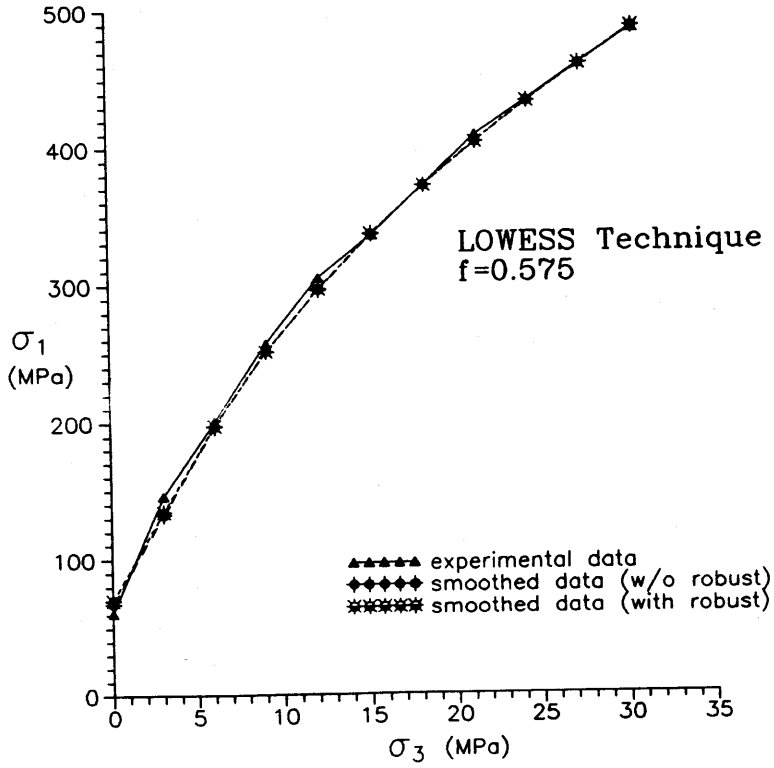

Figure 2.14: LOWESS Analysis of Basalt Rock Data with $f = 0.575$

lowessing the data and the residuals from lowessing the residuals in this case also. However, the values of the residuals have decreased considerably, especially near the origin. Figure 2.14 shows the experimental and smoothed values of σ_1' for $f = 0.575$. It can be observed from this figure that the smoothed values are closer to the experimental values all along the curve. Since $f = 0.575$ causes linear regression to be performed in the "local" region, i.e., to a fraction of the total number of data points, the higher curvature of the nonlinear envelope in the region near the origin has been captured in a better fashion. Therefore, the trend and form underlying the variation of σ_1' with respect to σ_3' has been obtained with a closer approximation.

2.6 Comparison of Results

In order to compare the three data analysis techniques described in this chapter, data for the Basalt rock mass (Lee, 1987) as shown in Table 2.15 was taken and analyzed by these methods to obtain the parameters m and s of the Hoek–Brown failure criterion.

2.6.1 Comparison of Linear Regression, Simplex Reflection and LOWESS Techniques

			Linear Regression			
			Lowess Technique		Lowess Technique	
	Linear Regression	Simplex Reflection Technique	(with Robust Method) $f = 0.575$	(with Robust Method) $f = 1.0$	(w/o Robust Method) $f = 0.575$	(w/o Robust Method) $f = 1.0$
m	22.343	21.773	22.107	22.107	22.15	21.89
s	0.00421	0.03226	0.0	0.0103	0.0	0.0
$\sum \epsilon^2$	1859.1	409.5	381.4 (L)	3878.1 (L)	357.1 (L)	2076.3 (L)
$\sum \epsilon^2$			4997.0 (LR)	7926.5 (LR)	5293.2 (LR)	9431.4 (LR)
σ_{cmass}	19.8	54.8	0.0	30.96	0.0	0.0

L = LOWESS; LR = Linear Regression; $\sigma_c = 305.1$ MPa

Table 2.19: Comparison of results for Basalt Rock Mass with Linear Regression, Simplex Reflection and Lowess Techniques

	Lowess Technique		Simplex Reflection Lowess Technique	
	(with Robust Method) $f = 0.575$	(with Robust Method) $f = 1.0$	(w/o Robust Method) $f = 0.575$	(w/o Robust Method) $f = 1.0$
m	21.42	20.31	21.399	20.76
s	0.03329	0.09796	0.03632	0.05409
$\sum \epsilon^2$	381.4(L)	3878.1 (L)	357.1 (L)	2076.3 (L)
$\sum \epsilon^2$	1107.6 (SR)	2065.8 (SR)	1062.1 (SR)	2631.5 (SR)
σ_{cmass}	55.7	95.5	58.1	70.9

L = LOWESS; SR = Simplex Reflection; $\sigma_c = 305.1$ MPa

Table 2.20: Comparison of results for Basalt Rock Mass with Simplex Reflection and Lowess Techniques

The way in which this comparison was carried out was that, first of all, the data set was analyzed by linear regression analysis and secondly by the Simplex reflection technique. Finally, the LOWESS technique was utilized to obtain smoothed values of σ_1' by taking $f = 0.575$ and $f = 1.0$, and the resulting data set was analyzed firstly by linear regression analysis and secondly by Simplex reflection analysis. The results of these analysis are shown in Tables 2.19 and Table 2.20. The first row of $\sum \epsilon^2$ indicates the values obtained from the analysis using the method for that particular column. The second row of $\sum \epsilon^2$ indicates the values obtained from the linear regression analysis of the smoothed data in Table 2.19 and from Simplex reflection analysis of the smoothed data in Table 2.20.

It is interesting to note that the value of s is an order of magnitude high for the Simplex reflection analysis as compared to that from linear regression analysis. The residuals $\sum \epsilon^2$ have also decreased by a factor of 7.7, while the value of m remains almost constant. From Table 2.19, it can be seen that the value of s is 0.0 from linear regression analysis of the Lowessed data for $f = 0.575$, with and without the *robust* procedure, and $f = 1.0$ without the *robust* procedure, and $s = 0.0103$ for $f = 1.0$ with the *robust* procedure. However, the value of the residuals obtained from linear regression analysis of the Lowessed data are very high compared to the Simplex Reflection or Linear Regression values. Although the value of the residuals from the LOWESS procedure is lower when the *robust* procedure is not used, the value of the residuals from linear regression analysis of the Lowessed data is

higher for the smoothed data set generated without the *robust* procedure.

As shown in Table 2.20, when the Simplex technique is used to analyze the smoothed data, the value of s is closer to that obtained from Simplex Reflection analysis only except when $f = 1.0$ with the *robust* procedure. Again, the value of the $\sum \epsilon^2$ is much higher than that for pure Simplex analysis only. It can be concluded from this analysis that the Simplex Reflection technique seems to be the most suitable technique for analyzing laboratory strength data. Since the number of data points available from experiments is usually less than 10, it is impractical to perform the LOWESS analysis on the data with any degree of confidence. In case a large number of data points are available, then the most suitable way to analyze them would be either to perform only Simplex Reflection analysis or to perform Simplex Reflection Analysis on the smoothed data set obtained from LOWESS analysis using $f < 1.0$ (around 0.5 to 0.6). Since the use of smoothed data from LOWESS analysis will involve a two–step process, it is more justifiable to use the Simplex Reflection Analysis only.

2.6.2 Comparison of Linear Regression and Simplex Reflection Techniques

Two data sets are considered in this section for comparing the results of linear regression analysis and the Simplex technique for obtaining the parameters of the Hoek-Brown criterion.

It has been found (Shah and Hoek, 1992) that both techniques give similar values of m, σ_c or s and $\sum \epsilon^2$ when the experimental data points corresponding to σ_1' and σ_3' follow a fairly uniform distribution. An example of this is the data set given in Table 2.21 for intact samples of Tennessee marble (Wawersik and Fairhurst, 1970). The results of the analyses of this data set are give in Table 2.22.

From Table 2.22 we can observe that the value of m, σ_c, σ_t (tensile strength), and $\sum \epsilon^2$ are similar for both types of analyses, however, the Simplex values are better since the $\sum \epsilon^2$ are lower. The triaxial strength and Mohr envelopes for this data set are shown in Figure 2.15. The χ^2 test can be used to assess the fit of the residuals to a normal distribution with zero mean, and it is given by

σ_3' (MPa)	σ_1' (MPa)
0.00	137.10
3.52	147.65
7.03	158.20
14.06	189.84
21.09	200.38
28.12	217.96
35.16	246.09
49.22	288.27

Table 2.21: Triaxial Test Data for Intact Tennesse Marble

	Linear Regression Analysis	Simplex Reflection Technique
m	5.653	5.482
σ_c	133.89 MPa	135.03 MPa
σ_t	-22.99 MPa	-23.86 MPa
$\sum \epsilon^2$	165.1	160.8
χ^2	0.808	0.761

Table 2.22: Comparison of Linear Regression and Simplex Reflection Techniques for Intact Tennesse Marble

	Linear Regression Analysis	Simplex Reflection Technique
m	22.34	21.77
s	0.004213	0.03227
σ_{cmass}	19.8 MPa	54.8 MPa
σ_{tmass}	-0.06 MPa	-0.45 MPa
$\sum \epsilon^2$	1859.0	409.5
χ^2	86.377	2.428

Table 2.23: Comparison of Linear Regression and Simplex Reflection Techniques for Basalt Rock Mass

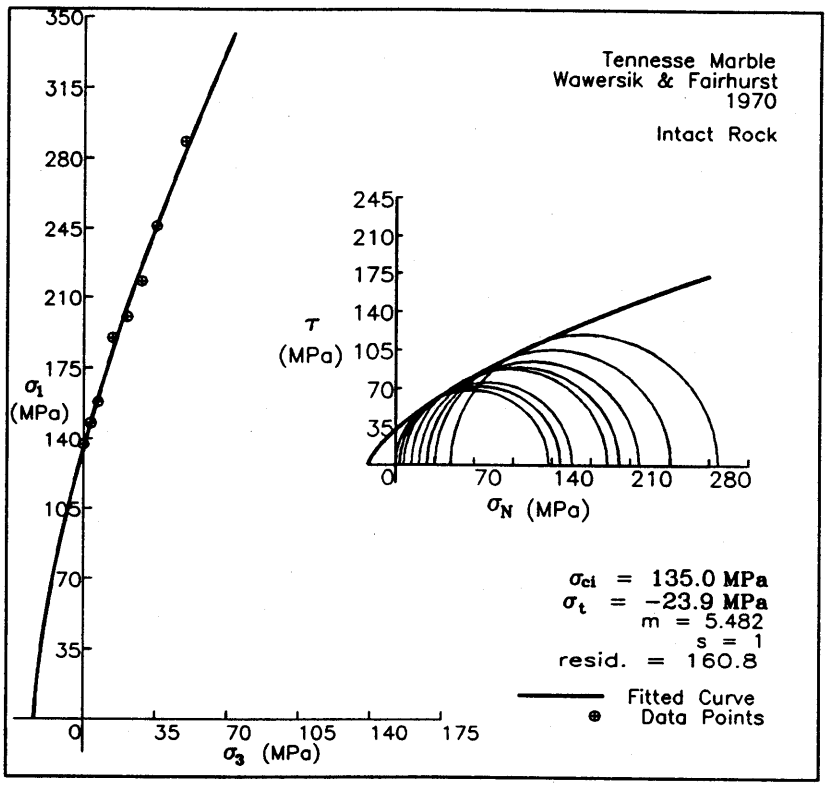

Figure 2.15: Triaxial Strength and Mohr Envelopes for Hoek–Brown failure criterion using Simplex Reflection Technique

$$\chi^2 = \sum_{j=1}^{n} \frac{(o_j - e_j)^2}{e_j} \tag{2.71}$$

where,

o_j are the observed or experimental values, and

e_j are the estimated or fitted values.

At the 95% significance level, for a degree of freedom, $\nu = n-1 = 7$, the value of $\chi^2 = 2.167$ (Crow, Davis and Maxfield, 1960, & Draper and Smith, 1981). The χ^2 values for linear regression and Simplex fitted data are 0.808 and 0.761, respectively. Since these χ^2 values are less than the $\chi^2_{0.95,\nu=7}$ value, the null hypothesis that the distribution function for the residuals follows a normal distribution cannot be rejected.

However, the difference arises when the data does not follow a uniform distribution but has some degree of bias and scatter. The goodness of fit can be ascertained from the fact that the use of the Simplex technique results in a lower value of $\sum \epsilon^2$ and χ^2. An example of this is the data set in Table 2.15 for a basalt rock mass (Ames, 1985) with $\sigma_c = 305.1$ MPa. The values obtained from linear regression and Simplex reflection techniques are summarized in Table 2.23.

It can be observed from Table 2.23 that the value of s has increased by a factor of 7.7 and the $\sum \epsilon^2$ has decreased by a factor of 4.5 for the Simplex reflection analysis. It is also significant to notice that the rock mass compressive strength σ_{cmass} and the rock mass tensile strength σ_{tmass} have increased considerably. The nature of this tightly interlocking basalt rock mass (Lee, 1987) suggests that σ_{cmass} should be higher than 19.8 MPa as obtained from linear regression and should be closer to 55 MPa which is obtained from the Simplex technique. The significantly different results for the fitted values from the two techniques was tested by using the Run test to assess if there was any serial correlation among the residuals. For the linear regression fitted values, the number of positive residuals $n_1 = 7$ and the number of negative residuals $n_2 = 4$ with a total of $R = 6$ runs, and for the Simplex fitted values, $n_1 = 4$, $n_2 = 7$ and $R = 5$. From the tables for the critical values for runs (Crow, Davis and Maxfield, 1960, & Draper and Smith, 1981), $R_{.975} = 2$ and $R_{.025} = 10$ for these values of n_1 and n_2. Therefore, a number of runs greater than 2 but less than 10 is consistent with the null hypothesis of randomness at the 5% level of significance. Since the value of R for both techniques lies within this range, it can be said that there is no serial

σ_3 (MPa)	σ_1 (MPa) experimental	σ_1 (MPa) linear regression	σ_1 (MPa) simplex technique
0.00	61.00	19.80	54.81
3.05	146.10	148.59	155.57
6.10	200.90	210.96	214.72
9.15	257.20	259.67	261.69
12.20	304.80	301.24	302.09
15.26	335.60	338.38	338.31
18.31	371.50	372.13	371.32
21.36	408.20	403.43	401.99
24.41	434.10	432.78	430.78
27.46	460.00	460.54	458.03
30.51	485.50	486.96	484.00

Table 2.24: Comparison of Linear Regression and Simplex Reflection fitted values for Basalt Rock Mass

correlation among the residuals.

If the value of χ^2 is calculated for the fitted values for this data set, the values obtained are 86.377 and 2.428, respectively, for linear regression and the Simplex technique. For $\nu = n - 1 = 10$ and at a 95% significance level, the value of $\chi^2 = 3.94$. Since the value of χ^2 for linear regression is much higher than $\chi^2_{0.95,\nu=10}$, the null hypothesis that residuals follow a normal distribution has to be rejected. However, for the Simplex technique $\chi^2 < \chi^2_{0.95,\nu=10}$, and hence, it can be concluded that the residuals for the Simplex technique follow a normal distribution. Therefore, it can be said that the fitted values obtained from the Simplex technique give a better fit to the experimental values.

The fitted values of σ_1' corresponding to the two techniques are listed in Table 2.24. From this table and from Figure 2.16, it can be observed that there is a significant difference in the curvature of the triaxial strength envelope at low values of confining pressures. The curve generated from the parameters obtained from the Simplex technique follow the experimental data more closely while that of linear regression shows large deviation near the origin of the axes and at low confining stresses. At higher values of confining pressures,

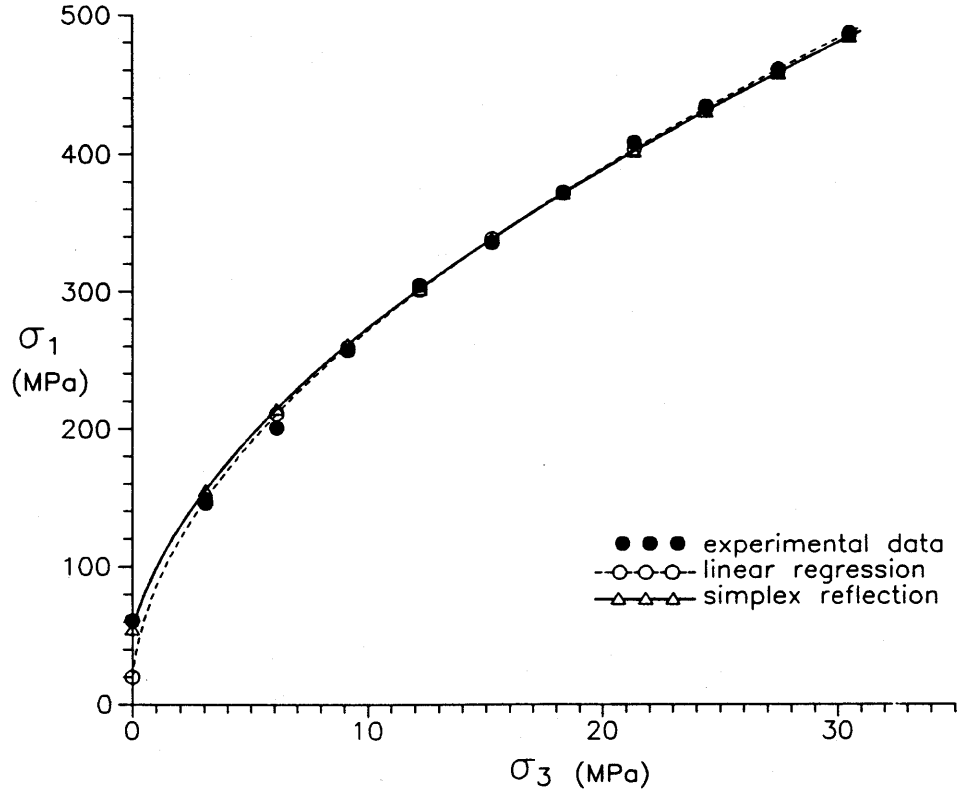

Figure 2.16: Comparison of Triaxial Strength Envelopes for Basalt Rock Mass corresponding to Hoek–Brown failure criterion using Simplex Reflection Technique and Linear Regression Analysis

the curves for the two techniques are similar. Hence, it can be concluded that the Simplex technique gives a better estimate of the Hoek-Brown parameters.

In a series of analyses carried out by Doruk (1991) of 177 data sets for triaxial tests on intact rock samples using ROCKDATA, it was found that the parameters m and σ_c of the Hoek–Brown failure criterion for well–fitted data sets were similar for linear regression and Simplex reflection techniques. In case of data sets which had some clusters or were scattered, the difference in the value of m and σ_c from the two techniques was found to be of the order of 10 to 75% with the Simplex reflection values giving better estimates with lower values of $\sum \epsilon^2$. The analyses for broken rock data also showed that the Simplex reflection technique gave better estimates of m and s. A classification scheme was developed to decide on the reliability of the results obtained from the analyses. The analyzed data sets were divided into seven classes according to their degree of fit, the total number of data points and the range of applied confining pressures. The results of the analyses of these seven classes of data sets reflected clearly the fact that for data sets which had a good range of confining pressures $\left(\left[\sigma'_{3_{max}} - \sigma'_{3_{min}}\right] \geq 0.3\sigma_c\right)$ and the number of data points were greater than five with almost even spacing, the results of the two techniques were similar. However, for data sets with scattered and clustered points or with too few points, the results of the Simplex technique were much better.

2.6.3 Application of Simplex Technique to Linear Criterion

The Simplex reflection technique was used for the analysis of linear failure envelopes such as the Mohr-Coulomb failure criterion (equation (2.1)). A number of analyses were carried out for direct shear test data. It was found that the results were identical for both linear regression analysis and the Simplex Reflection technique. The reason for this is that since this criterion is represented by a linear equation, the function to be minimized by both techniques is the sum of the square of the residuals of τ, and if the same function is being minimized, then the results must be identical. Therefore, the use of the Simplex technique for fitting linear functions to strength data is not advantageous. However, the advantage of this technique is in fitting nonlinear relations of the type of equation (2.3) for which a linearization of variables is to be done for linear regression analysis.

2.7 Conclusion and Recommendations

Statistical techniques for the analysis of laboratory strength data have been presented in this chapter. The advantages and disadvantages of Linear Regression analysis, Simplex Reflection Analysis and the LOWESS technique have been discussed with reference to their application towards the determination of the parameters of linear and nonlinear strength envelopes for soil and rock masses. It has been shown that the Simplex technique has a definite advantage over the other techniques for fitting a nonlinear strength criterion to laboratory strength data. The majority of triaxial or shear test data available do not have a uniform distribution, and hence, it is justified to use the Simplex Reflection method to analyze them. In conclusion, it can be said that although linear regression analysis may, at best, give similar estimates of the parameters of the Hoek-Brown criterion, the use of the Simplex technique will always give better estimates of the parameters of this criterion or any nonlinear criterion.

Furthermore, nonlinear regression analysis and regression techniques which take into account the error in the measurement of both variables should be studied, and their effectiveness should be assessed. However, it should be remembered that although statistics is mainly used in extracting information from the results of experiments that have already been carried out, the importance of statistics in planning experiments cannot be trivialized. With an appropriate program more information can be obtained from an experimental effort rather than if the tests are made in a haphazard manner and the use of statistics is only brought in as a posteriori. While carrying out a laboratory program for the determination of the strength of soil or rock masses, the experimental program should be designed such that in case of triaxial tests, the confining pressures σ_3' should be evenly spaced, and there should be more than one test carried out for each confining pressure. For this reason, statistics should not be viewed merely as an aid in the interpretation of experimental results but also as an integral part of the design of experiments.

Chapter 3

Failure Criteria for Rock Mass

3.1 Introduction

The stability of an underground excavation depends not only on the structural conditions in the rock mass, but also on the relationship between the stress in the rock and the strength of the rock. By defining the prevailing conditions in the rock mass in an analytically tractable way, the mechanical performance of the excavation configuration can be predicted using appropriate analytical or numerical techniques. In the last few decades, the field of geotechnical engineering has seen extraordinary developments, particularly in the application of computers for the analyses of stress distribution and stability of surface and subsurface problems. There have also been significant advances in the field of equipment and instrumentation for assessing and monitoring the behaviour of geotechnical construction. However, in order to utilize the knowledge of induced stresses around excavations, it is essential to have a criterion which will predict the strength of a rock mass and its response to the state of stress induced in it. This criterion is termed as the **failure criterion** for the rock mass.

A **failure criterion** or **strength criterion** is a relation between stress components which will permit the peak strengths developed under various stress combinations to be predicted. It defines the ultimate strength of the material under a complex, multi–axial state of stress.

The data available for the strength of rock masses indicate that the general form of the peak strength criterion should be

$$\sigma_1 = \mathcal{F}(\sigma_2, \sigma_3) \tag{3.1}$$

where,

σ_1 = major principal stress at failure;

σ_2 = intermediate principal stress at failure;

σ_3 = minor principal stress at failure.

Because the available data also suggest that the intermediate principal stress, σ_2, has less influence on peak strength than the minor principal stress, σ_3, most of the criteria used in practice are reduced to the form

$$\sigma_1 = \mathcal{F}(\sigma_3) \tag{3.2}$$

The failure criterion is also written in terms of the shear, τ, and normal stresses, σ_n, on a particular weakness plane or a shear zone in the form

$$\tau = \mathcal{F}(\sigma_n) \tag{3.3}$$

This representation of the failure criterion is most familiar to soil mechanics engineers in dealing with slope stability problems where limit equilibrium methods of analyses are used. On the other hand, the process of analyzing the stability of underground excavations involves the prediction of the response of the rock to the principal stresses acting upon each element. Consequently, a plot of triaxial test data in terms of σ_1 and σ_3, as expressed by equation (3.2), is the most useful form for the underground excavation engineer.

As discussed in Hoek (1983) and Hoek and Brown (1980), the difficulty associated with obtaining a realistic failure criterion for rock masses is emphasized in Figure 3.1 which shows the transition from intact rock material to a heavily jointed rock mass. The geotechnical engineer is concerned with all the stages in this transition. The stability of the entire system of underground openings or surface excavations, which make up a mine or an underground hydroelectric scheme, depends upon the behaviour of the entire rock mass surrounding these excavations. The combined effect of the strength of the intact rock and the behaviour of existing individual discontinuity surfaces determines the behaviour of the rock mass under the induced stresses. Depending on the number, orientation and nature of

	Description	Strength characteristics	Strength testing	Theoretical considerations
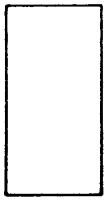	Hard intact rock	Brittle, elastic and generally isotropic	Triaxial testing of core specimens in laboratory relatively simple and inexpensive and results usually reliable	Theoretical behaviour of isotropic elastic brittle rock adequately understood for most practical applications
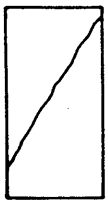	Intact rock with single inclined discontinuity	Highly anisotropic, depending on shear strength and inclination of discontinuity	Triaxial testing of core with inclined joints difficult and expensive but results reliable. Direct shear testing of joints simple and inexpensive but results require careful interpretation	Theoretical behaviour of individual joints and of schistose rock adequately understood for most practical applications
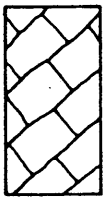	Massive rock with a few sets of discontinuities	Anisotropic, depending on number, shear strength and continuity of discontinuities	Laboratory testing very difficult because of sample disturbance and equipment size limitations	Behaviour of jointed rock poorly understood because of complex interaction of interlocking blocks
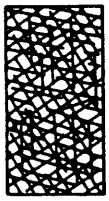	Heavily jointed rock	Reasonably isotropic. Highly dilatant at low normal stress levels with particle breakage at high normal stress	Triaxial testing of undisturbed core samples extremely difficult due to sample disturbance and preparation problems	Behaviour of heavily jointed rock very poorly understood because of interaction of interlocking angular pieces
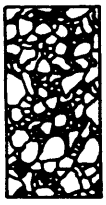	Compacted rockfill	Reasonably isotropic. Less dilatant and lower shear strength than in situ jointed rock but overall behaviour generally similar	Triaxial testing simple but expensive because of large equipment size required to accommodate representative samples	Behaviour of compacted rockfill reasonably well understood from soil mechanics studies on granular materials
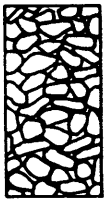	Loose waste rock	Poor compaction and grading allow particle rotation and movement resulting in mobility of waste rock dumps	Triaxial or direct shear testing relatively simple but expensive because of large equipment size required	Behaviour of waste rock adequately understood for most applications

Figure 3.1: Idealized diagram showing the transition from intact rock to a heavily jointed rock mass with increasing sample size (from Hoek, 1983)

discontinuities, the intact rock pieces will translate, rotate or crush in response to stresses imposed on the rock mass. The problem at hand will require that the engineer ascertain the properties of the intact rock material for processes of drilling and blasting or the use of tunnel boring machines, and the behaviour of existing discontinuities to stabilize the rock in the immediate vicinity of the underground openings and to assess the behaviour of the support systems. In certain situations the rock mass may be so heavily jointed that it will tend to behave like an assemblage of tightly interlocking angular particles with insignificant strength under unconfined conditions. Since there are a large number of possible combinations of block shapes and sizes, it is necessary to find behavioural trends which are common in all of these combinations.

In order to consider the behaviour of different rock mass configurations, i.e. from intact rock to heavily jointed rock mass (Figure 3.1), it must be stressed that the quantity and quality of experimental data decrease rapidly as one moves from intact rock sample to rock mass. There is a vast amount of data available in the literature for the behaviour of intact rock due to the ease of collecting and testing these specimens in the laboratory under all possible loading conditions. The degree of difficulty in testing samples with discontinuities increases exponentially as the number of discontinuities increases because of the fact that the process of collecting "undisturbed" samples of the rock mass becomes extremely difficult. The testing of these "undisturbed" samples is an even harder task. Full scale tests on heavily jointed rock masses are excessively difficult because of the experimental problems of preparing and loading the samples and are very expensive because of the scale of the operation. As a result, test data for heavily jointed rock mass is seldom available. Most of the failure criteria for heavily jointed rock mass are based on very few actual experimental tests of the rock mass, and hence, most of them are empirical in nature. In recent years, there has been a trend towards simulating the behaviour of heavily jointed rock masses by the use of synthetic materials.

This chapter deals with the assessment and development of failure criteria for rock. The first part consists of a review of the existing failure criteria for rock. The assumptions involved in the development of these criteria, their advantages and disadvantages for predicting the strength of rock mass are also discussed. The need for a new criteria is demonstrated on the basis of the requirements for predicting the strength in the brittle range of confining stresses, particularly in low confining stress values. The development of the *Mod-*

ified Hoek–Brown failure criterion and its properties, characteristics and advantages are discussed with its application for heavily jointed rock mass. Failure criteria for *intact* rock are also examined. A methodology is developed to correlate the parameters of the *Modified Hoek–Brown failure criterion* with rock mass characteristics and classification schemes, viz. RMR and Q systems.

3.2 Review of Existing Failure Criteria

A vast amount of information is available on the strength of intact rock and this information has been reviewed by Jaeger (1971). However, there is very little information available for the strength of rock mass. Although a failure criterion for a rock mass is at best only an approximate fit to the observed data, it should attempt to satisfy the following conditions as outlined in Hoek (1983):

1. The failure criterion should give good agreement with experimentally determined rock strength values;
2. The failure criterion should be expressed by mathematically simple equations based, to the maximum extent possible, upon dimensionless parameters;
3. The failure criterion should offer the possibility of extension to deal with anisotropic failure and the failure of jointed rock masses.

A brief review of the prominent failure criteria, among numerous criteria available in the literature, is given in Table 3.1 in which the development of each criteria and the constants involved are outlined. Many of these criteria provide good explanation of some aspects of rock behaviour, but fail to explain others. A brief description of each criterion is presented in this section.

3.2.1 Coulomb's Criterion

Coulomb's criterion is a classical strength criterion and is generally considered to be the most acceptable for describing the behaviour of soil, rock or other frictional materials. Coulomb (1776) postulated that the shear strengths of soil or rock comprises of two components — a

Failure Criterion	Mathematical Form	Remarks
Coulomb's criterion 1776	$\tau = c + \sigma_n \tan\phi$	shear strength comprises of cohesion and normal stress-dependent frictional component
Griffith's criterion (1921, 1925)	$\tau = 2\left(\mid \sigma_t \mid \left(\mid \sigma_t \mid + \sigma'_n\right)\right)^{1/2}$	predominantly for tensile stress fields; fracture initiates when stresses at pre-existing cracks exceed tensile strength of rock
Modified Griffith criterion McClintock & Walsh (1962)	$\tau = 2 \mid \sigma_t \mid + \sigma'_n \tan\phi'$	ϕ' is friction angle on crack surfaces; valid for $\sigma'_n > 0$; allows for frictional strength of closed cracks
Murrel's criterion 1965	$\tau^2_{oct} = 8\sigma_t\sigma_{oct}$ $J_2 = 4\sigma_t I_1$	extended 3D Griffith theory 1 empirical constant σ_t
Hobbs' criterion 1966	$\sigma_1 = B\sigma_3^b + \sigma_3$ $\tau = K_2\sigma_n^a$	empirical criterion for intact rock; 2 constants
Hoek's criterion 1968	$\sigma_1 - \sigma_3 = 2C + A\left(\sigma_1 + \sigma_3\right)^B$ $\tau_{max} = \tau_{maxO} + A\sigma_m^b$	empirical criterion for intact rock; 3 parameters (2D criterion)
Bieniawski's criterion 1974	$(\sigma_1/\sigma_c) = 1 + A\left(\sigma_3/\sigma_c\right)^k$ $(\tau_m/\sigma_c) = 0.1 + B\left(\sigma_m/\sigma_c\right)^c$ where $\tau_m = \frac{1}{2}\left(\sigma_1 - \sigma_3\right)$; $\sigma_m = \frac{1}{2}\left(\sigma_1 + \sigma_3\right)$	$k \approx 0.75$ and $c \approx 0.9$; for *intact* rocks 2 constants A and B depending on rock type; empirical criterion; valid for $\sigma_3 \geq 0$
Hoek–Brown criterion 1980	$\sigma_1 = \sigma_3 + \sqrt{m\sigma_c\sigma_3 + s\sigma_c^2}$ $\tau = A\left(\sigma_n - \sigma_t\right)^B$	for *intact* and *broken* rock; two empirical constants m and s; m and s related to *RMR* and Q
Ramamurthy's criterion 1987	$\left(\sigma_1 - \sigma_3\right)/\sigma_3 = B\left(\sigma_c/\sigma_3\right)^\alpha$	empirical 2D criterion valid for $\sigma_3 > 0$
Pan & Hudson's criterion 1988	$\frac{3}{\sigma_c}J_2 + \frac{\sqrt{3}}{2}m\sqrt{J_2} - \frac{m}{3}I_1 = s\sigma_c$	simplified Hoek-Brown criterion 3D criterion; for soft rocks
Yoshida, Morgenstern & Chan's criterion (1990)	$\sigma_1 = \sigma_3 + A\sigma_c\left(\frac{\sigma_3}{\sigma_c} - S\right)^{1/B}$	3 empirical constants; valid for *intact* and *broken* rock

Table 3.1: Review of Failure Criteria for Rock

constant cohesion and a normal stress dependent frictional component. The shear strength developed on a plane in the material can be expressed as

$$\tau = c + \sigma_n \tan \phi \tag{3.4}$$

where

c = cohesion; and

ϕ = angle of internal friction.

The values of compressive strength σ_c and tensile strength σ_t of the material are given by

$$\sigma_c = \frac{2c\cos\phi}{1 - \sin\phi} \tag{3.5}$$

$$\sigma_t = \frac{2c\cos\phi}{1 + \sin\phi} \tag{3.6}$$

The measurement of uniaxial tensile strength of rock is very difficult, and even if it is measured with great precision, its value is considerably lower than that given by equation (3.6). For this reason, a *tension cutoff* is usually applied at a selected value of uniaxial tensile stress, which corresponds to the **Rankine** criterion that is an extension of the **Coulomb** criterion.

Although the **Coulomb** criterion is very widely used, it is not a particularly satisfactory peak strength criterion for rock material for the following reasons:

1. It implies that a major shear fracture exists at peak strength. However, experimental observations by Wawersik and Fairhurst (1970) show that this is not always the case;
2. It implies a direction of shear failure which does not always agree with experimental observations;
3. Experimental peak strength envelopes are generally nonlinear as evident from data presented in Hoek (1983) for rock.

In spite of these limitations, the Coulomb criterion can provide a good representation of residual strength conditions, and especially, the shear strength of discontinuities in rock.

3.2.2 Griffith's Criterion

In one of the classic papers of engineering science, Griffith (1921) postulated that fracture of brittle materials, such as glass, is initiated when the tensile stress concentrations at the tips of minute, thin cracks or microscopic flaws in the material distributed through an otherwise isotropic, elastic material exceeds the tensile strength of the material. In rock, such flaws could be pre-existing cracks, grain boundaries or other discontinuities. Griffith's theory predicts a parabolic Mohr envelope (Hoek, 1968) and is defined by the equation

$$\tau = 2\left(|\,\sigma_t\,|\,(|\,\sigma_t\,| + \sigma_n)\right)^{1/2} \tag{3.7}$$

where,

τ = shear stress;

σ_n = effective normal stress; and

σ_t = uniaxial tensile strength of material.

Griffith's theory was originally developed for predominantly tensile stress fields. He based the determination of the conditions under which a crack would extend on his **energy instability concept** according to which

> "A crack will extend only when the total potential energy of the system of applied forces and material decreases or remains constant with an increase in crack length."

Griffith applied this theory to the extension of an elliptical crack of initial length $2c$ that is perpendicular to the direction of loading of a plate of unit thickness subjected to a uniform uniaxial tensile stress, σ. He found that the crack will extend when

$$\sigma \geq \sqrt{\frac{2E\alpha}{\pi c}} \tag{3.8}$$

where,

α = surface energy per unit area of the crack surface; and

E = Young's modulus of the uncracked material.

Griffith extended his theory to the case of applied compressive stresses. Neglecting the influence of friction on the cracks which will close under compression, and assuming that the elliptical crack will propagate from the points of maximum tensile stress concentration,

he obtained the following criterion for crack extension in plane compression:

$$(\sigma_1 - \sigma_2)^2 - 8\sigma_t(\sigma_1 + \sigma_2) = 0 \qquad \text{if } \sigma_1 + 3\sigma_2 > 0$$
$$\sigma_2 + \sigma_t = 0 \qquad \text{if } \sigma_1 + 3\sigma_2 < 0 \tag{3.9}$$

where,

σ_1 and σ_2 are major and intermediate principal stresses;

σ_t = uniaxial tensile strength of uncracked material.

This theory predicts that the uniaxial compressive stress at crack extension will always be eight times the uniaxial tensile strength.

The classic plane compression Griffith theory did not provide a very good model for the peak strength of the rock under multi–axial compression because of the fact that it did not allow for the frictional strength of closed cracks in rock subjected to compressive stresses. Quite often, σ_2 in the plane stress criterion was simply replaced by σ_3 so that the criterion could be applied to triaxial test results. However, the triaxial stress state is quite different from the plane stress condition. This theory is applicable for *intact* rocks only and it does not define the strength of *rock mass.*

3.2.3 Modified Griffith's Criterion

McClintock and Walsh (1962) proposed a modification to Griffith's theory to account for frictional forces once it was realized that when rock is subjected to compressive stress conditions, the frictional strength of closed cracks is activated. The Mohr failure envelope for the modified Griffith theory is defined by the equation

$$\tau = 2 \mid \sigma_t \mid + \sigma'_n \tan \phi' \tag{3.10}$$

where

ϕ' = angle of friction on the crack surfaces.

It should be noted that this equation is valid for $\sigma'_n > 0$.

Detailed studies on fracture initiation and propagation by Hoek & Bieniawski (1965) and Hoek (1968) showed that the original and modified Griffith theories are adequate for the prediction of fracture initiation and failure of brittle materials under conditions where the

effective normal stress acting across a pre-existing crack is tensile. This is because fracture propagation follows very quickly upon fracture initiation under tensile stress conditions, and hence, fracture initiation and failure of the specimen are practically indistinguishable. However, these theories fail to describe fracture propagation and failure of a sample subjected to compressive stresses.

In spite of the inadequacy of the original and modified Griffith theories in predicting the failure of intact specimens, Griffith's energy instability concept has formed the basis of the science of **fracture mechanics** which is being applied increasingly to the study of the fracture of rock.

3.2.4 Murrel's Criterion

In the last three decades, a number of investigators, including Murrel (1965), have performed studies to try and fit a nonlinear criterion to the observed experimental data. These investigators recognized the difficulty involved in developing a mathematical model which adequately predicts fracture propagation and failure in rock which led them to propose empirical relationships between principal stresses or between shear and normal stresses. Murrel's criterion is a three-dimensional extension of Griffith's criterion and involves one constant. It is expressed as

$$\tau_{oct}^2 = 8\sigma_t \sigma_{oct} \tag{3.11}$$

or,

$$J_2 = 4\sigma_t I_1 \tag{3.12}$$

where,

τ_{oct} = octahedral shear stress;
σ_{oct} = octahedral normal stress;
J_2 = second invariant of deviatoric stress tensor;
I_1 = first invariant of stress tensor;
σ_t = uniaxial tensile strength of material.

This criterion represents a parabolic relation between τ_{oct} and σ_{oct} or J_2 and I_1. Although it has σ_t as one of the constants, the value of uniaxial compressive and tensile strengths are *zero* as $I_1 = 0$ when $J_2 = 0$.

3.2.5 Hobbs' Criterion

Hobbs (1966) developed an empirical criterion relating the major and minor principal stresses or the shear and normal stresses at failure in the form

$$\sigma_1 = B\sigma_3^b + \sigma_3 \tag{3.13}$$

$$\tau = K_2\sigma_n^a \tag{3.14}$$

where B, b, K_2 and a are empirical constants.

This criterion was developed on the basis of fitting experimental test data for *intact* rocks. It also gives a nonlinear relation between σ_1 and σ_3 or τ and σ_n, but at $\sigma_3 = 0$, $\sigma_1 = 0$ resulting in *zero* uniaxial compressive strength. This equation is valid only for $\sigma_3 \geq 0$.

3.2.6 Hoek's Criterion

In 1968 Hoek proposed an empirical two-dimensional failure criterion for *intact* rock which involves three constants. It relates the major and minor principal stresses or the maximum shear and mean normal stresses at failure in the form:

$$\sigma_1 - \sigma_3 = 2C + A(\sigma_1 + \sigma_3)^B \tag{3.15}$$

$$\tau_{max} = \tau_{max0} + A\sigma_m^b \tag{3.16}$$

where,

$\tau_{max} = \frac{1}{2}(\sigma_1 - \sigma_3)$ = maximum shear stress;
$\sigma_m = \frac{1}{2}(\sigma_1 + \sigma_3)$ = mean normal stress;
τ_{max0} = intercept of τ_{max} *vs* σ_m plot when $\sigma_m = 0$;
A, B, C and b are material constants.

This criterion is based on Griffith's criterion for fracture initiation in brittle materials. The values of the three material constants are available only for a few types of rock.

3.2.7 Bieniawski's Criterion

The empirical criteria proposed by various investigators are in the form of a power law in recognition of the fact that peak σ_1 *vs* σ_3 and τ *vs* σ_n envelopes for rock material are generally concave downwards. In order to ensure that the parameters used in the power laws

are dimensionless, these criteria are best written in normalized form with all stress components being divided by the uniaxial compressive strength of the rock. Bieniawski (1974) proposed that the peak triaxial strengths of a range of rock types were well represented by the criterion

$$\frac{\sigma_1}{\sigma_c} = 1 + A\left(\frac{\sigma_3}{\sigma_c}\right)^k \tag{3.17}$$

or

$$\frac{\tau_m}{\sigma_c} = 0.1 + B\left(\frac{\sigma_m}{\sigma_c}\right)^c \tag{3.18}$$

where,

$\tau_m = \frac{1}{2}(\sigma_1 - \sigma_3)$;
$\sigma_m = \frac{1}{2}(\sigma_1 + \sigma_3)$;
A, B, c and k are material constants.

Bieniawski found that for the range of rock types tested $k \simeq 0.75$ and $c \simeq 0.90$. Although this criterion is a definite improvement over the criteria described previously, it can be observed from equation (3.17) that it is valid only for $\sigma_3 \geq 0$. For the rock types tested, it was found that both the material constants A and B take relatively narrow range of values.

3.2.8 Hoek–Brown Criterion

Based upon the observations of the predictions of Griffith's theory of fracture initiation in brittle materials and that of the Modified Griffith criterion for fracture initiation and propagation in materials subjected to compressive stress fields, Hoek and Brown (1980) experimented with a number of distorted parabolic curves to find one which gave good coincidence with the original Griffith theory for tensile effective normal stresses, and which fitted the observed failure conditions for brittle rocks subjected to compressive stress conditions.

Hoek and Brown had used a process of pure trial and error in deriving their empirical criterion. The triaxial strength criterion that they have adopted is the one proposed originally in 1936 by Leon for estimating the shear strength of concrete under combined tension-compression. Pramano and Kasper (1989) explain that this strength formulation combines the two-parameter Mohr-Coulomb friction law and the one-parameter tension-

cutoff condition of Rankine, similar to the Griffith criterion for brittle failure under combined tension-compression. In the case of the Leon model, the two strength parameters suffice to define the smooth transition between tension and frictional strength regimes. As described in Hoek (1983), there is no fundamental relationship between the empirical constants included in the criterion and any physical characteristics of the rock. The authors justification for choosing this particular criterion over numerous alternatives lies in the adequacy of its predictions of observed rock fracture behaviour, and the convenience of its application to a range of typical engineering problems.

Hoek and Brown's background in designing underground excavations in rock resulted in the decision to present the failure criterion in terms of the major and minor principal stresses at failure. This empirical *isotropic* failure criterion defining the relation between these stresses is conveniently expressed as

$$\sigma_1' = \sigma_3' + \sqrt{m\sigma_c\sigma_3' + s\sigma_c^2} \tag{3.19}$$

where,

σ_1' = major principal effective stress at failure;
σ_3' = minor principal effective stress at failure;
σ_c = uniaxial strength of intact rock;
m and s are empirical material strength parameters.

The influence of the intermediate principal stress is omitted similar to the Tresca and Coulomb conditions of maximum shear. The *isotropy* postulate infers that failure in tension or shear is not associated with any preferred material direction and depends only on the magnitude but not the direction of the principal stresses.

The material strength parameter m always has a finite positive value which ranges from about 0.001 for highly disturbed rock masses, to about 25 for hard intact rock. The value of the constant s ranges from 0 for jointed rock masses to 1 for intact rock material.

Equation (3.19) is applicable for designing underground excavations where the response of the individual rock elements to in situ and induced stresses is important. However, it is unsuitable to use this expression in designing rock slopes where the shear strength of a failure surface under specified normal stress conditions is required. The nonlinear Mohr failure envelope corresponding to this empirical failure criterion was derived by Dr. John

Bray of Imperial College (Hoek, 1983) and similar relationships have been developed by Ucar (1986) and Londe (1988). The equations developed by Bray are as follows:

$$\tau = \left(\cot \phi'_i - \cos \phi'_i\right) \frac{m\sigma_c}{8} \tag{3.20}$$

where,

τ = shear stress at failure;

ϕ'_i = instantaneous friction angle at the given values of τ and σ'_n, i.e., the inclination of the tangent to the Mohr failure envelope at the point (σ'_n, τ) as shown in Figure 2.2.

The value of the instantaneous friction angle ϕ'_i is given by

$$\phi'_i = \tan^{-1}\left(4h\cos^2\left(\frac{\pi}{6} + \frac{1}{3}\sin^{-1}\frac{1}{\sqrt{h^3}}\right) - 1\right)^{-\frac{1}{2}} \tag{3.21}$$

where

$$h = 1 + \frac{16\left(m\sigma'_n + s\sigma_c\right)}{3m^2\sigma_c} \tag{3.22}$$

The instantaneous cohesive strength c'_i, shown in Figure 2.2, is given by

$$c'_i = \tau - \sigma'_n \tan \phi'_i \tag{3.23}$$

From the Mohr circle construction given in Figure 2.2, the failure plane inclination β is given by

$$\beta = \frac{\pi}{4} - \frac{1}{2}\phi'_i \tag{3.24}$$

An alternative expression for the failure plane inclination, in terms of principal stresses σ'_1 and σ'_3 is given in Hoek and Brown (1980) as

$$\sin 2\beta = \frac{\tau_m}{\tau_m + m\sigma_c/8}\sqrt{1 + \frac{m\sigma_c}{4\tau_m}} \tag{3.25}$$

and,

$$\cos 2\beta = \frac{m\sigma_c/8}{(\tau_m + m\sigma_c/8)} \tag{3.26}$$

where,

$$\tau_m = \frac{1}{2}\left(\sigma'_1 - \sigma'_3\right) \tag{3.27}$$

The uniaxial compressive strength σ_{cmass} of the rock mass can be obtained by substituting $\sigma'_3 = 0$ in equation (3.19) to get

$$\sigma_{cmass} = \sqrt{s}\sigma_c \tag{3.28}$$

For intact rock, $s = 1$. Hence, $\sigma_{cmass} = \sigma_c$.

The uniaxial tensile strength σ_{tmass} of the rock mass is the value of σ_3' at which $\sigma_1' = 0$. From Figure 2.2, this is the value of σ_n' when the instantaneous friction angle $\phi_i' = \frac{\pi}{2}$. Substituting this condition in equation (3.21), the condition to be satisfied is $h = 0$. Therefore, the tensile strength of rock mass is

$$\sigma_{tmass} = -\frac{s\sigma_c}{m} \tag{3.29}$$

The process for obtaining the parameters σ_c, m and s for *intact* rock and *broken* rock mass from triaxial or shear test data using linear regression analysis or Simplex Reflection Technique have already been described in Chapter 2.

3.2.9 Ramamurthy's Criterion

Ramamurthy (1985) has proposed a failure criterion for *intact* rock and *broken* rock mass as

$$\left(\frac{\sigma_1 - \sigma_3}{\sigma_3}\right) = B\left(\frac{\sigma_c}{\sigma_3}\right)^{\alpha} \tag{3.30}$$

where,

σ_1 = major principal stress at failure;
σ_3 = minor principal stress at failure;
σ_c = uniaxial strength of intact rock; and
B and α are material parameters for *intact* rock.

He has proposed another set of parameters B_j and α_j which correspond to broken or jointed rock mass. It can be observed that this criterion is valid only for $\sigma_3 > 0$. It predicts *zero* uniaxial tensile strength for the *intact* or *broken* rock. For sandstones, the value of α was found to be 0.8 and the values of B were in a close range from 2.13 to 2.69. This criterion is based on the introduction of nonlinearity into the Mohr-Coulomb failure criterion and covers the entire range of brittle and ductile range of confining stresses, however, the problem arises in predicting the strength of the rock at low confining stresses.

3.2.10 Pan & Hudson's Criterion

In 1988, Pan & Hudson proposed a simplified three-dimensional version of the Hoek–Brown failure criterion. It is expressed as

$$\frac{3}{\sigma_c}J_2 + \frac{\sqrt{3}}{2}m\sqrt{J_2} - \frac{m}{3}I_1 = s\sigma_c \tag{3.31}$$

where,

I_1 = first invariant of stress tensor;

J_2 = second invariant of deviatoric stress tensor;

σ_c = uniaxial strength of intact rock; and

m and s are Hoek–Brown strength parameters.

This criterion has been obtained by transforming the original curved hexagonal shape of the Hoek–Brown failure surface into a paraboloid surface of circular cross-section. The cross-section along the hydrostatic axis is a 'mean' surface between the 'inner apices' and the 'outer apices' of the Hoek–Brown surface. This criterion has been found to predict the strength of weak rocks adequately, but it under-estimates the strength of strong rocks.

3.2.11 Yoshida, Morgenstern and Chan's Criterion

Yoshida (1990) and Yoshida, Morgenstern and Chan (1990) proposed a three–parameter empirical relation to estimate the strength of *intact* rock and *broken* rock mass. It is expressed as

$$\sigma_1 = \sigma_3 + A\sigma_c\left(\frac{\sigma_3}{\sigma_c} - S\right)^{1/B} \tag{3.32}$$

This criterion can be converted into a linear form by putting the value of $B = 1$ and into a nonlinear form by putting $B > 1$. Special cases of this criterion have been derived to conform to the Mohr–Coulomb criterion by substituting $B = 1$, and to the Hoek–Brown criterion by substituting $B = 2$. This criterion has been used for studying the time-dependent instability in fissured, over-consolidated clays and mudstones.

3.2.12 Hoek–Brown Failure Criterion — Reasons for Wide Acceptance

Out of the eleven prominent failure criteria that have been discussed in this section, the Hoek–Brown failure criterion has been used widely by geotechnical engineers around the world and has come to be accepted as the criterion describing the strength of rock mass in an adequate fashion. Most of these criteria have been found to be adequate by their developers for providing explanations for *specific* aspects of rock behaviour, but, in general, they fail to explain others. The Hoek–Brown failure criterion has been found to explain the behaviour of rock in a variety of engineering applications. The important characteristics of this criterion are described below which explain its popularity among geotechnical engineers.

- The empirical Hoek–Brown failure criterion, as described in section 3.2.8, contains three constants: m, s and σ_c. The constants m and s are both dimensionless and are approximately analogous to the friction angle, ϕ', and the cohesive strength, c', respectively, of the linear Mohr–Coulomb criterion. According to Hoek and Brown (1980), m and s "depend upon the properties of the rock, and upon the extent to which it has been broken before being subjected to the failure stresses". They also explain that "the manner in which fracture initiates and propagates is reflected in the value of m", which is an obvious reference to its origins from Griffith's theory. Efforts have been made in recent years to provide an explanation to the characteristics of the parameters m and s and to correlate them with the geological characteristics of the rock mass. These explanations suggest (Wood, 1991) that m is a geological parameter and is related to the properties of the material, crystalline matrix and geological history. Large values of m tend to be associated with brittle igneous and metamorphic rocks such as andesites, gneisses and granites. The larger values of m, in the range of 15-25, result in steeply inclined nonlinear Mohr envelopes and high instantaneous friction angles at low effective normal stresses. The lower values of m, in the range 3–7, give lower instantaneous friction angles and tend to be associated with more ductile carbonate rocks, e.g. limestone and dolomite. Therefore, it can be said that m has characteristic values for certain rock types. Doruk (1991) and Wood (1991) have developed a table which relates the type of rock and its grain size to the value of m for intact rocks. Table 3.2 illustrates these values of m for intact rock by the classification of the rock type. These values of m were reported by

Doruk (1991) from analyses of triaxial test data for each rock type using the Simplex Reflection technique for curve-fitting which has been incorporated into the program ROCKDATA (developed by the author in 1991).

Grain size	Sedimentary		Metamorphic		Igneous		
	Calcic	Silica	Calcic	Acidic	Acid	Basic	Basic
Coarse	Dolomite	(Conglom.)	Marble	Gneiss	Granite	Gabbro	Norite
	6.8		10.6	24.5	29.2	23.9	23.2
Medium	Limestone	Sandstone		Amphibolite		Dolerite	
	5.4	14.3		25.1		15.2	
Fine	(Micrite)	(Siltstone)		Quartzite	(Rhyolite)	Andesite	(Basalt)
				16.8		18.9	
V.Fine	(Chalk)	Mudstone		Slate	(Obsidian)		
		7.3		12.5			

Table 3.2: Hoek–Brown parameter m for *intact* rock (from Doruk, 1991 & Wood, 1991)

In the case of *broken* rock, the parameter m is sensitive to the degree of particle interlock in the rock mass and it gives a clear indication of a geological component and the dependence of m on granularity and mineralogy. It also represents the relation between m and the shear behaviour of intact rock and joints. This parameter can, therefore, be evaluated from the degree of weathering of the rock and the discontinuity surfaces.

The maximum value of the parameter s is 1, and this is applicable to intact rock specimens which have a finite tensile strength given by equation (3.29). Heavily jointed or broken rock in which the tensile strength has been reduced to zero and where the rock mass has *zero* cohesive strength when the effective normal stress is *zero* is characterized by a minimum value of s equal to *zero*. This implies that s is a geometric parameter (Wood, 1991) of the rock mass associated with the block size and can be derived from the joint volume or block volume.

The third constant, σ_c, is the uniaxial compressive strength of the intact rock material. This constant was adopted to represent the rock strength because it is "probably the

most widely quoted constant in rock mechanics, and it is likely that an estimate of this strength will be available in cases where no other rock strength data are available" (Hoek, 1983).

- Existing rock mass classification schemes such as the NGI "Q" system by Barton, Lien and Lunde (1974) and the Geomechanics "RMR" scheme proposed by Bieniawski (1983) are widely used by the rock engineering community to estimate the support requirements for underground excavations. The use of these classification schemes for the estimation of rock mass strength and deformability has, however, proved to be unsatisfactory. This is due to the fact that the factors relevant to support design are distinct from those required for the estimation of strength and deformability. Hoek and Brown (1988) have suggested that the characteristic of the rock mass which control its strength and deformation behaviour are similar to the characteristics which have been adopted in the RMR and Q systems. However, some of the parameters in these schemes are related to properties of the rock mass while others are a function of the design factors. Hence, if these classification schemes are used as tools to predict the strength characteristics, some modifications have to be made.

  The parameters of the Geomechanics classification system can be divided into general conceptual divisions, i.e., *block size, discontinuity friction* and *stress factor.* Of these three categories, both *block size* and *discontinuity friction* are closely related to the intrinsic properties of the rock mass. The *stress factor* should not be involved in the use of classification schemes for strength estimates as it is a parameter which is taken care of during stress analysis. Similarly, the parameters of the Q system can also be categorized into three divisions, i.e., *block size, block shear strength* and *active stress.* The arguments against including the *active stress* parameter in the Geomechanics classification scheme holds for this system, too.

  In order to estimate the strength of a rock mass from a classification scheme, Hoek and Brown (1988) proposed a set of relationships between the Rock Mass Rating (RMR) and the constants m and s. These relations have been derived on the basis of experience gained from the application of the table published by Hoek and Brown (1980) relating rock mass classification to material properties. Actual field applications of this table showed that the estimated rock mass strengths were reasonable when used for slope stability studies in which the rock mass is usually disturbed and loosened by

relaxation due to excavation of the slope. However, the estimated rock mass strengths generally appeared to be too low in applications involving underground excavations where the confining stresses do not permit the same degree of loosening as would occur in a slope. Following Priest and Brown (1983), the relationships were presented in the form of the following equations:

– *Disturbed rock masses:*

$$\frac{m}{m_i} = \exp\left(\frac{\text{RMR} - 100}{14}\right) \tag{3.33}$$

$$s = \exp\left(\frac{\text{RMR} - 100}{6}\right) \tag{3.34}$$

– *Undisturbed or interlocking rock masses:*

$$\frac{m}{m_i} = \exp\left(\frac{\text{RMR} - 100}{28}\right) \tag{3.35}$$

$$s = \exp\left(\frac{\text{RMR} - 100}{9}\right) \tag{3.36}$$

where,

m and s are the rock mass constants and
m_i is the value of m for the *intact* rock.

Equations 3.33 to 3.36 have been used to develop Table 3.3 (Hoek, 1988) which shows the approximate relationship between rock mass quality and the Hoek–Brown strength parameters. The values of RMR and Q have been quoted in this table as they are related by the following equation (Bieniawski, 1976):

$$\text{RMR} = 9 \log_e \text{Q} + 44 \tag{3.37}$$

- The calibre of a rock mass as an engineering medium is an inherent property which is a function of the strength of the intact rock material, the geometry and size of the blocks formed in the rock mass as a consequence of intersecting discontinuities, and the strength of these discontinuities. The behaviour of the rock mass is also dependent on the purpose for which it is being utilized, e.g., for civil engineering excavations, mining excavations, foundation engineering, hydraulic fracturing in the oil industry, etc.. These specific engineering applications introduce more variables in the determination of the strength of the rock mass. However, the above-mentioned three factors are applicable to engineering activities and, hence, constitute the generic rock mass

Disturbed rock mass m and s values					undisturbed rock mass m and s values	
EMPIRICAL FAILURE CRITERION $\sigma_1' = \sigma_3' + \sqrt{m\sigma_c\sigma_3' + s\sigma_c^2}$ σ_1' = major principal effective stress σ_3' = minor principal effective stress σ_c = uniaxial compressive strength of intact rock, and m and s are empirical constants.		CARBONATE ROCKS WITH WELL DEVELOPED CRYSTAL CLEAVAGE *dolomite, limestone and marble*	LITHIFIED ARGILLACEOUS ROCKS *mudstone, siltstone, shale and slate (normal to cleavage)*	ANENACEOUS ROCKS WITH STRONG CRYSTALS AND POORLY DEVELOPED CRYSTAL CLEAVAGE *sandstone and quartzite*	FINE GRAINED POLYMINERALLIC IGNEOUS CRYSTALLINE ROCKS *andesite, dolerite, diabase and rhyolite*	COARSE GRAINED POLYMINERALLIC IGNEOUS & METAMORPHIC CRYSTALLINE ROCKS – *amphibolite, gabbro gneiss, granite, norite, quartz-diorite*
INTACT ROCK SAMPLES						
Laboratory size specimens free	m	7.00	10.00	15.00	17.00	25.00
from discontinuities	s	1.00	1.00	1.00	1.00	1.00
CSIR rating: RMR = 100	*m*	*7.00*	*10.00*	*15.00*	*17.00*	*25.00*
NGI rating: Q = 500	*s*	*1.00*	*1.00*	*1.00*	*1.00*	*1.00*
VERY GOOD QUALITY ROCK MASS						
Tightly interlocking undisturbed rock	m	2.40	3.43	5.14	5.82	8.56
with unweathered joints at 1 to 3m.	s	0.082	0.082	0.082	0.082	0.082
CSIR rating: RMR = 85	*m*	*4.10*	*5.85*	*8.78*	*9.95*	*14.63*
NGI rating: Q = 100	*s*	*0.189*	*0.189*	*0.189*	*0.189*	*0.189*
GOOD QUALITY ROCK MASS						
Fresh to slightly weathered rock, slightly	m	0.575	0.821	1.231	1.395	2.052
disturbed with joints at 1 to 3m.	s	0.00293	0.00293	0.00293	0.00293	0.00293
CSIR rating: RMR = 65	*m*	*2.006*	*2.865*	*4.298*	*4.871*	*7.163*
NGI rating: Q = 10	*s*	*0.0205*	*0.0205*	*0.0205*	*0.0205*	*0.0205*
FAIR QUALITY ROCK MASS						
Several sets of moderately weathered	m	0.128	0.183	0.275	0.311	0.458
joints spaced at 0.3 to 1m.	s	0.00009	0.00009	0.00009	0.00009	0.00009
CSIR rating: RMR = 44	*m*	*0.947*	*1.353*	*2.030*	*2.301*	*3.383*
NGI rating: Q = 1	*s*	*0.00198*	*0.00198*	*0.00198*	*0.00198*	*0.00198*
POOR QUALITY ROCK MASS						
Numerous weathered joints at 30-500mm,	m	0.029	0.041	0.061	0.069	0.102
some gouge. Clean compacted waste rock	s	0.000003	0.000003	0.000003	0.000003	0.000003
CSIR rating: RMR = 23	*m*	*0.447*	*0.639*	*0.959*	*1.087*	*1.598*
NGI rating: Q = 0.1	*s*	*0.00019*	*0.00019*	*0.00019*	*0.00019*	*0.00019*
VERY POOR QUALITY ROCK MASS						
Numerous heavily weathered joints spaced	m	0.007	0.010	0.015	0.017	0.025
<50mm with gouge. Waste rock with fines.	s	0.0000001	0.0000001	0.0000001	0.0000001	0.0000001
CSIR rating: RMR = 3	*m*	*0.219*	*0.313*	*0.469*	*0.532*	*0.782*
NGI rating: Q = 0.01	*s*	*0.00002*	*0.00002*	*0.00002*	*0.00002*	*0.00002*

Table 3.3: Approximate relationship between rock mass quality and material constants (from Hoek, 1988)

properties. From this discussion, it is evident that in order to predict the strength of a rock mass, the parameters suggested above must be investigated and related to a classification scheme which does not associate its parameters with any specific engineering usage. The Engineering Geological Classification scheme being proposed by Wood (1991) tends to associate its parameters to these intrinsic parameters of the rock mass, and seems to be suitable for estimation of strength. Wood (1991) has developed a comprehensive classification scheme to estimate the Hoek–Brown strength parameters from the geological description of the rock mass.

The Hoek–Brown failure criterion deals only with failure of a rock mass, and it does not provide any basis for estimating its deformability. Since deformation of a rock mass is as important as its strength, Serafim and Pereira (1983) have correlated the in situ modulus of deformation (E, in GPa) with RMR according to:

$$E = 10^{\left(\frac{\text{RMR} - 10}{40}\right)} \tag{3.38}$$

This relation is useful in estimating the modulus of deformation of rock masses, particularly during the early stage of a project when relatively little field information is available.

It should be emphasized here that the values of RMR and Q used in equations 3.33 to 3.36 and 3.38 are the ones which take into account the *stress conditions*. However, as suggested earlier, in order to eliminate the affect of the engineering use of the rock mass, the values of RMR and Q should be modified as suggested by Yamamoto (1990).

- *Limitations on use of Hoek–Brown criterion:*

  The limitations in rock mass conditions under which this criterion itself is considered valid should be carefully studied. Figure 3.3 illustrates different scales of rock mass geometries relative to the size of a design excavation for which the criterion is considered valid. Scale factors associated with the size of the prototype design excavation to the host rock mass geometry or block size should be considered to ensure that the Hoek–Brown strength parameters estimated are to be used in an analysis for which truly intact or jointed rock mass conditions prevail.

  When the volume of rock being considered is small enough that it does not contain any structural discontinuities, equation (3.19) can be applied using the m and s values

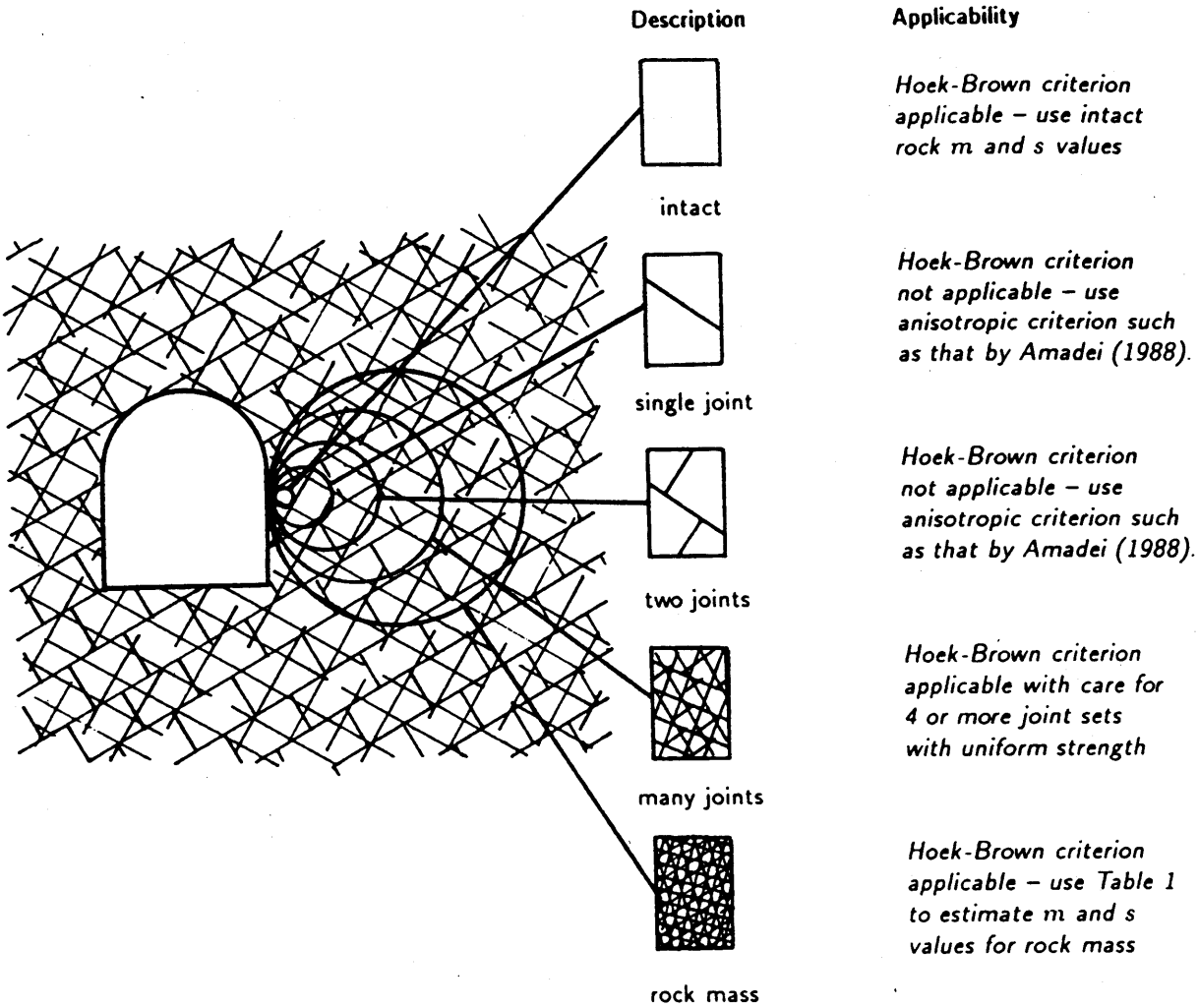

Figure 3.2: Applicability of the Hoek–Brown failure criterion to different scales of rock mass. Source: Hoek and Brown, 1988

for intact rock. This conditions will apply to small scale specimens which have been extracted for laboratory testing or to the analysis of excavations in massive rock which can be deemed to be *isotropic* and *intact* in behaviour.

When the volume of rock being considered is such that only a few structural discontinuities are contained in this volume, the Hoek–Brown criterion should not be used as the behaviour of this rock mass is likely to be highly anisotropic. The Hoek–Brown criterion, which is applicable to *isotropic* rock only, will give erroneous results.

When the volume of rock under consideration contains four or more closely spaced discontinuity sets and where none of these discontinuity sets is significantly weaker than any of the others, a requirement for the condition of *isotropy*, the Hoek–Brown criterion can be used and the m and s values can be estimated from Table 3.3.

Hoek (1983) showed that the criterion can be modified to allow for two-dimensional anisotropy. Amadei (1988) has published a detailed discussion on the strength of a regularly jointed rock mass subjected to a three-dimensional state of stress. When analyzing the stability of an excavation where the span or height of the excavation is only two or three times the spacing of the discontinuities in the rock mass, an anisotropic criterion such as that discussed by Amadei (1988) must be used. It should also be stressed that the stability of a small structurally defined wedge or block in the roof or the sidewall of an excavation will be controlled by the shear strength of the individual discontinuities, and the Hoek–Brown criterion should not be used for the analysis of this type of problem.

3.3 Need for a New Failure Criterion

The Hoek–Brown failure criterion is expressed in a simple mathematical form involving a minimal number of parameters which is suitable for practical excavation design. In various applications of this criterion in actual field problems, it has been found that the strength predicted by this criterion is adequate for the range of stresses associated with the brittle failure of rock masses at moderate confining stresses and for assessing the overall stability of an excavation. For modelling the behaviour of a rock mass, the quadratic approximation of the curvature of the strength envelope seems to be realistic and suitable because of its simplicity and relative accuracy.

However, when the Hoek-Brown failure criterion equation (3.19) was published in 1980, the philosophy behind the development of this criterion at that time attributed little significance to the behaviour of rock masses at very low or negative minor principal stress or effective normal stress values. Most analyses of underground excavation stability were concerned with overall stability and with the extent of zones of overstressed rock. In these analyses, as for most slope stability problems, all the stresses are compressive and equation (3.19) and, indeed, a number of failure criteria described in the section 3.2, work reasonably well. Hence, it is not too surprising that the Hoek–Brown criterion with its links to rock mass classification schemes for estimating m and s became popular.

Developments in recent years have forced the author to re-examine the adequacy of the Hoek–Brown failure criterion, defined by equation (3.19), in predicting the strength of jointed rock masses subjected to uniaxial compressive or tensile stress conditions and in ranges of low effective normal or confining stress values. These concerns are as described below:

- In studying the failure of rock in the immediate vicinity of underground excavation boundaries for the purpose of understanding how rock support works, it has become evident that equation (3.19) does not work very well in regions of very low or negative confining stress or effective normal stresses;
- Ross Hammett's work using NFOLD which has resulted in estimates of the strength of in situ pillars, and in general, he has found that these estimated strengths do not agree very well with the relationship $\sigma_{cmass} = \sqrt{s}\sigma_c$ given by the Hoek–Brown criterion. While one may argue that the stress distribution in a pillar is seldom equivalent to that in a uniaxially loaded specimen (see Figures 54 to 58 in *Underground Excavations in Rock*, Hoek & Brown, 1980), there is considerable justification in Hammett's criticism;
- From a practical consideration, the strength of a rock mass in uniaxial compression and tension conditions should be *zero* indicating that there is no cohesion in a rock mass. The Hoek–Brown failure criterion, however, predicts a finite value of $\sigma_{cmass} = \sqrt{s}\sigma_c$ and $\sigma_{tmass} = -s\sigma_c/m$ even for heavily jointed and broken rock mass; and
- The quadratic approximation of the Hoek–Brown failure criterion introduces simplicity into the form of the equation, but this restriction on the curvature of the failure

envelope imposes an artificial restraint on it, especially in the low range of confining or normal stresses.

The reason for the failure of equation (3.19) at low confining stresses lies in the form of the equation itself. Intuition suggests that the tensile strength of a jointed rock mass should be *zero* but forcing this condition by substituting $s = 0$ in equation (3.19) results in a curve which under-estimates the strength of the rock mass at low confining stresses. This is because the curve defined by equation (3.19) cannot be "bent" sufficiently to accommodate the rock mass behaviour in this low stress region.

Many failure criteria, some of which have been discussed in section 3.2, use complicated empirical curved surfaces which usually involve many parameters. An alternative form of equation (3.19) has been proposed by Pan and Hudson (1988), which is:

$$\frac{\sigma_1'}{\sigma_c} - \frac{\sigma_3'}{\sigma_c} = \left(m\frac{\sigma_3'}{\sigma_c} + s\right)^a \tag{3.39}$$

This equation is, in fact, a modification to the Hoek–Brown criterion to take into account a more precise curve fitting by introducing a third parameter a. The parameter a is a variable exponent and, as such, removes the constraint on the degree of curvature of the failure envelope. Pan and Hudson (1988) state that if $a = 0.65$ is chosen for Melbourne mudstone of Johnston (1986), this criterion fits the test data very well using the original parameter $m = 10$. This equation can be used for applications in which a specific curve fitting or higher precision is required.

The limitations of equation (3.39) are that, first of all, by introducing a third parameter, the degree of complexity of the equation is increased. It will be difficult to relate these three parameters to the geological characteristics of the rock mass. Secondly, the rock mass will have a finite value of unconfined compressive strength $\sigma_{cmass} = (s)^a\sigma_c$ and tensile strength which can be solved by substituting $\sigma_1' = 0$ in equation (3.39).

3.4 Modified Hoek–Brown Failure Criterion

Realizing these limitations of equation (3.39) in predicting the strength of a rock mass, the author proposes a new failure criterion which is based on the Hoek–Brown criterion (equation (3.19) and equation (3.39)) and is expressed in a non-dimensional form as

$$\frac{\sigma_1'}{\sigma_c} = \frac{\sigma_3'}{\sigma_c} + \left(m_b \frac{\sigma_3'}{\sigma_c}\right)^a \tag{3.40}$$

where,

σ_1' = effective major principal stress at failure;
σ_3' = effective minor principal stress at failure;
σ_c = uniaxial compressive strength of intact rock;
m_b and a are material strength parameters.

This equation has been called the *Modified Hoek–Brown Failure Criterion* and is illustrated in Figure 3.3. This is also an empirical failure criterion which contains two material strength parameters, viz., m_b and a, that are obtained from analyzing triaxial test data. The unconfined compressive strength of intact rock, σ_c, is required in this criterion.

3.4.1 Salient Features

The salient features of the *Modified Hoek–Brown failure criterion* are:

1. This criterion is a simple analytical relation between the major and minor principal effective stresses at failure and consists of only two parameters, m_b and a;
2. The constant power index (square root exponent) has been replaced by a variable exponent a which enhances the flexibility of the curve, and thereby, the degree of fit by removing the restraint on the curvature;
3. The rock mass strength under uniaxial conditions is equal to *zero* as dictated by intuition and practical considerations of no cohesion for broken rock. In equation (3.40), the rock mass unconfined compressive strength can be obtained by solving for σ_1' when $\sigma_3' = 0$. This results in $\sigma_1' = \sigma_{cmass} = 0$. Similarly, the unconfined tensile strength for the rock mass can be obtained by calculating σ_3' when $\sigma_1' = 0$. This evaluation gives $\sigma_3' = \sigma_{tmass} = 0$;

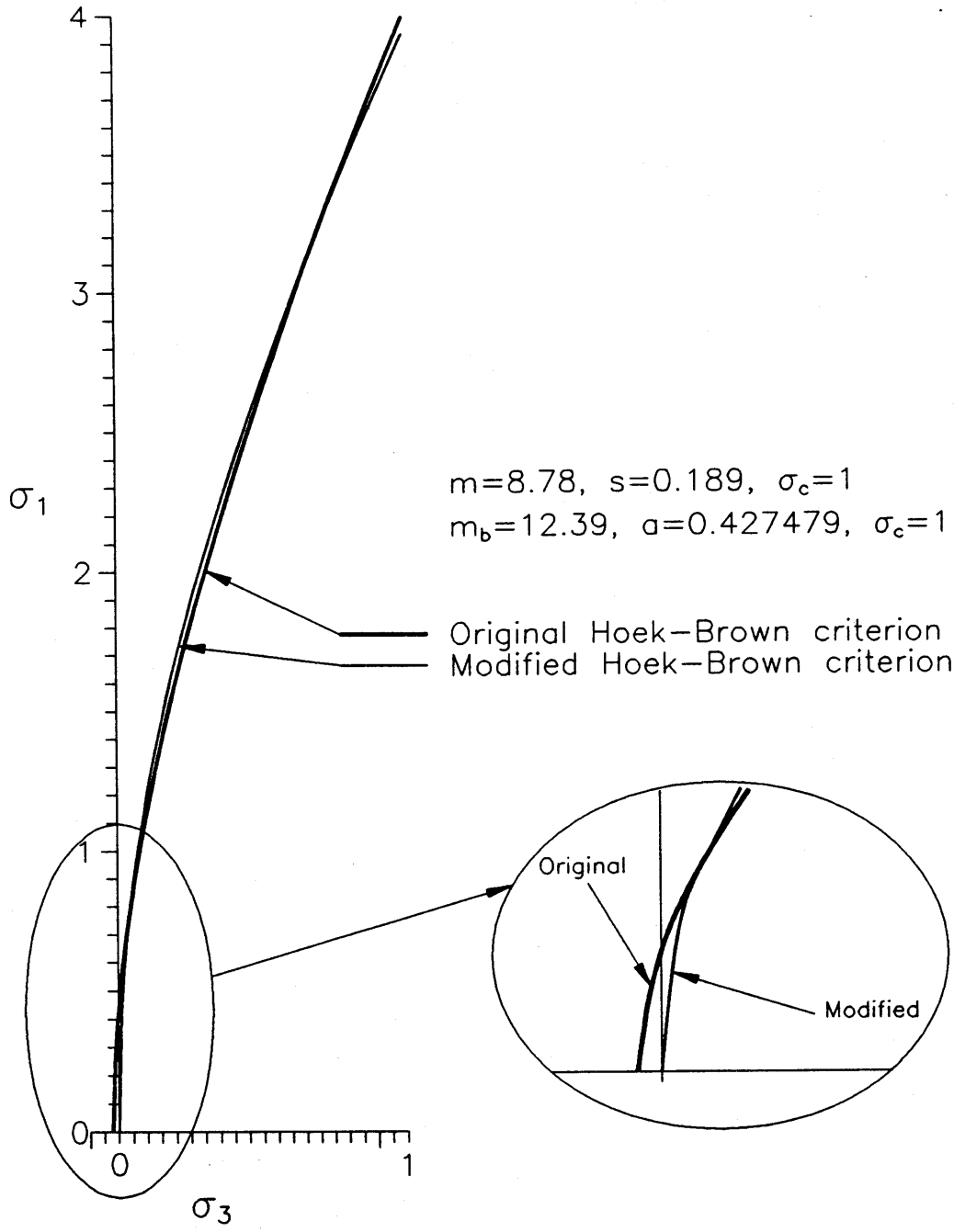

Figure 3.3: Modified and Original Hoek–Brown Failure Criterion - plot of triaxial strength envelopes

4. From Figure 3.3 it can be observed that this strength envelope is highly nonlinear in the region near the origin of the principal stress axes showing the fact that the strength of the rock mass increases very rapidly with the increase in confining pressure as compared to the strength envelope corresponding to the original Hoek-Brown failure criterion;

5. When the strength of in situ pillars are being estimated, it should be realized that the state of stress does not correspond exactly to uniaxial conditions and that there is a small amount of confinement present in the pillar. As can be seen from Figure 3.3, the strength of the rock mass increases very rapidly for small increases in the confining pressure. Therefore, the strength of the pillar is not $\sqrt{s}\sigma_c$ as obtained from equation (3.19) and not *zero* as calculated from equation (3.40), but it is equal to the value of σ_1' calculated from equation (3.40) at very small values of σ_3'. The difference in the predictions of strengths of the pillar for these small confining stresses lies in the fact that the *modified* criterion results in higher values of strength at lower confining pressures due to the increased flexibility of the envelope;

6. The *Modified Hoek–Brown strength envelope* follows the *Original Hoek–Brown strength envelope* at moderate and high confining stresses indicating that the two criteria predict similar strengths in these range of stresses.

3.4.2 Assumptions and Limits of Validity

The **assumptions and limits of validity** involved in the *Modified Hoek–Brown Failure Criterion* are similar to that of the *Original Hoek–Brown failure criterion* and are outlined below:

1. This criterion assumes *isotropic* conditions in the rock mass. The volume of rock under consideration should contain four or more discontinuity sets with all of these discontinuity sets having similar strength characteristics;

2. It is assumed that this failure criterion is valid only for effective stress conditions. Hoek (1983) suggests that the concept of effective stress will be satisfied in the case of jointed rocks since it is similar to porous rocks such as sandstones under normal

laboratory loading rates which generally satisfy effective stress conditions (Handin, Hager, Friedman & Feather, 1963);

3. The influence of the intermediate principal stress σ_2' has been neglected in deriving the failure criterion as it is assumed that the failure process is controlled by the major and minor principal stresses σ_1' and σ_3' and that σ_2' has no significant influence on this process. Mogi (1967) has pointed out that the influence of σ_2' on the strength of rock does exist, but it is relatively small. This assumption is almost certainly an over-simplification, and there is sufficient evidence (reviewed by Jaeger & Cook, 1969) to suggest that by ignoring σ_2' the strength of the rock mass is under-estimated and that the error in the estimation of strength is on the safer side;

4. A study of the failure characteristics of a variety of rock types by Mogi (1966) led him to conclude that the brittle–ductile transition for most rocks occurs at an average principal stress ratio $\sigma_1'/\sigma_3' = 3.4$. The *Modified* and the *Original* Hoek–Brown failure criterion are valid only for brittle failure of rock, and therefore, triaxial test data which are in the range $\sigma_1'/\sigma_3' > 3.4$ have only been considered in the statistical analysis for calculating the strength parameters. A rule of thumb used by Hoek (1983) is that the confining pressure must always be less than the unconfined compressive strength of the material for the behaviour to be considered brittle.

With the removal of the restriction imposed by the square-root term in the *original* Hoek–Brown criterion, the flexibility in the curvature of the strength envelope has been enhanced considerably compared to what was possible using the constants m and s only. However, the development of the *Modified Hoek–Brown failure criterion* has introduced two significant practical problems. The first is that Dr. John Bray's closed-form solution (equations 3.20–3.23) for the nonlinear Mohr shear strength envelope corresponding to the *Original Hoek–Brown failure criterion* no longer applies and it is not possible to obtain a direct solution for the more general case defined by equation (3.40). The second problem is the limited use and applicability of the least squares curve fitting process which has been used for the determination of m and s. The use of this procedure has its limitations in fitting laboratory strength data for rock mass to nonlinear relations such as equation (3.19) and (3.40) as discussed in Chapter 2. These two problems have been investigated and the techniques to overcome them are presented in subsequent sections.

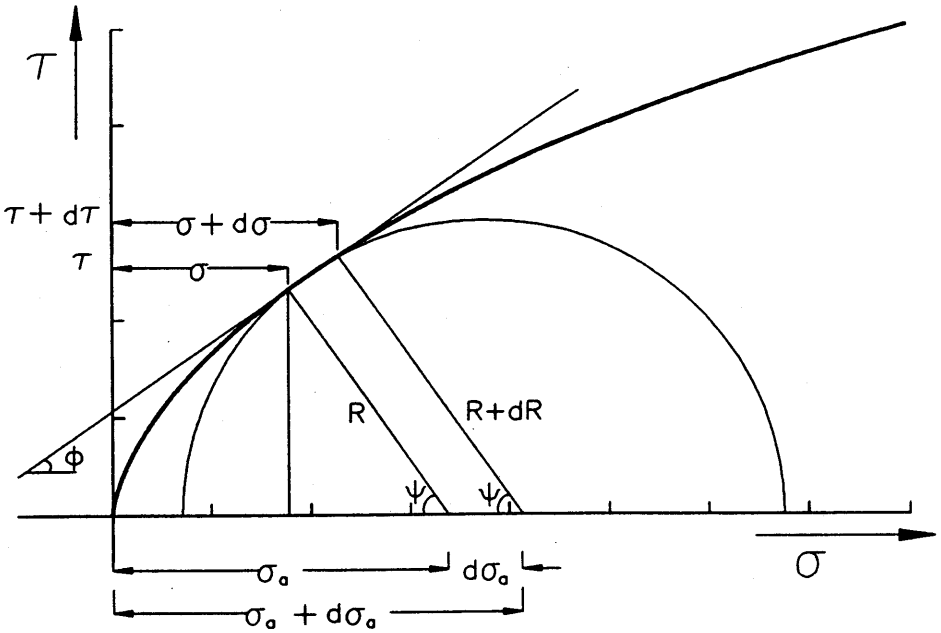

Figure 3.4: Solution for a Nonlinear Mohr Envelope

3.4.3 Mohr Envelope for Modified Hoek–Brown Failure Criterion

The first issue of obtaining a nonlinear Mohr shear strength envelope corresponding to the *Modified Hoek–Brown failure criterion* was solved on the lines of the development of the solution for the Mohr strength envelope for the *original* Hoek–Brown criterion by Dr. Bray. The difference that arose in the solution for the *modified* criterion is that a closed-form direct solution cannot be obtained as in the case of the *original* criterion. In solving for the Mohr envelope for the *original* criterion, Dr. Bray was able to use a series of analogies and mathematical tricks to obtain a direct solution due to the fact that this criterion has a square-root term and the resulting equation can be solved analytically. However, the variable exponent a in the *modified* criterion does not allow the solution of the equation analytically, and hence, a numerical technique involving the Newton–Raphson procedure was resorted to. The details of the derivation of the Mohr envelope for the *Modified Hoek–Brown criterion* are given in this section. Figure 3.4 represents the nonlinear Mohr

envelope corresponding to the *Modified Hoek–Brown failure criterion*. From this figure,

$$\sigma_a = \frac{1}{2}\left(\sigma_1' + \sigma_3'\right) \tag{3.41}$$

$$R = \frac{1}{2}\left(\sigma_1' - \sigma_3'\right) \tag{3.42}$$

$$\sigma_n' = \sigma_a - R\cos\Psi \tag{3.43}$$

$$\tau = R\sin\Psi \tag{3.44}$$

where,

R = radius of curvature of Mohr Envelope = radius of Mohr circle formed by (σ_1', σ_3') tangential to the Mohr envelope at (σ_n', τ);

ϕ_i' = instantaneous friction angle;

$\Psi = \frac{\pi}{2} - \phi_i'$;

It is assumed in this analysis that the rate of change of R, i.e. dR, in the small interval of normal stress, $d\sigma_a$, is constant. Therefore,

$$\frac{dR}{d\sigma_a} = \cos\Psi \tag{3.45}$$

Also,

$$\sigma_1' - \sigma_3' = 2R \tag{3.46}$$

$$\sigma_3' = \sigma_a - R \tag{3.47}$$

Rearranging equation (3.40),

$$\frac{\sigma_1'}{\sigma_c} - \frac{\sigma_3'}{\sigma_c} = \left(m_b\frac{\sigma_3'}{\sigma_c}\right)^a \tag{3.48}$$

or,

$$\left(\frac{\sigma_1' - \sigma_3'}{\sigma_c}\right)^{1/a} = m_b\frac{\sigma_3'}{\sigma_c} + s \tag{3.49}$$

Substituting equations (3.46) and (3.47) into (3.49),

$$m_b\left(\frac{\sigma_a - R}{\sigma_c}\right) + s = \left(\frac{2R}{\sigma_c}\right)^{1/a} \tag{3.50}$$

Differentiating σ_a with respect to R in this equation,

$$m_b\left(\frac{\partial\sigma_a}{\partial R} - 1\right) = \frac{2^{1/a}}{a}\left(\frac{R}{\sigma_c}\right)^{\frac{1-a}{a}} \tag{3.51}$$

or,

$$\frac{\partial\sigma_a}{\partial R} = 1 + \frac{2^{1/a}}{m_b a}\left(\frac{R}{\sigma_c}\right)^{\frac{1-a}{a}} \tag{3.52}$$

Therefore, from equation (3.45),

$$\cos \Psi = \frac{1}{1 + \frac{2^{1/a}}{m_b a}\left(\frac{R}{\sigma_c}\right)^{\frac{1-a}{a}}} \tag{3.53}$$

From equation (3.50),

$$\sigma_a = \frac{1}{m_b \sigma_c^{(1-a)/a}}(2R)^{1/a} + R \quad - \frac{s\sigma_c}{m} \tag{3.54}$$

Then equation (3.43) gives,

$$\sigma'_n = \frac{1}{m_b \sigma_c^{(1-a)/a}}(2R)^{1/a} + R(1 - \cos \Psi) \quad - \frac{s\sigma_c}{m} \tag{3.55}$$

Substituting the value of $\cos \Psi$ into this equation and rearranging,

$$\sigma'_n = (2R)^{1/a}\left[\frac{1}{m_b \sigma_c^{(1-a)/a}} + \frac{\frac{1}{m_b a}(1/\sigma_c)^{(1-a)/a}}{1 + \frac{2^{1/a}}{m_b a}\left(\frac{R}{\sigma_c}\right)^{\frac{1-a}{a}}}\right] \quad - \frac{s\sigma_c}{m} \tag{3.56}$$

or, $\left(\sigma_n + \frac{s\sigma_c}{m}\right)$

$$\sigma'_n\left[m_b \sigma_c^{(1-a)/a}\right]\left[1 + \frac{2^{1/a}}{m_b a}\left(\frac{R}{\sigma_c}\right)^{\frac{1-a}{a}}\right] = (2R)^{1/a}\left[1 + \frac{2^{1/a}}{m_b a}\left(\frac{R}{\sigma_c}\right)^{\frac{1-a}{a}} + \frac{1}{a}\right] \tag{3.57}$$

or,

$$2^{\frac{2}{a}} R^{\frac{2-a}{a}} + (2R)^{\frac{1}{a}} \sigma_c^{\frac{1-a}{a}} m_b [a+1] - \sigma'_n\left[m_b \sigma_c^{\frac{1-a}{a}}\right]\left[m_b a \sigma_c^{\frac{1-a}{a}} + 2^{\frac{1}{a}} R^{\frac{1-a}{a}}\right] = 0 \tag{3.58}$$

This is the nonlinear equation relating the radius of curvature R, the effective normal stress σ'_n and the material constants m_b, a and σ_c. This equation can be solved for R at a particular value of σ'_n, and then equation (3.53) can be used to calculate Ψ. Since $\Psi = \frac{\pi}{2} - \phi'_i$, the instantaneous friction angle can be evaluated. The shear stress can be computed from equation (3.44), and the following relation can be used to calculate the instantaneous value of cohesion:

$$c_i = \tau - \sigma'_n \tan \phi'_i \tag{3.59}$$

The failure plane inclination in terms of principal stresses σ'_1 and σ'_3 is given by

$$\sin 2\beta = \frac{1}{1 + a\tau_m/3}\sqrt{1 + \frac{2}{3}a\tau_m} \tag{3.60}$$

where,

$\tau_m = \frac{1}{2}(\sigma'_1 - \sigma'_3)$

The procedure described above is general in nature and can be used for the solution of the Mohr envelope for any nonlinear failure criterion relating the major and minor principal stresses by substituting the relation into equations (3.46) and (3.47).

The special cases of equation (3.58) are when $a = \frac{1}{2}$ and $a = \frac{1}{3}$. The first case is that for the *original* Hoek–Brown failure criterion with $s = 0$, and the second case is that for the a simplified version of the *modified* Hoek–Brown criterion with $a = \frac{1}{3}$ which will be discussed in a later section. For $a = \frac{1}{2}$, equation (3.58) reduces to

$$R^3 + \frac{3}{8} m\sigma_c R^2 - \frac{\sigma_c}{4} \left[m_b \sigma'_n\right] \left[R + \frac{m_b \sigma_c}{8}\right] = 0 \tag{3.61}$$

This is a cubic equation in R, and Dr. Bray has used subtle transformations to solve for R and has obtained the equations (3.20–3.23).

For $a = \frac{1}{3}$, equations (3.58) takes the form

$$R^5 + \frac{m_b \sigma_c^2}{12} R^3 - \sigma'_n m_b \sigma_c^2 \left[\frac{m_b \sigma_c^2}{192} + \frac{R^2}{8}\right] = 0 \tag{3.62}$$

Perhaps this equation can also be solved analytically, but a numerical equation solving procedure involving the Newton–Raphson technique has been used to solve this equation and the more general form of the equation represented by equation (3.58). This solution procedure is presented in the following section.

3.4.3.1 Solution procedure for Mohr Envelope

For ease of computation, the stresses should be calculated in a dimensionless form; therefore, all stresses should be normalized with σ_c. The Newton-Raphson technique is an iterative procedure and involves the computation of successive approximations of the root of the equation till consecutive values of the root differ only by a pre-assigned tolerance value. This procedure calculates the root (R) as

$$R_{i+1} = R_i - \frac{f(R_i)}{f'(R_i)} \tag{3.63}$$

where,

R_i and R_{i+1} are successive approximations of the root;
$f(R_i)$ is the value of the function evaluated at $R = R_i$; and

$f'(R_i)$ is the derivative of the function evaluated at $R = R_i$.

In the case of the Mohr envelope for the *Modified Hoek–Brown Failure Criterion*, the functions $f(R_i)$ and $f'(R_i)$ are

$$f(R_i) = 2^{\frac{2}{a}} R_i^{\frac{2-a}{a}} + (2R_i)^{\frac{1}{a}} \sigma_c^{\frac{1-a}{a}} m_b [a+1] - \sigma'_n \left[m_b \sigma_c^{\frac{1-a}{a}}\right] \left[m_b a \sigma_c^{\frac{1-a}{a}} + 2^{\frac{1}{a}} R_i^{\frac{1-a}{a}}\right] \tag{3.64}$$

$\left(\sigma_n + \frac{S\sigma_c}{m}\right)$

and,

$$f'(R_i) = 2^{\frac{2}{a}} \left(\frac{2-a}{a}\right) R_i^{\frac{2(1-a)}{a}} + 2^{\frac{1}{a}} \sigma_c^{\frac{1-a}{a}} m_b \left(\frac{a+1}{a}\right) R_i^{\frac{1-a}{a}} - 2^{\frac{1}{a}} \sigma'_n \left[m_b \sigma_c^{\frac{1-a}{a}}\right] \left(\frac{1-a}{a}\right) R_i^{\frac{1-2a}{a}} \tag{3.65}$$

In order to evaluate the values of τ, ϕ'_i and c_i for a range of normal stress, $(0 \leq \sigma'_n \leq \sigma'_{nmax})$, the steps to be followed are described below:

1. Assume $R_i = R_{i+1} = 1$. Normalize σ'_{nmax} with σ_c.
2. Start calculations with $\sigma'_n = 0$ and do until $\sigma'_n \leq \sigma'_{nmax}$ with increments given in Step 11.
3. Check: if $(R_1 < 1)$ then put $R_1 = 1$; else put $R = R_1$.
4. The number of iterations to reach convergence should be kept track of and should not be allowed to exceed the maximum allowable number of iterations (e.g. 200). Do the following calculations in this loop.
5. Calculate $f(R)$ using equation (3.64).
6. Calculate $f'(R)$ using equation (3.65).
7. Calculate new root $R_1 = R - f(R)/f'(R)$.
8. Check if the difference in the absolute values of R_1 and R is less than the tolerance limit $= 10^{-6}$, i.e. $(|(R_1 - R)| \leq 10^{-6})$. If this condition is true, break out of the loop and go to Step 10.
9. If the convergence condition in Step 8 is not satisfied, set $R = R_1$ and go to Step 4.
10. Calculate Ψ from equation (3.53), ϕ'_i from the relation $(\phi'_i = \frac{\pi}{2} - \Psi)$, τ from equation (3.44), and c_i from equation (3.59).

11. Calculate the next value of σ'_n by an increment depending on the condition listed below. Here σ'_n are normalized values of normal stress.

$$\begin{aligned} \text{for } 0.0 \leq \sigma'_n \leq 0.1 \qquad & \text{increment} = 0.0005 \\ \text{for } 0.1 < \sigma'_n \leq 0.5 \qquad & \text{increment} = 0.005 \\ \text{for } 0.5 < \sigma'_n \leq 10.0 \qquad & \text{increment} = 0.01 \\ \text{for } 10.0 < \sigma'_n \qquad & \text{increment} = 0.1 \end{aligned} \tag{3.66}$$

Go to Step 3.

These steps can be easily programmed on a computer and the Mohr envelope for various combinations of m_b, a and σ_c can be obtained.

3.4.4 Simplex Reflection Analysis for Modified Hoek–Brown Criterion

The Linear Regression Method of fitting a curve through a set of experimental data points is unsuitable for nonlinear relations such as those given by equation (3.40) or (3.19) as discussed in Chapter 2. In order to fit the triaxial test data to the *Modified Hoek–Brown failure criterion*, the Simplex Reflection technique presents a powerful alternative. This technique and its algorithm have been discussed in sections 2.4 and 2.4.1. This section will deal with the application of this technique for the calculation of the material strength parameters of the *Modified Hoek–Brown failure criterion.*

The parameters of the *Modified Hoek–Brown failure criterion* for *broken* rocks are m_b and a. Since the number of parameters are two for this case, the *simplex* formed will have three vertices, i.e., it is a triangle, with the coordinate pair (m_b, a). In order to minimize the number of iterations during the *simplex* procedure, a suitable starting point is required for the coordinates (m_b, a). For convenience, the value of m_b for the initial point is obtained by carrying out linear regression analysis on the broken rock data corresponding to the original Hoek–Brown Criterion. However, the initial value of a is kept as $\frac{1}{2}$ since this value of the exponent is the same as the square-root exponent for the *original* Hoek–Brown Criterion and hence, is a good starting point for the value of the curvature of the envelope. In order to set up the initial *simplex* triangle, two more points are required whose coordinates are obtained by providing appropriate step sizes for the values of m_b and

a as given in Table A.1 and A.3. These coordinates of the *simplex* are calculated by the operations outlined in Appendix A in such a way to obtain a stable triangle. As discussed in section 2.4.1, the function $\mathcal{S}(b)$ to be minimized is the sum of the square of the residuals of the σ_1', i.e.,

$$\mathcal{S}(b_i) = \sum \epsilon^2 = \sum_{j=1}^{n} \left(\sigma'_{1j_{experimental}} - \sigma'_{1j_{calculated}}\right)^2 = \text{minimum} \tag{3.67}$$

at each vertex of the triangle for the coordinates (m_i, a_i) to ascertain the highest b_H, next-to-highest b_N, and lowest b_L points of the triangle. The test conditions to be satisfied to obtain the minimum of the functions are:

$$\begin{aligned} (\mathcal{S}(b_H) - \mathcal{S}(b_L))/\mathcal{S}(b_H) &\leq \text{tolerance for residuals} \\ (m_{b_H} - m_{b_L})/m_{b_H} &\leq \text{tolerance for } m_b \\ (a_H - a_L)/a_H &\leq \text{tolerance for } a \end{aligned} \tag{3.68}$$

The values of the tolerance for m_b, a and $\sum \epsilon^2$ are given in Tables A.1 and A.3.

3.4.5 Comparison of Modified and Original Hoek–Brown Criteria

In order to ascertain the suitability of the *Modified Hoek–Brown failure criterion* for estimating the strength of rock mass, a number of triaxial test data for broken rock were fitted to this criterion using the Simplex Reflection technique, discussed in the previous section, and their goodness of fit were compared to that of the *original* Hoek–Brown Criterion. As stated earlier, one of the major problems in attempting to derive a failure criterion for jointed rock masses is that there is a dearth of reliable experimental data available for these materials. Due to the immense cost of carrying out tests on *undisturbed* samples of broken rock, various researchers have resorted to simulation of broken rock in the laboratory by creating "broken" rock from intact rock material or by using synthetic materials in the form of blocks. Out of the very few available data sets for triaxial tests on broken rock the best ones are those reported by Gerogiannopoulous (1979) on "granulated" marble and the tests by Jaeger (1969) on Panguna andesites. These data sets have been analyzed and their results are discussed in this section.

3.4.5.1 Gerogiannopoulous' Tests on Carrara Marble

Gerogiannopoulous (1979) had carried out tests on *intact* samples of Carrara marble and on "granulated" Carrara marble created by a technique originally used by Rosengren and Jaeger (1968). The process of creating the "granulated" marble involved the heating of the specimen in air to about 600°C due to which the anisotropy of thermal expansion of calcite caused almost complete separation at grain boundaries. The resulting material retained its shape and consisted of a mass of crystals in contact, with a porosity of about 4% and very small direct tensile strength. It was regarded as a laboratory model of randomly jointed, tightly interlocking rock mass.

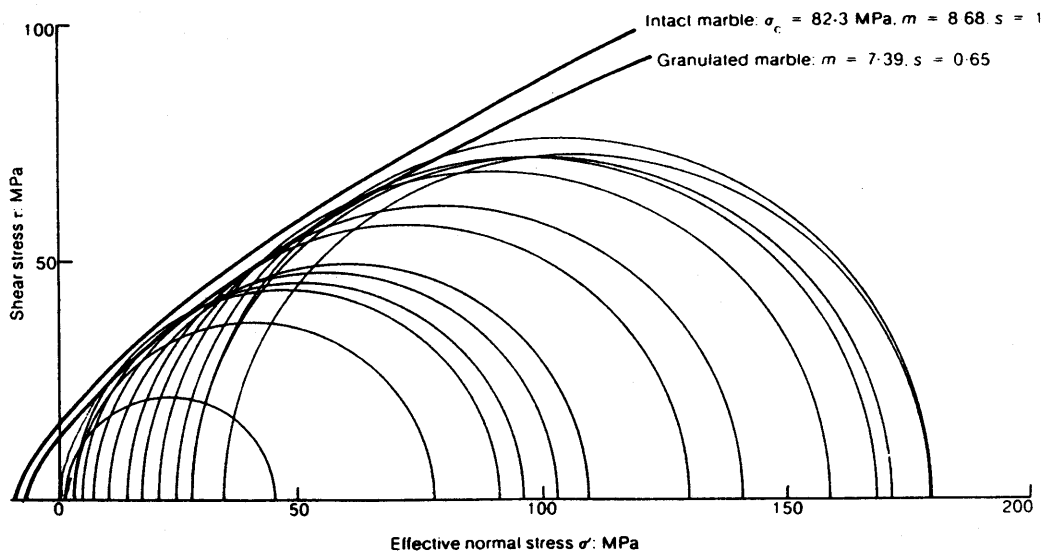

Figure 3.5: Mohr Envelopes comparing strength of *intact* and *granulated* Carrara marble (Gerogiannopoulous, 1979) for *Original* Hoek–Brown criterion

The triaxial test data for the *intact* and "granulated" samples of the Carrara marble tested by Gerogiannopoulous are given in Tables 2.11 and 2.13, respectively. The results of the analysis of the "granulated" specimens for the *original* and *modified* Hoek–Brown criteria are presented in Table 3.4. Gerogiannopoulous' results for "granulated" Carrara marble are reproduced as Mohr circles in Figure 3.5 which includes envelopes defined by the *original* Hoek–Brown criterion, fitted using Linear regression analysis.

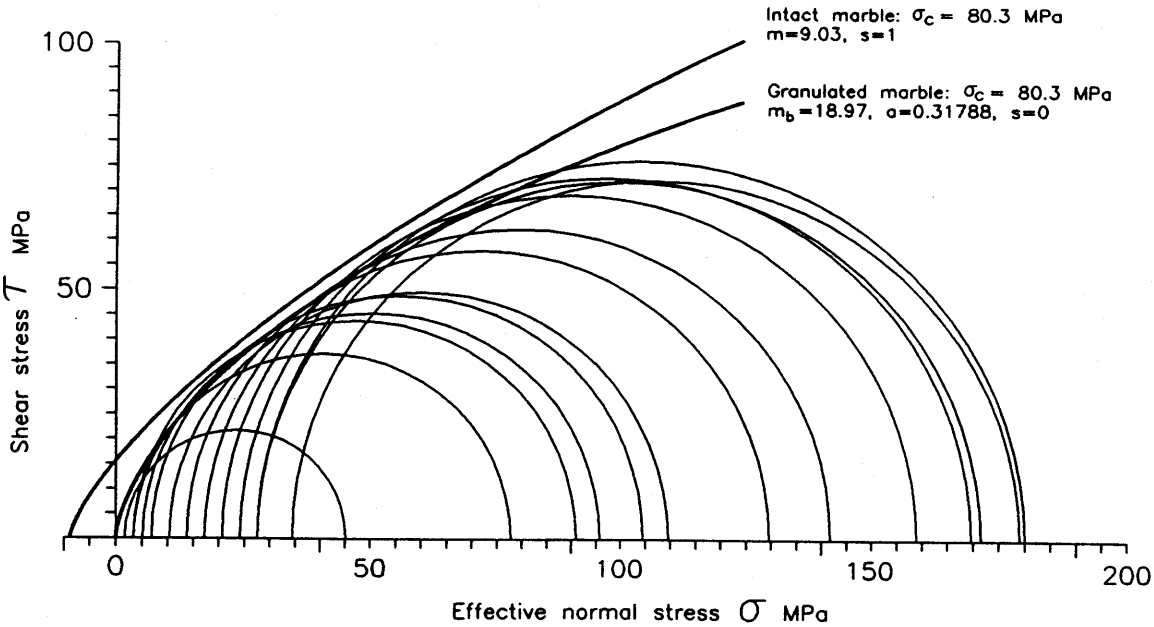

Figure 3.6: Mohr Envelopes defining strength of *intact* and *granulated* Carrara marble (Gerogiannopoulous, 1979) for *modified* Hoek–Brown criterion

In Figure 3.5, the poor fit of the Mohr envelope to the experimental data at very low effective normal stress values is evident as is the fact that the Mohr envelope predicts a significant tensile strength for this broken material. This is an unjustified extrapolation of the failure envelope in the tensile region of effective normal stress. Once the effective normal stress exceeds about 5 MPa, the curve fit is acceptable and it is unlikely that serious errors would arise from the application of this curve for $\sigma'_n > 5$ MPa.

Original Hoek–Brown criterion		Modified Hoek–Brown criterion	
σ_c	80.3 MPa	σ_c	80.3 MPa
m	8.55	m_b	18.97
s	0.551	a	0.31788
$\sum \epsilon^2$	1316	$\sum \epsilon^2$	784

Table 3.4: Comparison between results of *Original* and *Modified* Hoek–Brown criteria for *granulated* Carrara marble tested by Gerogiannopoulous (1979)

Figure 3.6 gives the results for *intact* rock corresponding to the *original* Hoek–Brown criterion and for the "granulated" marble corresponding to the *modified* Hoek–Brown criterion using the Simplex Reflection technique for fitting the data. The Mohr envelope for this criterion was plotted using the procedure described in section 3.4.1. In the case of the "granulated" marble, it is clear from Figure 3.6 that the values of $m_b = 18.97$ and $a = 0.31788$ result in a very good fit to the experimental data. This is also evident from Table 3.4 since the value of the sum of the squares of the residuals of σ_1' is 784 for the *modified* criterion as compared to 1316 for the *original* criterion. The Mohr envelope shows a highly nonlinear nature at very low effective normal stresses with very high values of instantaneous friction angle ϕ_i' indicating a rapid increase in strength. The fit of the Mohr envelope of the *modified* criterion is especially good in the range of low effective normal stresses, i.e., $\sigma_n' <= 5$ MPa, where the *original* criterion gave misleading results, and the fact that it gives *zero* tensile strength suggests that it is suitable for practical applications where the prediction of the strength of the rock mass at low confining or normal stresses is of prime importance. It is interesting to note that the envelope for the *modified* criterion is similar to that for the *original* criterion for $\sigma_n' > 5$ MPa. This suggests that the *Modified Hoek–Brown failure criterion* is similar to the *Original Hoek–Brown failure criterion* in estimating the strength of the rock mass in the range of medium and high effective normal stresses, corresponding to brittle fracture, and is a definite improvement in the low range of effective normal stresses.

3.4.5.2 Gerogiannopoulous' Tests on Wombeyan Marble

Gerogiannopoulous (1979) had also carried out triaxial tests on *intact* and "granulated" samples of Wombeyan Marble. The "granulated" samples of the marble were created as described in the previous section to simulate a tightly interlocking rock mass. The triaxial test data for the *intact* and "granulated" samples of the marble are listed in Table 3.5 and the results of the analysis of the "granulated" marble for the *original* and *modified* Hoek–Brown criterion are compared in Table 3.6.

For the *intact* marble, $\sigma_c = 84.1$ MPa and $m = 4.44$ corresponding to the *Original Hoek–Brown failure criterion.* Figure 3.7 shows the triaxial and Mohr strength envelopes

Intact Marble		Granulated Marble	
σ_3 (MPa)	σ_1 (MPa)	σ_3 (MPa)	σ_1 (MPa)
3.44	87.88	1.72	53.14
3.44	89.82	3.44	53.93
5.17	101.75	3.44	61.57
5.17	104.05	5.17	82.52
6.89	105.48	5.17	84.97
6.89	110.06	6.89	86.32
10.34	113.31	6.89	90.20
10.34	114.07	10.34	101.37
13.79	130.49	10.34	106.17
17.24	136.80	13.79	117.00
17.24	139.23	13.79	126.11
20.68	154.31	17.24	139.57
27.58	168.68	20.68	137.88
31.03	166.17	20.68	142.10
34.48	171.69	27.58	153.64
34.48	172.99	34.48	164.34

Table 3.5: Triaxial test data for *intact* and *granulated* Wombeyan Marble tested by Gerogiannopoulous (1979)

Original Hoek–Brown criterion		Modified Hoek–Brown criterion	
σ_c	84.1 MPa	σ_c	84.1 MPa
m	6.63	m_b	11.15
s	0.33164	a	0.33513
$\sum \epsilon^2$	1124.5	$\sum \epsilon^2$	654.6

Table 3.6: Comparison between results of *Original* and *Modified* Hoek–Brown criteria for "granulated" Carrara marble tested by Gerogiannopoulous (1979)

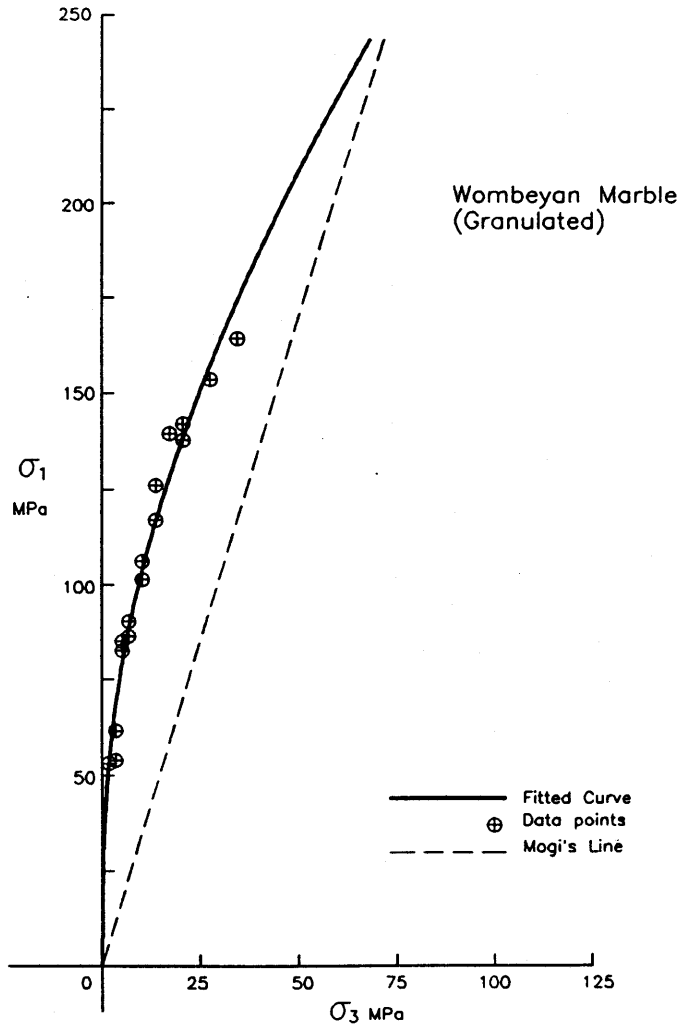

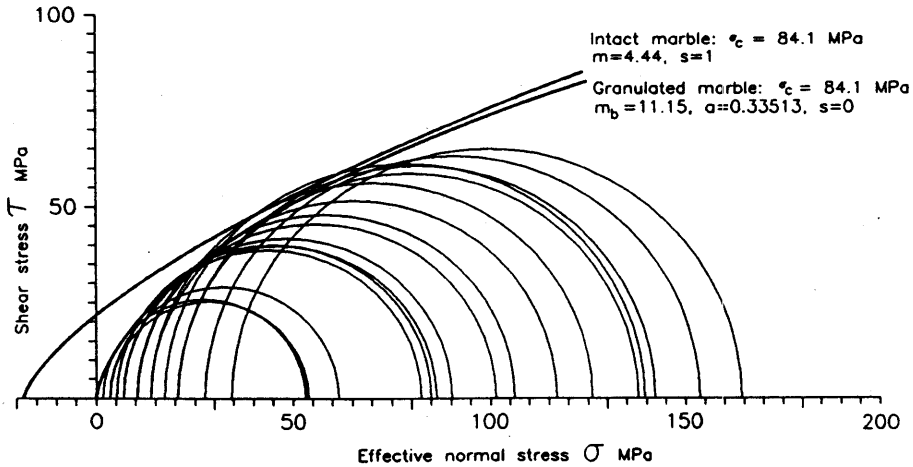

Figure 3.7: Triaxial and Mohr envelopes for "granulated" Wombeyan Marble for Modified Hoek–Brown failure criterion

for the "granulated" marble corresponding to the *Modified Hoek–Brown failure criterion*, and Figure 3.8 compares the Mohr envelopes for the *original* and *modified* criteria.

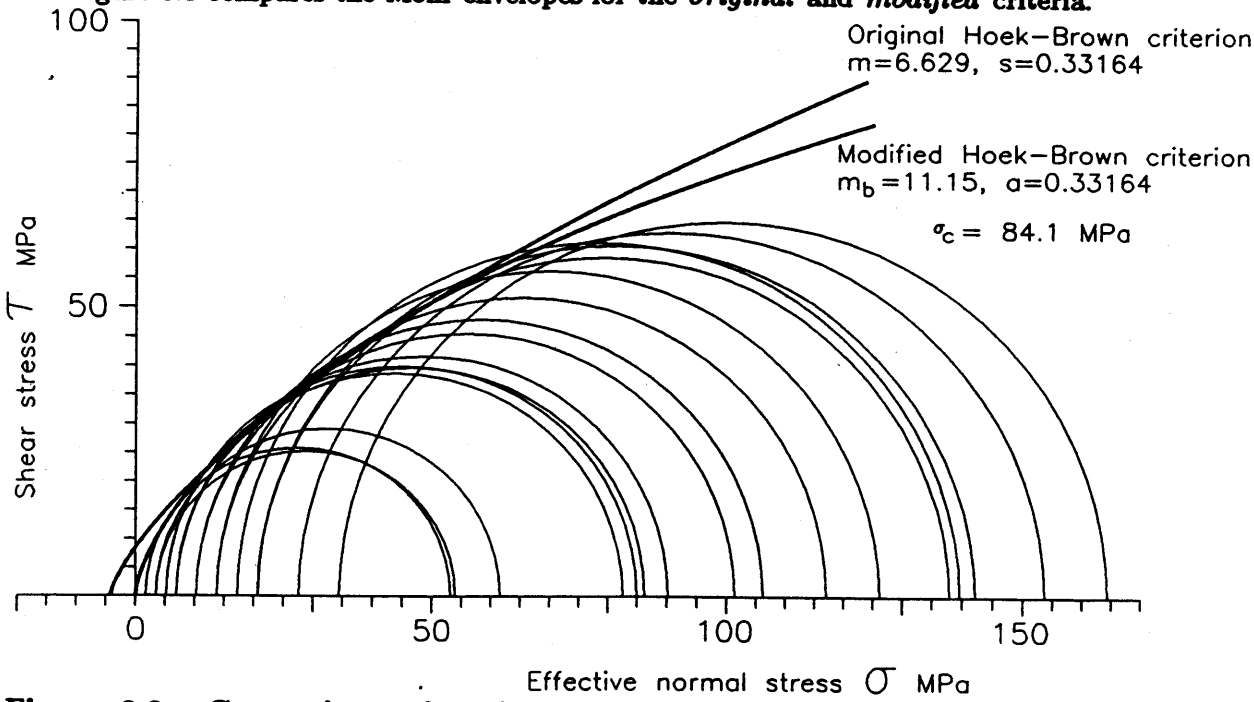

Figure 3.8: Comparison of Mohr envelopes for the *original* and *modified* Hoek–Brown failure criterion for "granulated" Wombeyan Marble

From Table 3.6 it can be observed that the *modified* criterion gives a better fit to the triaxial test data which is reflected in the fact that the sum of the square of the residuals of σ_1' for the *modified* criterion is 654.6 and that for the *original* criterion is 1124.5, a reduction of approximately 42%. This can also be seen in Figure 3.8 where the fit of the *modified* criterion in the range of low effective normal stress values is very good. It does not predict any tensile strength for the "granulated" rock whereas the *original* criterion extrapolates the curve in the tensile region where there are no data points available and predicts a significant tensile strength. Figure 3.7 also shows that the triaxial strength envelope of the *modified* criterion gives a better fit to the experimental triaxial data.

3.4.5.3 Jaegers' Tests on Panguna Andesite

Until now, the "undisturbed" samples of jointed Panguna Andesite, from Bougainville in Papua, New Guinea, tested by Jaeger (1969) have been accepted as the most reliable data sets on heavily jointed rock mass. Hoek and Brown (1983, 1988) have based the table relating rock mass quality and their empirical strength constants m and s on the analysis of the data from these tests.

Jaeger (1969) explains that in an attempt to study the properties of closely jointed rock, a triaxial pot to take specimens 6 in. diameter by 12 in. long was constructed and a number of cores of Panguna andesite were carefully drilled. This material is divided up by a network of open joints and of veins with a rather weak filling, the spacing of these being so close that a cross-section of the core would usually contain 50 to 100 individual areas separated by planes of weakness. The handling of this broken rock for testing presented a great deal of difficulty. After drilling, it was transferred from a split core barrel to a split aluminium tube and shipped in this to the laboratory. The core was next surrounded with a copper jacket 0.004 in. thick by removing the halves of the aluminium tube successively. This jacket was tack-soldered at a few points. The core, surrounded by the copper jacket and the split tubes, was then cut to length by a diamond saw. Copper end plates $\frac{1}{16}$ in. thick were tack-soldered to the jacket. The result was that a cylinder of rock which would otherwise have fallen to pieces on handling was lightly encased in a copper sheath outside which a conventional rubber jacket was used to exclude oil. This process of extraction and preparation of samples of rock mass was a landmark in rock mechanics and it highlights the degree of difficulty, care and expense involved in carrying out triaxial tests on rock mass. A summary of the important details of these tests (Hoek and Brown, 1980) is listed below and the results from the analyses of the data using the *original* and *modified* Hoek– Brown criterion are compared:

Intact Panguna andesite – The results for the tests carried out by Jaeger in 1968 on 1 in. diameter core samples and those on 2 in. diameter cores carried out by Golder Associates in 1978 were combined and analyzed by means of the Simplex Reflection Technique. The analysis gave $\sigma_c = 265.4$ MPa, $m = 18.9$, $s = 1$ for the *Original Hoek–Brown failure criterion.*

Undisturbed core samples – These samples were prepared as described earlier and were

tested triaxially by Jaeger in Canberra. The values of the strength parameters for the *original* criterion were obtained for $\sigma_c = 265.4$ MPa using Simplex Reflection method: $m = 0.282$, $s = 0.0002$ with $\sum \epsilon^2 = 1.397$. For the *modified* criterion for $\sigma_c = 265.4$ MPa, $m_b = 0.1029$, $a = 0.4215$ and $\sum \epsilon^2 = 0.6104$.

Recompacted graded samples – Samples were obtained from bench faces in the mine and typical grading curves were established for these samples. These grading curves were scaled down, as suggested by Marsal (1973), and the samples were compacted to as near the in situ density as possible before testing in a 6 in. diameter triaxial cell in the mine laboratory. For the *original* criterion, $m = 0.116$, $s = 0$ with $\sum \epsilon^2 = 13.85$. The analysis with the *modified* criterion gave: $m_b = 0.664$, $a = 0.648$ and $\sum \epsilon^2 = 6.1$.

Fresh to slightly weathered Panguna andesite – Substantial quantities of this material were shipped to Cooma in Australia where samples were tested in a $22\frac{1}{2}$ in. diameter triaxial cell by the Snowy Mountains Engineering Corporation. These samples were compacted to densities between 1.94 and 2.07 tonnes/m^3 (intact rock $\gamma = 2.55$ tonnes/m^3) before testing. Analysis of this data set gave: $m = 0.041$, $s = 0$ with $\sum \epsilon^2 = 0.3583$. Modified Hoek–Brown criterion parameters were obtained as: $m_b = 0.394$, $a = 0.655$ and $\sum \epsilon^2 = 0.1315$.

Moderately weathered Panguna andesite – Tested by Snowy Mountains Engineering Corporation in their $22\frac{1}{2}$ in. diameter triaxial cell after compaction to 1.97 tonnes/m^3, these samples gave $m = 0.03$ and $s = 0$ for $\sum \epsilon^2 = 0.2206$ for the *original* criterion. For the *modified* criterion, $m_b = 0.94$, $a = 0.768$ and $\sum \epsilon^2 = 0.006$.

Highly weathered Panguna andesite – Tested by Snowy Mountains Engineering Corporation in a 6 in. diameter triaxial cell after compaction to 1.97 tonnes/m^3, this material gave $m = 0.012$ and $s = 0$ with $\sum \epsilon^2 = 0.04384$ for the *original* criterion, and for the *modified* criterion, the parameters were $m_b = 0.638$, $a = 0.781$ and $\sum \epsilon^2 = 0.000842$.

The Mohr failure envelopes for the *intact* and *undisturbed jointed* Panguna andesite are shown in Figure 3.9. It can be observed from this figure that the drop in strength from the intact rock to the jointed rock mass is sharp. The reason for this decrease in strength can be explained by the undeveloped interlocking process of the broken rock, and therefore, the occurrence of block rotation. For the *undisturbed jointed* samples the *Modified Hoek–Brown failure* envelope shows that the increase in strength is very rapid at low confining pressures.

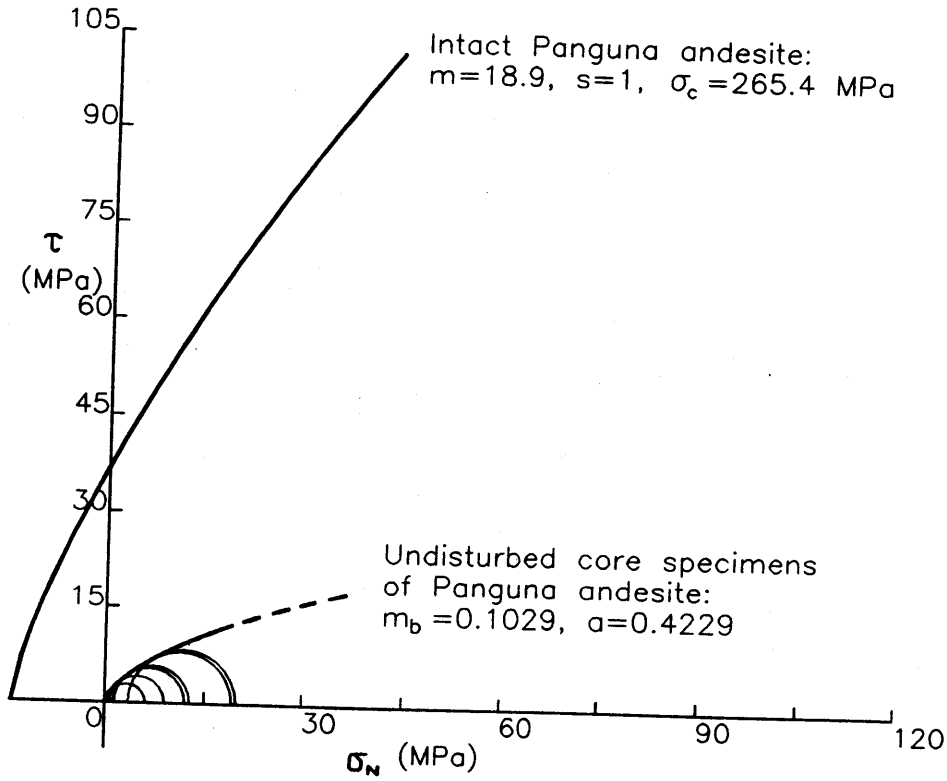

Figure 3.9: Mohr strength envelopes for *Intact* and *Undisturbed Jointed* Panguna Andesite

The Mohr failure envelopes for all the types of jointed Panguna andesite are plotted in Figures 3.10 and 3.11 corresponding to the *modified* and *original* Hoek– Brown criterion, respectively. It is evident that there is a systematic decrease in the strength of the rock mass as the degree of jointing and weathering increases which is reflected in the decrease in the values of m and s and also in the increase in the value of a. The value of a increases from 0.422 for *undisturbed jointed* samples to 0.781 for *highly weathered* samples indicating a tendency towards linearity of the Mohr envelope. The values of m_b, however, do not show any specific pattern. Comparing the values of the $\sum \epsilon^2$ for the two criteria, it can be seen that the values for the *modified* criterion are always much lower than that for the *original* criterion resulting in better fits to the triaxial test data. This is more evident at lower confining or effective normal stresses where the flexibility of the curve has been increased by the use of the variable power exponent a.

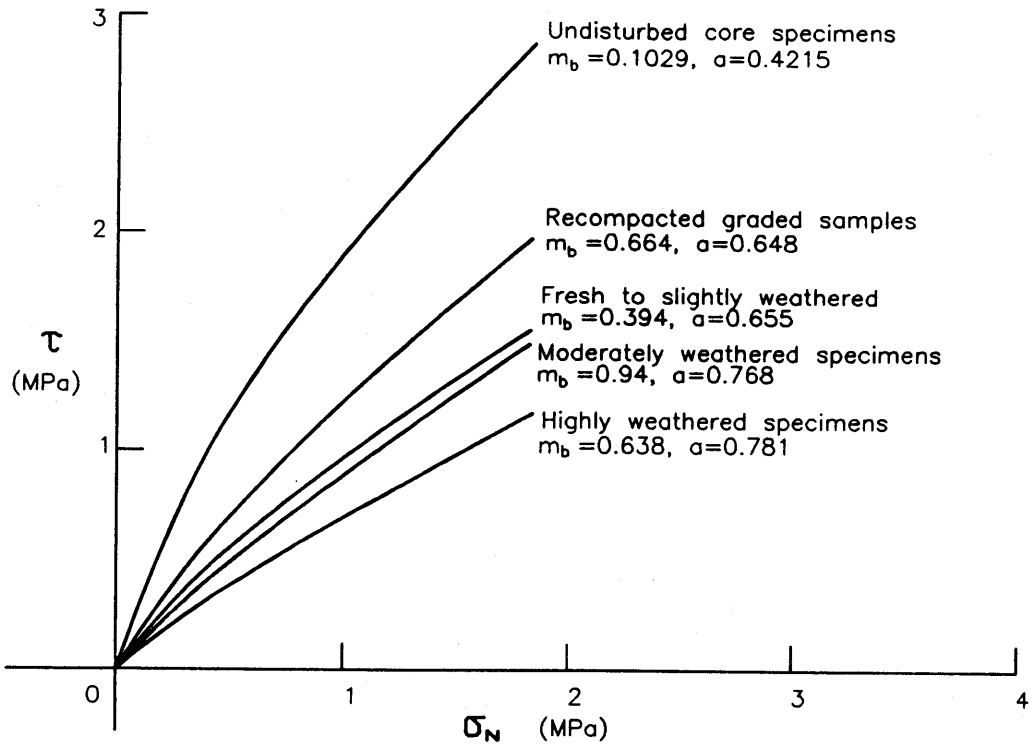

Figure 3.10: Mohr envelopes for Triaxial test results on *Jointed* Panguna Andesite for Modified Hoek–Brown Criterion

3.4.5.4 Analysis of Other "broken" Rock Mass Data

Doruk (1991) had carried out analysis of triaxial test data for residual strength data, triaxial test data for crushed model material and rockfill materials using a research version of the computer program ROCKDATA developed by the author in 1990, which included the *original* and the *modified* Hoek–Brown failure criteria. The residual strength data were taken for Westerly Granite tested by Wawersik and Brace (1971), and Doddington Sandstone by Santarelli and Brown (1989). The results of triaxial tests conducted on a model material similar to that of a soft rock, by Yudhbir, Lemanza and Prinzi (1983), under disintegrated conditions were also analyzed. The intact samples were a mixture of gypsum and celite, and the disintegrated or "broken" specimens were composed of 75% coarse and 25% fine particles. The rockfill materials were heavily compacted sandstones (Charles and Watt, 1980). The reason for analyzing rockfill materials with a criterion applicable for rock mass is that the overall strength behaviour of a heavily jointed rock mass, i.e., the high degree of

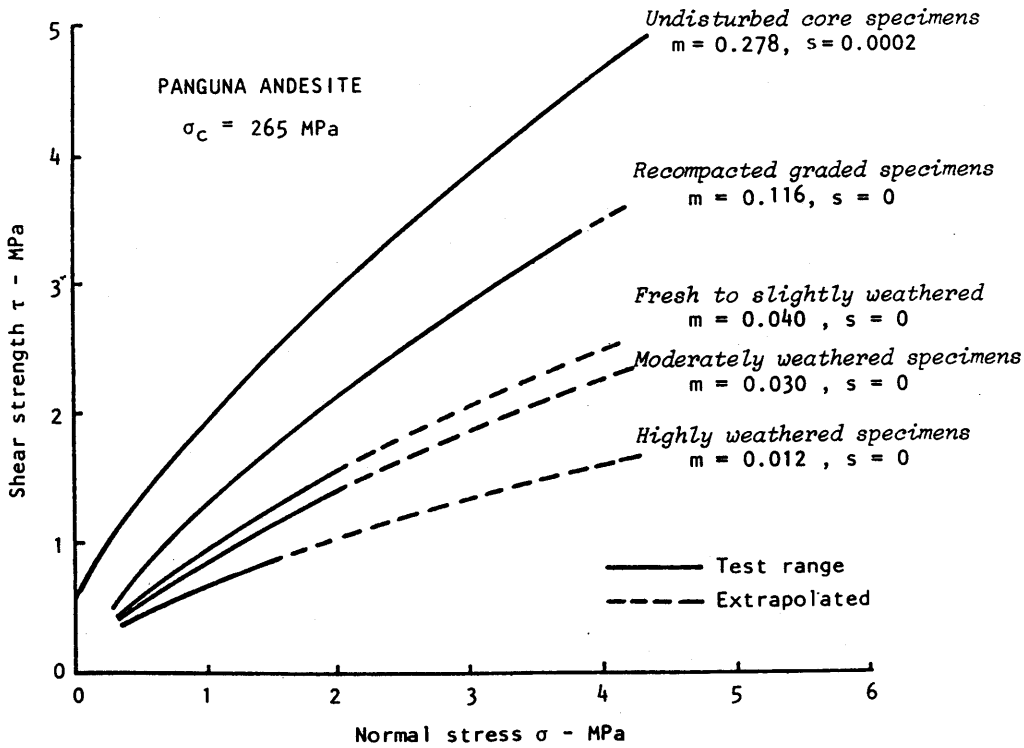

Figure 3.11: Mohr strength envelopes for *Intact* and *Undisturbed Jointed* Panguna Andesite for Original Hoek–Brown Criterion

dilation due to interlocking of individual particles under low effective normal stress values and particle crushing under high effective normal stress values, is generally similar to the overall strength behaviour of a heavily compacted rockfill. The analysis of the data for these type of "broken" rock also indicated that the *Modified Hoek–Brown failure criterion* gave a better fit to the triaxial data as compared to the *original* criterion. The values of the parameters m_b and a for these materials and the samples of Panguna Andesites and the Granulated marbles are listed in Table 3.7.

It can be observed from Table 3.7 that the values of the parameter a for the granulated marble and the crushed model material show a very narrow range with values smaller than 0.5. The small values of a result in very high curvatures at low effective normal stress values.

As shown in Doruk (1991), for the case of the analysis of residual strengths of the Westerly Granite and the Doddington sandstone, the plots of the Mohr envelope showed that

	Data Type	Range of a values	Range of m_b values
1.	Panguna Andesites (Undisturbed core samples to Highly weathered samples)	0.422 – 0.781	0.105 – 0.940
2.	Granulated Marble (Carrara and Wombeyan)	0.318 – 0.335	7.80 – 20.00
3.	Residual Strength (Granite and Sandstone)	0.344 – 0.842	1.82 – 15.42
4.	Crushed Model Material (Gypsum and celite)	0.431 – 0.462	1.12 – 2.79
5.	Rockfill materials (sandstone)	0.637	0.334

Table 3.7: Values of m_b and a for different rock types

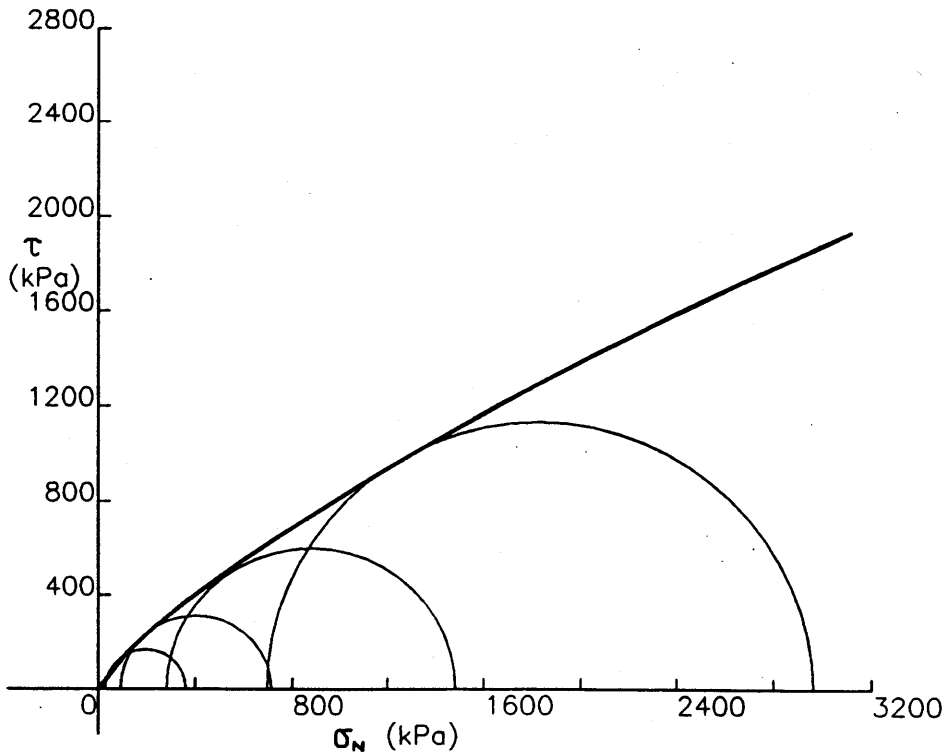

Figure 3.12: Mohr envelope for Sandstone Rockfill for Modified Hoek–Brown criterion

the *Modified Hoek–Brown failure criterion* was able to model the relationship between the residual strengths and the confining pressures adequately. However, it should be emphasized that, while the rock specimens are progressing from peak to residual strength, the loose broken particles are not permitted to move far along their fracture surfaces and are still tightly interlocking. For this reason, the decrease in the strength from the intact to the "broken" rock mass for these rock types are relatively small as compared to that of the Panguna andesite. Similarly, for the Carrara marble tested by Gerogiannopoulous, the decrease in the strength of the "granulated" marble is relatively small compared to that of the intact marble. This can be explained on the basis of the process involved in the granulation of the marble. Since this process does not involve shearing or displacement during the heating process, the grain boundaries of the "granulated" marble are tightly interlocking, and consequently, the Mohr envelope for the granulated marble represents the absolute upper bound for jointed rock masses.

The Mohr envelope corresponding to the *Modified Hoek–Brown failure criterion* for the Sandstone rockfill (Charles & Watt, 1980) is shown in Figure 3.12. It can be observed from this figure that the Mohr envelope gives a very good fit to the experimental data for the values of $m_b = 0.334$ and $a = 0.637$ obtained from Simplex Reflection analysis of the data for σ_c = 120,000 kPa. As shown in Figure 3.12, the Mohr envelope shows a marked curvature upto $\sigma'_n \leq 400$ kPa. This curvature can be explained by the dilation behaviour of the rockfill. The reduction in the rate of increase of the shear strength can be observed at $\sigma'_n > 600$ kPa. This is due to the fact that the dilatancy is suppressed because of particle breakage. Hence, it can be said the *Modified Hoek–Brown failure criterion* is able to model the behaviour of rockfill materials quite well, too. It appears that the result of stability analyses carried out for rockfills using the *Modified Hoek–Brown failure criterion* should be more precise, especially in the region where the shear strength at low effective normal stresses are important, as compared to those of the *Original Hoek–Brown criterion* or the Mohr–Coulomb criterion defined by c', cohesion, and friction, ϕ'.

3.4.6 Characteristics of Modified Hoek–Brown Failure Criterion

It has been shown in the previous section that the *Modified Hoek–Brown failure criterion* is able to model the behaviour of a variety of rock masses. Its parameters m_b and a provide greater flexibility to the curvature of the envelope. In order to study the influence of the strength parameters, m_b and a, on the strength and frictional properties of the rock mass, the characteristics of the criterion were investigated and are discussed in this section.

3.4.6.1 Influence of Parameter a on Strength Envelope

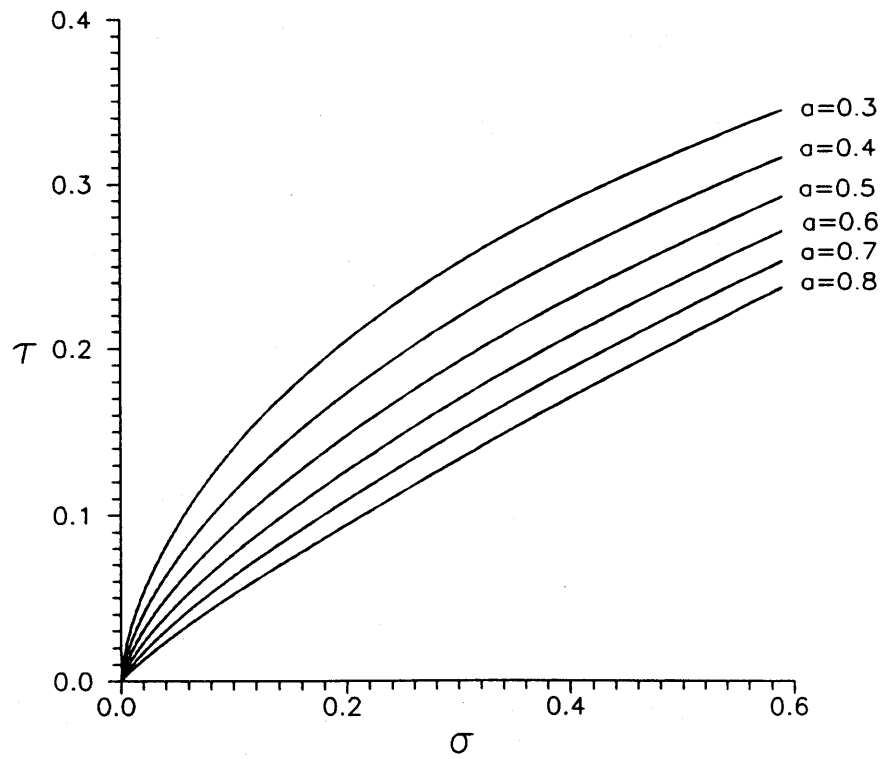

Figure 3.13: Variation of Mohr Strength Envelope with parameter a

It has been described in section 3.4.3.3 that the value of parameter a is directly proportional to the degree of jointing and weathering as in the case of the Panguna andesites. The value of a increase with the degree of jointing and weathering. Figure 3.13 shows the influence of a on the shear strength of broken rock mass. In plotting these curves, the values of m_b and σ_c have been taken as unity and the value of a has been varied from 0.3 to 0.8.

As observed, the parameter a reflects the curvature of the strength envelopes. The smaller the value of a, the greater is the curvature of the strength envelope at low confining or effective normal stresses indicating a high rate of increase of strength with the application of confining stress.

3.4.6.2 Influence of Parameter m_b on Strength Envelopes

It has been seen that the values of m_b do not follow any regular pattern for the Panguna andesites. In order to study this behaviour, the influence of m_b on the strength envelopes and the interaction of m_b and a were studied with the plots shown in Figure 3.14 in which the shear strength envelopes were calculated for fixed values of a with variations in the value of m_b taking $\sigma_c = 1$. It can be observed from this figure that an increase in the value of m_b results in an increase in the strength for the broken rock for all values of a. However, the rate of increase in strength with increasing m_b is governed by the value of a. The rate of increase of strength is higher for lower values of a for a given value of m_b. Consequently, it can be concluded that both a and m_b are sensitive to the degree of particle interlock in the rock mass, an therefore, both parameters characterize the curvature of the strength envelope. Therefore, it can be concluded that the strength predicted by the *modified* criterion is a function of both m_b and a, and that is why m_b was not showing any particular trend with the degree of jointing and weathering in the Panguna andesites.

3.4.6.3 Influence of a on Friction Angle ϕ'_i

The variation of the instantaneous friction angle, ϕ'_i, with the effective normal stress for various values of a is plotted in Figure 3.15 for the values m_b and σ_c equal to unity. It can be observed from this figure that the value of ϕ'_i at $\sigma'_n = 0$ is 90° for all values of a since this is the value of σ'_n at which the shear strength envelope originates. For lower values of a, the value of ϕ'_i is higher than that for higher values of a at low effective normal stress values. This indicates the fact that for the envelopes corresponding to low values of a, i.e. $a < 0.5$, the frictional strength of the rock mass is higher at low values of σ'_n, and the rate of decrease of the friction angle with σ'_n is also lower. The decrease in the value of friction angle with σ'_n with increase in σ'_n is greater for higher values of a. The values of ϕ'_i decrease

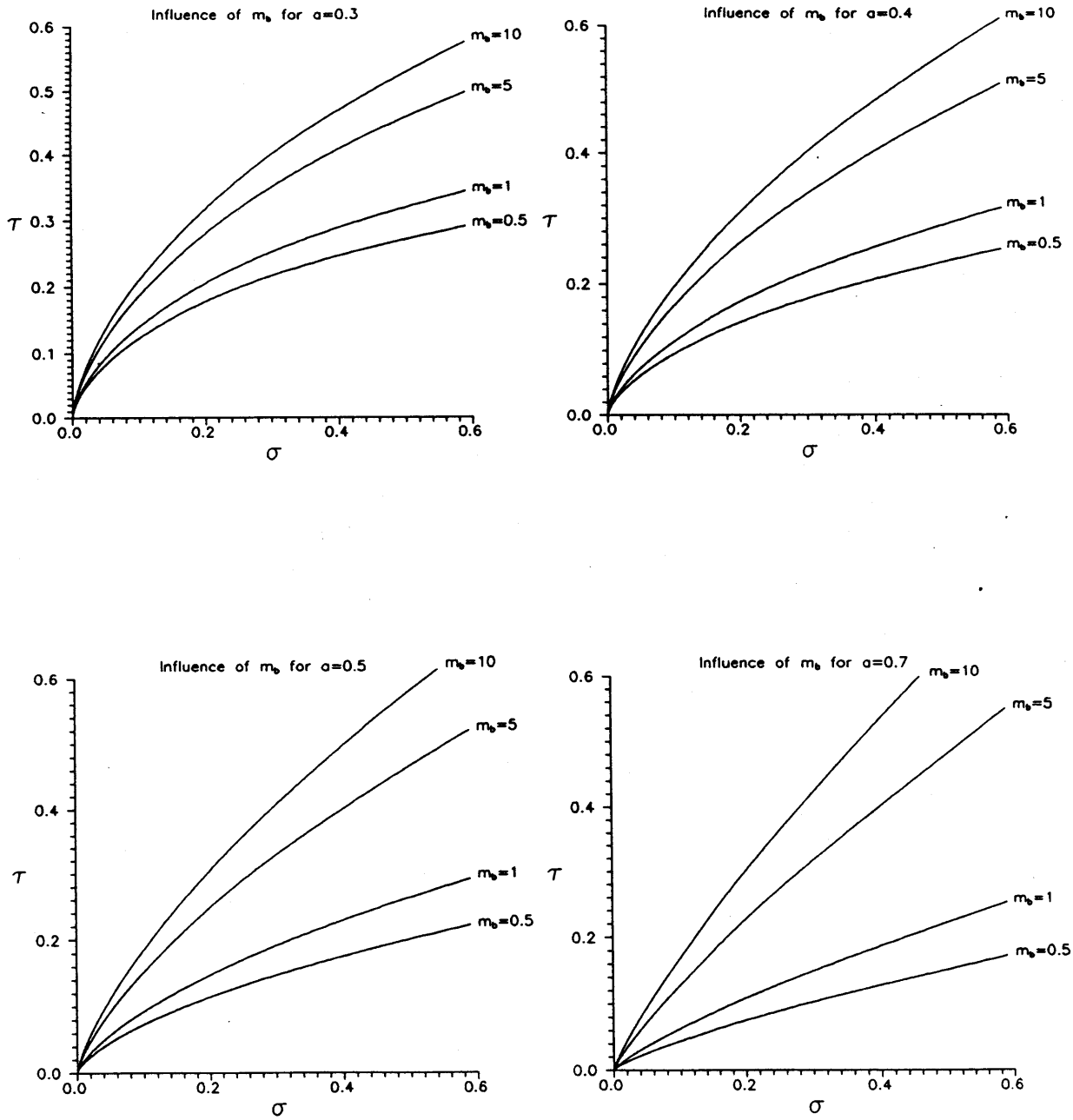

Figure 3.14: Variation of Mohr Strength Envelope with parameter m_b for different values of a

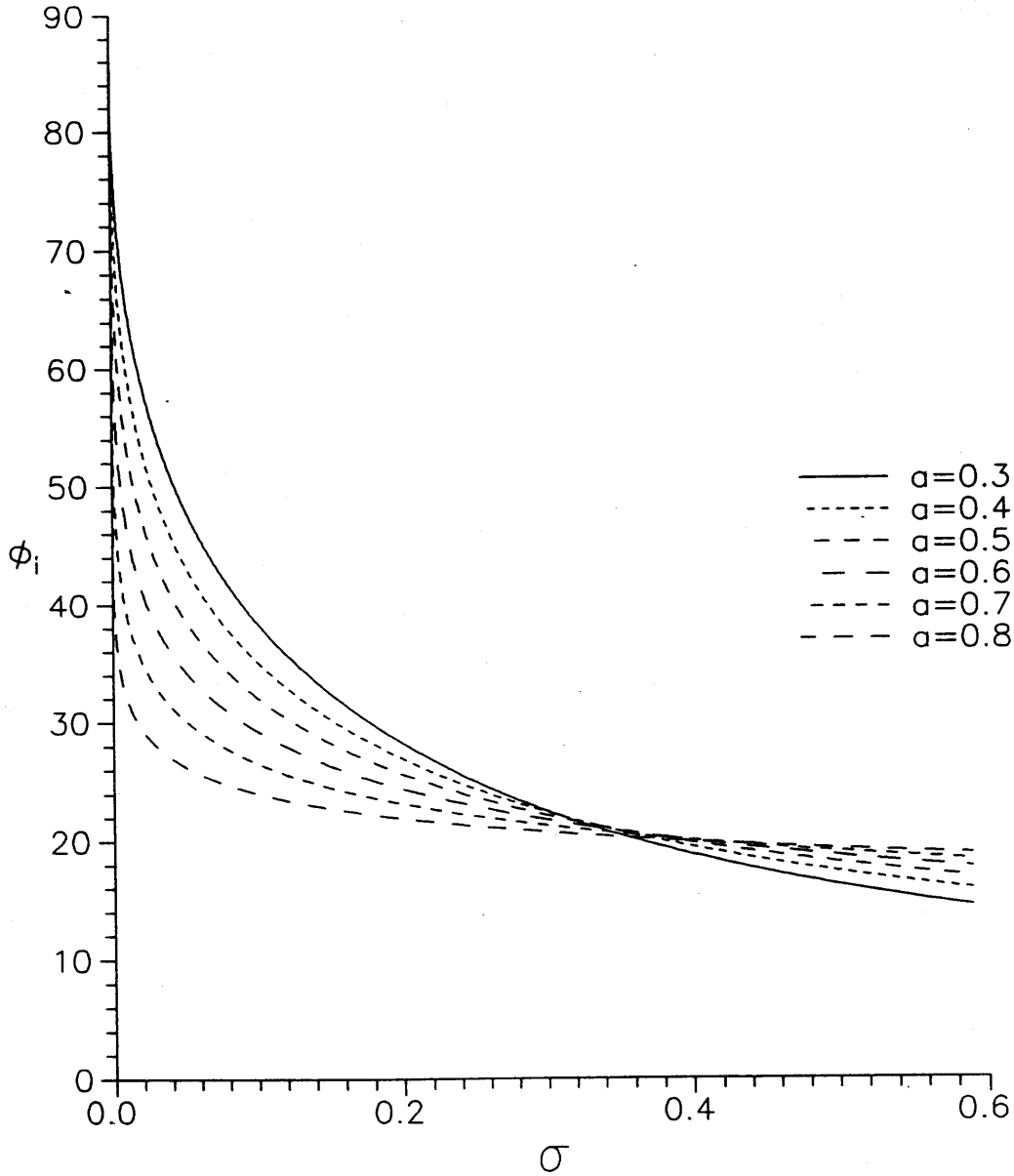

Figure 3.15: Variation of ϕ_i' with σ_n' for different values of a

less rapidly at higher values of σ'_n for higher values of a. Therefore, it can be concluded that the parameter a controls the value of shear strength as well as the friction angle of the rock mass at various values of σ'_n.

3.4.6.4 Variation of Friction Angle ϕ'_i with m_b

Figure 3.16 shows the variation of the instantaneous friction angle, ϕ'_i, with the effective normal stress σ'_n for various values of m_b. These curves have been plotted for $a = 0.3$ and $\sigma_c = 1$. It can be observed from this figure that as the value of m_b is increased from 0.5 to 20, the values of ϕ'_i increase for the same value of σ'_n. All of the curves originate from $\phi'_i = 90°$ and the rate of decrease of ϕ'_i with increasing σ'_n is faster for lower values of m_b. This figure makes it clear that the variation in ϕ'_i is dependent on m_b as well.

3.4.7 Investigation of Simplifications to Modified Hoek–Brown Failure Criterion

The choice of *Modified Hoek–Brown criterion* as a criterion for estimating the strength of a rock mass is quite heartening since it has only two parameters, viz. m_b and a. A further simplification to this criterion is to fix the value of a at, say, $\frac{1}{3}$ or 0.4. This thought is strengthened from the fact that the results of the analysis of the "granulated" Carrara and Wombeyan marbles suggest that the value of a is close to $\frac{1}{3}$. In order to investigate the possibility of obtaining a simplification to the *Modified Hoek–Brown failure criterion*, analyses of available triaxial test data were carried out with $a = \frac{1}{3}$. This simplification is represented by the equation:

$$\frac{\sigma'_1}{\sigma_c} = \frac{\sigma'_3}{\sigma_c} + \left(m_b \frac{\sigma'_3}{\sigma_c}\right)^{\frac{1}{3}} \tag{3.69}$$

The results of the fitting of these triaxial data sets to equation (3.69), using the Simplex Reflection technique, and the comparison of the value of the $\sum \epsilon^2$ with *Modified Hoek–Brown failure criterion* are given in Table 3.8.

It can be seen from Table 3.8 that for the "granulated" marbles the difference in the values of the parameters m_b and a and $\sum \epsilon^2$ are relatively small. However, for the Panguna Andesites the value of the residuals are significantly different. Therefore, it can

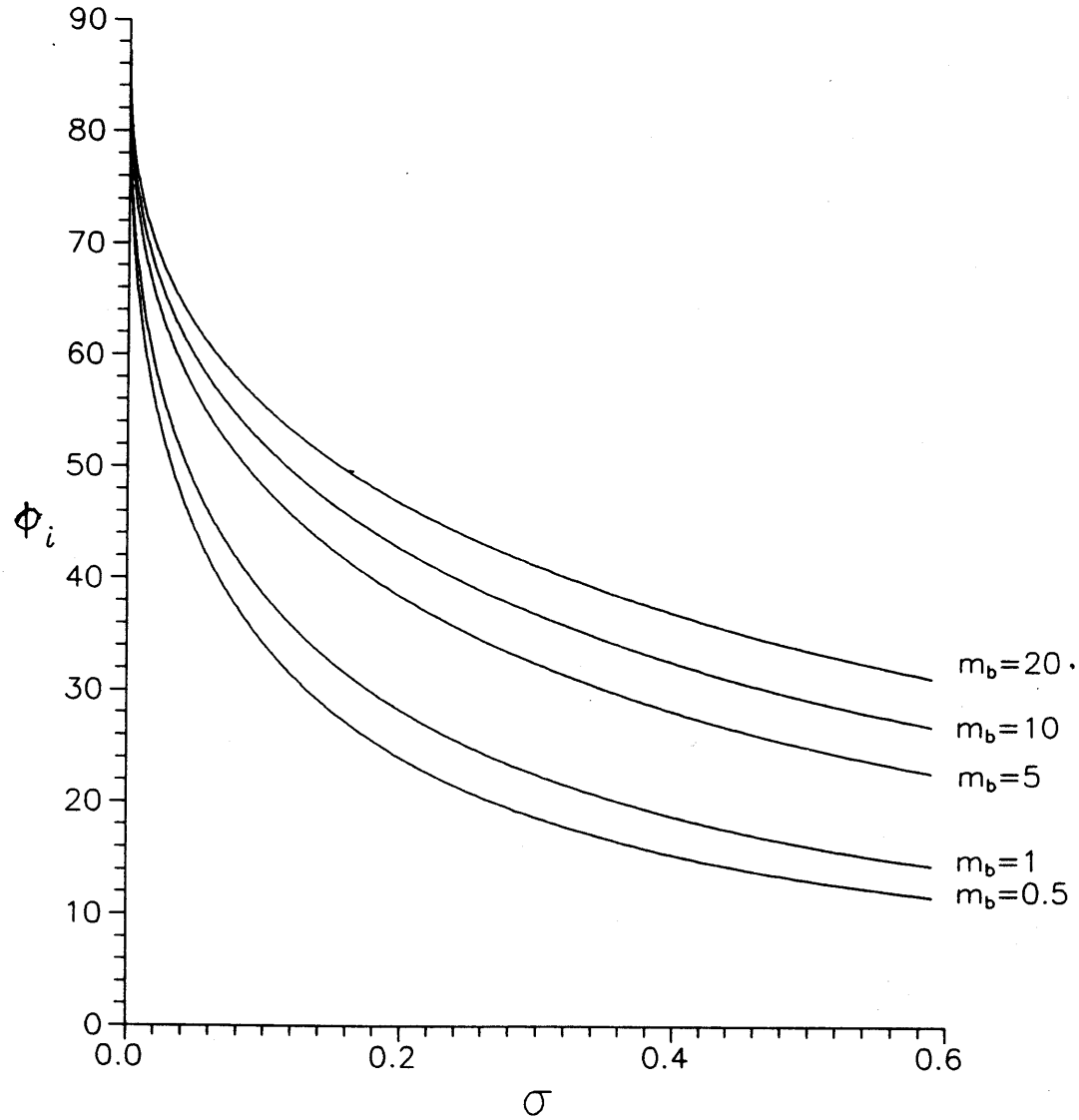

Figure 3.16: Variation of ϕ'_i with σ'_n for different values of m_b

Data Set	Modified Hoek–Brown a - variable			Modified Hoek–Brown $a = \frac{1}{3}$		
	m_b	a	$\sum \epsilon^2$	m_b	a	$\sum \epsilon^2$
1. Carrara Marble	18.97	0.31788	784	17.78	$\frac{1}{3}$	809.5
2. Wombeyan Marble	11.15	0.33514	654.6	11.17	$\frac{1}{3}$	653.9
3. Panguna Andesites						
a. Undisturbed core samples	0.1029	0.4215	1.397	0.0155	$\frac{1}{3}$	3.936
b. Recompacted graded samples	0.664	0.648	6.104	0.0024	$\frac{1}{3}$	45.22
c. Slightly weathered samples	0.394	0.655	0.1315	0.00031	$\frac{1}{3}$	1.138
d. Moderately weathered samples	0.94	0.768	0.006	0.00018	$\frac{1}{3}$	0.5864
e. Highly weathered samples	0.638	0.781	0.0008	0.00005	$\frac{1}{3}$	0.113

Table 3.8: Comparison of results for Modified and Simplification to Modified Hoek–Brown Failure criterion for rock mass

be concluded that although this simplification of assuming $a = \frac{1}{3}$ is very promising, it cannot be generalized for all types of rock mass. Similar types of results were obtained for $a = 0.4$. Therefore, it has been decided that the more general *Modified Hoek–Brown failure criterion* is to be used for the estimation of rock mass strength.

3.4.8 Investigation of Failure criteria for Intact Rock

In an effort to investigate the suitability of the *original* Hoek–Brown failure criterion for estimating the strength of *intact* rock mass, a series of analyses were carried out on numerous triaxial test data sets for *intact* rock specimens using the Simplex Reflection technique for curve-fitting. A generalized form of the Hoek–Brown criterion proposed by Pan and Hudson (1988), equation (3.39) was also used with $s = 1$ for intact rocks. This equation results in three material parameters, viz. m, σ_c and a for *intact* rocks. By setting $s = 1$, this expression becomes similar to the *Modified Hoek–Brown failure criterion* except that in the *modified* criterion $s = 0$. The Simplex Reflection technique for fitting the curve through the data points was applied to this equation, too. The results of the analysis of the data sets showed that the value of a deviated little from 0.5 and gave similar good fits as the values of $\sum \epsilon^2$ were approximately equal.

The substitution of $a = 0.5$ in equation (3.39), in fact, converts it to the *original*

Hoek–Brown criterion. Therefore, it was concluded that the *Original* Hoek–Brown failure criterion should be used for predicting the strength of *intact* rocks and that the Simplex Reflection technique, and not linear regression analysis, should be used for analyzing triaxial test data for *intact* rock specimens.

3.5 Field Estimates of Parameters of Modified Hoek–Brown Criterion

An important aspect in the development of a failure criterion for rock mass is to establish a set of relations which correlate the parameters of the criterion with rock mass characteristics or a classification scheme such as the RMR or Q systems. As discussed earlier, it is practically impossible to carry out triaxial or shear tests on rock masses at a scale which is of the same order of magnitude as surface or underground excavations used in mining or civil engineering (Hoek and Brown, 1988). Due to the problems associated with the preparation and transportation of samples of the rock mass, testing of strength of rock mass in the laboratory is an extremely difficult and expensive proposition.

In the absence of such strength data, attempts have to be made to provide a basis for linking the parameters of the criterion to measurements or observations which can be carried out by a competent geologist in the field. Hoek and Brown (1980, 1988) recognized that the characteristics of the rock mass which control its strength and deformation behaviour are similar to the characteristics which had been adopted by Bieniawski (1974) and by Barton, Lien and Lunde (1974) for their rock mass classification schemes. Hoek and Brown proposed a set of approximate relations between rock mass quality and material constants which is illustrated in Table 3.3. These relations were formulated on the basis of tests on Panguna andesites conducted by Jaeger (1969) which were later revised on the basis of lessons learned from practical applications. This table has been used extensively in the field in civil and mining engineering applications, and it has been found to provide competent results in the estimation of strength of the rock mass and for assessing the overall stability of excavations.

It is evident from the discussions in the previous sections that the *Modified Hoek–Brown failure criterion* models the behaviour of a jointed rock mass in a better fashion

than the *Original Hoek–Brown criterion*. Whereas the *original* criterion was found to be suitable for the prediction of the strength of the rock mass at moderate confining stresses associated with brittle failure and for assessing the overall stability of an excavation, its predictions of strengths at low values of confining stresses were inadequate. The *modified* criterion predicts zero tensile strength for rock mass and has improved the estimation of the strength of the rock mass in the range of low effective normal or confining stresses. The estimates of strength from this criterion in the moderate range of stresses are similar to that of the *original* criterion. Therefore, along with being adequate for predicting the overall strength and stability of the rock mass, the *modified* criterion is more suitable for assessing the strength and stability of the rock mass in regions close to the excavation, i.e. in regions of low confining stress, where it is vital to predict the behaviour of the rock mass alone and in conjunction with support systems.

Taking these facts into consideration, it was decided to develop relationships between the material strength parameters m_b and a of the *Modified Hoek–Brown failure criterion* and rock mass quality. A methodology was developed to obtain these parameters from the relationships of the material strength parameters m and s of the *original* criterion with rock mass quality. This methodology eliminates the deficiencies of the *original* criterion and presents the strength envelope in the form of the *modified* criterion.

3.5.1 Methodology for Correlating m_b and a with Rock Mass Quality

As discussed in section 3.4.8, it has been decided that the Original Hoek–Brown criterion is to be used for estimating the strength of intact rock samples. Therefore, the values of m_b and a are to be generated for RMR < 100 or for very good to very poor quality rock mass.

The *original* Hoek–Brown criterion predicts a finite value of tensile strength for the rock mass, and hence, the failure envelope is pivoted at $(\sigma_1' = 0, \sigma_3' = \sigma_{tmass})$ as shown in Figure 3.3. In the case of the *modified* criterion, rock mass is assumed to have no tensile strength, and therefore, the failure envelope is anchored at $(\sigma_1' = 0, \sigma_3' = 0)$. Thus, in order to obtain the curve corresponding to the *modified* criterion from the envelope of the *original* criterion, the generated curve has to be bent sufficiently in the region near the origin. This process introduces a high degree of curvature in the envelope in this region.

Table 3.3 lists the values of m and s for *disturbed* as well as *undisturbed* rock mass. The parameters m_b and a are generated for the undisturbed state of rock mass only as the strength parameters should correspond to their intrinsic property only because disturbance is an externally induced effect. The method by which the parameters m_b and a were generated from Table 3.3 is outlined below:

1. For a particular combination of the undisturbed values of m and s from Table 3.3, the *original* Hoek–Brown failure envelope was plotted with $\sigma_c = 1$, and six points were picked from this curve at equal intervals in the region $0.001 \leq \sigma_3'/\sigma_c \leq 1.0$. The limits for the range of σ_3'/σ_c were chosen by a systematic procedure of varying the upper and lower limits for σ_3'/σ_c since the values of the parameters m_b and a are very sensitive to the stress range adopted. This procedure is discussed in section 3.5.2.
2. These six points were fitted to the *Modified Hoek–Brown failure criterion* using the program ROCKDATA with the Simplex technique for fitting the data points to the curve. This process resulted in the values of m_b and a.
3. The previous two steps were repeated for all the sets of values in Table 3.3 and the values of m_b and a were obtained.

The resulting set of values relating the strength parameters m_b and a of the *Modified Hoek–Brown failure criterion* with the rock mass characteristics is presented in Table 3.9.

The significant features of the values of m_b and a in Table 3.9 and their trends are described and compared to the values of m and s from Table 3.3:

- At high values of RMR, both m and s are high resulting in high values of the tensile strength of the rock mass σ_{tmass}. Therefore, the *modified* criterion curve has to be bent to a higher degree which causes the value of a, for instance, to decrease upto 0.356 compared to 0.5 for the *original* criterion. The value of m_b increases to 6.84 compared to m of 4.10. Both m_b and a interact to provide a higher curvature to the envelope.
- At low values of RMR, the values of m and s are very small resulting in insignificant values of σ_{tmass}. Thus, the *modified* and the *original* criteria curves follow a similar

Undisturbed Rock Mass m_b and a Values						
MODIFIED HOEK–BROWN FAILURE CRITERION $\frac{\sigma_1'}{\sigma_c} = \frac{\sigma_3'}{\sigma_c} + \left(m_b \frac{\sigma_3'}{\sigma_c}\right)^a$ σ_1' = major principal effective stress σ_3' = minor principal effective stress σ_c = uniaxial compressive strength of intact rock, and m_b and a are material strength parameters.		CARBONATE ROCKS WITH WELL DEVELOPED CRYSTAL CLEAVAGE *dolomite, limestone and marble*	LITHIFIED ARGILLACEOUS ROCKS *mudstone, siltstone, shale and slate (normal to cleavage)*	ANENACEOUS ROCKS WITH STRONG CRYSTALS AND POORLY DEVELOPED CRYSTAL CLEAVAGE *sandstone and quartzite*	FINE GRAINED POLYMINERALLIC IGNEOUS CRYSTALLINE ROCKS *andesite, dolerite, diabase and rhyolite*	COARSE GRAINED POLYMINERALLIC IGNEOUS & METAMORPHIC CRYSTALLINE ROCKS – *amphibolite, gabbro gneiss, granite, norite, quartz-diorite*
VERY GOOD QUALITY ROCK MASS *Tightly interlocking undisturbed rock with unweathered joints at 1 to 3m.* CSIR rating: RMR = 85 NGI rating: Q = 100	m_b a	6.842 0.3557	8.972 0.3957	12.390 0.4275	13.740 0.4349	18.970 0.4534
GOOD QUALITY ROCK MASS *Fresh to slightly weathered rock, slightly disturbed with joints at 1 to 3m.* CSIR rating: RMR = 65 NGI rating: Q = 10	m_b a	2.096 0.4625	3.022 0.4717	4.537 0.4797	5.134 0.4821	7.516 0.4870
FAIR QUALITY ROCK MASS *Several sets of moderately weathered joints spaced at 0.3 to 1m.* CSIR rating: RMR = 44 NGI rating: Q = 1	m_b a	0.943 0.4906	1.355 0.4931	2.039 0.4952	2.314 0.4961	3.402 0.4973
POOR QUALITY ROCK MASS *Numerous weathered joints at 30-500mm, some gouge. Clean compacted waste rock* CSIR rating: RMR = 23 NGI rating: Q = 0.1	m_b a	0.446 0.4982	0.638 0.4986	0:958 0.4989	1.088 0.4998	1.598 0.5001
VERY POOR QUALITY ROCK MASS *Numerous heavily weathered joints spaced <50mm with gouge. Waste rock with fines.* CSIR rating: RMR = 3 NGI rating: Q = 0.01	m_b a	0.219 0.5000	0.313 0.5001	0.470 0.5006	0.533 0.5006	0.783 0.5007

Table 3.9: Approximate Relationship Between Rock Mass Quality and material constants m_b and a of Modified Hoek–Brown Criterion

path. This is the reason why for RMR < 23, we can observe that $m_b \approx m$ and $a \approx 0.5$.

- As we go across a row in Table 3.3, the values of m increase while the values of s remain constant. This signifies that the tensile strength of the rock mass σ_{tmass} is decreasing across the row. Therefore, the values of a increase across a row and are approximately equal to 0.5 on the right columns of Table 3.9 for lower values of RMR.

3.5.2 Selection of Stress Range

During the process of carrying out the analysis outlined in the previous section, it became obvious that the values of m_b and a are quite sensitive to the stress range selected for the generation of values of σ_1' and σ_3' from the *original* Hoek–Brown criterion. The selection of the range of σ_3'/σ_c is described below:

- *Selection of upper limit of σ_3'/σ_c:*

  The upper limit of σ_3'/σ_c was chosen as 1.0 since this ensures that the two envelopes match over a sufficiently large range of confining stresses. If the upper limit is reduced to, say 0.5, then the two curves will match upto $\sigma_3'/\sigma_c = 0.5$ and will tend to deviate from each other beyond this range. This is due to the fact that no data is available in the range where the *modified* criterion curve is being extrapolated.

- *Selection of lower limit of σ_3'/σ_c:*

  The selection of the lower limit of σ_3'/σ_c is critical as this determines the amount of curvature that has to be introduced into the curve to shift the anchor of the curve from $\sigma_3' = \sigma_{tmass}$ to $\sigma_3' = 0$. This is the location where the major difference in the predictions of the two curves arise. A series of tests were conducted to ascertain this lower limit of the stress range. The procedure adopted was to fix the upper limit of σ_3'/σ_c at 1.0 and move the lower limit of σ_3'/σ_c starting at 0.2 and moving to 0.01, 0.001 and 0.0001 in order to obtain an optimum value of the lower limit. It was found that the value of a decreased and that of m_b increased as the lower limit was reduced upto 0.001 indicating the increase in the curvature of the envelope. However, when the lower limit was further reduced to 0.0001, the values of a increased and m_b decreased and became similar to that for the lower limit at 0.2. This indicated that the optimum value of the lower limit had been obtained.

3.5.3 Procedure for Estimating Values of Strength Parameters for Practical Applications

In order to estimate the values of strength parameters for practical applications, the following guidelines should be used:

- For intact rock samples which are laboratory size specimens free from discontinuities or, as shown in Figure 3.2, if the scale of the rock mass being considered in the analysis is sufficiently small such that no discontinuities exist within the volume in consideration, then the strength of the rock should be estimated as that for intact rock from the *Original* Hoek–Brown criterion. The intact values of m can be obtained from Table 3.2 or from Table 3.3 for RMR = 100, and the values of σ_c can be obtained from standard geological references.
- For heavily jointed *isotropic* rock mass which consists of various sizes of blocks with varying degrees of weathering or, as shown in Figure 3.2, if the scale of the rock mass in consideration is sufficiently large such that more than four joint sets with isotropic properties exist in the volume, then strength estimates should be made from the *Modified Hoek–Brown failure criterion.* The values of m_b and a can be obtained from Table 3.9.

3.6 Comparison of Overstress Factors using Modified and Original Hoek–Brown Criterion

The properties of the *Modified Hoek–Brown failure criterion* in describing the behaviour of the rock mass in different ranges of effective normal stress or confining stress along with its ability to provide a better fit to laboratory strength data for rock mass have been dealt with in previous sections. In order to establish its suitability for predicting the behaviour of the rock mass for a typical field problem, where all the regimes of effective normal or confining stress will be encountered, the zones of *overstress* predicted around an underground excavation has been analyzed in this section and compared to that predicted by the *Original Hoek–Brown criterion.*

A typical underground excavation design situation that an engineer faces is shown

in Figure 3.17. Two tall rectangular excavations with arched roofs each having a span of 16 m and a height of 32 m are located at a separation of 20 m. The stress distribution and the predictions of the zones of *overstress* around these excavations have been analyzed with EXAMINE^{2D}, a two-dimensional indirect boundary element linear, static stress analysis program[1]. The excavations were analyzed for an *in situ* stress field of $\sigma_1 = 20$ MPa and $\sigma_3 = 10$ MPa aligned along the horizontal and vertical directions, respectively. The elasticity parameters of the rock mass were taken as $E = 15000$ MPa and $\nu = 0.25$.

The distribution of the major and minor principal stresses around the excavation are shown in Figures 3.17 and 3.18, respectively. The contours of minor principal stress distribution indicate that there is a fairly large zone in the pillar between the two excavations that has tensile stresses.

In order to compare the zones of *overstress* predicted by the *original* and the *modified* Hoek–Brown failure criterion around the two excavations, the values of the material strength parameters of the rock mass for the two criteria were taken for the same type of rock and RMR value. It was assumed that the rock mass is sandstone with RMR = 85 and $\sigma_c = 50$ MPa. The corresponding values of strength parameters are listed below:

- *Original Hoek–Brown criterion parameters*:
  $m = 8.78$, $s = 0.189$.
- *Modified Hoek–Brown criterion parameters*:
  $m_b = 12.39$, $a = 0.4275$.

Figures 3.19 and 3.20 show the distribution of the *zones of overstress* around the two excavations for the *original* and *modified* Hoek–Brown failure criterion, respectively.

An examination of Figures 3.19 and 3.20 reveals that the general trend of overstress around the excavations are similar which is indicative of the overall stability of the excavations. The contours of strength factor, which is the ratio of available strength to induced stress, are similar for values ≥ 2. However, there are significant differences between the predictions of *overstress*, especially in the low confinement and tensile region of stresses. These differences are illustrated below:

[1]Developed in the Department of Civil Engineering at the University of Toronto in 1990

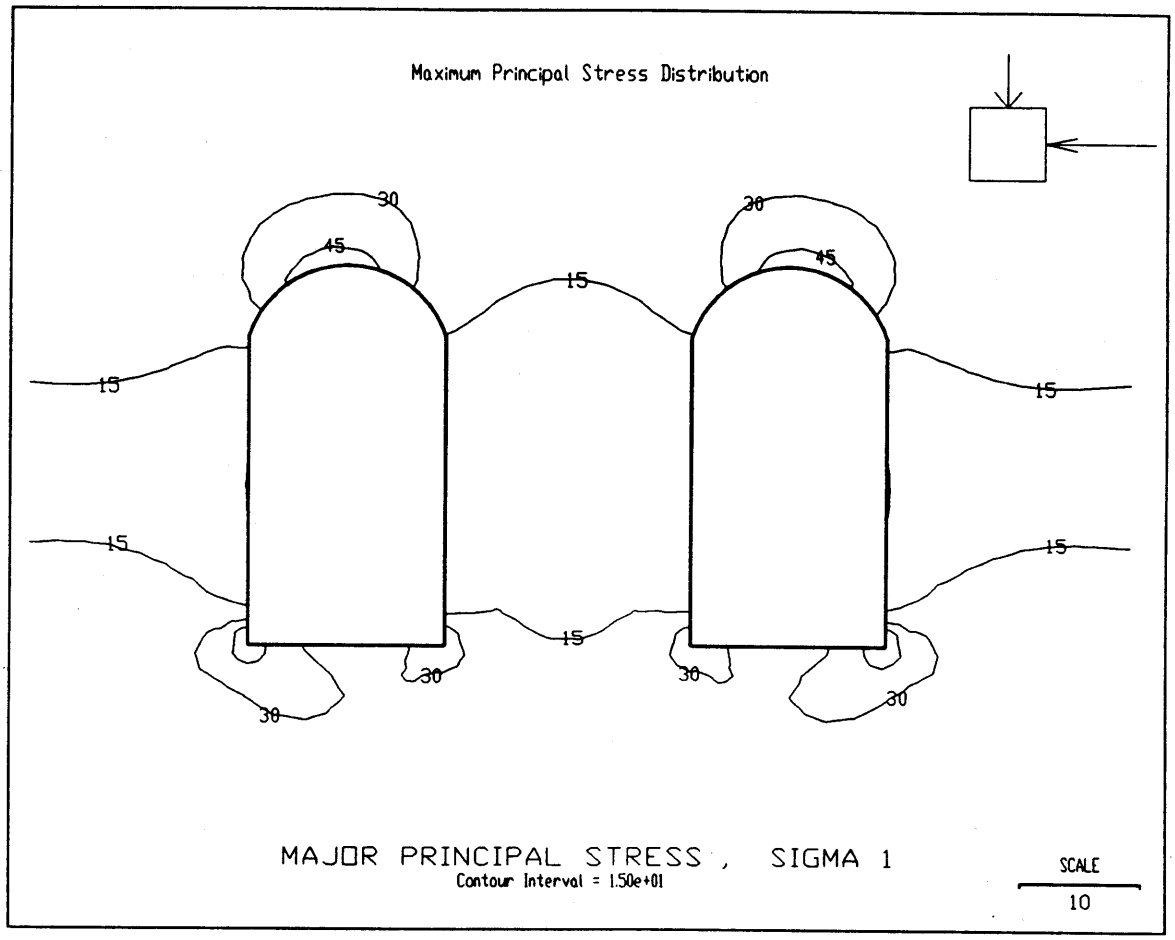

Figure 3.17: Maximum Principal Stress Distribution around Excavations

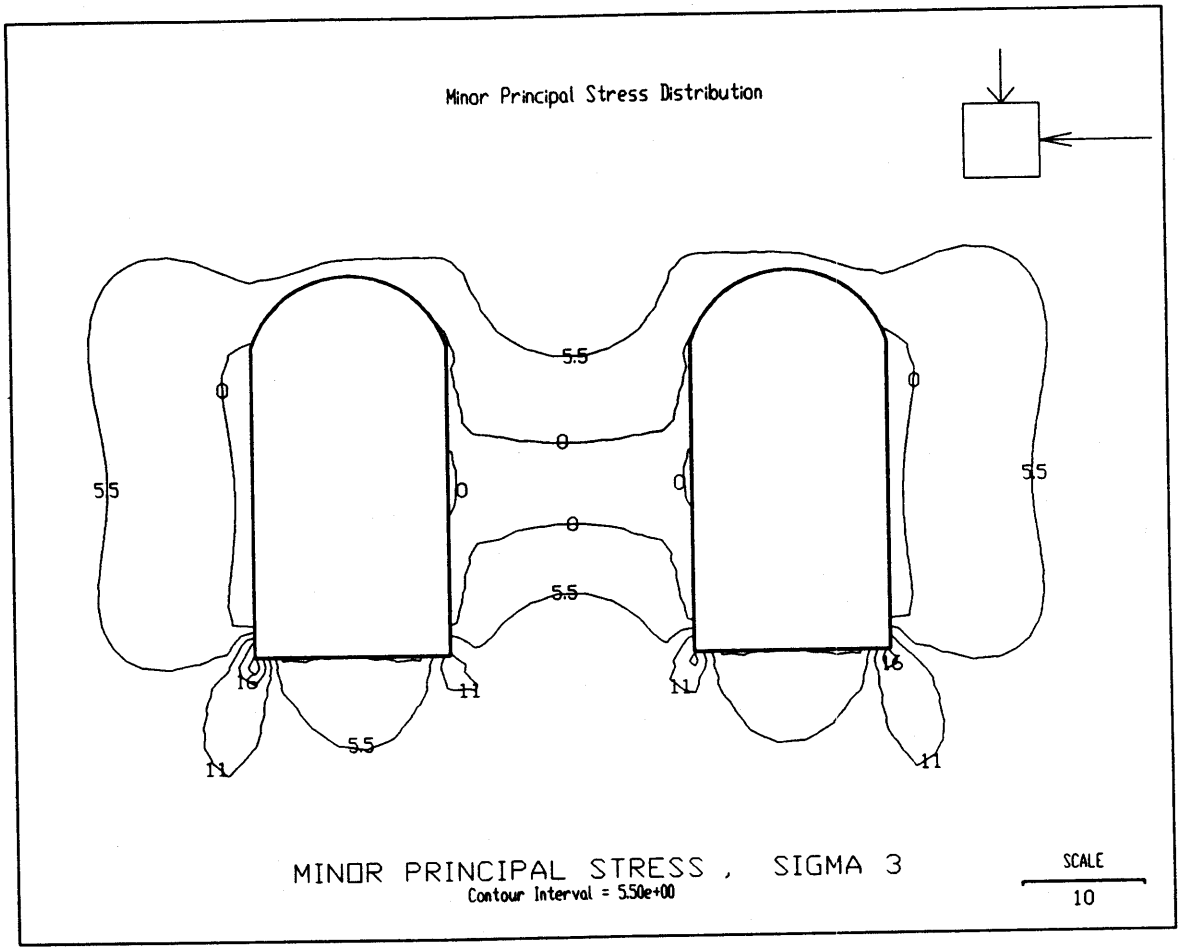

Figure 3.18: Minimum Principal Stress Distribution around Excavations

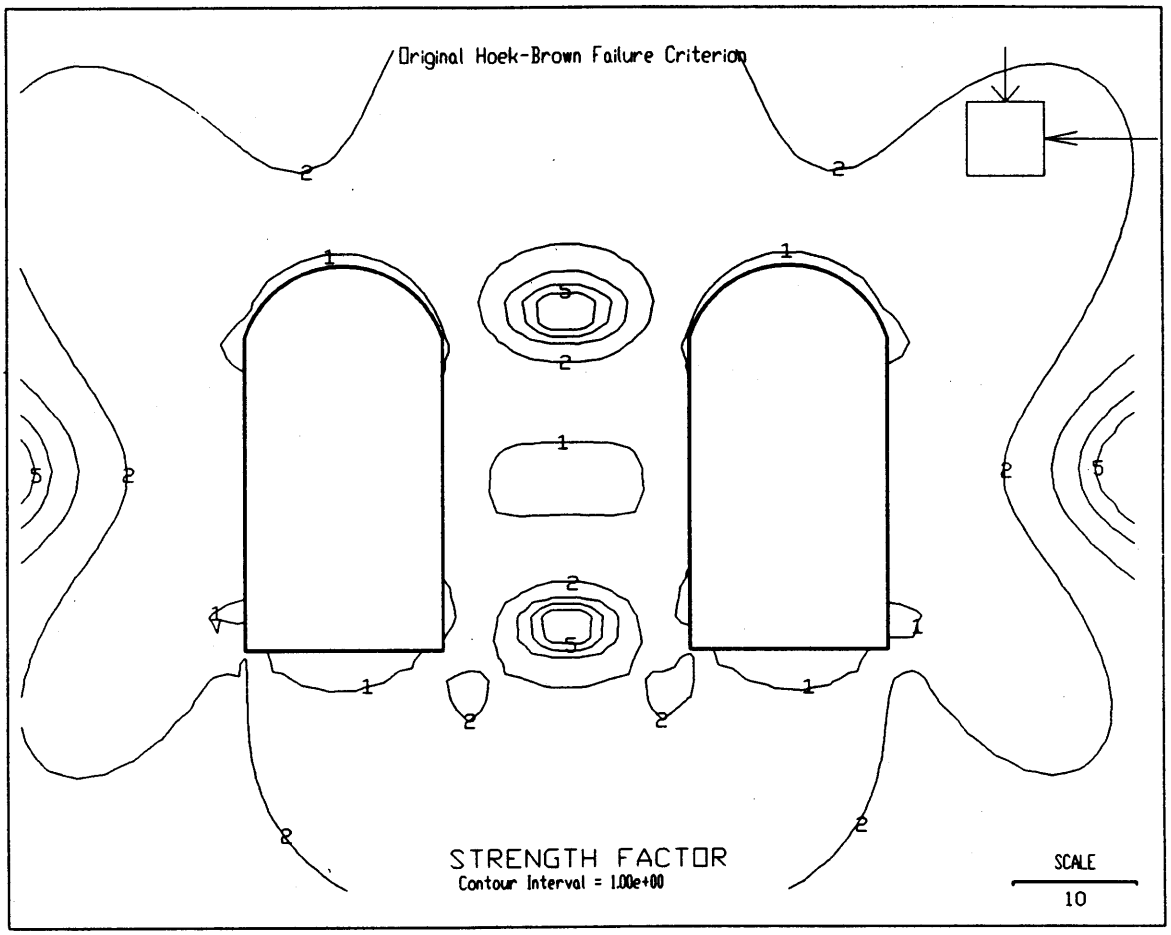

Figure 3.19: Overstress zone around excavations for Original Hoek–Brown Criterion

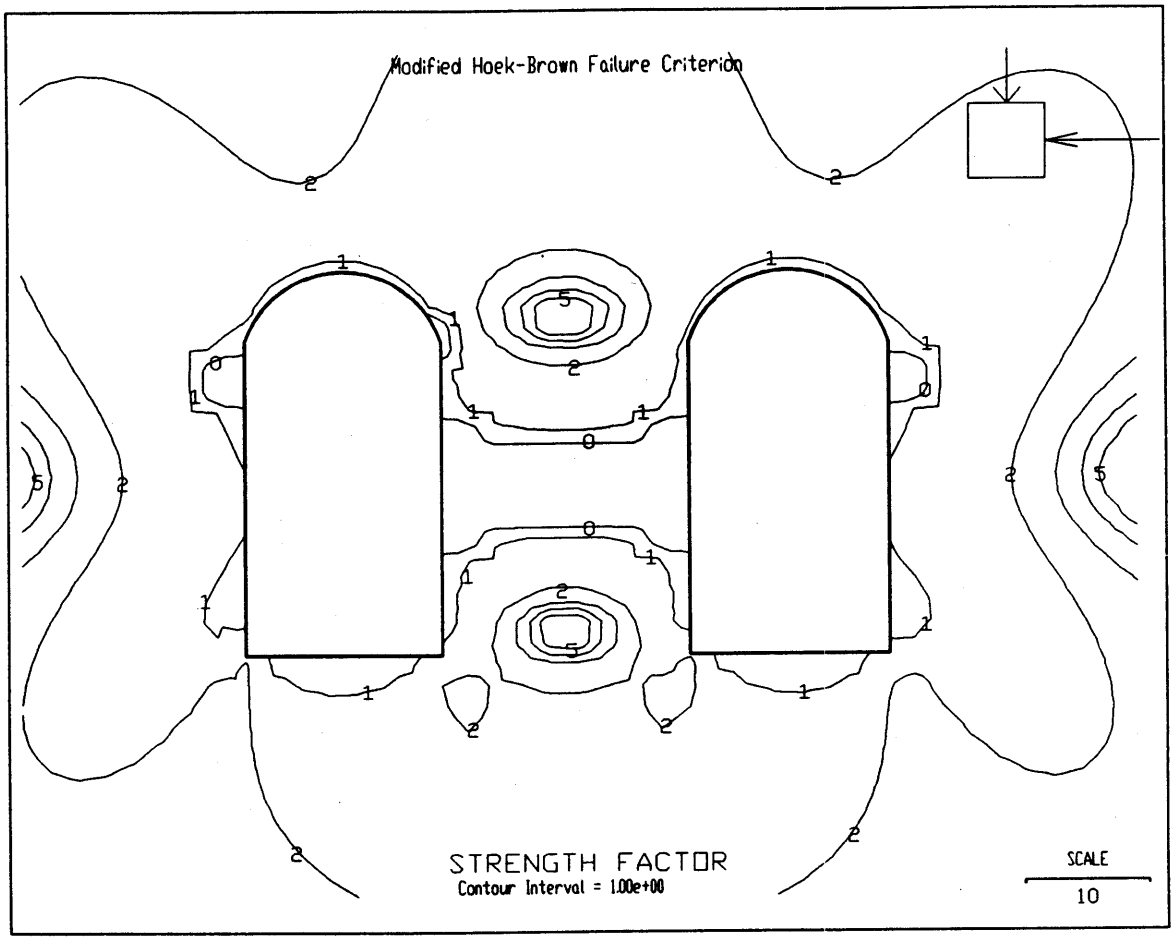

Figure 3.20: Overstress zone around excavations for Modified Hoek–Brown Criterion

1. *Tensile overstress in the Pillar*:

   The contours of zero strength factor for the *modified* criterion suggest that there is significant tensile fracturing of the rock in the pillar as compared to that predicted by the *original* criterion (Figure 3.19). It can be seen from Figure 3.18 that the value of the confining stress is less than or equal to zero in a large region in the pillar. Since the *modified* criterion assumes zero tensile strength for the rock mass, it predicts a zone of tensile fracturing of the rock mass. However, the value of the confining stresses have a very small tensile value, and hence, the tensile fracturing of the rock mass will be minimal resulting in the redistribution of the stresses in this region. From a practical point of view, for two excavations situated at close proximities with a horizontal to vertical *in situ* stress ratio of 2, there is bound to be considerable tensile fracturing in the pillar which is predicted adequately by the *modified* criterion.

2. *Zones of compressive overstress*:

   (a) In the vicinity of the boundaries of the two excavations, the *modified* criterion predicts a larger zone of shear failure in the rock mass as compared to the *original* criterion. This is due to the fact that in regions of very small compressive confining stresses, the *original* criterion predicts slightly higher strengths than the *modified* criterion. However, this difference fades away at slightly higher values of confining stresses, and the predictions of overstress by both criteria is similar. In actual field problems, larger zones of shear failure are to be expected if the excavations are located too close with high *in situ* stress ratios.

   (b) The zones of compressive overstress are larger on the outer side walls of the excavations for the *modified* criterion. This is due to lower confining stresses in these regions as the stress trajectories are deflected by the excavation. The *modified* criterion predicts a small zone of tensile fracture near the haunches of the outer sidewalls of the excavation where there are negative confining stresses.

The analysis of the two excavations at such a close proximity was presented in this section to highlight the difference in the predictions of the *original* and *modified* Hoek–Brown criterion. It has been observed that for the prevailing conditions of the layout of the excavations and the *in situ* stress ratios, the *modified* criterion provides a better explanation for the behaviour of the rock mass in the field.

3.7 Conclusions

An extensive discussion on existing failure criteria for rock has been presented in this chapter. The suitability of various failure criteria are described with special reference to the Hoek–Brown failure criterion which has gained popularity among geotechnical engineers. The *Modified Hoek–Brown failure criterion* has been introduced and its characteristics have been described. The advantage of this criterion over the *original* Hoek–Brown criterion have been successfully demonstrated with the help of a typical field problem. It has been established that the *modified* criterion gives a better fit to the laboratory strength data for *broken* rock mass, and that it predicts the behaviour of the rock mass in the low range of confining or normal stresses in a much better fashion. It has introduced a greater flexibility into the curvature of the strength envelope and has made it capable of modelling highly to slightly nonlinear trends in the envelope.

A methodology has been developed to estimate the values of the parameters m_b and a of the *Modified Hoek–Brown failure criterion* from observations of rock mass characteristics and quality made in the field. These estimates are presented in the form of a table, and in the absence of actual test data of the rock mass, the geotechnical engineer can use this table to estimate the values of m_b and a for use in subsequent analyses. It is, therefore, concluded that for predicting the behaviour of rock mass around underground excavations, the *Modified Hoek–Brown failure criterion* should be used in practice.

Chapter 4

Strength Criteria for Rockfill Materials

4.1 Introduction

As a natural extension to the development of a strength criterion for rock mass, the characteristics of existing strength criteria for rockfill materials is investigated in this chapter since their behaviour of dilation at low effective normal stress values and particle crushing at high effective normal stress values is akin to that of rock mass.

The suitability of rockfills as fill materials in embankment construction is well established. In the last two decades, there has been an increasing trend towards building high dams, mainly for hydroelectric and water resources development purposes, with a thin clay core supported by rockfill shoulders. This method of construction has been found to be safe and economical stemming from the fact that rockfills have properties of shear strength, deformability and permeability which are superior to those of earthfills.

4.2 Strength Criterion for Rockfills

In order to determine the stability of rockfill slopes, the shear strength of the rockfill material has to be obtained. Several researchers, including Marachi, Chan & Seed (1972), Marsal (1973), de Mello (1977), Charles and Watt (1980) and Charles and Soares (1984) have

presented criteria for assessing the strength of rockfills with emphasis on the design of rockfill dams. Of particular interest is the shear strength criterion proposed by Charles and Watt (1980). They carried out several large-scale drained triaxial compression tests on heavily compacted samples of different types of rockfill materials over a range of confining stresses typical of those encountered in the analysis of the stability of slopes. They found that the Mohr failure envelopes exhibit pronounced curvature particularly at low and medium confining stresses. In order to describe the shear strength of rockfills, they proposed an equation of the form

$$\tau = A\sigma_n^b \tag{4.1}$$

where,

τ = shear stress at failure;

σ_n = normal stress at failure; and

A and b are material parameters.

Charles and Watt (1980) reported the values of the material parameters A and b for sandstone, slate and basalt for a limited range of normal stresses (40 kPa < σ_n <400 kPa). These values are summarized in Table 4.1.

The important point to note about this criterion is that the parameter A is not non-dimensional; it depends upon the system of measurement of stress, i.e., *psi, kPa, MPa,* etc., and has the units of $stress^{1-b}$. This limitation leads to the fact that this material parameter cannot be generalized for all rocks of the same geological type. The value of A will be the same for the rock of the same type and origin only if the stress measurements have been made in the same system of units.

Rock Type	A	b
Sandstone	6.8	0.67
Slate (B1)	5.3	0.75
Slate (B2)	3.0	0.77
Basalt	4.4	0.81

Table 4.1: Values of Parameters A and b for various Rockfill Materials, stress measured in *kPa* (Charles & Watt)

4.3 Non-dimensional Failure Criterion

Considering the limitation of equation (4.1), a non-dimensional form of the shear strength criterion is proposed as below:

$$\frac{\tau}{\sigma_c} = \alpha \left(\frac{\sigma_n}{\sigma_c}\right)^{\beta} \tag{4.2}$$

where,

τ = shear stress at failure;

σ_n = normal stress at failure;

σ_c = uniaxial strength of intact rock; and

α and β are material parameters.

The **salient features** of this failure criterion are:

1. For this equation, the material parameters α and β are non-dimensional, and hence, can be related to rocks of the same geological type but of different origins having different values of intact strength.
2. This equation also implies that the rockfill material does not have any unconfined compressive and tensile strengths.
3. If $\sigma_c = 1$, then equation (4.2) reduces to the form of equation (4.1) and α corresponds to A and β corresponds to b. Therefore, if the unconfined compressive strength of the intact rock is not known, the parameters of equation (4.1) can be used directly provided that the stress units are defined and used in ensuing calculations in kPa.

4.3.1 Estimation of Material Parameters A and b

Charles and Soares (1984) outlined the method by which the parameters A and b of equation (4.1) were obtained. It is essential that the large scale triaxial tests be conducted on samples of the rockfill materials compacted to a dry density and a moisture content similar to that which will be obtained in the field and at appropriate confining pressures. Charles and Soares have provided a graph which can be used to obtain the maximum normal stress on the critical failure surface, and this value can be used to estimate the values of the confining pressures to be used in the triaxial tests.

At the first stage, the values of the major and minor principal stresses at failure (σ_1, σ_3) are plotted as Mohr circles on the (τ, σ_n) plane. A failure envelope can then be drawn tangential to these Mohr circles by hand, with the origin at ($\tau = 0$, $\sigma_n = 0$). A set of values of τ and σ_n is taken from this curve within the desired range of σ_n and is used to estimate A and b corresponding to equation (4.1). By taking the natural logarithm of both sides of equation (4.1), we get

$$\log \tau = b \log \sigma_n + \log A \tag{4.3}$$

Consequently if the set of points obtained from the failure envelope is replotted on log–log graph paper, a straight line is obtained with a gradient of b and an intercept of $\log A$. An alternative to this step is to carry out linear regression analysis on the set of (τ , σ_n) points using equation (4.3) which is the linearized version of equation (4.1). However, it should be realized that linear regression analysis has its limitations when applied for fitting a nonlinear failure curve through experimental data points as discussed in Chapter 2 and in Shah and Hoek (1992), especially when the data points are not evenly spaced and have scatter.

4.3.2 Estimation of Parameters α and β from Triaxial Test Data

A similar technique as outlined in the previous section can be used to determine the parameters α and β of equation (4.2) from a triaxial test data set. However, in order to overcome the inaccuracies introduced in the fitting of data by hand or the inaccuracies of the linear regression technique for fitting a nonlinear curve through a set of data points, a more rigorous method is presented here which utilizes the Simplex Reflection Technique (Nash (1979), Shah and Hoek, 1992) of curve-fitting as explained in Chapter 2. This method comprises of a two-step process, in which, in the first step, the triaxial test data is fitted to a curve similar to equation (4.2), but it relates the major and minor principal stresses at failure as follows:

$$\frac{\sigma_1}{\sigma_c} = \alpha' \left(\frac{\sigma_3}{\sigma_c}\right)^{\beta'} \tag{4.4}$$

where,

σ_1 = major principal stress at failure;

σ_3 = minor principal stress at failure; and

α' and β' are non-dimensional material parameters.

The experimental triaxial test data is fitted to equation (4.4) using the Simplex Reflection technique which is described in sections 2.4 and 2.4.1.

4.3.3 Estimation of α' and β'

In order to use the Simplex Reflection analysis to fit the triaxial data to equation (4.4) and to obtain the parameters α' and β', the function $\mathcal{S}$ to be minimized is the sum of the square of the residuals, $\sum \epsilon^2$, of the calculated σ_1 and the experimental σ_1, i.e.,

$$\mathcal{S} = \sum \epsilon^2 = \sum_{i=1}^{n} \left(\sigma_{1i_{calculated}} - \sigma_{1i_{experimental}} \right)^2 = \text{minimum} \tag{4.5}$$

where,

n = number of data pairs.

The number of parameters in this equation are two, viz., α' and β', and therefore, the *simplex* formed will have three vertices, i.e., it is a triangle with the coordinate pair (α', β'). The initial values of the parameters α' and β' can be taken as 1.0 and 0.5, respectively, and the step values can be taken as 0.1 and 0.01, respectively. The *simplex* procedure continues until the following test conditions are satisfied:

$$\begin{aligned} \left(\mathcal{S}(b_H) - \mathcal{S}(b_L)\right) / \mathcal{S}(b_H) &\leq \text{tolerance for residuals} = 0.00001 \\ \left(\alpha'_H - \alpha'_L\right) / \alpha'_H &\leq \text{tolerance for } \alpha' = 0.001 \\ \left(\beta'_H - \beta'_L\right) / \beta'_H &\leq \text{tolerance for } \beta' = 0.0001 \end{aligned} \tag{4.6}$$

where,

b_H = highest point of simplex, i.e., point at which $\mathcal{S}$ is maximum;
b_L = lowest point of simplex, i.e., point at which $\mathcal{S}$ is minimum;
α'_H and α'_L are the values of α' at the highest and lowest points, respectively; and
β'_H and β'_L are the values of β' at the highest and lowest points, respectively.

This minimization process results in the values of α' and β' which are used in the second step of the analysis.

In the second step, a set of τ and σ_n values are generated by applying the solutions derived by Balmer (1952) for obtaining the values of τ and σ_n for a nonlinear Mohr envelope

from triaxial test data. These are as follows:

$$\tau = \frac{\sigma_1 - \sigma_3}{\frac{\partial\sigma_1}{\partial\sigma_3} + 1}\sqrt{\frac{\partial\sigma_1}{\partial\sigma_3}} \tag{4.7}$$

and

$$\sigma_n = \sigma_3 + \frac{\sigma_1 - \sigma_3}{\frac{\partial\sigma_1}{\partial\sigma_3} + 1} \tag{4.8}$$

Taking the partial derivative of σ_1 with respect to σ_3 for the relation given by equation (4.4) we get,

$$\frac{\partial\sigma_1}{\partial\sigma_3} = \alpha'\beta'\left(\frac{\sigma_3}{\sigma_c}\right)^{\beta'-1} \tag{4.9}$$

Substituting equations (4.4) and (4.9) into equations (4.7) and (4.8) and solving for τ and σ_n, we get

$$\tau = \frac{\sigma_1 - \sigma_3}{\alpha'\beta'\left(\frac{\sigma_3}{\sigma_c}\right)^{\beta'-1} + 1}\sqrt{\alpha'\beta'\left(\frac{\sigma_3}{\sigma_c}\right)^{\beta'-1}} \tag{4.10}$$

and

$$\sigma_n = \sigma_3 + \frac{\sigma_1 - \sigma_3}{\alpha'\beta'\left(\frac{\sigma_3}{\sigma_c}\right)^{\beta'-1} + 1} \tag{4.11}$$

The values of σ_3/σ_c at which τ/σ_c and σ_n/σ_c are calculated are taken in a geometric progression in order to capture the highly nonlinear nature of the curve in the region near the origin. These values are as listed below:

$$\frac{\sigma^0_{3m}}{256},\ \frac{\sigma^0_{3m}}{128},\ \frac{\sigma^0_{3m}}{64},\ \frac{\sigma^0_{3m}}{32},\ \frac{\sigma^0_{3m}}{16},\ \frac{\sigma^0_{3m}}{8},\ \frac{\sigma^0_{3m}}{4},\ \frac{\sigma^0_{3m}}{2},\ \sigma^0_{3m} \tag{4.12}$$

where,

$\sigma^0_{3m} = \sigma_{3m}/\sigma_c =$ the normalized maximum confining pressure in the given triaxial data set.

Once these values of τ/σ_c and σ_n/σ_c are generated, they are fitted to equation (4.2) using the Simplex Reflection technique to obtain the parameters α and β. The function $\mathcal{S}$ to be minimized in this case is the sum of the square of the residuals, $\sum \epsilon^2$, of the calculated and the generated values of τ, i.e.,

$$\mathcal{S} = \sum \epsilon^2 = \sum_{i=1}^{n}\left(\tau_{i_{calculated}} - \tau_{i_{generated}}\right)^2 = \text{minimum} \tag{4.13}$$

where,

$n = 9$, the number of generated data pairs.

The Simplex procedure is performed till the conditions of equation (4.6) are satisfied except that α' and β' in equation (4.6) are replaced by α and β. The starting point and the steps for the initial *simplex* can be taken as that for α' and β'.

4.3.4 Estimation of Strength Parameters from Shear Test Data

For the case in which the experimental data is from shear tests, the reverse procedure is adopted to obtain the values of the material parameters α and β, and α' and β'. The difference in this procedure is in the generation of the triaxial data from the fitted Mohr envelope.

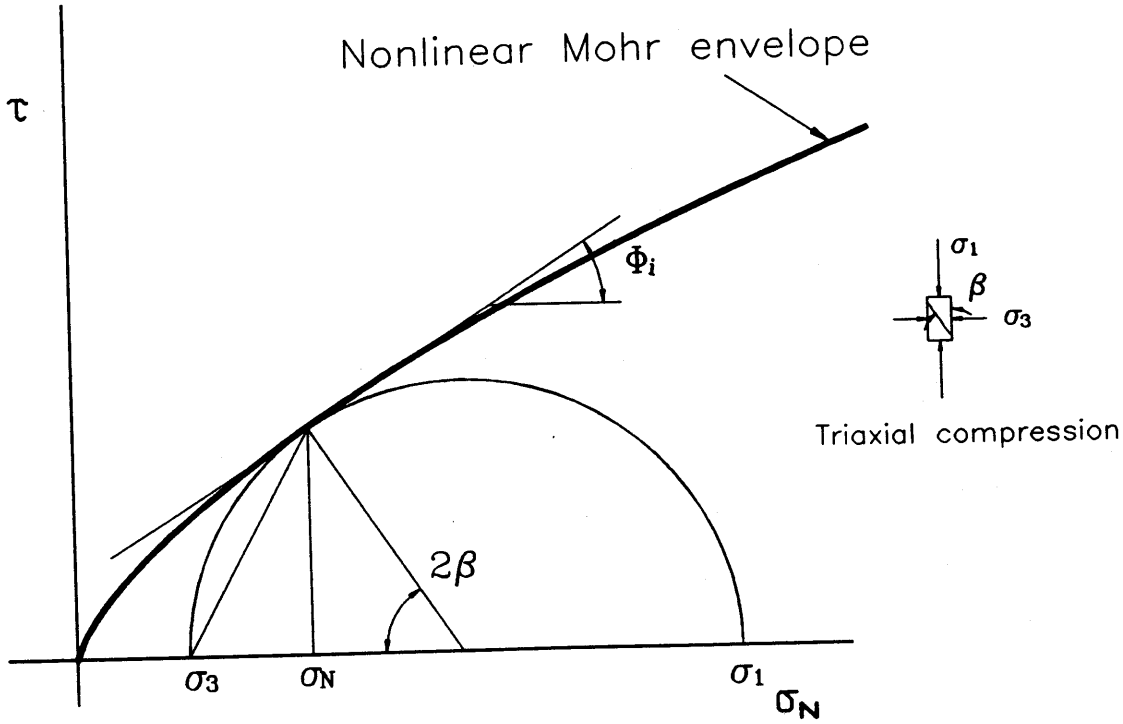

Figure 4.1: Balmer's solution for Nonlinear Mohr envelopes

As a first step, the shear test data is fitted to equation (4.2) using the Simplex Reflection Technique to obtain the parameters α and β. The function S to be minimized

in this case is

$$\mathcal{S} = \sum \epsilon^2 = \sum_{i=1}^{n} \left(\tau_{i_{calculated}} - \tau_{i_{experimental}} \right)^2 = \text{minimum} \tag{4.14}$$

where,

n = number of experimental data pairs.

For the Simplex procedure, the initial values of the variables, α and β are taken as 1.0 and 0.5, respectively, and the step values for the formation of the *initial* simplex are 0.1 and 0.01. This curve-fitting procedure results in the values of the strength parameters α and β.

The next step involves the generation of the triaxial strength values corresponding to this nonlinear Mohr envelope. Due to the nonlinear nature of the strength envelope, the values of σ_1 and σ_3 have to be generated in a nonlinear manner. This process is achieved as described below. From Figure 4.1,

$$\tan \phi_i = \frac{d(\tau/\sigma_c)}{d(\sigma_n/\sigma_c)} = \alpha\beta \left(\frac{\sigma_n}{\sigma_c}\right)^{\beta-1} \tag{4.15}$$

where,

ϕ_i = the instantaneous friction angle.

The values of σ_1 and σ_3 corresponding to (σ_n, τ) are calculated as

$$\frac{\sigma_3}{\sigma_c} = \frac{\sigma_n}{\sigma_c} - \frac{\tau/\sigma_c}{\tan\left(\frac{\pi}{4} + \frac{\phi_i}{2}\right)} \tag{4.16}$$

and

$$\frac{\sigma_1}{\sigma_c} = \frac{\sigma_n}{\sigma_c} + \frac{\tau}{\sigma_c}(\tan \phi_i + \cos \phi_i) \tag{4.17}$$

From equation (4.15),

$$\cos \phi_i = \frac{1}{\sqrt{1 + \alpha^2\beta^2 \left(\frac{\sigma_n}{\sigma_c}\right)^{2(\beta-1)}}} \tag{4.18}$$

and

$$\sin \phi_i = \frac{\alpha\beta \left(\frac{\sigma_n}{\sigma_c}\right)^{\beta-1}}{\sqrt{1 + \alpha^2\beta^2 \left(\frac{\sigma_n}{\sigma_c}\right)^{2(\beta-1)}}} \tag{4.19}$$

Substituting equations (4.18) and (4.19) in equation (4.17),

$$\frac{\sigma_1}{\sigma_c} = \frac{\sigma_n}{\sigma_c} + \frac{\tau}{\sigma_c}\left(\alpha\beta \left(\frac{\sigma_n}{\sigma_c}\right)^{\beta-1} + \sqrt{1 + \alpha^2\beta^2 \left(\frac{\sigma_n}{\sigma_c}\right)^{2(\beta-1)}}\right) \tag{4.20}$$

Using the trigonometric relation between full and half angles

$$\tan\phi_i = \frac{2\tan\frac{\phi_i}{2}}{1-\tan^2\frac{\phi_i}{2}} \tag{4.21}$$

and substituting the value of $\tan\phi_i$ from equation (4.15),

$$\alpha\beta\left(\frac{\sigma_n}{\sigma_c}\right)^{\beta-1}\tan^2\frac{\phi_i}{2} - 2\tan\frac{\phi_i}{2} - \alpha\beta\left(\frac{\sigma_n}{\sigma_c}\right)^{\beta-1} = 0 \tag{4.22}$$

Solving this quadratic equation for $\tan\frac{\phi_i}{2}$ and taking the positive root for real values,

$$\tan\frac{\phi_i}{2} = \frac{1+\sqrt{1+\alpha^2\beta^2\left(\frac{\sigma_n}{\sigma_c}\right)^{2(\beta-1)}}}{\alpha\beta\left(\frac{\sigma_n}{\sigma_c}\right)^{\beta-1}} \tag{4.23}$$

or,

$$\tan\frac{\phi_i}{2} = \cot\phi_i + \frac{1}{\sin\phi_i} \tag{4.24}$$

Hence,

$$\tan\left(\frac{\pi}{4}+\frac{\phi_i}{2}\right) = \frac{1+\cot\phi_i+\frac{1}{\sin\phi_i}}{1-\cot\phi_i-\frac{1}{\sin\phi_i}} \tag{4.25}$$

Substituting this in equation (4.16),

$$\frac{\sigma_3}{\sigma_c} = \frac{\sigma_n}{\sigma_c} - \frac{\tau}{\sigma_c}\left[\frac{\alpha\beta\left(\frac{\sigma_n}{\sigma_c}\right)^{\beta-1} - 1 - \sqrt{1+\alpha^2\beta^2\left(\frac{\sigma_n}{\sigma_c}\right)^{2(\beta-1)}}}{\alpha\beta\left(\frac{\sigma_n}{\sigma_c}\right)^{\beta-1} + 1 + \sqrt{1+\alpha^2\beta^2\left(\frac{\sigma_n}{\sigma_c}\right)^{2(\beta-1)}}}\right] \tag{4.26}$$

The values of σ_n/σ_c at which σ_1/σ_c and σ_3/σ_c are calculated are taken in a geometric progression in order to capture the nonlinear nature of the curve in the region near the origin. These values are as listed below:

$$\frac{\sigma^0_{nm}}{256},\ \frac{\sigma^0_{nm}}{128},\ \frac{\sigma^0_{nm}}{64},\ \frac{\sigma^0_{nm}}{32},\ \frac{\sigma^0_{nm}}{16},\ \frac{\sigma^0_{nm}}{8},\ \frac{\sigma^0_{nm}}{4},\ \frac{\sigma^0_{nm}}{2},\ \sigma^0_{nm} \tag{4.27}$$

where,

$\sigma^0_{nm} = \sigma_{nm}/\sigma_c =$ the normalized maximum normal stress in the given shear data set.

These values of σ_3/σ_c and σ_1/σ_c are then fitted to equation (4.4) using the Simplex Reflection technique to obtain the parameters α' and β'. The function $\mathcal{S}$ to be minimized in this step is the sum of the square of the residuals, $\sum\epsilon^2$, of the calculated and generated values of σ_1, i.e.,

$$\mathcal{S} = \sum\epsilon^2 = \sum_{i=1}^{n}\left(\sigma_{1_{calculated}} - \sigma_{1_{generated}}\right)^2 = \text{minimum} \tag{4.28}$$

where,

$n = 9$, the number of generated data pairs.

The Simplex procedure is applied till the conditions of equation (4.6) are satisfied. The starting point and the steps for the initial *simplex* are to be taken as described in section 4.3.3.

σ_3 (kPa)	σ_1 (kPa)
27	362
92	714
282	1482
695	2962

Table 4.2: Triaxial Test Data for Sandstone Rockfill (Charles & Watt)

Example of Triaxial data An example is presented for the analysis of triaxial test data provided in Charles and Watt (1980) for sandstone rockfill material (Table 4.2) in order to determine the parameters of the triaxial and shear strength envelopes. The results of the analysis are provided in Table 4.3 and a comparison of the values for the shear strength parameters, α and β, with the parameters, A and b, of Charles and Watt is shown in Table 4.4. The analysis of the data was carried out for $\sigma_c = 120,000$ kPa.

Step 1.	$\alpha' = 0.957$	$\beta' = 0.7115$	(Triaxial	parameters)
Balmer's solution	σ_3/σ_c	σ_1/σ_c	σ_n/σ_c (generated)	τ/σ_c (generated)
	0.000023	0.000474	0.000051	0.000110
	0.000045	0.000776	0.000101	0.000193
	0.000090	0.001270	0.000198	0.000339
	0.000181	0.002080	0.000388	0.000592
	0.000362	0.003406	0.000758	0.001024
	0.000724	0.005577	0.001473	0.001753
	0.001448	0.009133	0.002848	0.002967
	0.002896	0.014956	0.005476	0.004945
	0.005792	0.024490	0.010456	0.008091
Step 2.	$\alpha = 0.285$	$\beta = 0.779$	(shear	parameters)

Table 4.3: Results of analysis of sandstone rockfill material ($\sigma_c = 120,000$ kPa)

In the first step of the analysis, the triaxial test data were fitted to equation (4.4)

	$\sigma_c = 120,000$ kPa	$\sigma_c = 1$	Charles & Watt
α	0.285	3.73	$A = 6.8$
β	0.779	0.779	$b = 0.67$
$\sum \epsilon^2$	6.42e-9	92.5	

Table 4.4: Results of analysis for Sandstone Rockfill

	$\sigma_c = 120,000$ kPa	$\sigma_c = 1$
α'	0.957	27.93
β'	0.7115	0.7115
$\sum \epsilon^2$	6.95e-7	10010.3
α	0.285	3.73
β	0.779	0.779
$\sum \epsilon^2$	6.42e-9	92.5

Table 4.5: Comparison of results of analysis for Sandstone Rockfill

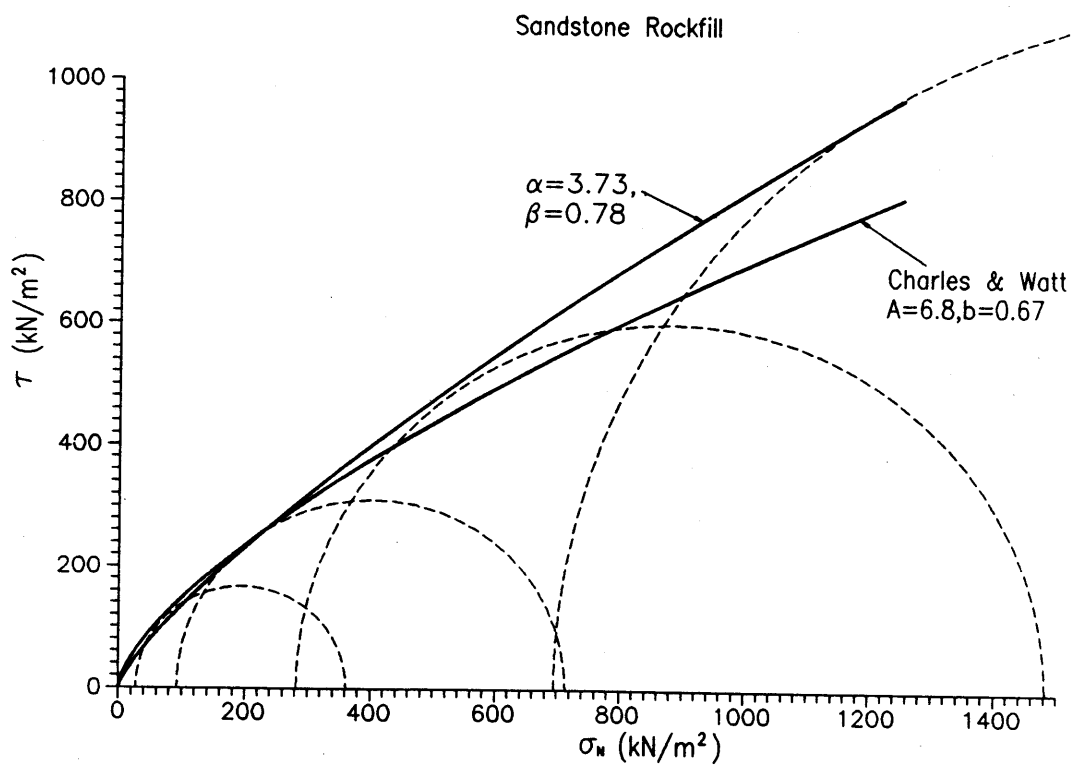

Figure 4.2: Comparison of results for Sandstone Rockfill

using the Simplex Reflection technique and the triaxial strength parameters α' and β' were obtained as 0.957 and 0.7115, respectively. Then equations (4.10) and (4.11) were used to generate the values of the normal and shear stresses for the set of values of the normalized confining pressures given by equation (4.12). Finally, these generated values were fitted to equation (4.2) using the Simplex Reflection technique to get the values of the shear strength parameters α and β as 0.285 and 0.779, respectively. The values of the parameters α and β are summarized in Table 4.4 for $\sigma_c = 120,000$ kPa and $\sigma_c = 1$, the latter corresponding to Charles and Watts' criterion. The corresponding values of A and b are also shown in Table 4.4. Table 4.5 contains the values of the strength parameters α', β', α and β for $\sigma_c = 120,000$ kPa and $\sigma_c = 1$. It can be observed from this table that the parameters controlling the curvature of both the envelopes, i.e. β' and β, are the same for any value of σ_c, but the values of the parameters α' and α change with a change in the value of σ_c.

The shear strength envelopes for the proposed non-dimensional criterion and the criterion proposed by Charles and Watt are drawn on the (σ_n, τ) plane in Figure 4.2 along with the Mohr circles corresponding to the principal stresses at failure. Charles and Watt considered a range of normal stress between 40 kPa and 400 kPa. If the two envelopes are compared in this range of normal stresses, it can be observed that the proposed criterion, with the more rigorous procedure for fitting data, gives a better fit to the experimental data, and hence, this criterion is better suited to the stability analysis of rockfills.

σ_n (MPa)	τ (MPa)
0.29	0.45
0.65	0.75
1.36	1.23
2.55	1.84
4.87	2.79

Table 4.6: Shear Test Data for Weathered Greywacke Joints (Martin & Miller)

Example of Shear Data An example of determining the shear strength and triaxial strength parameters from direct shear test data (Table 4.6) on weathered Greywacke joints (Martin and Miller, 1974) is demonstrated in this section. The uniaxial compressive strength of the intact rock was 80 MPa. The results of the analysis are shown in Table 4.7 and the

nonlinear triaxial and Mohr strength envelope are plotted in Figure 4.3.

Step 1.	$\alpha = 0.213$	$\beta = 0.6469$	(shear	parameters)
Nonlinear solution	σ_n/σ_c	τ/σ_c	σ_3/σ_c (generated)	σ_1/σ_c (generated)
	0.000238	0.000966	0.000415	0.005490
	0.000476	0.001512	0.000824	0.007045
	0.000951	0.002368	0.001626	0.009254
	0.001902	0.003708	0.003194	0.012545
	0.003805	0.005806	0.006231	0.017695
	0.007609	0.009091	0.012073	0.026126
	0.015219	0.014235	0.023243	0.040472
	0.030437	0.022291	0.044542	0.065664
	0.060875	0.034904	0.085155	0.111050
Step 2.	$\alpha' = 0.639$	$\beta' = 0.718$	(triaxial	parameters)

Table 4.7: Intermediate and Final results of analysis of Weathered Greywacke Joints ($\sigma_c = 80$ MPa)

	$\sigma_c = 80$ MPa	$\sigma_c = 1$
α	0.213	1.002
β	0.647	0.647
$\sum \epsilon^2$	2.09e-8	1.3e-4
α'	0.639	2.19
β'	0.718	0.718
$\sum \epsilon^2$	5.23e-5	0.334

Table 4.8: Comparison of results of analysis for Weathered Greywacke Joints

As shown in Table 4.7, at first, the shear test data were fitted to the nonlinear shear strength envelope defined by equation (4.2) using the Simplex Reflection technique, and the shear strength parameters α and β were obtained as 0.213 and 0.6469, respectively. In the second step of the analysis, a set of σ_3 and σ_1 values were generated according to equations (4.26) and (4.20) for the values of the normalized normal stress given in equation (4.27). This set of generated data was then fitted to the nonlinear triaxial strength envelope described by equation (4.4). The value of the triaxial strength parameters α' and β' were

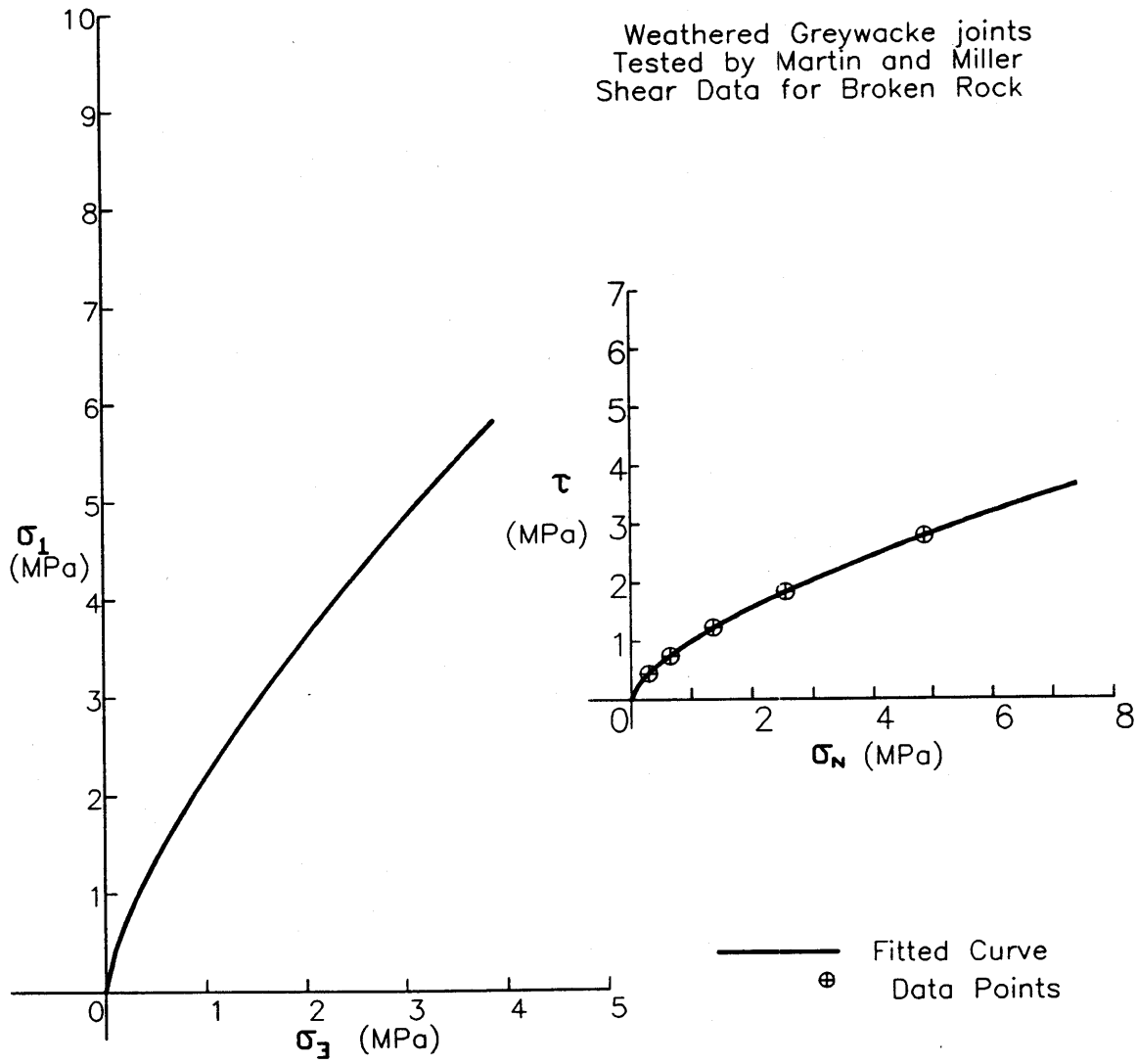

Figure 4.3: Results of analysis of Shear data for Weathered Greywacke joints

obtained as 0.639 and 0.718, respectively. In Table 4.8, the values of the four strength parameters, α, β, α' and β' are compared for $\sigma_c = 80$ MPa and $\sigma_c = 1$. As observed in the case of the example for triaxial test data, it can be deduced from this table that the values of the parameters controlling the curvature of the envelopes β and β' are independent of σ_c, but the parameters α and α' depend on the value of the σ_c.

A micro-computer program, ROCKFILL, which incorporates the procedures presented in this chapter for the determination of strength parameters of rockfill materials, has been developed by the author in 1991 and is available from the Department of Civil Engineering in the University of Toronto.

4.4 Conclusions

A non-dimensional form of the strength criterion for rockfill materials has been presented in this chapter in the shear as well as principal stress form. With the examples discussed in the previous section, it is evident that the proposed strength criteria for rockfill materials, and the method of obtaining the parameters of these criteria, is far superior to that proposed by Charles and Watt. It has been found (Shah and Hoek, 1992) that the new method gives excellent fit to laboratory test data, and introduces the flexibility of obtaining parameters of either the shear strength or triaxial strength envelopes or both from either triaxial or shear test data.

Chapter 5

Constitutive Relations for Rock Mass

5.1 Introduction

Constitutive or stress–strain laws or models of engineering materials play a significant role in providing reliable results from any solution procedure. Their importance has been enhanced significantly with the tremendous increase in development and application of many modern computer-based techniques such as the finite element, finite difference and boundary integral equation methods.

The simplest constitutive laws used in engineering are linear such as the Hooke's law. These laws are valid only for a very limited class of materials because most engineering systems are nonlinear and complex. The influence of nonlinear response becomes more prominent in the case of materials that are influenced by factors such as the state of stress, residual or initial stress, volume changes under shear, stress history or stress paths, inherent and induced anisotropy, change in the physical state, and fluid in the pores.

The rapidly growing use of three-dimensional finite element and other numerical simulations require sophisticated constitutive models which reproduce the prevalent material characteristics for every conceivable load history. Even elementary strength assessments in the form of ultimate load analyses necessitate realistic constitutive relations which remain fully operational during nonproportional and nonmonotonic loading, as progressive failure is

invariably accompanied by the localization of deformations and elastic unloading (Pramono and Willam, 1989). Thus, the local constitutive relations must cover the entire spectrum of triaxial strength, stiffness as well as fragility in tension and low confined compression when brittle–ductile materials such as concrete, soil or rock are considered.

An important phenomenon manifested by the rock mass in the vicinity of underground openings is their nonlinear response to induced stresses. *In situ* observations and experimental results show that this is caused by a combination of pre-peak nonlinear elasticity and post-peak behaviour. After failure, a rock mass may exhibit strain softening, perfect plastic or strain hardening behaviour depending on confining pressure, rate of loading and rheological characteristics of the rock mass (Pan and Hudson, 1988). For the mechanical description of nonlinear post failure behaviour of a rock mass, a yield criterion based on the theory of plasticity is usually used.

The *theory of plasticity* is an essential extension of the theory of elasticity as it deals with the analysis of stresses and strains in the structure in the plastic as well as elastic range of stresses. The combined effect of unknown initial stress, secondary stresses, and stress concentrations and redistribution due to discontinuities in the rock mass cannot be predicted accurately by the theory of elasticity, and therefore, the theory of plasticity has to be resorted to. It provides more realistic predictions for the strength and deformation in the rock mass. The engineer responsible for the design of any structure in the rock mass can get a better understanding of the role of the relevant mechanical variables that define the characteristic reaction of the rock mass to the applied or induced force field.

It should be emphasized that both the theory of elasticity and the theory of plasticity are phenomenological in nature. They are the mathematical formalization of experimental observations of the macroscopic behaviour of a deformable solid and do not inquire deeply into the microscopic, physical and chemical basis of this behaviour. Thus, the *mathematical theory* rather than the *physical theory* of plasticity is of interest to engineers.

The first task of the theory of plasticity is to set up relationships between stress and strain under a complex stress state that can adequately describe the observed deformation in the material. This theory has been well established for predicting the deformation behaviour of metals, in general, and in the last two decades, it has been applied to the prediction of the deformation behaviour of nonmetallic or geologic materials such as soil, rock and concrete.

The second task of this theory is to develop numerical solution techniques in order to incorporate these constitutive laws in the analysis of engineering structures. The nonlinear nature of the plastic deformation rules cause considerable difficulty in the solution of the basic equations of solid mechanics. This problem has been overcome by the incredible development of high-speed computers and techniques of finite element, finite difference and boundary integral equation methods. These developments have provided the engineer with powerful numerical tools that can be used for the solution of virtually any nonlinear problem. They have also provoked newer developments and wider applications of the plasticity theory.

It has now been realized by engineers and researchers that developments and sophistication in numerical solution techniques have by far exceeded the knowledge and comprehension of the behaviour of the materials defined by constitutive laws. The use of simple or less adequate constitutive models in the analysis of complex structures with these highly sophisticated solution techniques can result in predictions which will be of limited or doubtful validity.

It was with this realization in mind that the development of constitutive relations for rock mass was undertaken, and this subject is presented in this chapter. The constitutive relations for rock mass have been developed on the basis of the theory of plasticity with the Hoek–Brown criterion taken as the yield criterion for the rock mass. The deformational rules of the theory of plasticity have been incorporated in these constitutive relations and they are presented in a form that can be implemented directly in a numerical solution technique such as the finite element method. The inelastic dilation behaviour of rock mass has also been modelled with the development of a non-associative flow rule. The constitutive relations have been developed to model the rock mass as an elastic–perfectly plastic material in order to enhance the ease of using the model for practical rock engineering applications in the design of underground excavations where there is little information on post–failure behaviour of rock mass due to the immense cost of conducting tests on rock mass specimens in the pre-peak as well as post-peak regions of stress.

5.2 Definition of Constitutive Law

As stated in Desai and Siriwardane (1984), a **constitutive law** or **model** represents a mathematical model that describes our ideas of the behaviour of a material. In other words, a constitutive law simulates physical behaviour that has been perceived mentally. The main advantage of establishing a mathematical model is to apply the ideas for solving complex events quantitatively. Therefore, the power of a constitutive model depends on the extent to which the physical phenomenon has been understood and simulated. A solution to a boundary value problem in continuum mechanics requires constitutive equations in addition to the governing field equations. The basic principles governing Newtonian mechanics are

1. conservation of mass;
2. conservation of momentum;
3. conservation of angular momentum;
4. conservation of energy; and
5. laws of thermodynamics.

These principles are considered to be valid for all materials irrespective of their internal constitution. Therefore, a unique solution to a boundary value problem in continuum mechanics cannot be obtained only with the application of governing field equations. Hence, a unique determination of the response requires additional considerations that account for the nature of different materials. The equations that model the behaviour of a material are known as "constitutive equations" or "constitutive laws" or "constitutive models". Therefore, a **constitutive equation** can be defined as a mathematical model that can permit reproduction of the observed response of a continuous medium.

5.2.1 Steps in the Development of a Constitutive Law

Development of a viable constitutive law for successful implementation in numerical solution techniques is considered to consist of five main steps (Desai and Siriwardane, 1984) as listed below:

1. Mathematical formulation;

2. Identification of significant parameters;

3. Determination of parameters from laboratory tests, and verification, which can involve the following two additional steps:

4. Successful prediction of a majority of observed data from which the parameters were determined, and of other test data under different stress paths;

5. Satisfactory comparisons between predictions from a solution scheme in which the constitutive law is introduced, and observations or closed-form solutions for relevant practical boundary value problems.

The development of the constitutive model for rock mass described in this chapter incorporates all of these steps. The *mathematical formulation* of the model is based on the *theory of plasticity* with the Hoek–Brown criterion defining the yield criterion for rock mass. The *parameters* of the model deemed to be significant in describing the model are the material parameters m, s and σ_c of the Hoek–Brown criterion, Young's modulus (E) and poisson's ratio (ν), and a parameter controlling the inelastic dilation of the rock mass. The parameters m, s, σ_c, E and ν can be easily determined from triaxial tests, in situ tests or from standard tables available in the literature. The inelastic dilation parameter can be obtained from triaxial tests or, in case this parameter is not available, the engineer can use his or her judgement. The *successful prediction* of a majority of test cases, including uniaxial and triaxial tests, and comparison of the predictions of this model with standard solutions and observations is presented in Chapter 6.

5.3 Incremental Theory of Plasticity

In developing constitutive equations for materials, two basic approaches have been used. The first type of formulation is the *deformational theory* in the form of total stress-strain relations. This theory assumes that the state of stress determines the state of strain uniquely as long as the plastic deformation continues. However, the total stress-strain relation based on deformation theory is only valid in the case of *proportional loading*, and is found to

be inadequate in describing the phenomena associated with loading and unloading near the yield surface along a neutral loading path.

The second theory is the *incremental theory* or *flow theory*. This type of formulation relates the increment of plastic strain components $d\epsilon_{ij}^{p}$ to the state of stress σ_{ij}, and the stress increment $d\sigma_{ij}$. The simplest type of flow theory is the *theory of perfect plasticity*.

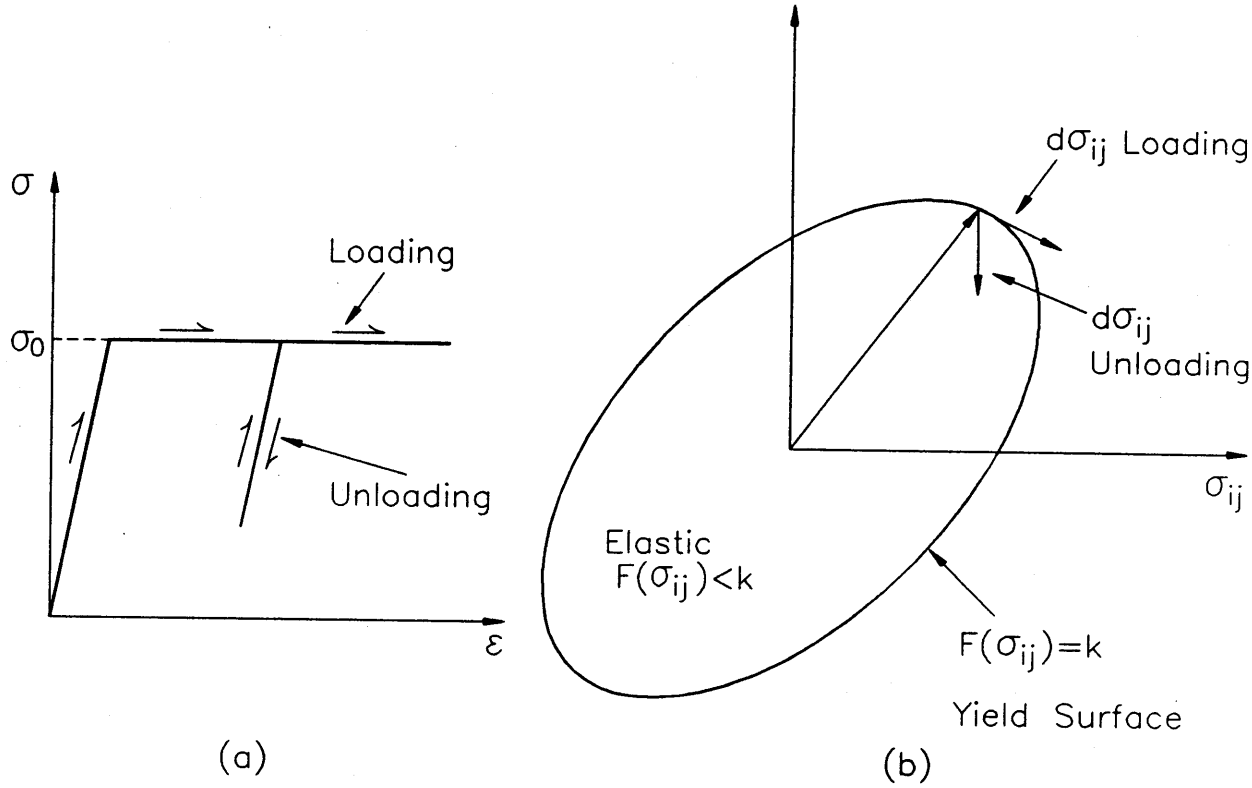

Figure 5.1: An elastic-perfectly plastic material. (a) Uniaxial stress-strain relation; (b) geometric representation of yield surface and criterion of loading and unloading

For many practical applications, a material may be idealized and assumed to have a negligible strain-hardening effect, i.e., its uniaxial stress-strain diagram beyond the yield point can be approximated by a horizontal straight line, with a constant stress level σ_o (Figure 5.1). Thus, plastic deformation is assumed to occur under a constant flow stress. This behaviour is called *perfectly* or *ideally plastic* behaviour. This idealization leads to a drastic simplification of the analysis of a complex problem. In particular, the upper- and lower-bound theorems can be established for a perfectly plastic material, from which

simple, direct and realistic methods for estimating the load-carrying capacity of structures in a direct manner can be developed.

This chapter deals with the stress-strain relation of rock mass assumed to be an isotropic, elastic-perfectly plastic material with the Hoek–Brown criterion taken as the yield criterion. The justification for the development of an elastic-perfectly plastic material model for rock mass is, firstly, the simplicity of its use for analyzing practical underground excavation problems, and secondly, the lack of sufficient data for the post-peak behaviour of rock mass during the design of an underground excavation. With the development of a simple elasto-plastic model with few parameters, a number of parametric studies can be carried out by varying these parameters in order to achieve an optimum design.

The stress-strain relation in the uniaxial case as shown in Figure 5.1 is rather simple. However, the general behaviour of the material under a complex stress state is not so straightforward since it involves six stress and six strain components. The development of the stress-strain relationships for any general combined state of stress in the rock mass is presented in subsequent sections. The major aspects involved in the development of the incremental theory of plasticity include:

1. The *existence* of an initial *initial yield* surface which defines the elastic limit of the material in a multiaxial state of stress;

2. The *flow rule* which is related to a plastic potential function and defines the direction of the incremental plastic strain vector in strain space; and

3. The *hardening rule* which describes the evolution of subsequent yield surfaces. The strength of a *perfectly plastic* material remains constant once it reaches its yield limit. Therefore, for such materials subsequent yield surfaces do not evolve, but the initial yield surface remains unchanged throughout the loading history.

These components of the incremental theory of plasticity are discussed in the following sections.

5.3.1 Yield Criterion

The *yield criterion* defines the limit of elastic deformation of a material under a multiaxial state of stress. For a one-dimensional state of stress, the yield criterion can be easily visualized: for instance, quantities such as measures of uniaxial compressive or uniaxial tensile strength. However, under a multiaxial state of stress this becomes complicated, and a mathematical expression involving all the stresses is required. Hence, the yield condition can generally be expressed as

$$f(\sigma_{ij}, k_1, k_2, \cdots) = 0 \tag{5.1}$$

where,

σ_{ij} is the stress tensor representing all the stresses;

k_1, k_2, $\cdots$ are material constants which are to be determined experimentally;

For isotropic materials, the orientation of the principal stresses is immaterial, and the values of the three principal stresses suffice to describe the state of stress uniquely. A yield criterion therefore consists in a relation of the form

$$f(\sigma_1, \sigma_2, \sigma_3, k_1, k_2, \cdots) = 0 \tag{5.2}$$

According to Nayak and Zienkiewicz (1972), the three principal stresses are related to the invariants of the stress tensor by the following relations

$$\begin{pmatrix} \sigma_1 \\ \sigma_2 \\ \sigma_3 \end{pmatrix} = \frac{1}{3}\begin{pmatrix} I_1 \\ I_1 \\ I_1 \end{pmatrix} + \frac{2\sqrt{J_2}}{\sqrt{3}}\begin{pmatrix} \cos\theta \\ \cos(\theta - 2\pi/3) \\ \cos(\theta + 2\pi/3) \end{pmatrix} \tag{5.3}$$

$$= \frac{1}{\sqrt{3}}\begin{pmatrix} \xi \\ \xi \\ \xi \end{pmatrix} + \frac{\sqrt{2}\rho}{\sqrt{3}}\begin{pmatrix} \cos\theta \\ \cos(\theta - 2\pi/3) \\ \cos(\theta + 2\pi/3) \end{pmatrix} \tag{5.4}$$

where, I_1 is first invariant of stress tensor σ_{ij}; J_2 is second invariant of deviatoric stress tensor and they are given by

$$I_1 = \sigma_{kk} \tag{5.5}$$

$$J_2 = \frac{1}{2}s_{ij}s_{ij} \tag{5.6}$$

where s_{ij} = deviatoric stress tensor and is expressed as

$$s_{ij} = \sigma_{ij} - \frac{1}{3} I_1 \delta_{ij} \tag{5.7}$$

δ_{ij} is Kronecker delta whose components are given by

$$\delta_{ij} = \begin{cases} 1, & \text{if } i = j; \\ 0, & \text{if } i \neq j. \end{cases} \tag{5.8}$$

ξ, ρ and θ are the coordinates of the Haigh-Westergaard stress space and are related to I_1, J_2 and J_3 (third invariant of deviatoric stress tensor) by

$$\xi = I_1/\sqrt{3} \tag{5.9}$$

$$\rho = \sqrt{2J_2} = \sqrt{3}\tau_{oct} \tag{5.10}$$

where τ_{oct} is the octahedral shear stress;

$$\cos 3\theta = \frac{3\sqrt{3}J_3}{2J_2^{3/2}} \qquad \text{for } 0 \leq \theta \leq \pi/3 \tag{5.11}$$

where, θ = Lode angle and

$$J_3 = \frac{1}{3} s_{ij} s_{jk} s_{ki} \tag{5.12}$$

Thus, one can replace equation (5.2) by

$$f(I_1, J_2, J_3, k_1, k_2, \cdots) = 0 \tag{5.13}$$

or

$$f(\xi, \rho, \theta, k_1, k_2, \cdots) = 0 \tag{5.14}$$

Yield criteria of materials have to be established experimentally. Original experimental works was done on metals, and hence the development of this subject started with metal plasticity. An important experimental fact for metals, shown by Bridgman and others (Hill, 1970), is that the influence of hydrostatic pressure on yielding is negligible. Therefore, the yielding of most of the metals is classified as hydrostatic pressure independent. The absence of a hydrostatic pressure effect means that the yield function can be reduced to the form

$$f(J_2, J_3, k_1, k_2, \cdots) = 0 \tag{5.15}$$

The Tresca and von Mises criteria are the most widely used yield criterion for metals exhibiting hydrostatic pressure independence.

The behaviour of many nonmetallic materials, such as soils, rocks and concrete, is characterized by their dependence on hydrostatic pressure. Therefore, the general form of equation (5.13) must be used to define the yield criteria for such materials. The Mohr–Coulomb and Drucker–Prager criteria are the most common yield criteria used for these materials. In this study, the Hoek–Brown criterion is taken as the yield criterion for rock mass.

The significance of the yield function can best be interpreted geometrically as a surface in stress space. For a perfectly plastic material, the yield function is assumed to remain unchanged. Thus, the parameters k_i in equation (5.2) are constant, and the yield surface is therefore fixed in stress space (Figure 5.1).

5.3.1.1 Haigh–Westergaard Stress Space

The geometric representation of the stress state at a point is very useful in the study of plasticity theory and failure criteria. The stress tensor σ_{ij} has six independent components, and hence, it is possible to consider these components as positional coordinates in a six-dimensional stress space. However, this is too difficult to deal with, and the simplest alternative is to take the three principal stresses σ_1, σ_2, σ_3 as coordinates and represent the state of stress at a point as a point in this three-dimensional stress space. This space is called the *Haigh–Westergaard stress space.* In this principal stress space, every point having coordinates σ_1, σ_2 and σ_3 represents a possible stress state. This stress space is shown in Figure 5.2.

The straight line ON passing through the origin and making equal angles with each of the coordinates axes is called the *Hydrostatic axis.* For every point on this line, the state of stress is such that $\sigma_1 = \sigma_2 = \sigma_3$. Thus, every point on this line corresponds to a hydrostatic or spherical state of stress, while the deviatoric stresses, $s_1 = (2\sigma_1 - \sigma_2 - \sigma_3)/3$, etc., are equal to *zero.* Any plane perpendicular to ON is known as the *deviatoric plane* and is defined by the equation

$$\sigma_1 + \sigma_2 + \sigma_3 = \sqrt{3}\xi \tag{5.16}$$

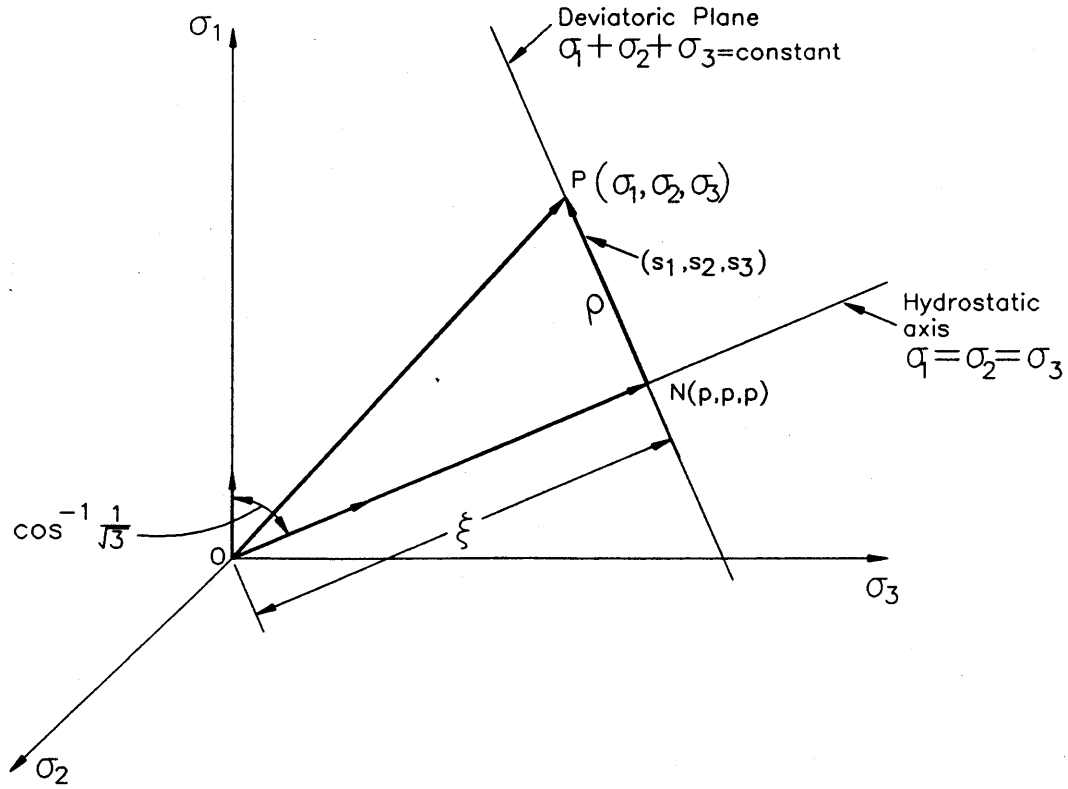

Figure 5.2: Haigh–Westergaard Stress Space

where, ξ is the distance from the origin to the plane measured along the normal ON. The particular deviatoric plane passing through the origin O,

$$\sigma_1 + \sigma_2 + \sigma_3 = 0 \tag{5.17}$$

is called the π-plane.

The distance of the point, representing the stress state, perpendicular to the *hydrostatic axis*, ξ, is determined by ρ, which is related to the second invariant of the deviatoric stress tensor, and θ, which is related to the second and third invariants of the deviatoric stress tensor.

5.3.2 Three-dimensional Hoek–Brown Criterion

The Hoek–Brown failure criterion is expressed as

$$\sigma_1 = \sigma_3 + \sqrt{m\sigma_c\sigma_3 + s\sigma_c^2} \tag{5.18}$$

or,

$$F(\sigma_{ij}) = \sigma_1 - \sigma_3 - \sqrt{m\sigma_c\sigma_3 + s\sigma_c^2} = 0 \tag{5.19}$$

Substituting the values of σ_1 and σ_3 from equations (5.3) and (5.4), the three-dimensional form of the Hoek–Brown criterion is expressed as

$$F = \sqrt{J_2}\left(\sqrt{3}\cos\theta + \sin\theta\right) - \sqrt{\frac{m\sigma_c I_1}{3} - \frac{m\sigma_c\sqrt{J_2}}{\sqrt{3}}\left(\cos\theta + \sqrt{3}\sin\theta\right) + s\sigma_c^2} = 0 \tag{5.20}$$

or,

$$F = \frac{\rho}{\sqrt{2}}\left(\sqrt{3}\cos\theta + \sin\theta\right) - \sqrt{\frac{m\sigma_c\xi}{\sqrt{3}} - \frac{m\sigma_c\rho}{\sqrt{2}}\left(\frac{\cos\theta}{\sqrt{3}} + \sin\theta\right) + s\sigma_c^2} = 0 \tag{5.21}$$

From equation (5.20), let

$$F = \sqrt{J_2}\left(\sqrt{3}\cos\theta + \sin\theta\right) - \sqrt{A} = 0 \tag{5.22}$$

where,

$$A = \left[\frac{m\sigma_c I_1}{3} - \frac{m\sigma_c\sqrt{J_2}}{\sqrt{3}}\left(\cos\theta + \sqrt{3}\sin\theta\right) + s\sigma_c^2\right] \tag{5.23}$$

Some of the yield criteria used in metal and nonmetal plasticity, are shown in Table 5.1 in the three-dimensional stress space representation. The three-dimensional Hoek–Brown and Modified Hoek–Brown criteria are also presented in this table.

Yield Criterion	$f(I_1, J_2, \theta)$	$f(\xi, \rho, \theta)$
Tresca	$2\sqrt{J_2}\sin\left(\theta + \frac{\pi}{3}\right) - \sigma_t = 0$	$\sqrt{2}\rho\sin\left(\theta + \frac{\pi}{3}\right) - \sigma_t = 0$
von Mises	$\sqrt{J_2} - \sigma_s = 0$	$\rho - \sqrt{2}\sigma_s = 0$
Drucker–Prager	$\alpha I_1 + \sqrt{J_2} - k = 0$	$\sqrt{6}\alpha\xi + \rho - \sqrt{2}k = 0$
Mohr–Coulomb	$\frac{1}{3}I_1\sin\phi + \sqrt{J_2}\sin\left(\theta + \frac{\pi}{3}\right)$ $+\frac{\sqrt{J_2}}{\sqrt{3}}\cos\left(\theta + \frac{\pi}{3}\right)\sin\phi - c\cos\phi = 0$	$\sqrt{2}\xi\sin\phi + \sqrt{3}\rho\sin\left(\theta + \frac{\pi}{3}\right)$ $+\rho\cos\left(\theta + \frac{\pi}{3}\right)\sin\phi - \sqrt{6}c\cos\phi = 0$
Hoek–Brown	$\frac{\rho}{\sqrt{2}}\left(\sqrt{3}\cos\theta + \sin\theta\right)$ $-\sqrt{\frac{m\sigma_c\xi}{\sqrt{3}} - \frac{m\sigma_c\rho}{\sqrt{2}}\left(\frac{\cos\theta}{\sqrt{3}} + \sin\theta\right) + s\sigma_c^2} = 0$	$\sqrt{J_2}\left(\sqrt{3}\cos\theta + \sin\theta\right)$ $-\sqrt{\frac{m\sigma_c I_1}{3} - \frac{m\sigma_c\sqrt{J_2}}{\sqrt{3}}\left(\cos\theta + \sqrt{3}\sin\theta\right) + s\sigma_c^2} = 0$
Modified Hoek–Brown	$\frac{\rho}{\sqrt{2}}\left(\sqrt{3}\cos\theta + \sin\theta\right)$ $-m^a\sigma_c^{1-a}\left[\frac{\xi}{\sqrt{3}} - \frac{\rho}{\sqrt{2}}\left(\frac{\cos\theta}{\sqrt{3}} + \sin\theta\right)\right]^a = 0$	$\sqrt{J_2}\left(\sqrt{3}\cos\theta + \sin\theta\right)$ $-m^a\sigma_c^{1-a}\left[\frac{I_1}{3} - \frac{\sqrt{J_2}}{\sqrt{3}}\left(\cos\theta + \sqrt{3}\sin\theta\right)\right]^a = 0$

where,

σ_t = yield stress in simple tension, σ_s = yield stress in pure shear, and $0 \leq \theta \leq \pi/3$

Table 5.1: Failure criteria expressed in three-dimensional stress space form

5.3.3 Plotting of Yield Criteria in Haigh-Westergaard Stress Space

The general shape of a failure surface, $f(I_1, J_2, J_3) = 0$ or $f(\xi, \rho, \theta) = 0$, in a three-dimensional stress space can be described by its cross-sectional shapes in the deviatoric planes and its meridians in the meridian planes or by plotting it as a surface in stress space.

5.3.3.1 Deviatoric Section

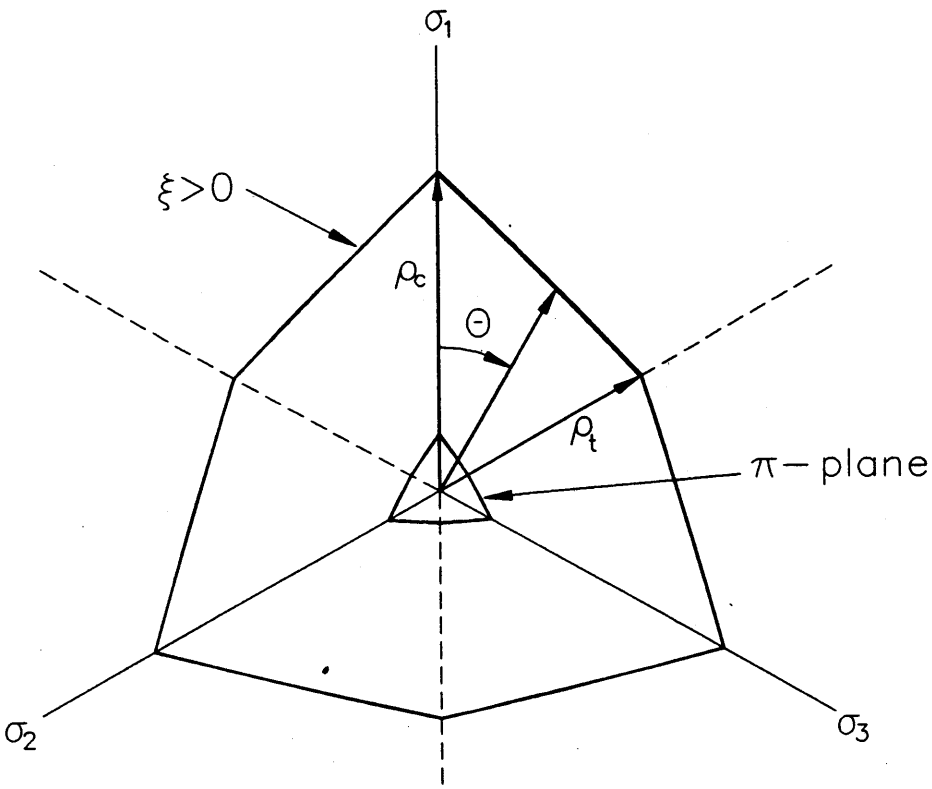

Figure 5.3: Deviatoric section of the Hoek–Brown surface (Compression +ve). Material parameters: $m = 7$, $s = 1$, $\sigma_c = 35$ MPa.

The cross-sections of the failure surface are the intersection curves between this surface and a deviatoric plane which is perpendicular to the hydrostatic axis with ξ = constant. For an isotropic material, the labels 1, 2, 3 attached to the principal stress coordinate axes are arbitrary. It follows that the cross-sectional shape of the surface has a three-fold symmetry as shown in Figure 5.3. Therefore, the shape of the cross-section is explored only in the sector $\theta = 0$ to $\pi/3$, the other sectors being known by symmetry.

The deviatoric section of the Hoek–Brown yield surface for $m = 7$, $s = 1$, $\sigma_c = 35$ MPa is shown in Figure 5.3. This section was generated by solving equation (5.21) for ρ at a fixed value of ξ and by varying θ from 0 to $\pi/3$ at intervals of $\theta = \pi/18$. The entire cross-section was then generated by the properties of symmetry.

The typical sector shown in Figure 5.3 by a heavy line corresponds to the regular ordering of the principal stresses, $\sigma_1 \geq \sigma_2 \geq \sigma_3$. Within this ordering there are two extreme cases:

1. $\theta = \pi/3$:

$$\sigma_1 = \sigma_2 > \sigma_3 \tag{5.24}$$

2. $\theta = 0$:

$$\sigma_1 > \sigma_2 = \sigma_3 \tag{5.25}$$

5.3.3.2 Meridians

The meridians of the failure surface are the intersection curves between the yield surface and a plane (the meridian plane) containing the hydrostatic axis with $\theta =$ constant.

The meridian corresponding to $\theta = 0$ is called the *compression meridian* since equation (5.24) represents a state of stress corresponding to a hydrostatic stress state with a compressive stress superimposed in one direction. The meridian determined by $\theta = \pi/3$, from equation (5.25), represents a hydrostatic state of stress with a tensile stress superimposed in one direction, and thus, is called the *tensile meridian.*

The *compression* and *tension* meridians of the Hoek–Brown yield surface are plotted in Figure 5.4. It can be observed from Figures 5.3 and 5.4 that the strength of the rock mass is considerably higher in compression than in tension.

5.3.3.3 Three-dimensional Surface

In order to plot the shape of the yield surface as an actual three-dimensional shape in principal stress space, the aid of computer graphics is taken in order to visualize the nature of the surface.

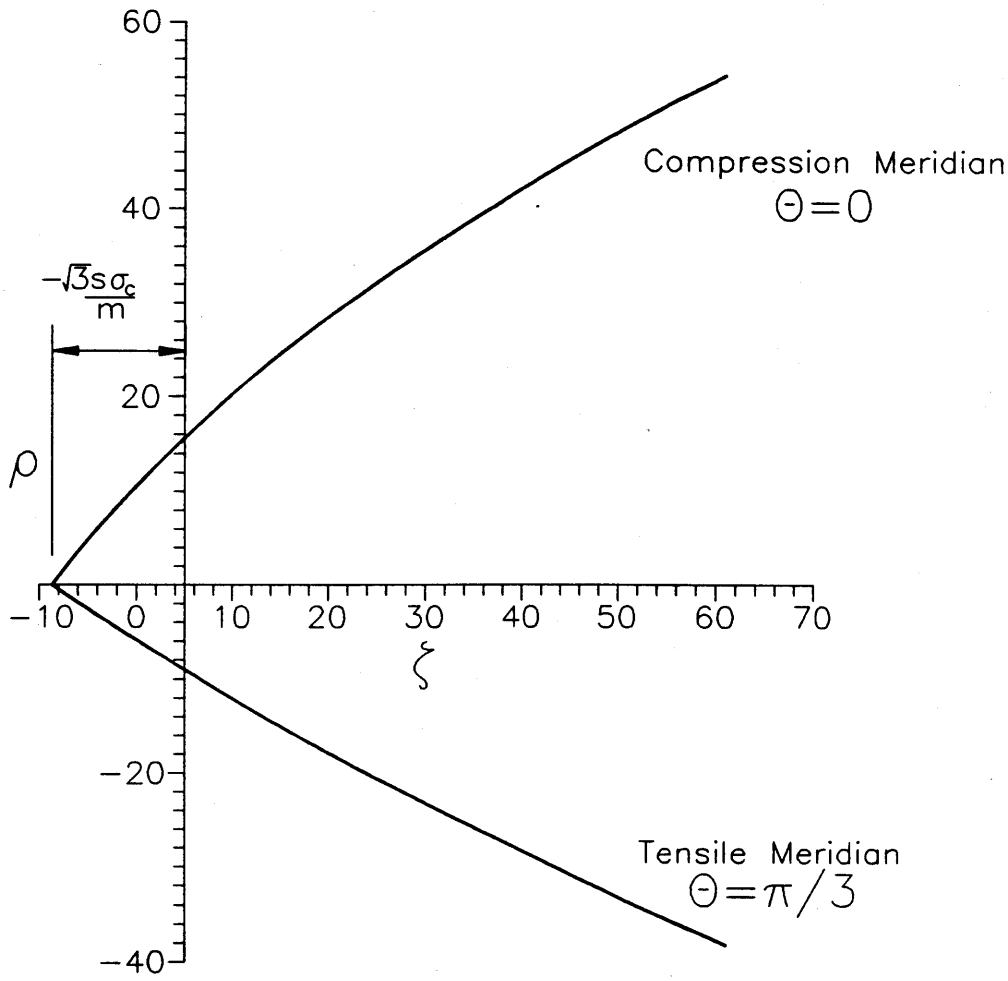

Figure 5.4: Meridians of the Hoek–Brown surface (Compression +ve). Material parameters: $m = 7$, $s = 1$, $\sigma_c = 35$ MPa.

The procedure by which the actual three-dimensional shape of the Hoek–Brown yield surface were generated is outlined below:

- The tensile strength of the rock mass in a general state of stress is given by $\sigma_{tmass} = -\sqrt{3}s\sigma_c/m$. This value is taken as the tip of the hexagonal paraboloid shaped yield surface.
- A series of deviatoric cross-sections of the yield surface are generated at different values of ξ. The values of ξ are taken at close intervals initially since the yield surface is highly nonlinear in this region. As shown in Figures 5.5 and 5.6, the deviatoric sections are generated for each value of ξ using the properties of symmetry as discussed in the section on Deviatoric Sections.
- The coordinates ξ, ρ and θ of the yield surface are transformed into σ_1, σ_2 and σ_3 or the X–Y–Z rectangular coordinate system using suitable transformations.
- These values of the coordinates are stored in a file with an extension ".geo". Each point on the deviatoric sections is given a node number and the node numbers are written to the ".geo" file such that the node numbers of successive deviatoric sections form closed polygons. Thus, the ".geo" file contains information of firstly, the coordinates of the nodes, and secondly, the nodal connectivities of the polygons.
- The ".geo" file was then imported into EXAMINE^{3D}[1]. The data visualization features of this program were used to generate the Hoek–Brown yield surfaces in Figures 5.5 and 5.6.

5.3.4 Features of the Hoek–Brown Yield Surface

The significant features of the Hoek–Brown yield surface and its differences with respect to the Mohr–Coulomb yield surface are outlined below:

- The Hoek–Brown yield surface has a hexagonal paraboloidal shape which is a combination of six parabolic surfaces. The Mohr–Coulomb yield surface has a hexagonal pyramid shape in three-dimensions.

[1] A three-dimensional direct boundary element stress analysis program, developed by Sanjiv Shah and Brent Corkum at the Dept. of Civil Engineering, University of Toronto in 1991.

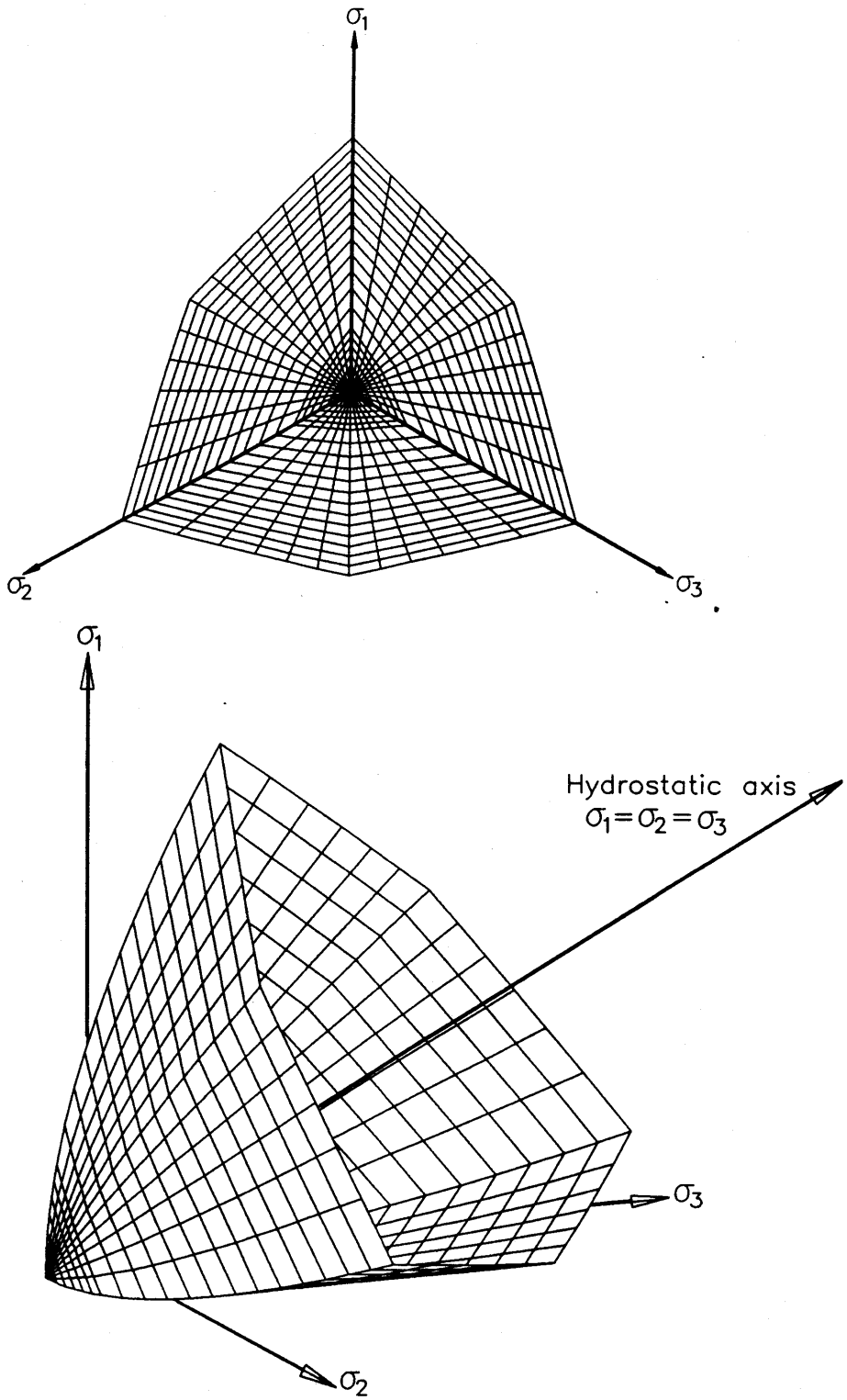

Figure 5.5: Hoek–Brown yield surface in three-dimensional stress space for strong rock. Material parameters: $m = 7$, $s = 1$, $\sigma_c = 35$ MPa. (a) view along hydrostatic axis, (b) general three-dimensional view.

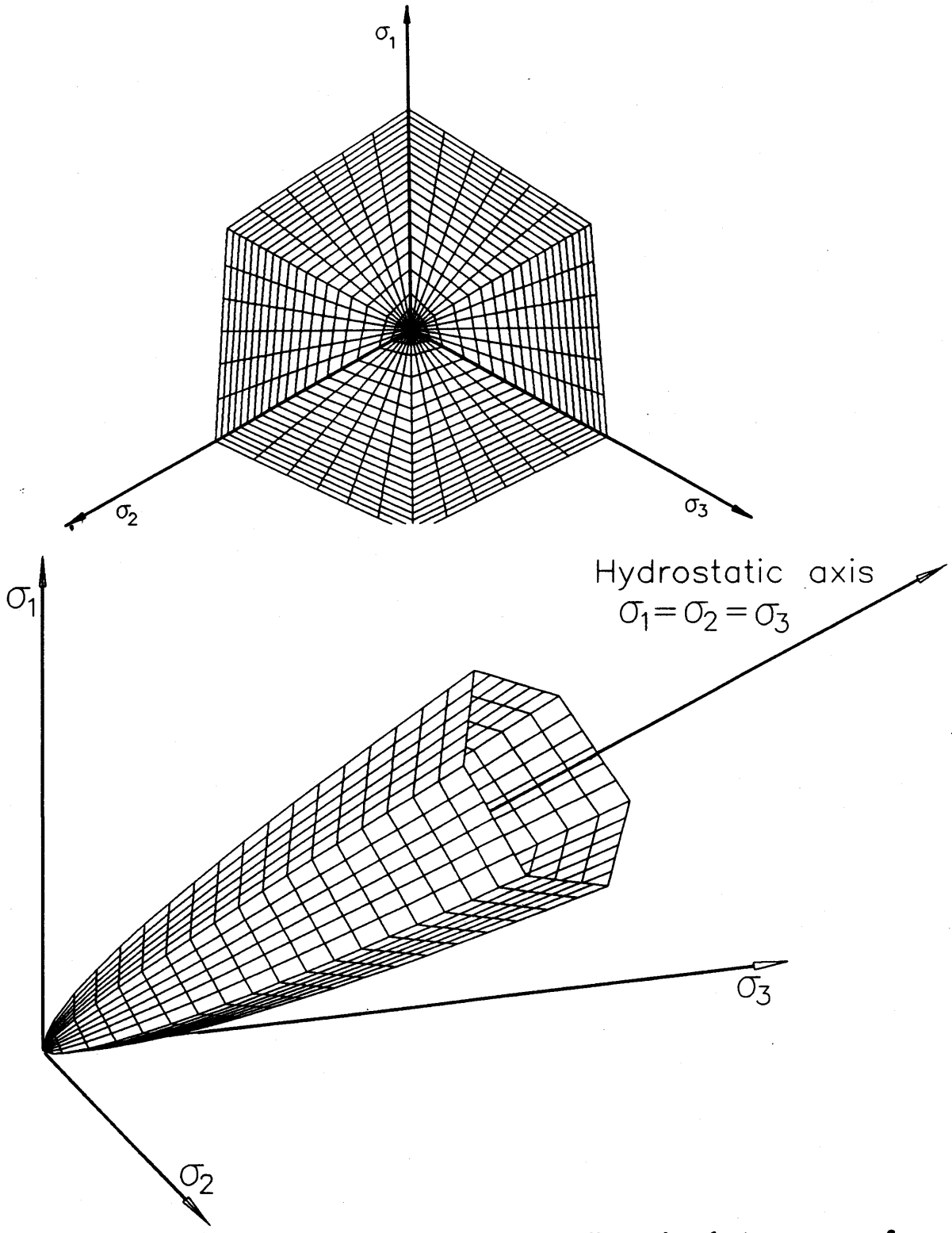

Figure 5.6: Hoek–Brown yield surface in three-dimensional stress space for weak rock. Material parameters: $m = 0.3$, $s = 0.0001$, $\sigma_c = 35$ MPa. (a) view along hydrostatic axis, (b) general three-dimensional view.

- It has a curved profile along a meridian indicating the nonlinear nature of the increase in shear strength with the increase in hydrostatic stress. This is in contrast to the Mohr–Coulomb surface which has a linear profile in the meridian sections.

- It has a curved profile in the deviatoric sections, too, indicating a nonlinear change in the shear strength with change in the Lode angle θ. The Mohr–Coulomb surface has a hexagonal shape in the deviatoric plane.

- The Hoek–Brown yield surface for a strong rock (Figure 5.5) with $m = 7$, $s = 1$ and $\sigma_c = 35$ MPa, shows a pronounced hexagonal shape. The radius of the deviatoric section along the compression meridian ρ_c, i.e. along $\theta = 0$, is much higher than the radius along the tensile meridian ρ_c, i.e. along $\theta = \pi/3$. This indicates that for strong rocks the ratio of the compressive to tensile strength is high. However, for a weak rock (Figure 5.6) with $m = 0.3$, $s = 0.0001$ and $\sigma_c = 35$ MPa, the yield surface is such that $\rho_c \approx \rho_t$. Thus, the yield surface for weak rocks has a tendency of taking the shape of a paraboloid. This realization had led Pan and Hudson (1988) to propose a simplified Hoek–Brown yield surface which forces $\rho_c = \rho_t$; thus, the deviatoric sections are circular.

- The Hoek–Brown yield surface has corners at the points where the six parabolic surfaces intersect. These points result in "corner" singularities when constitutive relations are derived for the rock mass.

5.3.5 Criterion for Loading and Unloading

Plastic deformation occurs in the material as long as the stress point is on the yield surface. For the plastic flow to continue, the state of stress must remain on the yield surface which is termed "loading". Otherwise, the stress state must drop below the yield value; in which case, no further plastic deformation occurs and all incremental deformations are elastic. This condition is termed "unloading".

The concept of loading and unloading for a complex stress state can be explained geometrically when the yield criterion is expressed as a surface and σ_{ij} and $d\sigma_{ij}$ as stress and stress increment vectors, respectively, in stress space as shown in Figure 5.1. For instance, a material is considered to be in a plastic state, characterized by the stress tensor

σ_{ij}. If an infinitesimal increment of stress $d\sigma_{ij}$ is applied to the current stress state, then for a perfectly plastic material, the stress point cannot move outside the yield surface. Plastic flow can occur only when the stress point is on the yield surface, and therefore, the additional loading $d\sigma_{ij}$ must move along the tangential direction. Thus, the condition for a continuation of further plastic flow or the criterion for loading is expressed mathematically as

$$f(\sigma_{ij}, k) = 0 \quad \text{and} \quad df = \frac{\partial f}{\partial \sigma_{ij}} d\sigma_{ij} = 0 \tag{5.26}$$

and the criterion for unloading is expressed as

$$f(\sigma_{ij}, k) = 0 \quad \text{and} \quad df = \frac{\partial f}{\partial \sigma_{ij}} d\sigma_{ij} < 0 \tag{5.27}$$

Hence, the yield function $f(\sigma_{ij})$ also serves as the *criterion of loading* for further plastic deformation and as the *criterion of unloading* for elastic deformation.

5.3.6 Elastic and Plastic Strain Increment Tensors

The total strain increment tensor during plastic flow is assumed to be the sum of the elastic and plastic strain increment tensors:

$$d\epsilon_{ij} = d\epsilon^e_{ij} + d\epsilon^p_{ij} \tag{5.28}$$

where,

$d\epsilon_{ij}$ = total strain increment vector;

$d\epsilon^e_{ij}$ = elastic strain increment vector;

$d\epsilon^p_{ij}$ = plastic strain increment vector;

The theory of elasticity can be used to provide the necessary relationship between the incremental changes of stress and elastic strain, the stress-strain relation for a plastic material reduces essentially to a relation involving the current stress state and the incremental changes of stress and plastic strain.

5.4 Plastic Potential and Flow Rule

The flow rule is the necessary kinematic assumption postulated for plastic deformation. It gives the ratio of the relative magnitudes of the components of the plastic strain increment

tensor $d\epsilon^p_{ij}$. The flow rule also defines the direction of the plastic strain increment vector $d\epsilon^p_{ij}$. von Mises proposed the concept of *plastic potential function* which is a scalar function of the stresses, $Q(\sigma_{ij})$. The plastic flow equations are written as

$$d\epsilon^p_{ij} = \lambda \frac{\partial Q}{\partial \sigma_{ij}} \tag{5.29}$$

where,

λ = a positive scalar factor of proportionality which is nonzero only when plastic deformation occurs.

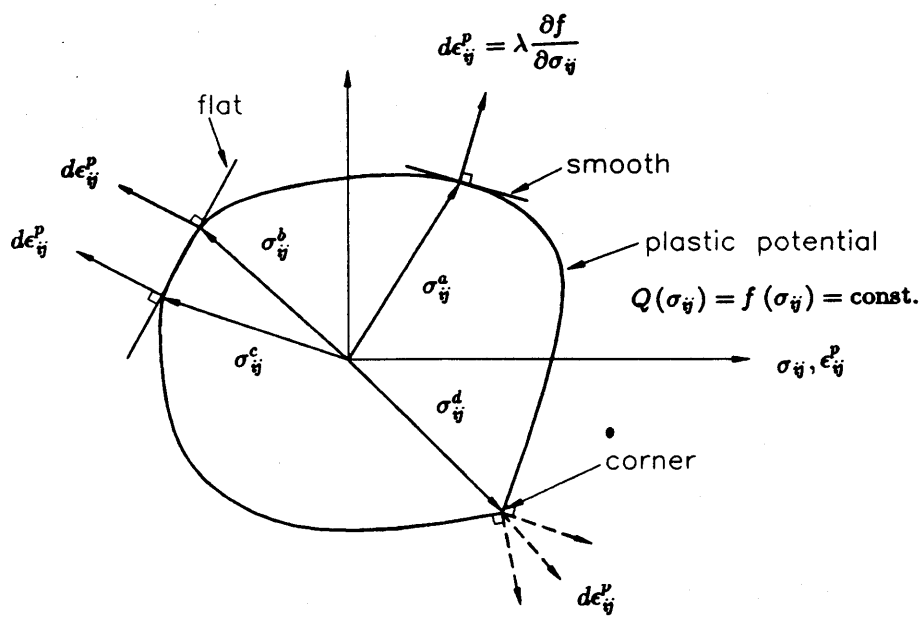

Figure 5.7: Geometric Illustration of Associated Flow Rule

The equation $Q(\sigma_{ij})$ = constant defines a *hypersurface* of plastic potential in nine-dimensional stress space. The direction cosines of the normal vector to this surface at the point σ_{ij} on the surface are proportional to the *gradient* $\partial Q/\partial \sigma_{ij}$. Therefore, equation (5.29) implies that the plastic flow vector $d\epsilon^p_{ij}$, if plotted as a free vector in stress space, is directed along the normal to the surface of the plastic potential, as shown in Figure 5.7.

Of great importance is the simplest case when the yield function and the plastic potential function coincide, i.e. $f = Q$. Thus,

$$d\epsilon_{ij}^{p} = \lambda \frac{\partial f}{\partial \sigma_{ij}} \tag{5.30}$$

and plastic flow develops along the normal to the yield surface $\partial f / \partial \sigma_{ij}$ as shown in Figure 5.7. Equation (5.30) is called the *associated flow rule* (AFR) because the flow is connected or associated with the yield criterion, while equation (5.29) with $f \neq Q$ is called a *nonassociated flow rule* (NAFR). The use of the associated flow rule is important for the following cases:

1. the AFR is valid for irreversible plastic materials where work expended on plastic deformation cannot be reclaimed;
2. the stress-strain law of a material based on the AFR will result in a *unique* solution of a boundary-value problem; and
3. the AFR makes it possible and convenient to formulate various generalizations of the plasticity equations by considering yield and loading surfaces of more complex form.

The associated as well as the nonassociated flow rules have been developed for the constitutive model corresponding to the Hoek–Brown criterion. For the associated flow rule, the function $Q(\sigma_{ij}) = f(\sigma_{ij})$ used is the one represented by equation (5.22).

The nonassociated flow rule used in this study corresponds to a plastic potential function, $Q(\sigma_{ij})$, which is a simplified version of the Hoek–Brown surface. This plastic potential function is constructed in such a manner that it is independent of the Lode angle θ, i.e., it is a volume of revolution around the hydrostatic axis, but has a nonlinear profile in the triaxial plane matching that of the Hoek–Brown yield surface. This plastic potential function is obtained by evaluating $f(\sigma_{ij})$ at Lode angle $\theta = \pi/6$, which gives a 'mean surface' between the inner and outer apices of the surface, and by introducing a variable dilation parameter α. This results in

$$Q(\sigma_{ij}) = 2\sqrt{J_2} - \sqrt{\alpha\sigma_c\left(\frac{I_1}{3} - \sqrt{J_2}\right) + s\sigma_c^2} = 0 \tag{5.31}$$

Let

$$Q(\sigma_{ij}) = 2\sqrt{J_2} - \sqrt{R} = 0 \tag{5.32}$$

where,

$$R = \left[\alpha\sigma_c\left(\frac{I_1}{3} - \sqrt{J_2}\right) + s\sigma_c^2\right] \tag{5.33}$$

and

$$\alpha = \mathcal{F}(m) = \begin{cases} \frac{m}{4}, & \text{for quasi-associated flow;} \\ 0, & \text{for zero-dilatant flow;} \end{cases} \tag{5.34}$$

For geotechnical materials like soils and rocks, it has been found that the associated flow rule tends to overestimate the plastic volume expansion. The nonassociated flow rule is therefore adopted in establishing constitutive relations for such materials.

5.4.1 Convexity, Normality and Uniqueness for Elastic-Perfectly Plastic Materials

The associated flow rule or *normality rule* discussed before has been established firmly in the mathematical theory of metal plasticity (Hill, 1970). Since the condition of irreversibility of plastic deformation implies that work expended on plastic deformation in a cycle is positive, the positive plastic work leads to convexity of the yield surface and normality of the plastic flow. The normality condition or the associated flow rule guarantees the uniqueness of the solution of an elastic-plastic boundary value problem.

Because of the irreversible character of plastic deformation, work expended on plastic deformation cannot be reclaimed. This means that the work of the stresses on the change of plastic strain is positive whenever a change of plastic strain occurs. The requirement that this work be positive for plastic deformation leads to

$$d\sigma_{ij}\, d\epsilon_{ij}^p \geq 0 \tag{5.35}$$

The associated flow rule and the conditions of convexity, normality and uniqueness are the consequences of Drucker's stability postulate (Chen and Han, 1988). These conditions are explained below:

1. **Convexity:**

   The yield surface must be convex. As shown in Figures 5.3, 5.5 and 5.6, the Hoek–Brown yield surface is convex in shape. Therefore, the angle between $d\sigma_{ij}$ and $d\epsilon_{ij}^p$ must always be $\leq \pi/2$ in order to satisfy the condition of equation (5.35).

2. **Normality:**

   The plastic strain increment vector $d\epsilon_{ij}^{p}$ must be normal to the yield surface at a smooth point and lie between adjacent normals at a corner. In the case of the Hoek–Brown yield surface, when the stress state is such that the Lode angle is $0 < \theta < \pi/3$, then as shown in Figure 5.3, the surface is smooth and convex and $d\epsilon_{ij}^{p}$ must be normal to the surface so that it makes a right angle or less with all possible $d\sigma_{ij}$ in order to satisfy the condition of irreversibility given by equation (5.35). However, when the stress state is at the corner, i.e. at $\theta = 0$ or $\theta = \pi/3$, then the direction of $d\epsilon_{ij}^{p}$ cannot be uniquely defined as the derivative of the yield surface with respect to the stress state does not exist. There is some freedom in the direction of $d\epsilon_{ij}^{p}$ but the vector must lie between the adjacent normals at an adjacent point to the corner so that equation (5.35) is satisfied. The manner in which the singularity of the Hoek–Brown surface has been "smoothed" is described in a later section.

3. **Uniqueness of solution:**

   If the normality condition is imposed on the stress-strain relation, the uniqueness requirement is also satisfied for an elastic–perfectly plastic material. This condition ensures that for a given mechanical state of a body and a system of infinitesimal increments of surface tractions, the resulting increments of stresses and strains (elastic and plastic) are unique.

However, it should be noted that the stability postulate of Drucker is a *sufficient* but not a *necessary* criterion. This postulate may not be *necessarily* required in a general formulation of any flow rule for elastic–plastic materials. It has been shown by Mroz (1963) that for an elastic–work–hardening–plastic material, the uniqueness allows a nonassociated flow rule to occur which does not necessarily satisfy Drucker's stability postulate. Further, when the uniqueness of stress and strain trajectories for a given loading history exists, the material can be regarded as locally stable, and thus, the condition of uniqueness rather than the stability postulate may be regarded as a basic criterion in establishing elastic–plastic stress-strain relationships.

5.5 Incremental Stress–Strain Relationships

In an elastoplastic stress analysis by a numerical approach, the most common technique is the incremental method using tangent stiffness. An incremental relationship between stress and strain is needed in forming the tangent stiffness. The constitutive relations for rock mass corresponding to the Hoek–Brown criterion are developed in this section. Multiaxial perfectly plastic behaviour requires that the stress increment vector be tangential to the yield surface and the plastic strain increment vector be normal to the loading surface. According to the concept of perfect plasticity, the magnitude of the plastic strain increment cannot be uniquely determined by the given current stress state σ_{ij} and stress increments $d\sigma_{ij}$. However, for a given current stress state σ_{ij} and a given plastic strain increment $d\epsilon^p_{ij}$ satisfying the flow rule, the stress increment $d\sigma_{ij}$ can be determined by the *consistency condition* which ensures that the stress state remains on the yield surface.

5.5.1 Constitutive Relations in General Form

The total strain increment is given by equation (5.28). The elastic strain increment can be determined from Hooke's law as

$$d\epsilon^e_{ij} = D_{ijkl} d\sigma_{kl} \tag{5.36}$$

or,

$$d\epsilon^e_{ij} = \frac{dI_1}{9K}\delta_{ij} + \frac{ds_{ij}}{2G} \tag{5.37}$$

where,

D_{ijkl} = matrix relating stresses to strains in the elastic range,

K and G are Bulk and Shear Modulii, respectively, of the material.

The plastic strain increment is obtained from the flow rule. Therefore, the complete stress-strain relations for an elastic-perfectly plastic material are expressed as

$$d\epsilon_{ij} = D_{ijkl} d\sigma_{kl} + \lambda \frac{\partial f}{\partial \sigma_{ij}} \tag{5.38}$$

or

$$d\epsilon_{ij} = \frac{dI_1}{9K}\delta_{ij} + \frac{ds_{ij}}{2G} + \lambda \frac{\partial f}{\partial \sigma_{ij}} \tag{5.39}$$

where λ is an as yet undetermined factor with the value

$$\lambda \begin{cases} = 0 & \text{wherever } f < 0 \text{ or } f = 0 \text{ but } df < 0 \\ > 0 & \text{wherever } f = 0 \text{ and } df = 0 \end{cases} \tag{5.40}$$

The value of λ can be determined by combining the stress-strain relations (equations (5.38) and (5.39) with the *consistency condition* which is defined by

$$df = \frac{\partial f}{\partial \sigma_{ij}} d\sigma_{ij} = 0 \tag{5.41}$$

which ensures that the stress state $(\sigma_{ij} + d\sigma_{ij})$ existing after the incremental change $d\sigma_{ij}$ has taken place still satisfies the yield criterion $f(\sigma_{ij})$

$$f(\sigma_{ij} + d\sigma_{ij}) = f(\sigma_{ij}) + df = f(\sigma_{ij}) \tag{5.42}$$

Solving equation (5.39) and using the flow rule, the stress increment tensor can be determined as

$$d\sigma_{ij} = C_{ijkl}\left(d\epsilon_{kl} - d\epsilon^p_{kl}\right) = C_{ijkl} d\epsilon_{kl} - \lambda C_{ijkl} \frac{\partial f}{\partial \sigma_{kl}} \tag{5.43}$$

Substituting equation (5.43) into equation (5.41) and solving for λ:

$$\lambda = \frac{\frac{\partial f}{\partial \sigma_{ij}} C_{ijkl} d\epsilon_{kl}}{\frac{\partial f}{\partial \sigma_{rs}} C_{rstu} \frac{\partial f}{\partial \epsilon_{tu}}} \tag{5.44}$$

It should be noted that all indices of the tensors in equation (5.44) are dummy indices, indicating the scalar nature of λ. Thus, if $f(\sigma_{ij})$ is defined for a particular material and strain increments $d\epsilon_{ij}$ are prescribed, the factor λ is determined uniquely.

Substituting equation (5.44) into equation (5.43), the incremental stress-strain relation can be expressed explicitly as

$$d\sigma_{ij} = \left[C_{ijkl} - \frac{C_{ijmn} \frac{\partial f}{\partial \sigma_{mn}} \frac{\partial f}{\partial \sigma_{pq}} C_{pqkl}}{\frac{\partial f}{\partial \sigma_{rs}} C_{rstu} \frac{\partial f}{\partial \sigma_{tu}}} \right] d\epsilon_{kl} \tag{5.45}$$

The coefficient tensor in the parentheses represents the elastic-plastic tensor of tangent moduli for an elastic-perfectly plastic material:

$$C^{ep}_{ijkl} = C_{ijkl} - \frac{C_{ijmn}\frac{\partial f}{\partial \sigma_{mn}}\frac{\partial f}{\partial \sigma_{pq}}C_{pqkl}}{\frac{\partial f}{\partial \sigma_{rs}}C_{rstu}\frac{\partial f}{\partial \sigma_{tu}}} \tag{5.46}$$

This equation is the most general form of the constitutive relation for an elastic-perfectly plastic material. The stress increments can be determined uniquely by the yield function $f(\sigma_{ij})$ and the total strain increment $d\epsilon_{ij}$. Therefore, if the current stress state σ_{ij} is known and the increments of strain $d\epsilon_{ij}$ are prescribed, the corresponding stress increments $d\sigma_{ij}$ can be obtained from equation (5.45).

5.5.2 Constitutive Relations for Hoek-Brown Criterion — Associated Flow Rule

The three-dimensional Hoek–Brown yield surface is defined by equation (5.20) and is a function of I_1, J_2 and J_3. Hence, if the yield surface for a isotropic material is expressed in the general form as

$$f(I_1, J_2, J_3) = 0 \tag{5.47}$$

the gradient of this yield surface is written as

$$\frac{\partial f}{\partial \sigma_{ij}} = \frac{\partial f}{\partial I_1}\frac{\partial I_1}{\partial \sigma_{ij}} + \frac{\partial f}{\partial J_2}\frac{\partial J_2}{\partial \sigma_{ij}} + \frac{\partial f}{\partial J_3}\frac{\partial J_3}{\partial \sigma_{ij}} \tag{5.48}$$

or

$$\frac{\partial f}{\partial \sigma_{ij}} = B_0\delta_{ij} + B_1 s_{ij} + B_2 t_{ij} \tag{5.49}$$

where,

$$B_0 = \frac{\partial f}{\partial I_1}, \quad B_1 = \frac{\partial f}{\partial J_2}, \quad B_2 = \frac{\partial f}{\partial J_3} \tag{5.50}$$

Here t_{ij} is the deviation of the square of the stress deviation s_{ij} and is given by:

$$t_{ij} = \frac{\partial J_3}{\partial \sigma_{ij}} = s_{ik}s_{kj} - \frac{2}{3}J_2\delta_{ij} \tag{5.51}$$

The Hoek–Brown yield surface is expressed by equation (5.20). In order to evaluate the derivatives B_0, B_1 and B_2, the following relations are also used

$$\frac{\partial \theta}{\partial J_2} = \frac{\cot 3\theta}{2J_2} \tag{5.52}$$

$$\frac{\partial \theta}{\partial J_3} = -\frac{\cot 3\theta}{3J_3} \tag{5.53}$$

Taking the derivatives of equation (5.20) with respect to I_1, J_2 and J_3, the values of B_0, B_1 and B_2 are obtained as

$$B_0 = -\frac{m\sigma_c}{6\sqrt{A}} \tag{5.54}$$

$$\begin{aligned} B_1 = \frac{1}{2\sqrt{J_2}} \Big[& \sqrt{3}\cos\theta + \sin\theta + \left(\cos\theta - \sqrt{3}\sin\theta\right)\cot 3\theta \\ & + \frac{m\sigma_c}{2\sqrt{3}\sqrt{A}} \left\{\cos\theta + \sqrt{3}\sin\theta + \left(\sqrt{3}\cos\theta - \sin\theta\right)\cot 3\theta\right\}\Big] \end{aligned} \tag{5.55}$$

$$B_2 = \frac{1}{2J_2 \sin 3\theta} \left[3\sin\theta - \sqrt{3}\cos\theta - \frac{m\sigma_c}{2\sqrt{A}}\left(\sqrt{3}\cos\theta - \sin\theta\right)\right] \tag{5.56}$$

It can be observed from equations (5.54, 5.55, 5.56) that only the constants B_i need be defined by the yield surface. Only these quantities are to be changed when changing a yield criterion in any numerical formulation. The constants B_i are given in Table 5.2 for prominent yield criteria used in metal and nonmetal plasticity. The values of B_i for the Hoek–Brown and the Modified Hoek–Brown criteria are also shown in this table.

Yield Criterion	B_0	B_1	B_2
Tresca	0	$\left[\sin\left(\theta+\frac{\pi}{3}\right)/\sqrt{J_2}\right]\left[1+\cot\left(\theta+\frac{\pi}{3}\right)\cot 3\theta\right]$	$\left[-\sqrt{3}\cos\left(\theta+\frac{\pi}{3}\right)/J_2\sin 3\theta\right]$
von Mises	0	1	0
Drucker–Prager	α	$\frac{1}{2\sqrt{J_2}}$	0
Mohr–Coulomb	$\frac{\sin\phi}{3}$	$\left[\sin\left(\theta+\frac{\pi}{3}\right)/2\sqrt{J_2}\right]\left\{\left[1+\cot\left(\theta+\frac{\pi}{3}\right)\cot 3\theta\right] + \sin\phi\left[\cot\left(\theta+\frac{\pi}{3}\right)-\cot 3\theta\right]\Big/\sqrt{3}\right\}$	$\frac{1}{2J_2\sin 3\theta}\left[\sin\left(\theta+\frac{\pi}{3}\right)\sin\phi - \sqrt{3}\cos\left(\theta+\frac{\pi}{3}\right)\right]$
Hoek–Brown	$-\frac{m\sigma_c}{6\sqrt{A}}$	$\frac{1}{2\sqrt{J_2}}\left[\sqrt{3}\cos\theta+\sin\theta+\left(\cos\theta-\sqrt{3}\sin\theta\right)\cot 3\theta + \frac{m\sigma_c}{2\sqrt{3}\sqrt{A}}\left\{\cos\theta+\sqrt{3}\sin\theta+\left(\sqrt{3}\cos\theta-\sin\theta\right)\cot 3\theta\right\}\right]$	$\frac{1}{2J_2\sin 3\theta}\left[3\sin\theta-\sqrt{3}\cos\theta - \frac{m\sigma_c}{2\sqrt{A}}\left(\sqrt{3}\cos\theta-\sin\theta\right)\right]$
Modified Hoek–Brown	$-\frac{am^a\sigma_c^{1-a}C^{1-a}}{3}$	$\frac{1}{2\sqrt{J_2}}\left[\sqrt{3}\cos\theta+\sin\theta+\left(\cos\theta-\sqrt{3}\sin\theta\right)\cot 3\theta + \frac{am^a\sigma_c^{1-a}C^{a-1}}{\sqrt{3}}\left\{\cos\theta+\sqrt{3}\sin\theta+\left(\sqrt{3}\cos\theta-\sin\theta\right)\cot 3\theta\right\}\right]$	$\frac{1}{2J_2\sin 3\theta}\left[3\sin\theta-\sqrt{3}\cos\theta - am^a\sigma_c^{1-a}C^{a-1}\left(\sqrt{3}\cos\theta-\sin\theta\right)\right]$

where,

$A = \left[\frac{m\sigma_c I_1}{3} - \frac{m\sigma_c\sqrt{J_2}}{\sqrt{3}}\left(\cos\theta+\sqrt{3}\sin\theta\right) + s\sigma_c^2\right]; \qquad C = \left[\frac{I_1}{3} - \frac{\sqrt{J_2}}{\sqrt{3}}\left(\cos\theta+\sqrt{3}\sin\theta\right)\right];$

and $0 \le \theta \le \pi/3$

Table 5.2: Constants B_i defined for different yield surfaces

In finite element applications, the constitutive relation of a material is reflected by the material stiffness matrix C^{ep}_{ijkl}, which is used in forming the tangent stiffness. This stiffness matrix relates the strain increment with the stress increment by

$$d\sigma_{ij} = C^{ep}_{ijkl} d\epsilon_{kl} \tag{5.57}$$

To obtain a general form of the fourth-order tensor C^{ep}_{ijkl}, equation (5.46) is written as

$$C^{ep}_{ijkl} = C_{ijkl} + C^{p}_{ijkl} \tag{5.58}$$

where,

C^{ep}_{ijkl} = elasto-plastic stiffness tensor;

C_{ijkl} = elastic stiffness tensor and is given by

$$C_{ijkl} = \frac{E}{2(1+\nu)} \left[\frac{2\nu}{(1-2\nu)} \delta_{ij}\delta_{kl} + \delta_{ik}\delta_{jl} + \delta_{il}\delta_{jk} \right] \tag{5.59}$$

C^{p}_{ijkl} = plastic stiffness tensor and is given by

$$C^{p}_{ijkl} = -\frac{H_{ij} H_{kl}}{h} \tag{5.60}$$

where,

$$h = \frac{\partial f}{\partial \sigma_{rs}} C_{rstu} \frac{\partial f}{\partial \sigma_{tu}} \tag{5.61}$$

and

$$H_{ij} = C_{ijmn} \frac{\partial f}{\partial \sigma_{mn}} \tag{5.62}$$

From equation (5.51),

$$t_{ii} = 0 \tag{5.63}$$

$$t_{ij} s_{ij} = s_{ij} s_{kj} s_{ki} = 3J_3 \tag{5.64}$$

$$t_{ij} t_{ij} = \frac{2}{3} J_2^2 \tag{5.65}$$

Substituting equation (5.59) for C_{ijkl} and equation (5.49) for $\partial f / \partial \sigma_{ij}$ into equations (5.61, 5.62), and using the relations given by equations (5.63, 5.64, 5.65) the expressions for h and H_{ij} are obtained in terms of the elastic constants G and ν and the coefficients B_0, B_1 and B_2 as

$$h = 2G \left[3B_0^2 \frac{1+\nu}{1-2\nu} + 2B_1^2 J_2 + \frac{2}{3} B_2^2 J_2^2 + 6B_1 B_2 J_3 \right] \tag{5.66}$$

$$H_{ij} = 2G\left[B_0\frac{1+\nu}{1-2\nu}\delta_{ij} + B_1 s_{ij} + B_2 t_{ij}\right] \tag{5.67}$$

The stress increment vector $d\sigma_{ij}$ and the strain increment vector $d\epsilon_{ij}$ are expressed explicitly in vector forms as

$$\{d\sigma_{ij}\} = \{d\sigma_x, d\sigma_y, d\sigma_z, d\tau_{xy}, d\tau_{yz}, d\tau_{zx}\} \tag{5.68}$$

$$\{d\epsilon_{ij}\} = \{d\epsilon_x, d\epsilon_y, d\epsilon_z, d\gamma_{xy}, d\gamma_{yz}, d\gamma_{zx}\} \tag{5.69}$$

where $d\gamma_{xy} = 2d\epsilon_{xy}$, etc., are the engineering shear strains. The corresponding vector for the tensor H_{ij} has the form

$$[H_{ij}] = \{H_x, H_y, H_z, H_{xy}, H_{yz}, H_{zx}\} \tag{5.70}$$

where,

$$\begin{aligned}
H_x &= 2G\left[B_0\frac{1+\nu}{1-2\nu} + B_1 s_x + B_2\left(s_x^2 + s_{xy}^2 + s_{zx}^2 - \frac{2}{3}J_2\right)\right] \\
H_y &= 2G\left[B_0\frac{1+\nu}{1-2\nu} + B_1 s_y + B_2\left(s_y^2 + s_{yz}^2 + s_{xy}^2 - \frac{2}{3}J_2\right)\right] \\
H_z &= 2G\left[B_0\frac{1+\nu}{1-2\nu} + B_1 s_z + B_2\left(s_z^2 + s_{zx}^2 + s_{yz}^2 - \frac{2}{3}J_2\right)\right]
\end{aligned} \tag{5.71}$$

and

$$\begin{aligned}
H_{xy} &= 2G\left[B_1 s_{xy} + B_2\left(s_x s_{xy} + s_{xy} s_y + s_{zx} s_{yz}\right)\right] \\
H_{yz} &= 2G\left[B_1 s_{yz} + B_2\left(s_{xy} s_{xz} + s_y s_{yz} + s_{yz} s_z\right)\right] \\
H_{zx} &= 2G\left[B_1 s_{zx} + B_2\left(s_{zx} s_x + s_{zy} s_{xy} + s_z s_{xz}\right)\right]
\end{aligned} \tag{5.72}$$

Thus, the tensor C_{ijkl}^{ep} can be expressed in a matrix form as

$$[C^{ep}] = [C] + [C^p] \tag{5.73}$$

where,

$$[C] = \begin{bmatrix} K+\frac{4}{3}G & K-\frac{2}{3}G & K-\frac{2}{3}G & 0 & 0 & 0 \\ K-\frac{2}{3}G & K+\frac{4}{3}G & K-\frac{2}{3}G & 0 & 0 & 0 \\ K-\frac{2}{3}G & K-\frac{2}{3}G & K+\frac{4}{3}G & 0 & 0 & 0 \\ 0 & 0 & 0 & G & 0 & 0 \\ 0 & 0 & 0 & 0 & G & 0 \\ 0 & 0 & 0 & 0 & 0 & G \end{bmatrix} \tag{5.74}$$

and

$$[C^p] = -\frac{1}{h}\begin{bmatrix} H_x^2 & H_xH_y & H_xH_z & H_xH_{xy} & H_xH_{yz} & H_xH_{zx} \\ & H_y^2 & H_yH_z & H_yH_{xy} & H_yH_{yz} & H_yH_{zx} \\ & & H_z^2 & H_zH_{xy} & H_zH_{yz} & H_zH_{zx} \\ & & & H_{xy}^2 & H_{xy}H_{yz} & H_{xy}H_{zx} \\ & \text{sym.} & & & H_{yz}^2 & H_{yz}H_{zx} \\ & & & & & H_{zx}^2 \end{bmatrix} \tag{5.75}$$

5.5.3 Constitutive Relations for Hoek-Brown Criterion — Nonassociated Flow Rule

The plastic potential function used in the derivation of the incremental stress-strain relations corresponding to the Hoek–Brown criterion is expressed by equation (5.31). The constitutive relations for the rock mass using the *nonassociated flow rule* are generated in a similar manner as that with *associated flow rule* except that the incremental plastic strain vector is now normal to the potential function $Q(\sigma_{ij})$. Therefore,

$$d\epsilon_{ij}^p = \lambda \frac{\partial Q}{\partial \sigma_{ij}} \tag{5.76}$$

In order to evaluate the gradient $\partial Q/\partial \sigma_{ij}$, the following steps are undertaken:

The plastic potential function, equation (5.31), is a function of I_1 and J_2 only. Hence,

$$\frac{\partial Q}{\partial \sigma_{ij}} = \frac{\partial Q}{\partial I_1}\frac{\partial I_1}{\partial \sigma_{ij}} + \frac{\partial Q}{\partial J_2}\frac{\partial J_2}{\partial \sigma_{ij}} \tag{5.77}$$

or,

$$\frac{\partial Q}{\partial \sigma_{ij}} = Q_0\delta_{ij} + Q_1 s_{ij} \tag{5.78}$$

where,

$$Q_0 = \frac{\partial Q}{\partial \sigma_{ij}}, \quad Q_1 = \frac{\partial Q}{\partial \sigma_{ij}} \tag{5.79}$$

Evaluating these partial derivatives,

$$Q_0 = -\frac{\alpha\sigma_c}{6\sqrt{R}} \tag{5.80}$$

$$Q_1 = \frac{1}{\sqrt{J_2}}\left[1 + \frac{\alpha\sigma_c}{4\sqrt{R}}\right] \tag{5.81}$$

The plastic tangent stiffness matrix C^p_{ijkl} represents the degradation of the stiffness of the material due to plastic flow and is given by

$$C^p_{ijkl} = -\frac{1}{h} H_{kl} H^*_{ij} \tag{5.82}$$

where,

$$h = \frac{\partial f}{\partial \sigma_{ij}} C_{ijkl} \frac{\partial Q}{\partial \sigma_{kl}} \tag{5.83}$$

$$H_{ij} = C_{ijmn} \frac{\partial f}{\partial \sigma_{mn}} \tag{5.84}$$

and

$$H^*_{ij} = C_{ijmn} \frac{\partial Q}{\partial \sigma_{mn}} \tag{5.85}$$

Therefore

$$h = 2G \left[3B_0 Q_0 \frac{1+\nu}{1-2\nu} + 2B_1 Q_1 J_2 + 3B_2 Q_1 J_3 \right] \tag{5.86}$$

$$H_{ij} = 2G \left[B_0 \frac{1+\nu}{1-2\nu} \delta_{ij} + B_1 s_{ij} + B_2 t_{ij} \right] \tag{5.87}$$

and

$$H^*_{ij} = 2G \left[Q_0 \frac{1+\nu}{1-2\nu} \delta_{ij} + Q_1 s_{ij} \right] \tag{5.88}$$

The vector corresponding to H_{ij} is given by equations (5.71, 5.72), and the vector corresponding to tensor H^*_{ij} is obtained from

$$\begin{aligned} H^*_x &= 2G \left[Q_0 \frac{1+\nu}{1-2\nu} + Q_1 s_x \right] \\ H^*_y &= 2G \left[Q_0 \frac{1+\nu}{1-2\nu} + Q_1 s_y \right] \\ H^*_z &= 2G \left[Q_0 \frac{1+\nu}{1-2\nu} + Q_1 s_z \right] \end{aligned} \tag{5.89}$$

and

$$\begin{aligned} H^*_{xy} &= 2G[Q_1 s_{xy}] \\ H^*_{yz} &= 2G[Q_1 s_{yz}] \\ H^*_{zx} &= 2G[Q_1 s_{zx}] \end{aligned} \tag{5.90}$$

For direct use in a finite element formulation

$$d\sigma_{ij} = \{[C_{ijkl}]^e + [C_{ijkl}]^p\}\, d\epsilon_{kl} \tag{5.91}$$

where, $[C_{ijkl}]^e$ is given by equation (5.74) and

$$[C_{ijkl}]^p = \begin{bmatrix} H_xH_x^* & H_x^*H_y & H_x^*H_z & H_x^*H_{xy} & H_x^*H_{yz} & H_x^*H_{zx} \\ H_xH_y^* & H_yH_y^* & H_y^*H_z & H_y^*H_{xy} & H_y^*H_{yz} & H_y^*H_{zx} \\ H_xH_z^* & H_yH_z^* & H_zH_z^* & H_z^*H_{xy} & H_z^*H_{yz} & H_z^*H_{zx} \\ H_xH_{xy}^* & H_yH_{xy}^* & H_zH_{xy}^* & H_{xy}H_{xy}^* & H_{xy}^*H_{yz} & H_{xy}^*H_{zx} \\ H_xH_{yz}^* & H_yH_{yz}^* & H_zH_{yz}^* & H_{xy}H_{yz}^* & H_{yz}H_{yz}^* & H_{zx}H_{yz}^* \\ H_xH_{zx}^* & H_yH_{zx}^* & H_zH_{zx}^* & H_{xy}H_{zx}^* & H_{yz}H_{zx}^* & H_{zx}H_{zx}^* \end{bmatrix} \tag{5.92}$$

It is obvious from equation (5.92) that the tensor C^p_{ijkl} lacks symmetry, and so does C^{ep}_{ijkl} when a nonassociated flow rule is used, i.e.,

$$\text{if } Q \neq f, \text{ then } C^{ep}_{ijkl} \neq C^{ep}_{klij} \tag{5.93}$$

Furthermore, in this case, the elastic-plastic tangent stiffness C^{ep}_{ijkl} may not be positive definite. The stiffness matrix generated during the finite element solution procedure is also nonsymmetric in this situation. Therefore, a **nonsymmetric** equation solver is to be used to evaluate the displacements and stresses.

5.5.4 Problems with Associated Flow Rule

The main problems involved with using the *associated flow rule* while deriving the constitutive relations for rock mass using the Hoek–Brown yield surface are inelastic dilation and corner singularities. These phenomena are discussed below:

5.5.4.1 Inelastic Dilation

An important feature of the use of the associated flow rule in the derivation of the constitutive relations is the *inelastic* or *plastic cubic* or *volumetric* dilation $d\epsilon^p_{kk}$. The constitutive relations indicate that if the parameter of the Hoek–Brown criterion $m \neq 0$, then plastic deformation must be accompanied by an *increase* in volume. This property is known as

dilatancy, and it is the consequence of the dependency of the yield function on hydrostatic stress.

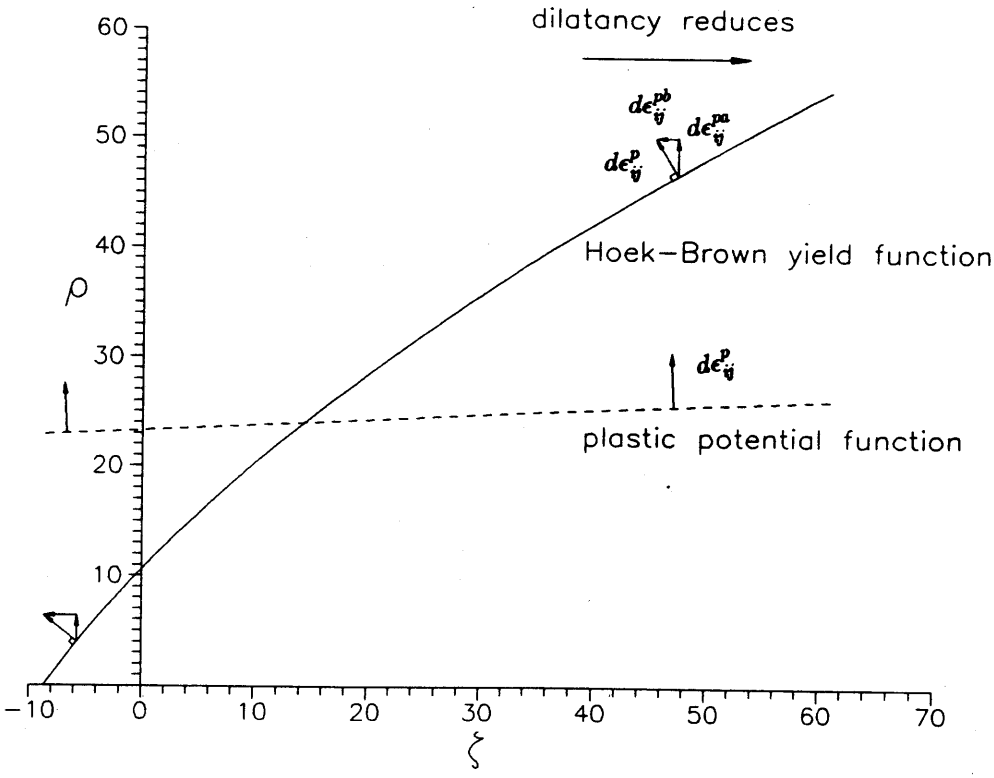

Figure 5.8: Plastic volume expansion (a) associated with Hoek–Brown Yield surface; (b) nonassociated.

This phenomenon can be explained geometrically as shown in Figure 5.8. The *compression* meridian of the Hoek–Brown yield surface is plotted in this figure. The *normality condition* or the associated flow rule requires that the plastic strain increment vector $d\epsilon_{ij}^{p}$ be perpendicular to the yield surface when the stress state is on the yield surface. It is therefore also perpendicular to the *compression* meridian. The vector $d\epsilon_{ij}^{p}$ is decomposed into a vertical and a horizontal component $d\epsilon_{ij}^{pa}$ and $d\epsilon_{ij}^{pb}$ parallel to the ρ and ξ axes, respectively. The horizontal component $d\epsilon_{ij}^{pb}$ represents the plastic volume change, which is always negative when the yield surface opens in the direction of the positive hydrostatic axis. This implies that plastic flow must always be accompanied by an *increase* in volume.

However, as stated earlier, geologic materials like rock, soil and concrete do not exhibit volume dilation, i.e. dilatancy is negligible or *zero* once failure has occurred. In

order to model this phenomenon, the nonassociated flow rule (equation 5.31) was used. The *compression* meridian of this plastic potential surface for $\alpha = 0.001$ is shown with dashed lines in Figure 5.8. The plastic strain increment vector $d\epsilon_{ij}^{p}$ is now normal to this potential surface. It can be observed from this figure that for a very small value of α, the potential surface is almost parallel to the ξ-axis. Therfore, the horizontal component of $d\epsilon_{ij}^{p}$ is approximately *zero*, indicating zero dilatancy. The slope of the potential function is governed by the value of α. If $\alpha = m$, then the flow is associated to the simplified Hoek–Brown surface (independent of Lode angle θ). If $\alpha = 0$, then dilatancy is *zero*. The range of values that can be used for α is $0 \leq \alpha \leq m$. Thus, by changing the value of α the person carrying out the analysis can model the actual volume dilation behaviour of the model. However, it should be remembered that α is a constant and is not a function of the accumulated plastic strain.

It can be observed from Figure 5.8 that since the Hoek–Brown yield surface has a nonlinear meridian, the dilatancy reduces as the hydrostatic stress increases. However, the dilatancy always has a finite negative value indicating volume *increase* after failure. In the case of the potential surface with $\alpha = 0.001$, the normal to the surface is near vertical, indicating very small inelastic volume increase. If $\alpha = 0.0$, then the potential surface will be parallel to the hydrostatic axis, and dilatancy will reduce to zero.

The advantages of using this *nonassociated flow rule* (equation (5.31)) are enumerated below:

1. The dilatancy reduces continuously in a nonlinear fashion with increasing confining pressure;
2. the numerical difficulties in dealing with singularities at corners of the potential surface are avoided; and
3. it is simple to calculate the first order derivative $\partial Q/\partial \sigma_{ij}$ of the potential surface as it involves I_1 and J_2 only.

5.5.4.2 Corner Singularity

As explained earlier the hexagonal paraboloidal shape of the Hoek–Brown surface results in corner singularity. At $\theta = 0$ and $\theta = \pi/3$, the derivatives of the yield surface with respect to the stress state $\partial f / \partial \sigma_{ij}$ cannot be evaluated. Therefore, the direction of the incremental plastic strain increment vector is not defined uniquely. In a numerical analysis code, this causes overflow in the calculations and the procedure is terminated.

In order to overcome this problem, several geometric and numerical smoothing procedures (Bathe (1982), Zienkiewicz (1977), Moreau (1975))have been suggested in the literature. These included fitting a circular arc near the corners with a radius equal to ρ at the location near the corner by keeping the tangents of the surface and the arc coincident at that location. The procedure adopted in this model is as follows:

- if $0 < \theta \leq 0.05°$, then the partial derivative $\partial f / \partial \sigma_{ij}$, i.e. B_0, B_1 and B_2, are evaluated explicitly at $\theta = 0.05°$ and these values are used in the stiffness calculations;
- if $59.95° \leq \theta < 60°$, then the partial derivative $\partial f / \partial \sigma_{ij}$, i.e. B_0, B_1 and B_2, are evaluated explicitly at $\theta = 59.95°$ and these values are used in further calculations.

This procedure has the effect of uniquely defining the direction of $d\epsilon^p_{ij}$ in the range of θ where $\partial f / \partial \sigma_{ij}$ does not exist. Since the range of θ where this procedure is applied is very small (0.05°), numerical solution of the finite element equations introduces only a very small error.

5.6 Properties of the Hoek–Brown Constitutive Model

The constitutive model for rock mass developed in this chapter is a simple, elastic–perfectly plastic one. It consists of only six parameters, viz. m, s, σ_c, E, ν and α. These six parameters are used to define the complete behaviour of the rock mass in the elastic as well as plastic range of stresses and deformations. The *associated* and the *nonassociated* flow rules have been incorporated into the model. The formulation of the *nonassociated* flow rule provides the user with the option of selecting the value of α in the range of $0 \leq \alpha \leq m$, corresponding to a zero-dilatant or a fully associated material. During the design of a

project, if the inelastic dilation behaviour of the rock mass is not available, the user can analyze the problem at hand, firstly, by taking $\alpha = m$ and, secondly, by taking $\alpha = 0$, to account for the extreme cases, and then use engineering judgement to select the analysis most representative of the actual field situation.

This constitutive model has been incorporated into the nonlinear finite element stress analysis program, ABAQUS (1989). The procedure for the incorporation of this model into the program is discussed in detail in Chapter 6.

Chapter 6

Implementation of Constitutive Relations for Rock Mass into ABAQUS and Verification of Model

6.1 Introduction

Constitutive Relations for rock mass have been developed in Chapter 5. They are presented in a form that can be directly implemented into a numerical solution procedure. These incremental stress-strain relations can be incorporated into any stress analysis computer program based on either the finite element method, finite difference method or the boundary integral equation method.

As discussed in Chapter 5, the second major task of the *theory of plasticity* is to develop numerical techniques for implementing these stress-strain relationships in the analysis of engineering structures. The general numerical solution procedure utilized for solving an elastic-plastic problem under the action of loads or displacements, each of which varies in a specified manner, should incorporate these stress-strain relations in order to predict the induced stresses, strains and displacements under a complex state of stress. The tremendous development of high-speed computers and techniques of finite element, finite difference and boundary integral equation analysis have supplied the engineer with powerful resources and enormous flexibility for the solution of virtually any nonlinear stress analysis problem.

Out of the three above-mentioned numerical analysis techniques, the *finite element* method has been firmly established as the prominent stress analysis technique. In contrast to the other techniques, the finite element method is essentially a product of the electronic digital computer age. Thus, although the approach shares many of the features common to the previous numerical approximations, it possesses certain characteristics that take advantage of the special facilities offered by high-speed computers. In particular, this method can be systematically programmed to accommodate such complex and difficult problems as nonhomogeneous materials, nonlinear stress–strain behaviour and complicated boundary conditions. A large number of publications on the theory, applicability and suitability of the finite element method are available in the literature (Zienkiewicz (1977), Desai and Abel (1972), Bathe (1982)). The reason for adopting this technique to implement the constitutive relations for rock mass is that this technique provides a large degree of flexibility for incorporating nonlinear constitutive relations for nonhomogeneous problems.

The finite element method has had an extremely active development since the late 1950s. During the first half of this period, research was concentrated on element formulation and the development of new approaches for solving problems involving linear elasticity, small and large strain. Element formulation, numerical integration techniques and development of efficient algorithms for the solution of the system of algebraic equations have reached a level of saturation. However, very little effort was concentrated on modelling nonlinear stress-strain behaviour of the material under a complex state of stress.

The majority of the applications of the finite element method are in the realm of solid mechanics including structural, soil and rock mechanics. This method has been applied to three major categories of boundary value problems: equilibrium of steady state problems, eigenvalue problems, and propagation of transient problems. These major categories of boundary value problems are used prominently in various fields of study, including structural engineering, structural mechanics, aerospace engineering, soil mechanics, foundation engineering, rock mechanics, heat conduction, hydrodynamics, hydraulic engineering, water resources, nuclear engineering, etc..

In spite of the broad range of fields in which this method is used, the development in the modelling of constitutive behaviour of the material is a fairly recent event. Thus, even though a very high level of sophistication is used in the analysis with a higher order

element and efficient solvers, the results predicted by the model will be of limited use if a linear, elastic or any simple material constitutive behaviour is used. Therefore, the aim of this chapter is to incorporate the elasto-plastic constitutive relations developed for rock mass in Chapter 5 into a finite element program in order to study and predict the response of the rock mass around underground excavations in a more realistic fashion.

6.2 ABAQUS – Finite Element Program

The constitutive model for rock mass was implemented into a commercially available finite element program rather than developing a nonlinear finite element program starting from basics. This decision was taken because developing a nonlinear finite element analysis program is in itself a major task. Because of the high degree of complexity of nonlinear solution and various other procedures involved in the development of such a program, the implementation and testing of the constitutive model would become a secondary issue. Therefore it was decided to use an existing finite element analysis program which has the facilities of incorporating the constitutive model. Out of the various commercially available and academic finite element programs, e.g. ABAQUS, ADINA, ANSYS, FEAP, etc., the program ABAQUS was selected to incorporate the constitutive model for rock mass. This was because ABAQUS has proved to be a very powerful program for analyzing geotechnical stress analysis problems among numerous other applications which it is used for.

6.2.1 Salient Features of ABAQUS

The salient features of ABAQUS (ABAQUS – User's Manual, 1989) are outlined below:

1. ABAQUS is designed as a flexible tool for numerical modelling of structural response. In order to provide for maximum flexibility in both linear and nonlinear analyses, a series of procedure has been written so as to offer a high degree of generality in modelling the history of loading of the structure to be analyzed.

2. The different types of analysis that can be undertaken with the procedures in ABAQUS are: static and dynamic stress analysis, heat transfer analysis, element removal and

replacement procedures, coupled diffusion/stress analysis, eigenvalue buckling prediction, coupled heat transfer/stress analysis, natural frequency extraction, Geostatic stress analysis, modal dynamic analysis including response spectrum, analyses for time history, steady-state and random response, procedures for substructuring or generation of superelements, and acoustic and coupled acoustic-structural analysis.

3. Among a vast element library of finite elements available in ABAQUS, the prominent ones are: solid (continuum) stress/displacement elements, truss elements, plane stress and plane strain elements, generalized plane strain elements, axisymmetric solid elements, three dimensional solid elements with variable nodes, membrane elements, beam elements, shell elements, gap elements, joint elements, interface elements, etc.. These elements are available with different integration schemes including reduced integrations schemes.

4. Nonlinear stress analysis problems can be carried out for material nonlinearity, geometric nonlinearity or boundary nonlinearity and any combination of these nonlinearities.

5. ABAQUS has several elastic, plastic, fluid flow, acoustic material models built into it which include elastic, hyperelastic, hypoelastic, porous elastic, Drucker–Prager, Clay Plasticity, Concrete models, foam model, permeability, porosity, viscoelasticity, viscoplasticity, creep, deformational plasticity, latent heat models, etc.. Besides this, the program also provides the users with the flexibility of implementing their own material constitutive models. This is in the form of a subroutine **UMAT** which is written by the user and compiled with the program during the process of running the program. The description of subroutine **UMAT** is given in a later section.

6. In nonlinear problems the challenge is always to obtain a convergent solution at minimum cost. The nonlinear procedures in ABAQUS offer two approaches to this. Direct user control of increment size is one choice, whereby the user specifies the incrementation scheme. This is particularly useful in repetitive analyses where the user has a very good "feel" of the problem. Automatic control of incrementation is an alternative choice: the user defines a period of history and at the same time specifies certain tolerances or error measures. ABAQUS then automatically selects the increments to model the step. This approach is usually more efficient since the user cannot predict

the response ahead of time. Automatic control will, in some cases, increase the cost of the analysis over the cost when the response is essentially predictable and direct user specification of increments is adopted, but automatic control can save enormously over repeated user controlled running of a problem to obtain a satisfactory incrementation scheme. In addition, automatic incrementation is extremely valuable in nonlinear problems when convergence is achieved quickly or is not achieved in certain steps. If convergence is achieved in the first iteration of the step, ABAQUS increases the step size for the next increment so as to reach the final solution stage in a quicker fashion. However, if convergence is not achieved in successive iterations of a step, ABAQUS automatically cuts back on the step size and tries to achieve convergence with a smaller step size. This is useful for problems in which the material exhibits nonlinearity with strain softening or hardening.

7. Nonlinear static analysis requires the solution of nonlinear equilibrium equations, and the program uses Newton's method for this purpose. Many problems involve history dependent response, so that the solution is usually obtained as a series of increments, with iteration within each increment to obtain equilibrium. Increments must sometimes be kept small so as to assure correct modelling of history dependent effects, but most commonly the choice of increment size is a matter of computational efficiency, i.e., if the increments are too large, more iterations will be required. Newton's method has a finite radius of convergence, which suggests that too large an increment can prevent any solution from being obtained because the initial state is too far away from the equilibrium state that is being sought, i.e. it is outside the radius of convergence. Thus, there is an algorithmic restriction on the increment size. For most cases the automatic incrementation is preferred.

8. For nonlinear static analysis, the increments or steps can be provided by two approaches. Firstly, the case where the loading variations over the step must follow a prescribed history. The definition of these increments are given directly by the user, or automatic incrementation can be used. The automatic scheme for this procedure is based on the convergence of the iteration process at each increment. The second approach is where the loading is proportional, but the load magnitude is considered to be part of the solution because buckling or collapse may occur. The modified Riks method is provided in ABAQUS for such cases, the basis of this method being to choose a

increments based on controlling the path length along the load-displacement response curve, and thus obtain solutions regardless of whether the response is stable or unstable (ABAQUS – Theory manual 1989). In this procedure, the variation of loading magnitude over the step is considered to be an unknown which is to be determined as part of the solution. During a RIKS step ABAQUS prints out a "load proportionality factor" at each increment. This defines the current local magnitudes according to:

$$P_{\text{total}} = P_0 + \lambda \left(P_{\text{ref}} - P_0 \right) \tag{6.1}$$

where,

P_{total} = current magnitude of the load component;
P_0 = magnitude of this load component at the start of the step;
P_{ref} = magnitude of this load component as defined in the data for the step; and
λ = "load proportionality factor".

The Riks algorithm is based on attempting to step along the equilibrium path by prescribing the path length along the curve to be traversed in each increment. This means that the load magnitude is determined by the solution, with the consequence that, when the Riks procedure is chosen, the user no longer has control over this magnitude. This causes a control problem – the user must specify when the step will be completed. This may be accomplished with any combination of the following two possibilities:

(a) by defining a maximum value of λ beyond which the solution is not of interest. The step terminates when this value is exceeded; and

(b) by specifying a finishing displacement at a specified degree of freedom. The step will terminate when this limiting displacement is crossed.

9. During the numerical solution of the equilibrium equations at each increment a tolerance value **PTOL** is provided. All forces at all nodes (except those with prescribed displacements) must fall below this tolerance for the solution to be accepted; otherwise ABAQUS continues to iterate the increment. If convergence is not achieved in the maximum number of iterations allowed for each step, the increment is subdivided if automatic incrementation is chosen, or the job is terminated. Usually PTOL is set to a small fraction $(10^{-2} - 10^{-4})$ of typical actual force values.

10. As discussed in Chapter 5, if an *associated flow rule* is used in generating the incremental stress-strain relations, a symmetric equation solver is used for solving the

equilibrium equations. However, if a *nonassociated flow rule* is used, the material stiffness matrix generated from the constitutive relations is unsymmetric, and therefore, an *unsymmetric* equation solver is to be used. ABAQUS provides the user with the facility to use either a symmetric or an unsymmetric solver depending on the requirements of the problem.

11. ABAQUS runs as a batch application program. The main input is a file which indicates which options are required, and gives the data associated with those options. There may also be supplementary files, such as restart or result files from previous analyses, or auxiliary data files, for example a file containing an earthquake record for dynamic analysis. An example input file is provided in Appendix B which was used for the analysis of the behaviour of rock mass around a circular excavation.

6.3 Subroutine UMAT

As discussed in the previous section, ABAQUS provides an interface whereby the user can write his own constitutive model in subroutine **UMAT** in a very general way. **UMAT** is the subroutine where the user can define the mechanical constitutive behaviour of the material to be used by ABAQUS. This subroutine is called at each material calculation point for which the definition of the material is in the form of *USER MATERIAL. The interface to this user subroutine is simple. When the subroutine is called, it is provided with the state at the start of the increment (stress, solution dependent state variables, temperature, etc.); with the increments in temperature and predefined state variables; and with the strain increments and the time increments. The subroutine performs two functions: it updates the stresses and the solution dependent variables to their values at the end of the increment, and it provides the material constitutive matrix for the constitutive model. The accuracy with which this matrix is defined is usually a major determinant of the rate of convergence of the solution, and so has a strong influence on computational efficiency.

The *USER MATERIAL option includes the parameter UNSYMM. Use of this parameter indicates that the material constitutive matrix is not symmetric, and invokes the program's unsymmetric equation solution capability. Most constitutive models require the storage of solution dependent state variables, e.g., plastic strains, failure state, etc..

The *DEPVAR option is used in the *MATERIAL definition to allocate storage for these variables.

Subroutine UMAT was developed for constitutive modelling of rock mass and is reproduced in Appendix B. An explanation of its arguments that are relevant to this model are explained below:

```
      SUBROUTINE UMAT (STRESS, STATEV, DDSDDE, SSE, SPD, SCD,
     1 RPL, DDSDDT, DRPLDE, DRPLDT,
     2 STRAN, DSTRAN, TIME, DTIME, TEMP, DTEMP, PREDEF, DPRED, CMNAME,
     3 NDI, NSHR, NTENS, NSTATV, PROPS, NPROPS, COORDS, DROT)

      IMPLICIT REAL*8(A-H, O-Z)
      CHARACTER*8 CMNAME
      DIMENSION STRESS(NTENS), STATEV(NSTATV),
     1 DDSDDE(NTENS,NTENS),
     2 DDSDDT(NTENS), DRPLDE(NTENS),
     3 STRAN(NTENS), DSTRAN(NTENS), PREDEF(1), DPRED(1),
     4 PROPS(NPROPS), COORDS(3), DROT(3,3)


      user coding


      RETURN
      END
```

The variables in the argument are as follows:

DDSDDE(NTENS,NTENS): This is the matrix of the constitutive model. DDSDDE(I,J) defines the change in the Ith stress component at the end of the time increment caused by an infinitesimal perturbation of the Jth component of the strain increment array. Unless the parameter UNSYMM is specified on the *USER MATERIAL option associated with this material, ABAQUS uses the symmetric part of DDSDDE only.

STRESS(NTENS): This array is passed in as the stress tensor at the beginning of the increment, and is updated in this routine to be the stress tensor at the end of the increment.

STATEV(NSTATV): This is the array of solution dependent state variables. They are passed in as the value at the beginning of the increment and they are returned as the values at the end of the increment. The size of this array is that defined on the *DEPVAR option associated with this material.

The variables passed in for information are:

STRAN(NTENS): This is the array of total strain components at the beginning of the increment.

DSTRAN(NTENS): This is the array of strain increments.

TIME: The total time value at the start of the increment.

DTIME: This is the time increment.

NDI: number of direct stress components at this point.

NSHR: number of engineering shear stress components at this point.

NTENS: NDI + NSHR: the size of the stress or strain component array.

PROPS(NPROPS): The array of material constants entered in the *USER MATERIAL option for this material.

NPROPS: The number of material constants (the value given to the CONSTANTS parameter of the *USER MATERIAL option).

Several utility routines exist in ABAQUS that are useful for the coding of the routine. They are used as follows:

1. Stress invariants:

```
CALL SINV(STRESS,SINV1,SINV2)
```

Given a stress tensor, STRESS, with NDI direct components and NSHR shear components, this routine returns the first invariant of the stress tensor and the second invariant of the deviatoric stress tensor.

$$\mathtt{SINV1} = \frac{1}{3}\sigma_{kk} = \frac{1}{3}I_1 \tag{6.2}$$

and

$$\mathtt{SINV2} = \sqrt{3J_2} \tag{6.3}$$

2. Principal values:

```
CALL SPRINC(S,PS,LSTR)
```

Given a stress tensor, S, with NDI direct components and NSHR shear components, this routine returns the three principal values in PS(1), PS(2) and PS(3). LSTR is an identifier that is supplied: LSTR = 1 indicates that S contains stresses, LSTR = 2 indicates that S contains strains. Principal values are ordered in ascending algebraic order.

Two other subroutines and one function were written which are called by UMAT for various procedures. These routines are described below:

1. Function **FAILUR**:

```
REAL*8 FUNCTION FAILUR(TPSTRS,PROPS,NTENS,NPROPS)
```

Function FAILUR checks whether the present stress state defined by TPSTRS is on the yield surface, i.e. $f(\sigma_{ij}) = 0$ or if the material is in an elastic state, i.e. $f(\sigma_{ij}) < 0$. The value of the Lode angle θ is evaluated from the principal stresses, and its magnitude is checked in order that its value is not in the region of corner singularity. If it is, then the smoothing procedure described in Chapter 5 is used to evaluate the Lode angle. This function then returns the value of $f(\sigma_{ij})$ to subroutine UMAT. NTENS, PROPS, NPROPS are as defined earlier.

2. Subroutine **HOEKBR**:

```
SUBROUTINE HOEKBR(TPSTRS,PROPS,NTENS,NPROPS,DEPSP,CONSTI)
```

TPSTRS, PROPS, NTENS, NPROPS are as defined earlier. DEPSP(6) is an array that stores the incremental plastic strain tensor, and CONSTI(6,6) is the matrix where the constitutive matrix is stored. This is the subroutine where the elasto-plastic constitutive matrix C^{ep}_{ijkl} is generated when plasticity calculations are done. The deviatoric stress tensor s_{ij} is evaluated from the total stress tensor since it is required in the calculation of the tensor H_{ij}. The derivative of the yield and plastic potential functions, $\partial f/\partial\sigma_{ij}$ and $\partial Q/\partial\sigma_{ij}$, respectively, are calculated by evaluating the coefficients

B_0, B_1, B_2 and Q_0, Q_1 as discussed in Chapter 5. Since a numerical singularity can occur while evaluating the partial derivative of the yield function with respect to the stress state near the corners, the value of the Lode angle θ is checked and modified if it lies in the "corner" region. The terms h, H_{ij} and H^*_{ij} are also evaluated which are then used in the generation of the plastic constitutive matrix C^p_{ijkl}. The elastic matrix C^e_{ijkl} is also generated and combined with C^p_{ijkl} to produce the elasto-plastic constitutive matrix C^{ep}_{ijkl}. The stress tensor is updated here with the value of C^{ep}_{ijkl} and the incremental strain vector $d\epsilon_{ij}$. This updated stress tensor TPSTRS and the constitutive matrix CONSTI are then returned to subroutine UMAT.

3. Subroutine **DERSTR**

```
SUBROUTINE DERSTR(ST,PROPS,NTENS,NPROPS,DFST)
```

This subroutine is used to calculate the derivative of the yield surface with respect to the stress state ST. The derivatives $\partial f/\partial\sigma_{ij}$ are stored in a vector DFST(6). These derivatives are used while evaluating whether the material is still loading or unloading from a plastic state.

6.3.1 Calculation Procedure in Subroutine UMAT

The procedure for calculating the material constitutive matrix is presented in this section. It is based on the procedures specified in Bathe (1982) and Nayak and Zienkiewicz (1972).

A major characteristic of inelastic analysis is that the constitutive matrix is dependent on the current conditions of stresses, strains and other state variables plus their history. For elastic-perfectly plastic analysis, it depends on the stress state. It follows that to obtain an accurate response prediction it is necessary to employ the stress calculation procedure in an integration process. Specifically, once the approximations to the displacement increments have been evaluated, the stresses corresponding to time $t+\Delta t$ are calculated as

$$^{t+\Delta t}\sigma = {}^{t}\sigma + \int_{t}^{t+\Delta t} C^{ep} d\epsilon \tag{6.4}$$

where,

$^{t}\sigma$ = the stress state at time t.

In order to solve for an accurate response prediction, equilibrium iterations are in general required, in which case equation (6.4) is generalized to the equation,

$$^{t+\Delta t}\sigma^{(i-1)} = {}^{t}\sigma + \int_{t}^{t+\Delta t(i-1)} C^{ep} d\epsilon \tag{6.5}$$

The general observation is that in inelastic analysis an integration of the stresses are to be carried out during each equilibrium iteration. This integration was performed in subroutine UMAT using the Euler forward integration scheme in which the solution is simply obtained by forward integrating over a sufficient number of subincrements in order to obtain the required accuracy in the integration process.

As stated earlier, ABAQUS provides the stress $({}^{t}\sigma_{ij})$, strain $({}^{t}\epsilon_{ij})$ from the previous step and the strain increment $(d\epsilon_{ij})$ for the current step to subroutine UMAT. The steps involved in this subroutine are explained below:

1. The stress increment corresponding to the strain increment $d\epsilon_{ij}$ is calculated assuming elastic behaviour

$$d\sigma_{ij} = C^{e}_{ijkl} d\epsilon_{kl} \tag{6.6}$$

2. The total stress is the calculated as

$$^{t+\Delta t}\sigma_{ij} = {}^{t}\sigma_{ij} + d\sigma_{ij} \tag{6.7}$$

3. With this new state of stress, the value of the yield function $f(\sigma_{ij})$ and the its derivative with respect to the stress state $\partial f / \partial \sigma_{ij}$ are determined.

4. The criterion for loading, unloading or neutral loading is evaluated in this step. If $f(\sigma_{ij}) < 0$, elastic behaviour assumption holds, i.e., the material is loading elastically. If $f(\sigma_{ij}) = 0$ and $df = (\partial f / \partial \sigma_{ij}) d\sigma_{ij} < 0$, then the material is unloading, and hence, elastic behaviour of the material is assumed. Therefore, for these two situations, the updated value of the stress is taken equal to $^{t+\Delta t}\sigma_{ij}$ and subroutine UMAT is exited. However, if $f(\sigma_{ij}) = 0$ and $df = (\partial f / \partial \sigma_{ij}) d\sigma_{ij} = 0$, the material is loading and, in this case, the following steps are undertaken.

5. If the previous state of stress was plastic as indicated by a flag stored in the state dependent variable `STATEV(1)`, then the variable `RATIO` is set to zero, and the command passes to step 7. Otherwise, there is a transition from elastic to plastic, and

RATIO, which is the portion of incremental strain taken elastically is determined. The variable RATIO is determined from the equation

$$f\left(\sigma_{ij} + \text{RATIO} * d\sigma_{ij}\right) = 0 \tag{6.8}$$

since at the stress $(\sigma_{ij} + \text{RATIO} * d\sigma_{ij})$ the yield function becomes equal to zero and yielding is initiated. The value of RATIO is obtained as

$$\text{RATIO} = -\frac{f\left({}^{t}\sigma_{ij}\right)}{\frac{\partial f}{\partial({}^{t}\sigma_{ij})} d\sigma_{ij}} \tag{6.9}$$

6. The stress σ_{ij} is redefined as that at start of yield, i.e.

$$^{t+\Delta t}\sigma_{ij} = {}^{t}\sigma_{ij} + \text{RATIO} * d\sigma_{ij} \tag{6.10}$$

and the plastic strain increment is calculated as

$$d\epsilon^{p}_{ij} = (1 - \text{RATIO}) * d\epsilon_{ij} \tag{6.11}$$

7. To obtain the final stresses, which include the effect of the complete strain increment $d\epsilon_{ij}$, the stresses corresponding to $d\epsilon^{p}_{ij}$ are to be added to ${}^{t}\sigma_{ij}$. Since the material constitutive law is dependent on the current stresses, $d\epsilon^{p}_{ij}$ is subdivided into subincrements $\Delta d\epsilon^{p}_{ij}$ and ${}^{t}\sigma_{ij}$ is updated for each interval by the increments in stresses corresponding to the increments in elastic-plastic strains in that interval. In this calculation, the constitutive matrix corresponding to the latest available stress conditions is used, i.e. the calculation is according to

$$^{t+\Delta t(i)}\sigma_{ij} = {}^{t+\Delta t(i-1)}\sigma_{ij} + C^{ep}\Delta d\epsilon^{p}_{ij} \tag{6.12}$$

for all elastic-plastic strain subincrements $\Delta d\epsilon^{p}_{ij}$.

It should be noted here that while performing checks for equality or inequality for terms such as $f\left(\sigma_{ij}\right)$ and df, the value used is a small tolerance limit instead of zero. This tolerance value is specified currently as 0.01 in the subroutine. A small tolerance value is used instead of zero because of the limit of precision of the computer.

The sign convention in ABAQUS is tension positive. However, since the constitutive model has been formulated for compression positive, the signs of the stresses and strains

passed to UMAT are changed at the initiation of the routine, and after they have been updated as required, their signs are reversed back to tension positive.

Subroutine UMAT has been developed for the general three-dimensional state of stress. In this subroutine, the stresses are updated for all the six components of stress and the constitutive matrix is generated as a 6 by 6 matrix. Depending on the type of problem being analyzed and the type of elements being used, ABAQUS passes the number of direct stress (`NDI`) components and the number of shear stress (`NSHR`) components with a total of `NTENS` = `NDI` + `NSHR` components to subroutine UMAT. When subroutine UMAT returns the updated values of the stresses, `STRESS`, and the constitutive matrix, `DDSDDE`, only those components specified by `NDI` and `NSHR` are returned to ABAQUS.

6.4 Testing of Model against Standard Solutions

Once the constitutive model for rock mass was programmed as subroutine UMAT for ABAQUS, the testing of the model against standard test cases was initiated in order to verify its correctness and its applicability for geotechnical applications. This procedure satisfies the final requirement of the Steps in the Development of Constitutive Law as outlined in Chapter 5 (section 5.2.1). Uniaxial tests, triaxial tests at various values of confining pressures and analysis of a circular hole in an infinite medium under hydrostatic stress conditions were carried out to verify the results of the constitutive model. These results were compared with standard values which are obtained from Lama and Vutukuri (1978), Brown, Bray, Ladanyi and Hoek (1983). The results of these tests are presented in the following sections.

6.4.1 Uniaxial Compression Test

Uniaxial or unconfined compression test of a rock mass was carried out with the *associated* and *nonassociated* flow rules for the following properties:

- *Rock mass properties*:

  $m = 7$, $s = 1$, $\sigma_c = 35$ MPa, $E = 20$ GPa, $\nu = 0.2$, and $\alpha = 0.25$.

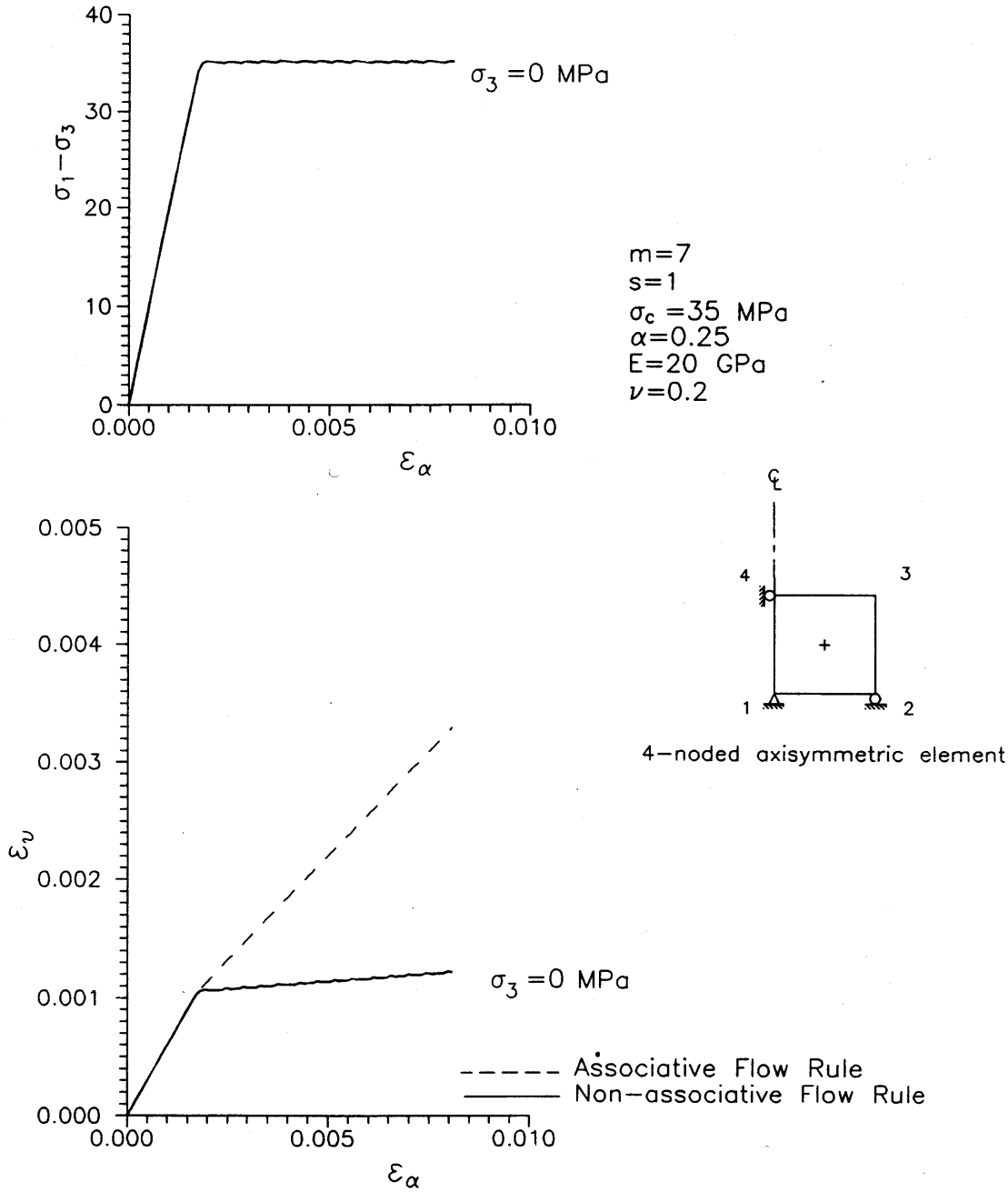

Figure 6.1: Results of Uniaxial Test on Rock Mass with $m = 7$, $s = 1$, $\sigma_c = 35$ MPa.

- *Element type*:

  The element used for the analysis was CAX4R which is a 4-noded bilinear, reduced integration axisymmetric solid element. The number of constitutive calculation points is one and this is at the center of the element. The size of the element used in the analysis was 1 m x 1 m.

- *Boundary conditions*:

  As shown in Figure 6.1, the boundary conditions are such that displacements are prevented in the vertical direction at nodes 1 and 2 and in the horizontal direction at nodes 1 and 4.

- *Loading*:

  The element was loaded in a displacement controlled fashion since this process simulates the actual loading of a specimen in the laboratory. The face corresponding to nodes 3–4 was displaced downwards to load the element. This type of loading does not cause convergence problems once the material has failed.

- *Solution procedure*:

  The analysis was carried out in a single step with an initial increment of 0.005 and a maximum increment of 0.014 and the maximum displacement at node 3 was limited to −0.008 m. The displacement of this node was limited to this value as the solution is to be stopped at a certain value of displacement otherwise the calculations will continue for ever. The Riks procedure was used and during the analysis, it was noticed that ABAQUS started with an initial increment of 0.005 and rapidly increased it to the maximum of 0.014. After failure had occurred the incrementation was cutback several times when convergence was not being achieved in one increment. The value of PTOL was taken as 0.3 which is approximately $1/100^{th}$ of the maximum load expected to be achieved in the analysis.

For the Hoek–Brown criterion, the compressive strength under uniaxial conditions, i.e. for $\sigma_3 = 0$ MPa, for a rock mass whose material parameters are $m = 7$, $s = 1$ and $\sigma_c = 35$ MPa is equal to 35 MPa which is clearly illustrated in Figure 6.1 depicting the variation of $(\sigma_1 - \sigma_3)$ or σ_1 (as $\sigma_3 = 0$ in this case) versus axial strain ϵ_a. The strength remains constant

at 35 MPa with the increase in axial strain after failure because the constitutive law models the material as an elastic-perfectly plastic material.

The uniaxial test was carried out for two cases: firstly, an analysis was done with the *associated* flow rule, and secondly, with the *nonassociated* flow rule for $\alpha = 0.25$. It can be observed from Figure 6.1 that for the *associated* flow, the volumetric strain ϵ_v keeps on increasing with the increase in axial strain ϵ_a indicating volume expansion of the rock mass after failure. However, in the case of *nonassociated* flow with $\alpha = 0.25$, the volumetric strain shows very little increase with increase in axial strain. If α is taken as zero, then the volumetric strain remains constant after failure. Thus, it can be deduced from this figure that the user can control the inelastic dilation of the material depending on the test data available.

6.4.2 Triaxial Tests at Different Confining Pressures

The second set of tests carried out for the verification of the constitutive model was triaxial tests with confining pressures σ_3 of 10 and 15 MPa. The *rock mass properties, element type* and *boundary conditions* were similar to that for the Uniaxial compression test. However, the *loading* of the model and the *solution procedure* were different and are described below:

- *Loading of the model*:

  The model was loaded in two steps. In the first step, an all-round confining pressure was applied to the model in the form of pressure loads on the faces corresponding to nodes 2–3 and 3–4. The model was allowed to reach an equilibrium solution, and then in the second step, the element was loaded in a displacement controlled fashion as described for the uniaxial compression test. The element face corresponding to nodes 3–4 was displaced downward to simulate the axial loading of the specimen in the lab.

- *Solution procedure*:

  The analysis was carried out in two steps. In the initial step pressure loading equal to the confining pressure was applied on element faces 2–3 and 3–4. The initial increment in the load was specified as 0.45 with a maximum increment of 1.0. The model

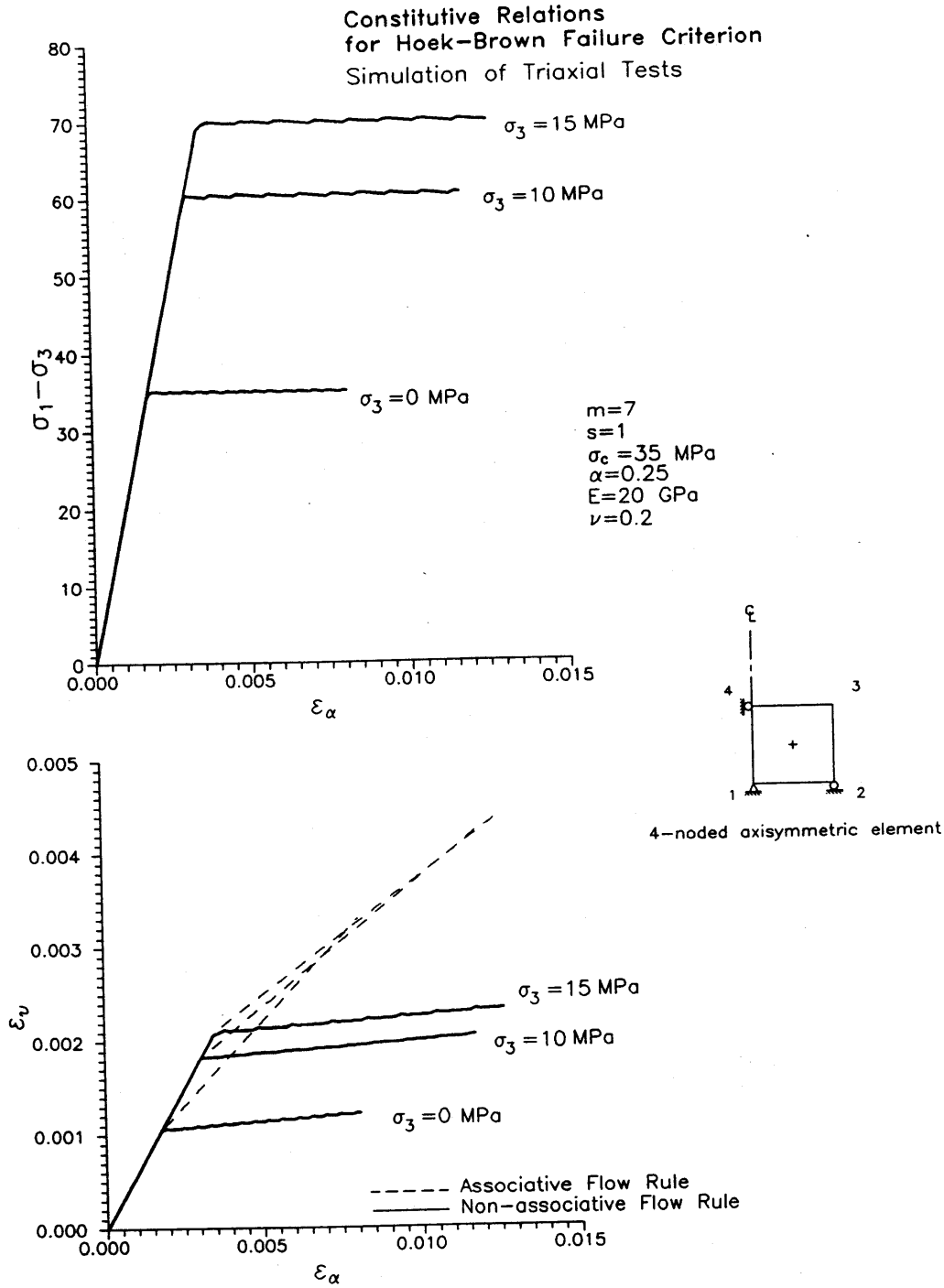

Figure 6.2: Results of Triaxial Test on Rock Mass with $m = 7$, $s = 1$, $\sigma_c = 35$ MPa for confining pressures $\sigma_3 = 10$ and 15 MPa.

reached equilibrium and it was observed from the results that the principal stresses at the constitutive calculation point were equal to the applied confining pressure. In the second step, displacement loading was applied on element face 3–4. The initial increment of load at this step was taken as 0.01 with a maximum of 0.015 and the limiting displacement at node 3 was taken as -0.012 m and -0.015 m for $\sigma_3 = 10$ MPa and $\sigma_3 = 15$ MPa, respectively. The Riks procedure was also used in the analysis and PTOL was specified as 0.1 for the first step and 0.5 for the second step.

According to the Hoek–Brown criterion, the strength of a rock mass, whose material strength parameters are $m = 7$, $s = 1$ and $\sigma_c = 35$ MPa, is 70.62 MPa for $\sigma_3 = 10$ MPa and 85 MPa for $\sigma_3 = 15$ MPa. The values of $(\sigma_1 - \sigma_3)$ for these confining pressures are 60.62 MPa and 70 MPa. As can be observed from Figure 6.2, the values of $(\sigma_1 - \sigma_3)$ for these two cases from the finite element solution are very close to the predicted values. The slight variation in the values of the strength can be attributed to the numerical solution process and the value of the tolerance specified for the inequality $f(\sigma_{ij}) \leq 0$.

These triaxial tests were carried out for the *associated* flow rule as well as the *nonassociated* flow rule for $\alpha = 0.25$. It can be observed from Figure 6.2 that for the *associated* flow rule, the volumetric strain ϵ_v keeps on increasing with the increase in axial strain ϵ_a. This indicates volume expansion in the rock mass after failure. However, in the case of *nonassociated* flow with $\alpha = 0.25$, ϵ_v shows very little increase with increase in ϵ_a. Again, if $\alpha = 0$, then there will not be any inelastic dilation after failure in the post peak region of deformations.

The variation of ϵ_v with ϵ_a of the triaxial tests as well as the uniaxial test is shown in Figure 6.2. An interesting phenomenon that can be observed from this figure is that the slope of the ϵ_v *vs.* ϵ_a curve for the *associative* flow rule case decreases with increase in confining pressure. This shows that the *dilatancy* of the rock mass reduces with the increase in confining pressure. The primary reason for this phenomenon is the nonlinear nature of the Hoek–Brown yield surface as was discussed in Figure 5.8 in Chapter 5.

6.4.3 Circular Tunnel Under Hydrostatic Stress

Analysis of stress distribution around a circular underground excavation under hydrostatic stress conditions was also carried out for a tunnel of 1 m radius. The *nonassociated* flow rule was used for the analysis with $\alpha = 0$. The tunnel is assumed to be excavated in a continuous, homogeneous, isotropic, elastic–perfectly plastic rock mass, complying with the Hoek–Brown yield criterion and the plastic potential surface developed corresponding to this criterion. Since this problem is symmetric about the horizontal and vertical axes, only a quarter of the circle was analyzed. The input data file for this example is listed in Appendix B. The parameters used in the analysis and the analysis procedure are described below:

- *Rock mass properties*:

  $m = 7$, $s = 1$, $\sigma_c = 8.6$ MPa, $E = 10$ GPa, $\nu = 0.25$, $\alpha = 0.0$.

- *In situ stress condition*:

  The *in situ stress condition* before excavation of the tunnel is hydrostatic, i.e., $\sigma_1 = \sigma_2 = \sigma_3 = 15$ MPa.

- *Element type and discretization*:

  The type of element used in the analysis is CPE8 which is a 8 noded biquadratic plane strain element with nine constitutive calculation points corresponding to the 3x3 Gaussian Quadrature integration scheme.

  The total number of elements used in the analysis was 80 out of which the inner most 8 elements were removed to model the excavation of the tunnel. The finite element mesh for this problem is shown in Figure 6.3. It can be seen in this figure that a finer mesh is used near the excavation which corresponds to a larger number of constitutive calculation points in the region where the stress gradient is expected to be high, and a gradual reduction in the density away from the excavation. The finite element mesh is terminated at a distance (d) corresponding to a ratio $d/r = 10$, where r is the radius of tunnel and is equal to 1 m. This distance is considered to be far enough so that the effect of the boundary on the stress distribution near the region of interest is negligible.

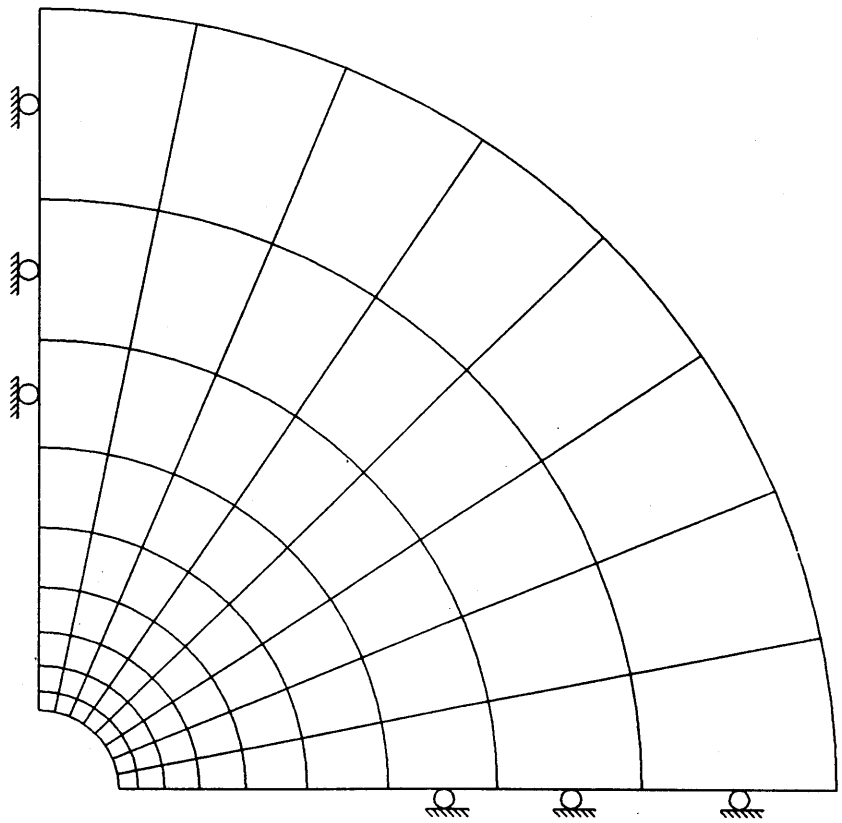

Figure 6.3: Finite Element Mesh for Circular Tunnel under Hydrostatic stress conditions $\sigma_1 = \sigma_2 = \sigma_3 = 15$ MPa.

- *Boundary conditions*:

  Since only a quarter of the circular excavation was analyzed, the boundary conditions for symmetry along the horizontal and vertical axes were applied. These conditions correspond to roller supports preventing displacements in the horizontal direction for the nodes of the elements on the left edge and in the vertical direction for the nodes of the elements along the bottom. These conditions are shown in Figure 6.3.

- *Loading*:

  This problem was loaded in two steps. In the first step, the entire model was subjected to *GEOSTATIC condition which loaded the domain with the *in situ* stress given in the *INITIAL CONDITIONS. All the elements were loaded to a hydrostatic state of stress equal to 15 MPa. In the next step, the tunnel was excavated by removing the first array of elements near the center.

- *Solution procedure*:

  The solution for the first step corresponding to GEOSTATIC loading was done with PTOL = 0.10. The entire system was allowed to equilibrate at the end of which all the constitutive points were loaded with the stresses corresponding to the *in situ* hydrostatic stress field. In the second step, the elements for the tunnel were removed and equilibrium iterations were carried out for PTOL = 0.05 with and initial and final increment of 0.02. The state of each constitutive point was monitored to ascertain whether it had failed or if it was still in the elastic stage. Since the *nonassociated* flow rule was used in the analysis, the unsymmetric equation solver facility of ABAQUS had to be used.

The variation of the tangential, radial and out-of-plane stresses with distance along a radial direction from the excavation boundary is depicted in Figure 6.4. The variation of these three stress components with distance is described below:

1. Tangential stress $\sigma_{\theta\theta}$ *vs* d:

   Figure 6.4 shows the variation of $\sigma_{\theta\theta}$ with radial distance for the case of elastic analysis as well as elasto-plastic analysis with the Hoek–Brown constitutive model. For the initial hydrostatic stress state corresponding to $\sigma_1 = \sigma_2 = \sigma_3 = 15$ MPa, the stress

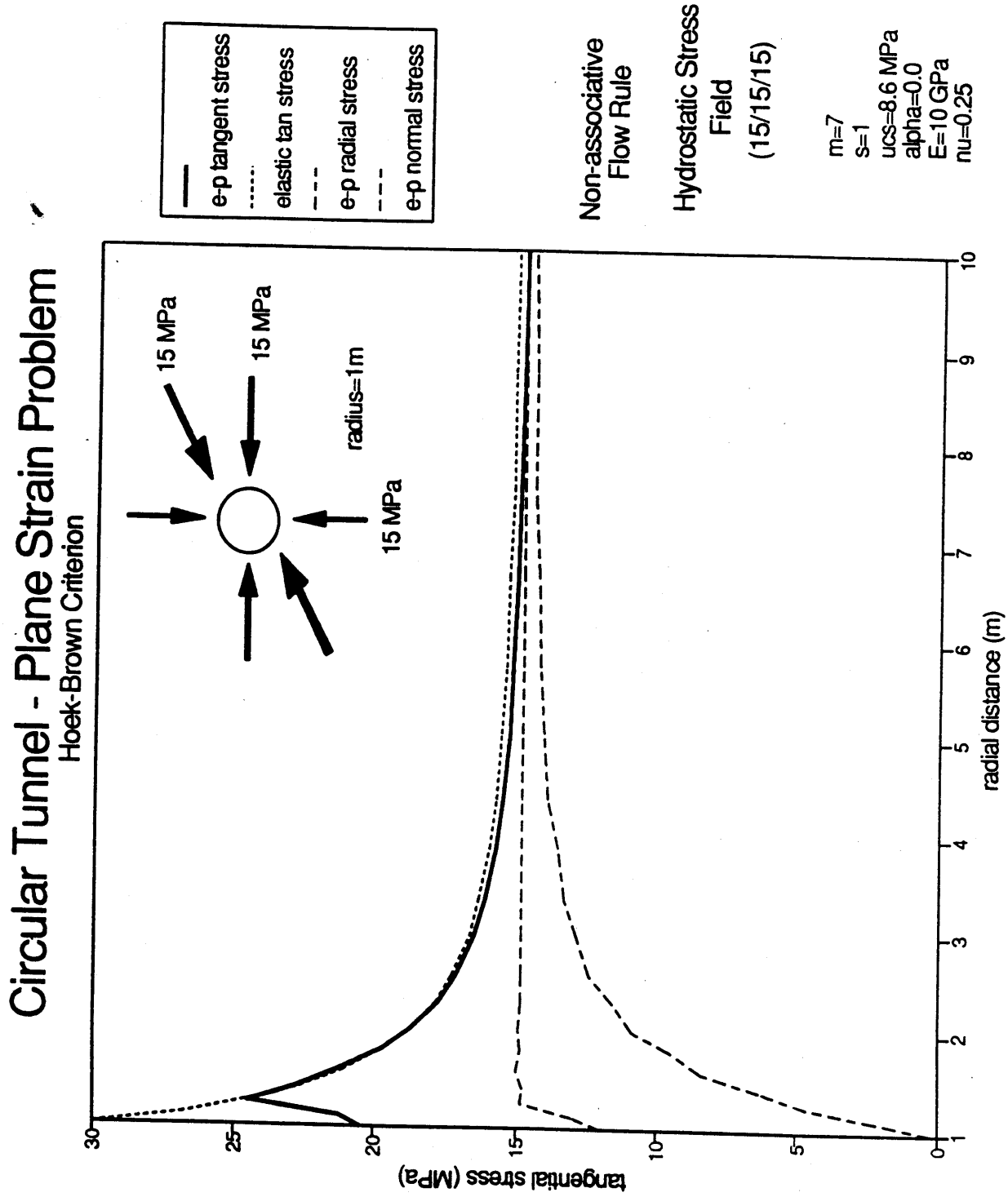

Figure 6.4: Variation of Tangential, Radial and Out-of-plane stresses with distance for Circular Excavation. Elastic stresses correspond to Kirsch's solution

concentration factor for tangential stress at the excavation boundary is $k = 2$. The value of $\sigma_{\theta\theta}$ from elastic analysis at the excavation boundary $d = r = 1$ m is 30 MPa. However, from elasto-plastic analysis, $\sigma_{\theta\theta}$ has dropped down to appx. 20.5 MPa at the boundary. This indicates that the constitutive calculation point in the rock mass next to the excavation has failed and is not able to sustain any additional load. This causes the load to be transferred further back into the rock mass. The confining stresses increase as we travel away from the excavation boundary. With the increase in the confining stress, the yield strength of the rock mass increases. Therfore, as shown in the figure, the value of $\sigma_{\theta\theta}$ increases. However, this value is much less than the elastic value of $\sigma_{\theta\theta}$ for that location. Therefore, the material in this region has also failed but is able to sustain higher loads due to the confinement. The curve for the variation of $\sigma_{\theta\theta}$ with radial distance (d) intersects the elastic $\sigma_{\theta\theta}$ *vs* d curve. This intersection point indicates the limit of the failure zone around the excavation. The variation of $\sigma_{\theta\theta}$ *vs* d follows the elastic variation after this point as the material in this region is still in an elastic state.

2. Radial stress σ_{rr} *vs* d:

   The radial stress σ_{rr} varies nonlinearly with radial distance (d) starting at 0 at the excavation boundary. Its value reaches the *in situ* stress value as we approach the domain boundary.

3. Out-of-plane stress σ_{zz} *vs* d:

   The out-of-plane stress σ_{zz} decreases in the region where the rock mass has failed. Its value is lowered from an *in situ* value of 15 MPa to appx. 12.5 MPa at the excavation boundary. The value of σ_{zz} then increases and reaches the *in situ* value at the end of the failed zone. It remains constant at 15 MPa after that.

The variation of radial displacement with radial distance is shown in Figure 6.5 for the cases of elastic and elasto-plastic analyses. The displacements corresponding to elasto-plastic analysis are much higher than that for elastic analysis near the excavation. This is because the material has failed in this region which has resulted in larger displacements. As we move away from the excavation boundary, this difference in displacements reduces. For the elasto-plastic analysis results, the displacement becomes zero at the domain boundary because of the introduction of the artificial restraint at that location. An analysis was also

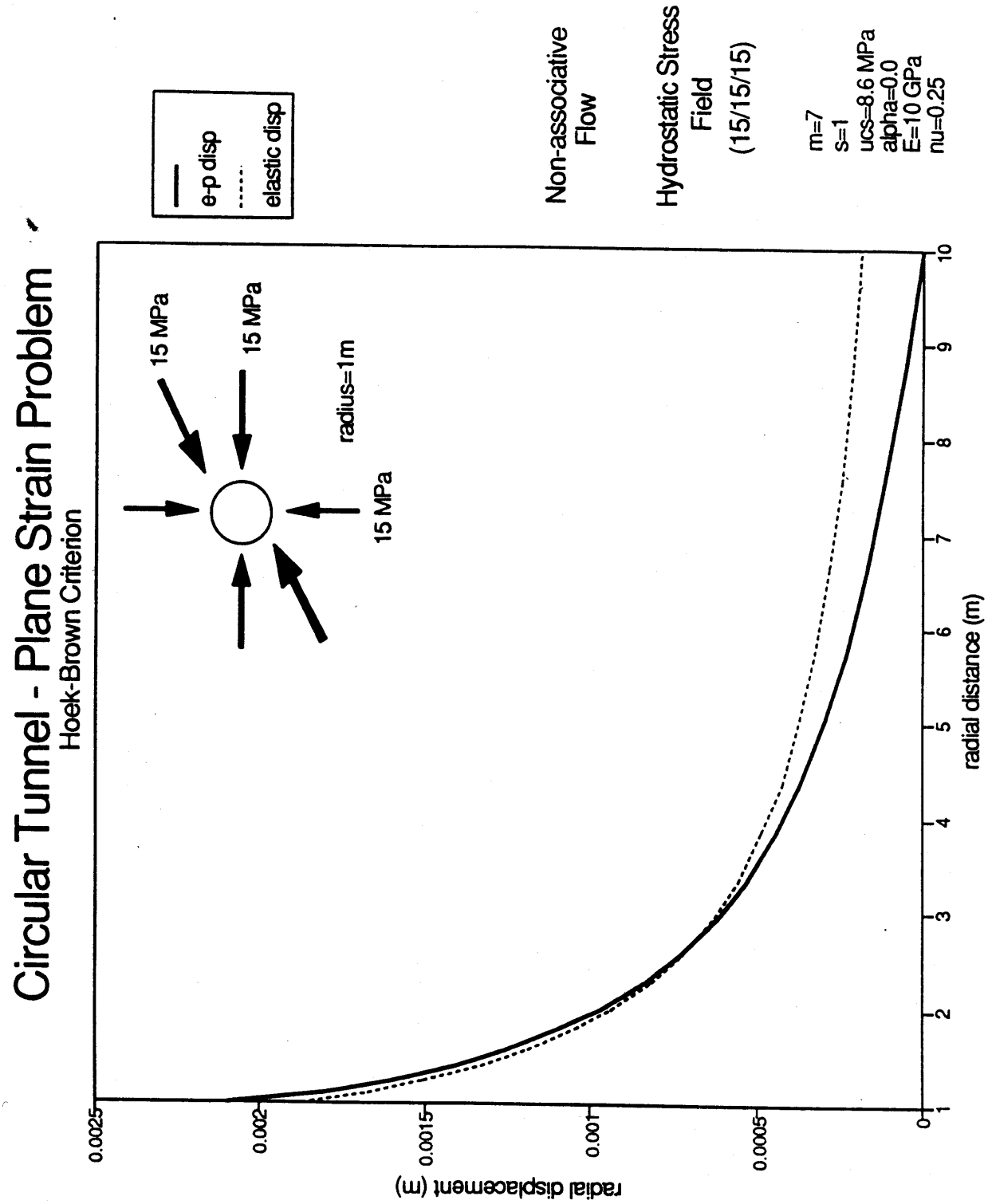

Figure 6.5: Variation of Displacement with Distance from Circular Tunnel Boundary. Elastic displacements correspond to Kirsch's solution.

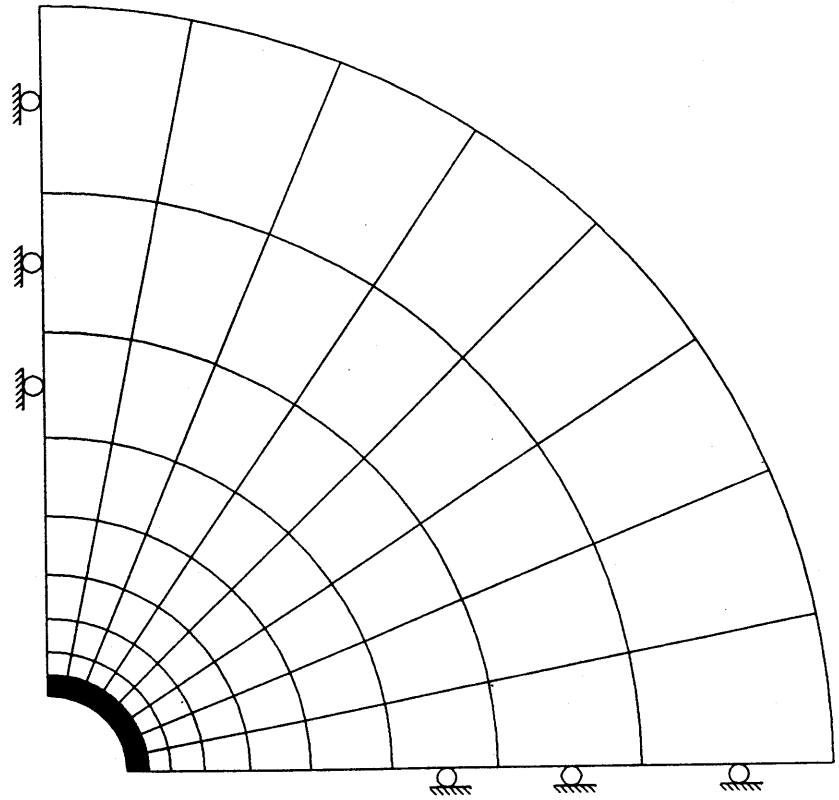

Plastic zone around Circular Tunnel
(radius of Plastic zone = 0.28m)

Figure 6.6: Zone of Plastic Failure around Circular Excavation

carried out with $\alpha = m = 7$. It was observed that the displacements around the excavation were larger for this case as compared to that for $\alpha = 0.0$. This is because $\alpha = 0$ causes *zero* inelastic volume dilation while $\alpha > 0$ causes a finite inelastic volume dilation resulting in higher values of displacements.

The zone of plastic failure around the circular excavation is indicated in Figure 6.6. The radius of this zone is 0.28 m from the excavation boundary. This zone has been obtained from those integration points for which the state dependent variable `STATEV(1)` has a value of 1, indicating plastic failure. All of the integration points of the first array of elements around the excavation and integration points number 1, 4 and 7 of the second array of elements had failed in shear. The zone of failure around the excavation is symmetric as the geometry as well as the loading are symmetric.

The predictions of the distribution of stresses and displacements are similar to that predicted by other constitutive models. These distributions and the zone of plastic failure are symmetric around the excavation indicating the stability of the constitutive calculation procedure.

6.5 Analysis of URL Underground Excavation

The constitutive model for rock mass has been tested successfully for standard situations. It can now be used to predict the distribution of stresses around any underground excavation under a general state of stress. The underground excavation problem analyzed here is that of the Underground Research Laboratory at Pinawa, Manitoba, in Canada. A brief description of this project is given here (Read, Martin, Talebi & Young, 1992).

The construction of the Underground Research Laboratory (URL) required the excavation of various tunnels and shafts ranging from 1.8 m in diameter to 8.0 m wide by 5 m high at depths between 240 and 443 m. The excavations were constructed using controlled drill and blast methods and raise-boring methods in massive unjointed granite of the Lac du Bonnet batholith, which is considered to be representative of many granitic intrusions of the Precambrian Canadian Shield. During construction of the excavations various degrees of microcracking, spalling and slabbing, as well as pop-ups of the excavation floors were observed. In some cases the amount of spalling resulted in the formation of pronounced V-shaped notches in the roof of the excavations.

The in situ stresses at the URL have been extensively investigated using traditional methods such as overcoring and hydraulic fracturing, and by non-traditional methods such as microseismic monitoring, convergence monitoring and under-excavation techniques. The maximum far-field stresses, in the vicinity of the above mentioned excavations varied from 25 to 55 MPa and the maximum to minimum stress ratio in the plane perpendicular to the axis of the excavation varied from 1.2 to 4.

The strength of the granite was determined from laboratory samples using a stiff MTS machine. The peak strengths of the brittle granite rock were obtained along with the strength at initial yield which occurs at the stage of closure of the existing microcracks and the formation of new microcracks. The strength at initial yield of the granite has been

considered to be the strength of the rock mass which exists at the time of the formation of microcracks in the massive granite.

6.5.1 Analysis Procedure

A typical excavation shown in Figures 6.7 and 6.8 was analyzed by ABAQUS using the constitutive relations developed for rock mass complying with the Hoek–Brown yield surface and the nonassociative flow rule developed for this model. This underground excavation problem was analyzed under plane strain conditions. The parameters used in the analysis and the solution procedure are explained below:

- *Rock mass properties*:

  $m = 8$, $s = 0.4$, $\sigma_c = 155$ MPa, $E = 15$ GPa, $\nu = 0.25$ and $\alpha = 0.0$.

- *In situ stresses*:

  $\sigma_1 = 55$ MPa, $\sigma_3 = 14$ MPa oriented at an angle of 10° to the horizontal, and out-of-plane stress $\sigma_{zz} = 47$ MPa. The in-plane stresses were resolved into σ_{xx}, σ_{yy} and τ_{xy} stresses while creating the input file for ABAQUS. These values are 53.8 MPa, 16.2 MPa and 6.84 MPa, respectively.

- *Element type and discretization*:

  Four element groups have been used in the discretization of the domain. The first group of elements corresponds to those inside the excavation which are of type CPE6 (six-noded quadratic element with 3 constitutive calculation points). The second and third group of elements are the ones around the excavation. The density of the elements in this region is very high and they consist of elements of type CPE6 and CPE8 (8-noded biquadratic). The fourth group of elements is of type CPE6 and is located after the second and third groups upto the domain boundary.

  The total number of elements used in the analysis is 1120 and the number of nodes is 2637. The discretization of the domain with these elements is shown in Figure 6.7.

- *Boundary conditions*:

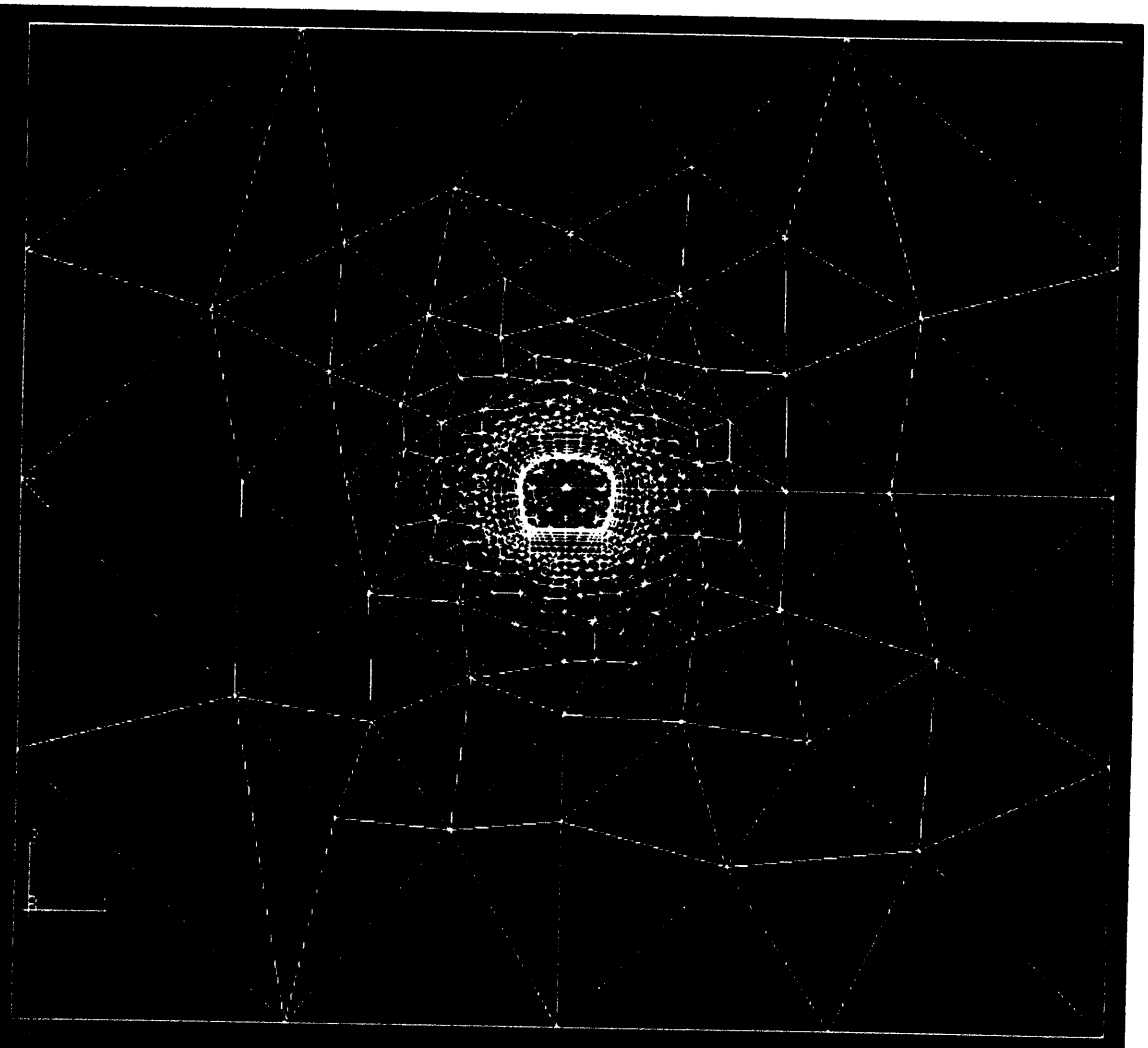

Figure 6.7: Finite Element Mesh for Discretization of Domain for URL Excavation

In order to model the far field stresses at a sufficient distance away from the excavation, the displacements along the domain boundary were fixed in the x- as well as y-directions.

- *Loading*:

  The model was loaded initially with GEOSTATIC loading equal to the *in situ* state of stress. In the next step the elements inside the excavation were removed.

- *Solution procedure*:

  The solution procedure adopted during the removal of the elements inside the excavation was with an initial increment of 0.02 and a maximum increment of 0.08. The value of PTOL was set at 0.1. The final equilibrium state of the model was achieved after 24 increments during which the automatic incrementation scheme was cut back 3 times.

6.5.2 Discussion of Results

The results of the analysis of the URL excavation with ABAQUS are presented in Figures 6.8, 6.9 and 6.10.

Figure 6.8 shows the contours of the major principal stress σ_1 around the excavation. It can be observed from this figure that the rock mass has failed in shear at the left side of the excavation roof and the stress has been redistributed further back into the rock mass. This is indicated by the contour of lower σ_1 near the excavation boundary, and the formation of a closed contour of higher σ_1 away from this zone. The confinement of the rock mass increases as we go away from the excavation, and therefore, the strength of the rock mass increases and it is able to take up higher stresses. The constitutive model is an elastic-perfectly plastic model, and hence, the strength of the material remains constant after failure. Thus, there is less redistribution of stresses after failure. There is a high concentration of major principal stress on the right end of the excavation floor, too.

The distribution of the minimum principal stress is shown in Figure 6.9. It can be noticed in this figure that there are some tensile stresses (shown by the red zone) in the side walls resulting in the formation of tensile cracks. The tensile strength of the rock mass

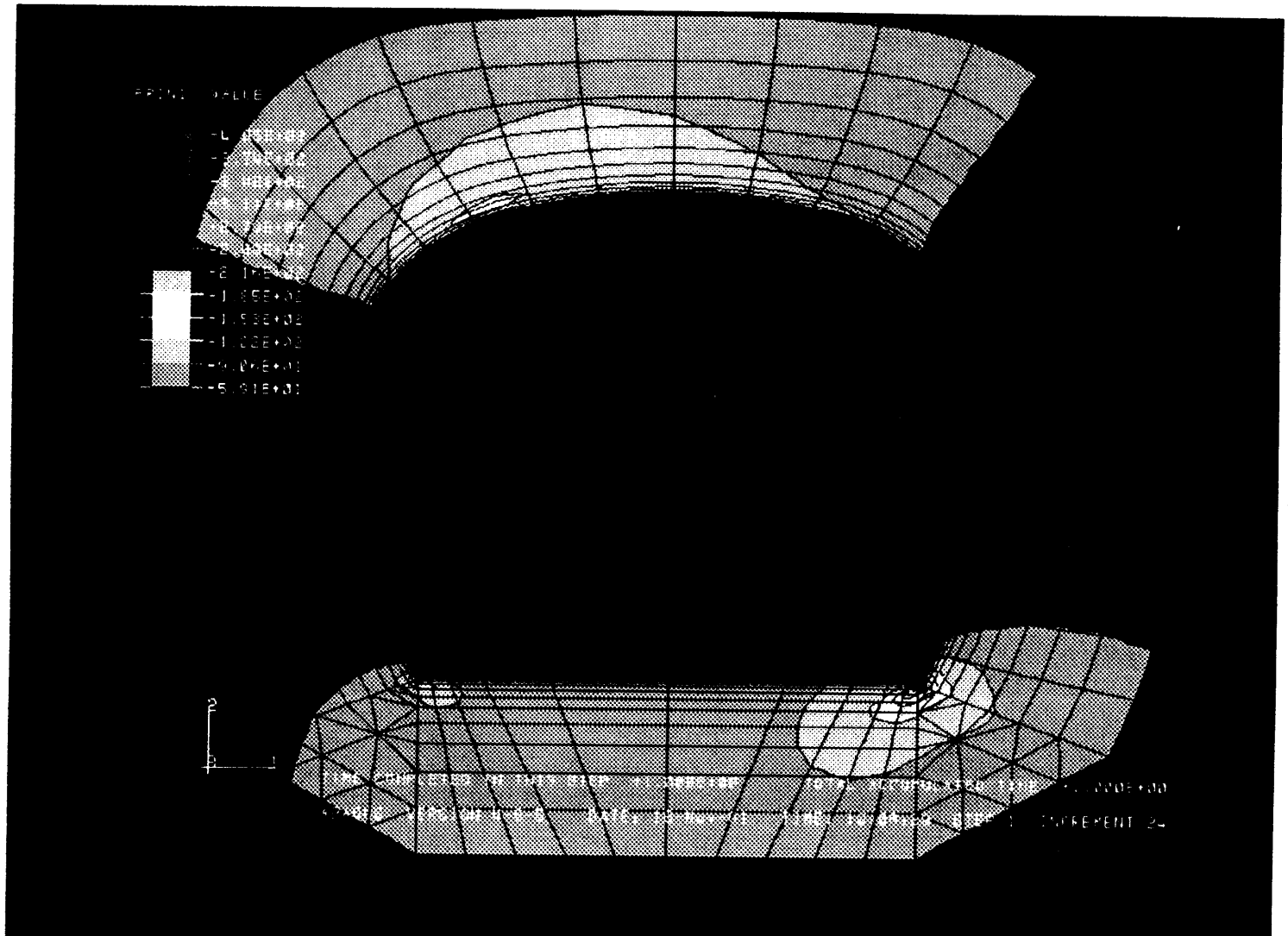

Figure 6.8: Maximum Principal Stress Distribution
around URL excavation

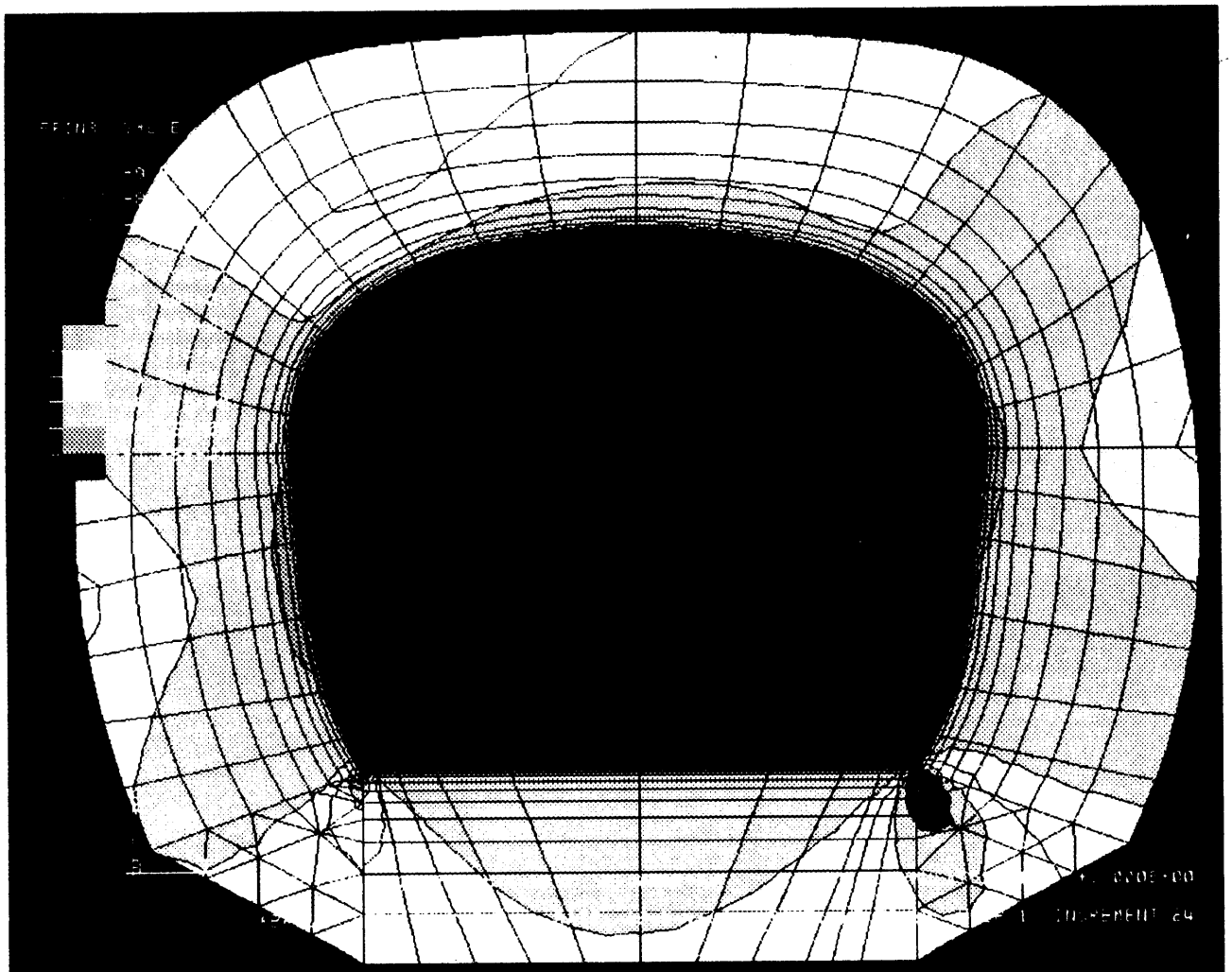

Figure 6.9: Minimum Principal Stress Distribution around URL excavation

is not reduced to *zero* after failure, but it is kept at the tensile strength limit. Therefore, the redistribution of stresses is lower in this case.

The zone of failure around the excavation is depicted in Figure 6.10. This figure was plotted as a distribution of the state dependent variable STATEV which has a value of 1 if the material is in a plastic state and 0 if it is in an elastic state. In the figure, it can be observed that failure has occurred on the roof, side walls and the floor of the excavation.

The analysis predicts that shear failure has occurred in the roof and in the floor of the excavation. As discussed previously, during the excavation process at the URL site, the presence of spalling and slabbing, and in some cases, pronounced V-shaped notches in the roof of the excavation were observed. If an approach of modelling the excavation by progressively removing the failed material is undertaken, it can be established that the final stable state of the excavation will be similar to that observed at the site.

Floor pop-ups have been observed in the URL excavation which are predicted very well by the model which shows shear failure in the floor region of the excavation.

A series of microcracks were observed in the side walls of the excavation suggesting tensile fracture of the rock mass in this zone. This behaviour of the rock mass is also predicted quite distinctively by the model.

In summary, it can be said that the predictions of the analysis of the URL excavation with the Hoek–Brown constitutive model are fairly accurate which justifies its use as a practical tool during the design of an underground excavation.

6.6 Conclusions

The elastic-perfectly plastic constitutive model for rock mass corresponding to the Hoek–Brown criterion has been successfully incorporated into the finite element program ABAQUS. The uniaxial and triaxial tests and the analysis of a circular excavation in an infinite rock mass indicate that the model is predicting the desired results. Parametric studies carried out for different values of the dilation parameter, α, show the variation in the inelastic

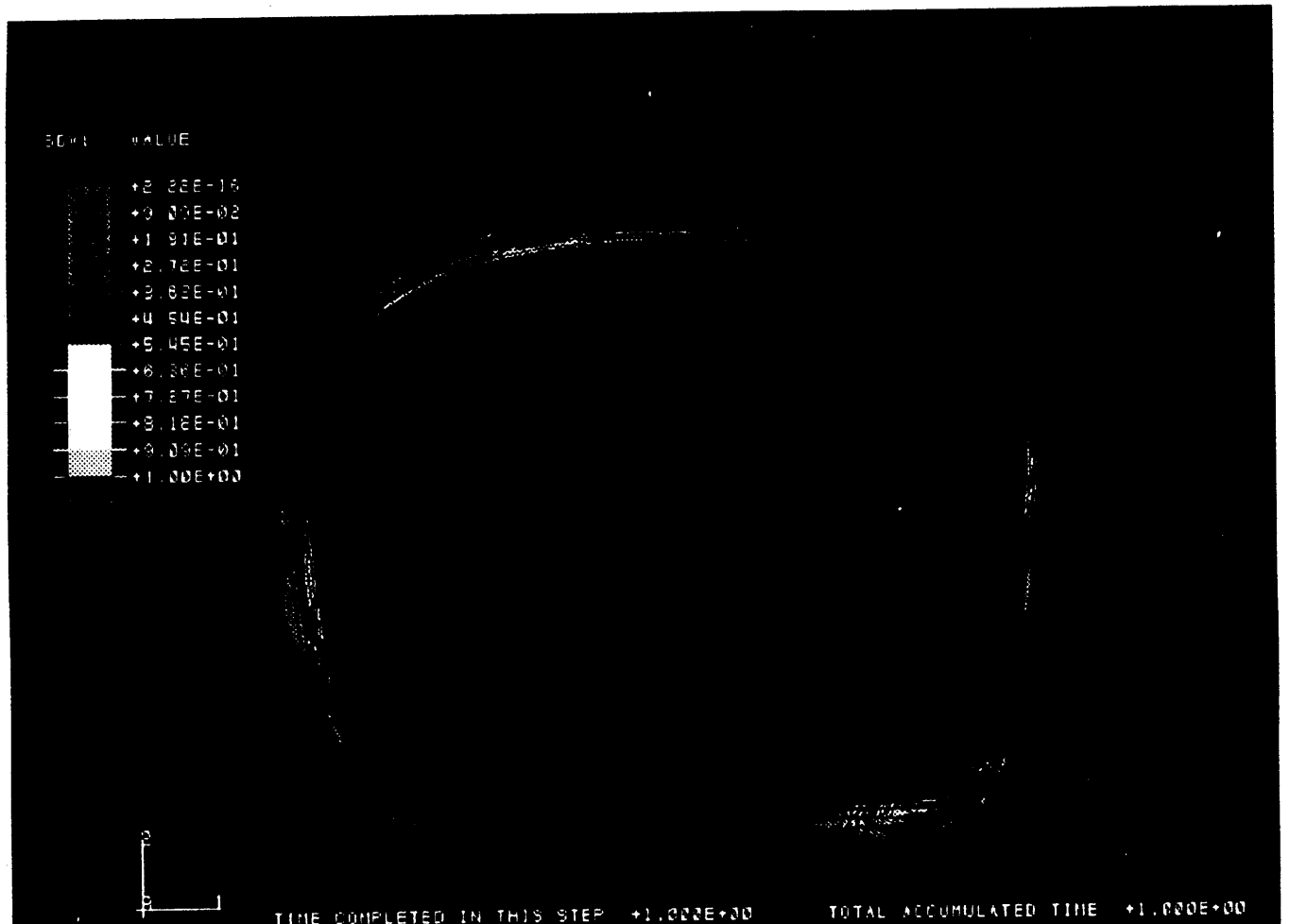

Figure 6.10: Failure Zone around URL excavation

volume dilation as expected. The predictions of stress and plastic zone distribution around an actual field problem match those observed at the site very well.

This constitutive model is a simple one with very few parameters and is now available in ABAQUS in a fully operational condition. It can be used to carry out parametric studies for the analysis of the behaviour of the rock mass around underground excavations, and by using elements available in ABAQUS to model rock reinforcement and support, the response of the rock mass to various types of support conditions can be studied in a more realistic fashion.

Chapter 7

Conclusions and Recommendations

7.1 Conclusions

The study on the behaviour of rock mass carried out during the span of this research has resulted in major advances in the discipline of rock mechanics. The three principal issues addressed in this thesis are, firstly, statistical analysis of laboratory strength data, secondly, failure or strength criterion for rock mass and rockfill materials, and finally, constitutive relations for rock mass.

In the first segment, the statistical techniques employed for the analysis of laboratory strength data were investigated. Linear regression analysis, Simplex reflection technique and the LOWESS technique were evaluated for fitting nonlinear failure envelopes through triaxial and shear test data for rock mass. It was established beyond any apprehension that the Simplex technique is by far the best procedure for fitting data to nonlinear failure criterion such as the Hoek–Brown criterion. The algorithm for this technique was incorporated into a computer program ROCKDATA which has demonstrated to be a powerful and robust tool for the analysis of strength data. This program has been used extensively in the estimation of the strength parameters of the *original* and the *modified* Hoek–Brown failure criteria. The parameters controlling the convergence of the simplex procedure were established in an optimum way such that the number of iterations required is a minimum without sacrificing the accuracy of results.

The second principal task of the research was to develop a failure criterion for rock mass which overcomes the limitations of the original Hoek–Brown failure criterion in estimating the strength of rock mass in the range of low confining stresses. The Hoek–Brown criterion predicts a tensile strength for jointed rock mass which by intuition should be zero. The quadratic approximation of this failure criterion introduces a restraint on the curvature of the strength envelope especially at low confining stresses. These limitations of the Hoek–Brown criterion were overcome by the development of a new criterion termed as the *Modified Hoek–Brown failure criterion* which reduces the tensile strength of rock mass to zero and institutes greater flexibility into the curvature of the envelope by incorporating a variable exponent. It has been illustrated effectively by the analysis of several sets of strength data for rock mass that this criterion fits the data in a better fashion. The Simplex technique was utilized for fitting the data to the proposed criterion. The removal of the square-root exponent of the *original* criterion resulted in the lack of a closed-form solution for the corresponding nonlinear Mohr envelope for the *modified criterion*. This predicament was overcome by the development of a procedure for solving the nonlinear Mohr envelope for this criterion. The predictions of the zones of overstress around a typical underground excavation layout from the two criterion were compared, and it was observed that the predictions of the *modified* criterion were closer to that observed in the field.

The correlation between the parameters of the *original* Hoek–Brown criterion and rock mass classification schemes, such as the RMR and the Q systems, is well established. In order to relate the parameters of the *Modified Hoek–Brown failure criterion* to these classification schemes, a methodology was developed to obtain these parameters from the *original* criterion. The product of this process is a table of values for the parameters m_b and a of the *modified* criterion related to different types of rock mass characteristics. It is proposed that this table be used to obtain the parameters of the criterion in the absence of actual triaxial test data on the rock mass, and the *Modified Hoek–Brown failure criterion* be used for estimating the strength of rock mass instead of the *Original Hoek–Brown criterion.*

Strength criteria for rockfill materials were also examined, and a set of non-dimensional nonlinear triaxial and shear strength criteria were proposed that can be used for the stability analyses of slopes. A rigorous technique was developed to estimate the triaxial or shear strength parameters for rockfill materials from either triaxial or shear test data. It

was demonstrated that the proposed strength criteria for rockfill materials fits the available data in a better fashion than that proposed by previous researchers.

The final facet of this research was the development of constitutive relations for rock mass and the implementation of these relations into an appropriate numerical solution procedure. Constitutive models which incorporated the linear Drucker–Prager or Mohr–Coulomb yield criterion were used till date for the analysis of the response of rock mass around underground excavations. The development of constitutive relations for rock mass using the theory of plasticity with the nonlinear Hoek–Brown criterion has resulted in a realistic model for rock mass. The Hoek–Brown constitutive model developed in this work is an elastic-perfectly plastic one with only six parameters which has enhanced the effectiveness of the model in conducting parametric studies of the elasto-plastic response of rock mass in the design of underground excavations. The constitutive model was developed with the *associated* and the *nonassociated* flow rules in order to provide the user with the facility of modelling inelastic volume dilation of the material. This material model has been successfully incorporated into the finite element program ABAQUS and several tests were carried out to ensure the accuracy and validity of the predicted results. The results of several standard and field problems indicate accurate response predictions. The Hoek–Brown constitutive model is now available in ABAQUS in a fully functional form.

7.2 Recommendations for Future Research

The study on the behaviour of rock mass presented in this thesis has encompassed several important issues and has provided the geotechnical engineer with a number of tools for predicting the behaviour of rock mass. Some of the areas where further research is recommended are outlined below:

1. The Simplex technique was established as the most appropriate technique for analyzing laboratory strength data. Nonlinear regression analysis and regression techniques which take into account the error in the measurement of both variables should be contemplated and their effectiveness for the determination of the strength parameters of rock mass should be assessed.

2. The importance of statistics in planning laboratory testing programs should be given greater emphasis. Efforts should be undertaken to establish a set of procedures for carrying out triaxial or shear tests at confining or normal stresses that are at even intervals with more than one test for each confining or normal stress value. The use of statistics as an integral part of the design of experiments and not merely as an aid in the interpretation of results should be duly accentuated.

3. The relationships between the parameters of the *original* and the *modified* Hoek–Brown criterion with rock mass classification schemes have been derived on the basis of very few test results on *broken* rock mass. Efforts should be made to conduct more tests of *rock mass* in the laboratory. In the absence of such results, further research into the techniques involving the determination of rock mass strength through convergence measurements in tunnelling (Tanimoto, et.al. 1988) in various types of rock mass should be investigated.

4. The importance of probabilistic techniques such as the Rosenbleuth's technique or Monte-Carlo simulation in rock mechanics cannot be trivialized. The immense amount of uncertainty and variability in rock mechanics measurements requires the interpretation of results in a probabilistic rather than a deterministic manner. Values of strength parameters obtained from analysis of triaxial tests should be interpreted as mean values with a certain amount of variation. Further research should be conducted to develop techniques for estimating these variabilities.

5. The constitutive model for rock mass presented in this thesis is an elastic-perfectly plastic model. Research should be conducted to develop constitutive models which incorporate *isotropic*, *kinematic* or *mixed* strain-softening or hardening of the material along with residual strength. Simple trilinear strain-softening models as proposed by Brown, Bray, Ladanyi and Hoek (1983) and more complicated models based on the degradation of stiffness of the material with progressive failure, e.g. the damage concept (Ofoegbu and Curran, 1980), should be incorporated into the model. However, in order to develop these models as practical tools for rock engineering design, they should be kept as simple as possible to enhance their effectiveness.

6. Since the *Modified Hoek–Brown criterion* was observed to describe the strength of rock mass in a better fashion than the *Original Hoek–Brown criterion*, consti-

tutive relations for rock mass using the *modified* criterion should be developed and incorporated into a numerical solution procedure.

7. Constitutive models for reinforced rock mass akin to reinforced concrete should be developed to study the interaction of rock mass and reinforcing support systems.

References

1. ABAQUS - USERS' Manual Version 4.8 (1989), Hibbit, Karlsson & Sorensen, Inc.

2. ABAQUS - Theory Manual Version 4.8 (1989), Hibbit, Karlsson & Sorensen, Inc.

3. AMES, R.R., 1985, "Rock mass strength parameters for the Cohassett dense interior based on the Hoek and Brown failure criterion", Computational Brief No. 00155, Rockwell Hanford Operation, Richland, Washington.

4. BALMER, G. (1952), "A General Analytical Solution for Mohr's Envelope", *Amer. Soc. Testing Materials*, Vol. 52, 1260-1271.

5. BARTON, N. (1976), "The Shear Strength of Rock and Rock Joints", *Int. Jrnl. Rock Mech. Min. Sci. & Geomech. Abstr.*, Vol. 13, 255-279.

6. BARTON, N., LIEN, R. & LUNDE, I. (1974), "Engineering Classification of Rock Masses for the Design of Tunnel Supports", *Rock Mech.* **6**, 189-236.

7. BARTON, N. & KJAERNSLI, B. (1981), "Shear Strength of Rockfill", *Journal of Geotechnical Engineering Division, Proc. ASCE*, Vol. 107, No. 7, 873-891.

8. BATHE, K.J. (1982), *Finite Element Procedures in Engineering Analysis*, Prentice-Hall, Englewood Cliffs, New Jersey, U.S.A..

9. BIENIAWSKI, Z.T. (1976), "Rock mass classification in rock engineering", in *Exploration for Rock Engineering* (ed. Z.T. Bieniawski), **1**, 97-106, A.A. balkema, Rotterdam.

10. BIENIAWSKI, Z.T. (1983), "The Geomechanics Classification (RMR system) in design Applications to Underground Excavations", *Proc. Int. Symp. Geol. Underground Constr.*, A. A. Balkema, Rotterdam, Vol. 2, 1133-1147.

11. BRADY, B.H.G. & BROWN, E.T. (1985), Rock Mechanics for Underground Mining, George Allen & Unwin (Publishers) Ltd, London, U.K..

12. BROWN, E.T. (ed) (1987), Analytical and Computational Methods in Engineering Rock Mechanics, Allen & Unwin, London, U.K..

13. BROWN, E.T., BRAY, J.W., LADANYI, B. & HOEK, E. (1983), "Ground Response Curves for Rock Tunnels", *Journal of Geotechnical Engineering, Amer. Soc. of Civil Engineers.*

14. CACECI & CACHERIS, 1984 (May), *Byte* magazine.

15. CHARLES, J.A. & SOARES, M.M. (1984), "Stability of compacted rockfill slopes", *Géotechnique* **34**, No. 1, 61-70.

16. CHARLES, J.A. & WATTS, K.S. (1980), "The influence of confining pressure on the shear strength of compacted rockfill", *Géotechnique* **30**, No. 4, 353-367.

17. CHEN, W.F. (1982), Plasticity in Reinforced Concrete, McGraw-Hill Inc., Toronto, Canada.

18. CHEN, W.F. & HAN, D.J. (1988), Plasticity for Structural Engineers, Springer-Verlag, New York, U.S.A..

19. CLEVELAND, W.S. (1979), "Robust Locally Weighted Regression and Smoothing Scatterplots", *Jounal of American Statistical Association*, Vol. 74, 829-836.

20. CROW, E.L., DAVIS, F.A. & MAXFIELD, M.W., 1960, *Statistical Manual*, Research Dept., U.S. Naval Ordnance Test Station, Dover Publications, Inc., New York.

21. de MELLO, V.F.B. (1977), "Seventeenth Rankine Lecture: Reflections on design decisions of practical significance to embankment dams", *Géotechnique* **27**, No. 3, 279-356.

22. DESAI, C.S. & ABEL, C.S. (1972), Introduction to the Finite Element Method - A Numerical Method for Engineering Analysis, Litton Educational Publishing, Inc., New York, U.S.A..

23. DESAI, C.S. & SIRIWARDANE, H.J. (1984), Constitutive Laws for Engineering Materials with Emphasis on Geologic Materials, Prentice-Hall, Inc., Englewood Cliffs, New Jersey, U.S.A..

24. DORUK, P. (1991), "Analysis of the Laboratory Strength Data Using the Original and Modified Hoek-Brown Failure Criteria", M.A.Sc. thesis, Dept. of Civil Engineering, University of Toronto, Canada.

25. DRAPER, N. & SMITH, H., 1981, *Applied Regression Analysis, Second Edition*, John Wiley & Sons, Inc., Toronto.

26. GEROGIANNOPOULOUS, R.E. (1979), "A Critical State Approach to Rock Mechanics", Ph.D. thesis, Imperial College, London, U.K..

27. GEROGIANNOPOULOUS, R.E. & BROWN, E.T. (1978), "The Critical State Concept Applied to Rock", *Int. Jrnl. Rock Mech. Min. Sci. & Geomech. Abstr.*, Vol. 15, 1-10.

28. HANDIN, J., HAGER, R., R.V., FRIEDMAN, M. & FEATHER, J.N. (1963), "Experimental deformation of sedimentary rocks under confining pressure; pore pressure tests", *Bull. Am. ass. Petrol. Geol.* , **47**, 717-755.

29. HILL, R. (1970), The Mathematical Theory of Plasticity, Oxford Clarendon Press, U.K..

30. HOBBS, D.W. (1970), "The behaviour of broken rock under triaxial compression", *Int. J. Rock Mech. Min. Sci.*, **7**, 125-148.

31. HOEK, E. (1968), "Brittle failure of rock", *Rock Mechanics in Engineering Practice*, (eds K.G. Stagg & O.C. Zienkiewicz), Wiley, London, 99–124.

32. HOEK, E. (1983), Strength of jointed rock masses - 23rd Rankine Lecture. *Geotechnique* **33**, 3, 187-223.

33. HOEK, E. & BROWN, E.T. (1980), *Underground Excavations in Rock*, Institution of Mining and Metallurgy, London, p. 527.

34. HOEK, E. & BROWN, E.T. (1988), "The Hoek-Brown Failure Criterion - A 1988 Update", Proc. of 15th *Canadian Rock Mech. Symp.*, Univ. of Toronto, Canada, 31-38.

35. HOEK, E. & SHAH, S. (1990), "Rock Mass Failure - Some New Thoughts", Internal Correspondence, Dept. of Civil Engg., Univ. of Toronto, Canada.

36. JAEGER, J.C. (1964), Elasticity, Fracture and Flow, with Engineering and Geological Applications, Methuen, London, U.K..

37. JAEGER, J.C. (1969), "Behaviour of Closely Jointed Rock", Proc. 11th *Symp. on Rock Mech.*, Berkeley, California, 57-68.

38. JAIN, S.K. (1980), Fundamental Aspects of the Normality Rule and theis Role in Deriving Constitutive Laws of Soils, Virginia Polytechnic Institute and State University, U.S.A..

39. KENNEDY, J.B. and NEVILLE, A.M. (1968), *Basic Statistical Methods for Engineers and Scientists*, Scranton International Textbook Co..

40. LAMA, R.D. & VUTUKURI, V.S. (1978), *Handbook on Mechanical Properties of Rocks*, Trans Tech Publications, Aedermannsdorf, Switzerland.

41. LEE, K. (1987), Golder Associates, Internal communication.

42. LONDE, P. (1988), "Determination of Shear Failure Envelope in Rock Masses", *Jrnl. Geotechnical Engineering Div., ASCE*, 106, No. GT9, 1013-1035.

43. LOWESS 1.0A (1987), "A computer Program for Robust, Locally-weighted Regression Analysis - Program and Documentation", Published by Golder Associates, Redmond, Washington, U.S.A..

44. MARACHI, N.D., CHAN, C.K. & SEED, H.B. (1972), "Evaluation of Properties of Rockfill Materials", *Jrnl. Soil Mechanics & Foundations, ASCE*, Vol. 1, 95-104.

45. MARSAL, R.J. (1973), "Mechanical Properties of Rockfill", in *Embankment-Dam Engineering*; *Casagrande Volume*, Ed. Hirschfeld, R.C. & Poulos, S.J., John Wiley & Sons, New York.

46. MARSDEN, J.R., WU, B., HUDSON, J.A. & ARCHER, J.S. (1989), "Investigation of Peak Rock Strength Behaviour for Wellbore Stability Application", in *Rock at Great Depth*, Maury & Fourmaintraux (eds.), Balkema, Rotterdam.

47. MARTIN, G.R. & MILLER, P.J. (1974), "Joint Strength Characteristics of a Weathered Rock", *Proc. 3rd Rock Mech. Congress, ISRM*, Denver, Vol. 2A, 263-270.

48. MOGI, K. (1966), "Pressure Dependence of Rock Strength and Transition from Brittle Fracture to Ductile Flow", *Bulletin Earthquake Research Institute*, Japan, Vol. 44, 215-232.

49. MOGI, K. (1967), "Effect of the Intermediate Principal Stress on Rock Failure", *Journal Geophysics Research*, Vol. 72, No. 20, 5117-5131.

50. MOREAU, J.J. (1975), "Application of Convex Analysis to the Treatment of Elasto-plastic Systems", *Application of methods of Functional Analysis to Problems in Mechanics, Joint Symp. IUTAM/IMU*, Marseille.

51. MURREL, S.A.F. (1965), "The effect of triaxial stress systems on the strength of rocks at atmospheric temperatures", *Geophys. J.*, **10**, 231-281.

52. NAYAK, G.C. & ZIENKIEWICZ, O.C. (1972), "Convenient forms of Stress Invariants for Plasticity", *Jrnl. Structural Div., Proc. ASCE*, Vol. 98, No. ST4, 949-954.

53. NAYAK, G.C. & ZIENKIEWICZ, O.C. (1972), "Elasto-Plastic Stress Analysis. A Generalization for Various Constitutive Relations Including Strain Softening", *Int. Jrnl. for Numerical Methods in Engineering*, Vol. 5, 113-135.

54. NAYLOR, D.J. & PANDE, G.N. (1981), Finite Elements in Geotechnical Engineering, Pineridge Press, Swansea, U.K..

55. NELDER J.A. & MEAD, R. (1965), "A simplex method for function minimisation", *Comput. J.*, 308-313.

56. OFOEGBU, G.I. & CURRAN, J.H. (1990), "Yielding and Damage of Intact Rock", Department of Civil Engineering, University of Toronto.

57. OWEN, D.R.J. & HINTON, E. (1980), Finite Elements in Plasticity: Theory and Practice, Pineridge Press, Swansea, U.K..

58. PAN, X.D. & HUDSON, J.A. (1988), "A Simplified Three Dimensional Hoek-Brown Yield Criterion", *Rock Mechanics and Power Plants*, Romana (ed), Balkema, Rotterdam.

59. PAN, X.D. & HUDSON, J.A. (1988), "Large deformation Analysis for Rock Excavations – A Numerical Study".

60. PANDE, G.N., BEER, G. & WILLIAMS, J.R. (1990), Numerical Methods in Rock Mechanics, John Wiley & Sons, New York, U.S.A..

61. PRAGER, W. (1959), An Introduction to Plasticity, Addison-Wesley Pub. Co., Reading, Mass., U.S.A..

62. PRIEST, S.D. & BROWN, E.T. (1983), "Probabilistic Stability Analysis of Variable Rock Slopes", *Trans. Instn Min. Metall.* **92**, Jan., A1-A12.

63. RAMAMURTHY, T. (1985), "Stability of Rock Mass", 8th *Indian Geotechnical Society Annual Lecture*, India.

64. READ, R.S., MARTIN, C.D., TALEBI, S. & YOUNG, R.P. (1992), "Strength of Massive Granite Around Underground Excavations", *International Symposium on Rock Support and 16th Canadian Rock Mechanics Symposium.*

65. ROSENGREN, K.J. & JAEGER, J.C. (1968), "The Mechanical Properties of an Interlocked Low-Porosity Aggregate", *Géotechnique*, **18**, Vol. 4, 317-326.

66. SANTARELLI, F.J. & BROWN, E.T. (1989), "Failure of Three Sedimentary Rocks in Triaxial and Hollow Cylinder Compression Tests", *Int. J. Rock Mech. Min. Sci. & Geomech. Abstr.*, Vol. 26, pp. 401-413.

67. SERAFIM, J.L. & PEREIRA, J.P. (1983), "Consideration of the Geomechanics Classification of Bieniawski", *Proc. Intnl. Symp. Engng. Geol. and Underground Construction*, Lisbon, Portugal, 1133-44.

68. SHAH, S. & HOEK, E. (1992), "Simplex Reflection Analysis of Laboratory Strength Data", to be published by *Canadian Geotechnical Journal.*

69. SHAH, S. & HOEK, E. (1992), 'Strength Criteria for Rockfills Materials", *in preparation.*

70. TANIMOTO, C., FUJIWARA, T., YOSHIOKA, H., HATA, K. & MICHIHIRO, K. (1988), "Determination of Rock Mass Strength Through Convergence Measurements in Tunnelling", *Second International Symposium on Field Measurements in Geomechanics*, Sakurai (Ed), Balkema, Rotterdam, pp. 1069-1078.

71. UCAR, R. (1986), "Determination of Shear Failure Envelope in Rock Masses", in *Journal of Geotechnical Engineering*, Vol. 112, No. 3, *Amer. Soc. of Civil Engineers.*

72. WAWERSIK, W.R. & BRACE, W.F. (1971), "Post Failure Behaviour of a Granite and a Diabase", *Rock Mechanics*, Vol. 3, No.2, pp. 61-85.

73. WAWERSIK, W.R. & FAIRHURST, C. (1970), "A Study of Brittle Rock Fracture in Laboratory Compression Experiments", *Int. Jnl. Rock Mech. Min. Sci.*, 7, 561-575.

74. WESTERGAARD, H. (1964), Theory of Elasticity and Plasticity, Dover Publications, New York, U.S.A..

75. WOOD, D. (1991), "Estimating Hoek–Brown Rock Mass Strength Parameters from Rock Mass Classifications", submitted to *Canadaian Geotechnical Journal.*

76. YAMAMOTO, T. (1990), "Suggestions for the Prediction of the Rock Mass deformability by means of Rock mass Classification", M.A.Sc. Thesis, Department of Civil Engineering, University of Toronto, Canada.

77. YOSHIDA, N. (1990), "Time-dependent Instability in Fissured Over-Consolidated Clays and Mudstones", Ph.D. thesis, Dept. of Civil Engineering, Univ. of Alberta, Edmonton, Canada.

78. YOSHIDA, N., MORGENSTERN, N.R. & CHAN, D.H. (1990), "Analysis of Softening Effects in Mudstone and Over-consolidated Clays", Soils and Foundations.

79. YOSHIDA, N., MORGENSTERN, N.R. & CHAN, D.H. (1990), "A Failure Criterion for Stiff Soils and Rocks Exhibiting Softening", in *Canadian Geotechnical Journal.*

80. YUDHBIR, LEMANZA, W. & PRINZI, F. (1983), "An Empirical Failure Criterion for Rock Masses", *Proc. 5th Congr. Int. Soc. Rock Mech.*, Melbourne, PB1-PB8.

81. ZIENKIEWICZ, O.C. (1977), Finite Element Method in Engineering, Tata-McGraw Hill Pub., New Delhi, India.

Appendix A

Pseudocode for Simplex Reflection Technique

pmodule Simplex (**imports**: parameters of equation, NP, σ_{1_i}, σ_{3_i};
exports: parameters of equation, $\sum \epsilon^2$)

* parameters for Hoek-Brown Criterion are m, s or σ_c
* values of m, s or σ_c are imported from linear regression analysis
* variables :
* $simp_{i,j}$ a $3 * 3$ matrix to store coordinates and residuals at three vertices
* $step_i$ a 1-D array of length 2 containing step sizes to set up initial simplex
* $maxerr_i$ a 1-D array of length 3 containing tolerance values for coordinates and residuals
* l_i a 1-D array of length 3 containing coordinates of lowest vertex
* h_i a 1-D array of length 3 containing coordinates of highest vertex
* $next_i$ a 1-D array of length 3 containing coordinates of next vertex
* $center_i$ a 1-D array of length 3 containing coordinates of centroid vertex
* M number of parameters $= 2$
* N $(M + 1) = 3$
* NP number of data points
* σ_{1_i} array of NP points containing experimental σ_1 values
* σ_{3_i} array of NP points containing experimental σ_3 values
* $simp_{i,1} = m$
* $simp_{i,2} = s$ or σ_c

```
* simp_{i,3} = Σ ε^2
* α = 0.5,   γ = 2.0,   β = β' = 0.5

call SumOfResiduals(simp_1, N, NP, σ_{1_i}, σ_{3_i})      * calculate residuals for first point
for i ← 1 to M do                                         * set up initial simplex with step values
    p_i ← step_i * (√N + M − 1)/(√2M)
    q_i ← step_i * (√N − 1)/(√2M)
end i for-loop
for i ← 2 to N do
    for j ← 1 to M do
        simp_{i,j} ← simp_{1,j} + q_j
    end j for-loop
    simp_{i,i−1} ← simp_{1,i−1} + p_{i−1}
    call SumOfResiduals(simp_i, N, NP, σ_{1_i}, σ_{3_i})
end i for-loop
for i ← 1 to N do                                         * initialize lowest and highest coordinates
    l_i ← 0
    h_i ← 0
end i for-loop
call Order(simp_{i,j}, l, h)                              * order the vertices as highest, next-to-highest, lowest
niter ← 0

do {
    done ← 1
    niter ← niter + 1
    for i ← 1 to N do                                     * calculate centroid of vertices except highest vertex
        if i ≠ h_N then
            for j ← 1 to M do
                center_j ← center_j + simp_{i,j}
            end j for-loop
        end if-loop
    end i for-loop
```

```
for i ← 1 to N do
    center_i ← center_i/M
    next_i ← (1 + α) * center_i − α * simp_{h_N,i}    * reflection of highest vertex about centroid
end i for-loop
call SumOfResiduals(next, N, NP, σ_{1_i}, σ_{3_i})
if next_N ≤ simp_{l_N,N} then
    call NewVertex(simp_{i,j}, h, next, N)
    for i ← 1 to M do
      next_i ← γ * simp_{h_N,i} + (1 − γ) * center_i    * expansion of reflected point
    end i for-loop
    call SumOfResiduals(next, N, NP, σ_{1_i}, σ_{3_i})
    if next_N ≤ simp_{l_N,N} then
      call NewVertex(simp_{i,j}, h, next, N)
    end if-loop
else
    if next_N ≤ simp_{h_N,N} then
      call NewVertex(simp_{i,j}, h, next, N)
    else
      for i ← 1 to M do
          next_i ← β * simp_{h_N,i} + (1 − β) * center_i    * reduction of simplex
      end i for-loop
      call SumOfResiduals(next, N, NP, σ_{1_i}, σ_{3_i})
      if next_N ≤ simp_{h_N,N} then
          call NewVertex(simp_{i,j}, h, next, N)
      else
          for i ← 1 to N do
              for j ← 1 to M do
                  simp_{i,j} ← (simp_{i,j} + simp_{l_N j}) * β    * contraction of simplex
              end j for-loop
              call SumOfResiduals(next, N, NP, σ_{1_i}, σ_{3_i})
          end i for-loop
      end if-loop
    end if-loop
```

```
        end if-loop

        call Order(simp_{i,j}, l, h)
        for j ← 1 to N do
            error_j ← (simp_{h_j,j} − simp_{l_j,j})/simp_{h_j,j}
            if done then
              if error_j > maxerror_j then done = 0
            end if-loop
        end j for-loop
        if niter > 50 then
            for i ← 1 to M do
              for j ← 1 to M do
                  if simp_{i,j} ≤ 10^{-10} then done = 1        * exit condition if very small values
              end j for-loop
            end i for-loop
        end if-loop
    } while ( not( done or (niter > maxiter))                   * maxiter can be set to 200
    for i ← 1 to N do
        mean_i ← 0.0
        for j ← 1 to N do
            mean_i ← mean_i + simp_{j,i}
        end j for-loop
        mean_i ← mean_i/N
    end i for-loop
    m ← mean_1
    s or σ_c ← mean_2
    ∑ ε^2 ← mean_3
end pmodule
```

smodule SumOfResiduals(**imports:** $X_i, N, NP, \sigma_{1_i}, \sigma_{3_i}$; **exports:** X_i)

* function to calculate $\sum \epsilon^2$

* X_i contains (m, σ_c) or (m, s) and residuals

$X_N \leftarrow 0.0$

if $((s < 0.0$ or $s > 1.0)$ **or** $m < 0.0$) **then** $X_N \leftarrow 10^{30}$

* penalty function to check the limits of applicability of parameters

else

for $i \leftarrow 1$ **to** NP **do**

$X_N \leftarrow X_N + (\text{Func}(X, \sigma_{3_i}) - \sigma_{1_i})^2$

end i **for-loop**

end if-loop

end smodule

fmodule Func(**imports:** X_i, σ_3; **returns:** $\sigma_{1_{calc}}$)

* function to calculate σ_1 corresponding to σ_3

$\sigma_{1_{calc}} \leftarrow \sigma_3 + \sqrt{m\sigma_c\sigma_3 + s\sigma_c^2}$ * for Hoek-Brown Criterion

$\sigma_{1_{calc}} \leftarrow \sigma_3 + \left(\frac{m\sigma_3}{\sigma_c}\right)^a \sigma_c$ * for Modified Hoek-Brown Criterion

end fmodule

smodule Order(**imports:** $simp_{i,j}$; **exports:** $low_i, high_i$)

* function to order the vertices of the simplex

for $i \leftarrow 1$ **to** N **do**

for $j \leftarrow 1$ **to** N **do**

if $simp_{i,j} < simp_{low_j, j}$ **then** $low_j \leftarrow i$

if $simp_{i,j} < simp_{high_j, j}$ **then** $high_j \leftarrow i$

end j **for-loop**

end i **for-loop**

end smodule

```
smodule NewVertex(imports: simp_{i,j}, high_i, next_i, N; exports: simp_{i,j})
  * function to assign new vertex to simp_{i,j}
  for i ← 1 to N do
      simp_{high_N,i} ← next_i
  end i for-loop
end smodule
```

Range of m	*step*	tolerance
$0.0 < m \leq 0.1$	0.01	0.0001
$0.1 < m \leq 0.5$	0.05	0.0001
$0.5 < m \leq 1.0$	0.1	0.001
$1.0 < m \leq 10.0$	0.5	0.001
$10.0 < m \leq 50.0$	1.0	0.01
$50.0 < m$	5.0	0.01

Table A.1: Step size and Tolerance value for m and m_b

Range of σ_c MPa	*step*	tolerance
$0.0 < \sigma_c \leq 10.0$	0.01	0.001
$10.0 < \sigma_c \leq 25.0$	0.05	0.001
$25.0 < \sigma_c$	0.1	0.01

Table A.2: Step size and Tolerance value for σ_c

parameter	*step*	tolerance
s	0.001	0.0001
a	0.001	0.0001
$\sum \epsilon^2$		0.001

Table A.3: Step size and Tolerance value for s, a and $\sum \epsilon^2$

Appendix B

FORTRAN Code for Subroutine UMAT in ABAQUS

B.1 Program listing for Rock Mass Constitutive Model

```
C     Subroutine UMAT
C     Hoek-Brown Failure Criterion
C     Elasto-Plastic Constitutive Model for Jointed Rock Masses
C     NON-ASSOCIATIVE FLOW RULE

      SUBROUTINE UMAT (STRESS, STATEV, DDSDDE, SSE, SPD, SCD,
     1 RPL, DDSDDT, DRPLDE, DRPLDT,
     2 STRAN, DSTRAN, TIME, DTIME, TEMP, DTEMP, PREDEF, DPRED, CMNAME,
     3 NDI, NSHR, NTENS, NSTATV, PROPS, NPROPS, COORDS, DROT)

      IMPLICIT REAL*8(A-H, O-Z)
      CHARACTER*8 CMNAME
      DIMENSION STRESS(NTENS), STATEV(NSTATV),
     1 DDSDDE(NTENS,NTENS),
     2 DDSDDT(NTENS), DRPLDE(NTENS),
     3 STRAN(NTENS), DSTRAN(NTENS), PREDEF(1), DPRED(1),
     4 PROPS(NPROPS), COORDS(3), DROT(3,3)
      DIMENSION DSTRES(6), DEPSP(6), STSS(6), DFST(6), DELSTN(6)
      DIMENSION TPSTRS(6), TPSTRN(6), TPDSTN(6), CONSTI(6,6)

      TERM1 = PROPS(1) + 4.0D0/3.0D0 * PROPS(2)
      TERM2 = PROPS(1) - 2.0D0/3.0D0 * PROPS(2)

C      WRITE(*,99) (DSTRAN(I), I=1,NTENS)
      SDNORM = 0.0D0
      SSNORM = 0.0D0
      DO 5200 I=1,NTENS
        SDNORM = SDNORM + DSTRAN(I)*DSTRAN(I)
        SSNORM = SSNORM + STRAN(I)*STRAN(I)
5200  CONTINUE
```

```
      SDNORM = DSQRT(SDNORM)
      SSNORM = DSQRT(SSNORM)
C     WRITE(*, 5210) SDNORM, SSNORM
5210  FORMAT('SDNORM = ', E15.5, ' SSNORM = ', E15.5)

      TOLER = 1.0D-2
C      WRITE(*,500) TIME, DTIME
500   FORMAT('TIME = ', F10.2, ' DTIME = ', F10.2)

C     INITIAL CONSTITUTIVE MATRIX

      IF(TIME .EQ. 0.0 .AND. SDNORM .LT. 1.0D-12) THEN
        STATEV(1) = 0
        STATEV(2) = TIME
C       WRITE(*, 5110)
5110    FORMAT('INITIAL')
C        WRITE(*,99) (DSTRAN(I), I=1,NTENS)
        GOTO 5000
      ENDIF

      DO 2 I=1,6
        TPSTRS(I) = 0.0D0
        TPSTRN(I) = 0.0D0
        TPDSTN(I) = 0.0D0
2     CONTINUE

      DO 5310 I=1,6
        DO 5310 J=1,6
5310      CONSTI(I,J) = 0.0D0


      DO 5 I=1,NDI
        TPSTRS(I) = -1.0D0*STRESS(I)
        TPSTRN(I) = -1.0D0*STRAN(I)
        TPDSTN(I) = -1.0D0*DSTRAN(I)
5     CONTINUE
      DO 6 I=1,NSHR
        TPSTRS(3+I) = -1.0D0*STRESS(NDI+I)
        TPSTRN(3+I) = -1.0D0*STRAN(NDI+I)
        TPDSTN(3+I) = -1.0D0*DSTRAN(NDI+I)
6     CONTINUE

C      WRITE(*, 99) (TPDSTN(I), I=1,6)
99    FORMAT('tpdstn ',6E13.5)

C      WRITE(*,5400) TIME, STATEV(2)
5400  FORMAT('TIME = ', F15.5, ' STATEV(2) = ', F15.5)

        DSTRES(1) = TERM1 * TPDSTN(1) + TERM2 * (TPDSTN(2) + TPDSTN(3))
        DSTRES(2) = TERM1 * TPDSTN(2) + TERM2 * (TPDSTN(1) + TPDSTN(3))
        DSTRES(3) = TERM1 * TPDSTN(3) + TERM2 * (TPDSTN(1) + TPDSTN(2))
        DO 10 KI = 4, 6
          DSTRES(KI) = PROPS(2) * TPDSTN(KI)
10      CONTINUE

        DO 20 KK = 1, 6
```

```
          TPSTRS(KK) = TPSTRS(KK) + DSTRES(KK)
20      CONTINUE

C     EVALUATE AND CHECK FAILURE STATE

        FAIL = FAILUR(TPSTRS, PROPS, NTENS, NPROPS)
        CALL DERSTR(TPSTRS,PROPS,NTENS,NPROPS,DFST)
        DF = 0.0D0
        DO 5350 I=1,6
5350      DF = DF + DFST(I)*DSTRES(I)
C       WRITE(*,5300) FAIL, DF
5300    FORMAT('FAIL = ', F15.5, ' DF = ', F15.5)

         IF(FAIL .LE. TOLER .OR. DF .LT. TOLER) THEN
C         WRITE(*, 27)
27        FORMAT('ELASTIC')
          STATEV(1) = 0
          DO 30 M=1,3
            CONSTI(M,M) = TERM1
            CONSTI(M+3, M+3) = PROPS(2)
30        CONTINUE
          DO 40 MM=2,3
            CONSTI(1,MM) = TERM2
            CONSTI(MM,1) = TERM2
            IF(MM .GT. 2) THEN
              CONSTI(2,MM) = TERM2
              CONSTI(MM,2) = TERM2
            ENDIF
40        CONTINUE
          GOTO 100
         ELSEIF(FAIL .GT. TOLER .OR. DABS(DF) .LE. TOLER) THEN
          DO 41 KK=1,6
            STSS(KK) = TPSTRS(KK) - DSTRES(KK)
            TPSTRS(KK) = STSS(KK)
41        CONTINUE
          DO 15 I=1,6
15          DELSTN(I) = TPDSTN(I)/10
          DSTRES(1) = TERM1 * DELSTN(1) + TERM2*(DELSTN(2) + DELSTN(3))
          DSTRES(2) = TERM1 * DELSTN(2) + TERM2*(DELSTN(1) + DELSTN(3))
          DSTRES(3) = TERM1 * DELSTN(3) + TERM2*(DELSTN(1) + DELSTN(2))
          DO 1020 KI = 4, 6
            DSTRES(KI) = PROPS(2) * DELSTN(KI)
1020      CONTINUE
          ICOUNT=1
1000      IF(ICOUNT .LE. 10) THEN
            WRITE(*, 1005) ICOUNT
1005        FORMAT('ICOUNT = ', I10)
            ICOUNT = ICOUNT + 1
            DO 1030 KK = 1, 6
              TPSTRS(KK) = TPSTRS(KK) + DSTRES(KK)
1030        CONTINUE
C           WRITE(*, 1040) TPSTRS(2)
1040        FORMAT('TPSTRS(2) = ', F10.5)

            FAIL1 = FAILUR(TPSTRS, PROPS, NTENS, NPROPS)
```

```
          WRITE(*, 1050) FAIL1
1050      FORMAT('FAIL1 = ' E13.5)

          IF(FAIL1 .LE. TOLER) THEN
            STATEV(1) = 0
            WRITE(*,1051)
1051        FORMAT('ELASTIC !!')
            GOTO 1000
          ELSEIF(FAIL1 .GT. TOLER .AND. IDINT(STATEV(1)) .EQ. 0) THEN
            STATEV(1) = 1
            WRITE(*, 43)
43          FORMAT('ELASTO-PLASTIC')
            DO 410 KK=1,6
              STSS(KK) = TPSTRS(KK) - DSTRES(KK)
410         CONTINUE
            FAILPR = FAILUR(STSS, PROPS, NTENS, NPROPS)
            NUMER = (-1.0D0)*FAILPR
            DENOM = 0.0D0
            CALL DERSTR(STSS, PROPS, NTENS, NPROPS, DFST)
            DO 45 I=1,6
              DENOM = DENOM + DFST(I) * DSTRES(I)
45          CONTINUE
            RATIO = NUMER / DENOM
C           WRITE(*,46) RATIO
46          FORMAT('RATIO = ', F10.5)
51          DO 52 KK=1,6
              TPSTRS(KK) = STSS(KK) + RATIO*DSTRES(KK)
52          CONTINUE

C     CALCULATE INCREMENTAL PLASTIC STRAIN

            DO 60 II=1,6
              DEPSP(II) = (1.0D0 - RATIO) * DELSTN(II)
60          CONTINUE
            CALL HOEKBR(TPSTRS, PROPS, NTENS, NPROPS, DEPSP, CONSTI)
            GOTO 1000
          ELSEIF((FAIL1 .GT. TOLER .OR. FAIL1 .LE. TOLER)
     1                .AND. IDINT(STATEV(1)) .EQ. 1) THEN
            STATEV(1) = 1
            WRITE(*, 39)
39          FORMAT('PLASTIC')
            DO 401 KK=1,6
              STSS(KK) = TPSTRS(KK) - DSTRES(KK)
401         CONTINUE

            DO 42 NN=1,6
              DEPSP(NN) = DELSTN(NN)
42          CONTINUE
            CALL HOEKBR(STSS, PROPS, NTENS, NPROPS, DEPSP, CONSTI)
            DO 70 I=1,6
              TPSTRS(I) = STSS(I)
70          CONTINUE
            GOTO 1000
          ENDIF
        ENDIF
      ENDIF
```

```
100   DO 105 I=1,NDI
        STRESS(I) = -1.0D0*TPSTRS(I)
        STRAN(I)  = -1.0D0*TPSTRN(I)
        DSTRAN(I) = -1.0D0*TPDSTN(I)
        DO 102 J=1,NDI
          DDSDDE(I,J) = CONSTI(I,J)
102     CONTINUE
105   CONTINUE
      DO 110 I=1,NSHR
        STRESS(NDI+I) = -1.0D0*TPSTRS(3+I)
        STRAN(NDI+I)  = -1.0D0*TPSTRN(3+I)
        DSTRAN(NDI+I) = -1.0D0*TPDSTN(3+I)
        DO 108 J=1,NSHR
          DDSDDE(NDI+I,NDI+J)=CONSTI(3+I,3+J)
108     CONTINUE
110   CONTINUE
      DO 120 I=1,NDI
        DO 115 J=1,NSHR
          DDSDDE(I,NDI+J) = CONSTI(I,3+J)
          DDSDDE(NDI+J,I) = CONSTI(3+J,I)
115     CONTINUE
120   CONTINUE
C      DO 121 I=1,NTENS
C        WRITE(*, 122) (DDSDDE(I,J), J=1,NTENS)
121    CONTINUE
C     WRITE(*, 122) (STRESS(I), I=1,NTENS)
122   FORMAT('STRESS ', 6E13.5)
      GOTO 5100

5000  DO 5020 I=1,NTENS
        DO 5020 J=1,NTENS
5020      DDSDDE(I,J) = 0.0D0
      DO 5030 I=1,NDI
5030    DDSDDE(I,I) = TERM1
      DO 5040 I=1,NSHR
5040    DDSDDE(I+NDI, I+NDI) = PROPS(2)
      DO 5050 I=2,NDI
        DDSDDE(1,I) = TERM2
        DDSDDE(I,1) = TERM2
        IF(I .GT. 2) THEN
          DDSDDE(2,I) = TERM2
          DDSDDE(I,2) = TERM2
        ENDIF
5050  CONTINUE

5100  RETURN
      END


C     FUNCTION FAILUR
C     EVALUATE STRESS STATE

      REAL*8 FUNCTION FAILUR(TPSTRS, PROPS, NTENS, NPROPS)
```

```
      IMPLICIT REAL*8(A-H, O-Z)
      DIMENSION PS(3), TPSTRS(6), PROPS(NPROPS)

      CALL SINV( TPSTRS, SINV1, SINV2)
C      WRITE(*, 1) SINV1, SINV2
1     FORMAT('SINV1 = ', E15.5, 'SINV2 = ', E15.5)

C     CALCULATE HYDROSTATIC STRESS (I-1), SQRT OF J-2, J-3
      HYDROS = 3.0D0 * SINV1
      DVTR02 = SINV2 / DSQRT(3.0D0)

      CALL SPRINC(TPSTRS, PS, 1)
C      WRITE(*, 2) PS(1), PS(2), PS(3)
2     FORMAT( 'PS(1) = ', E15.5, 'PS(2) = ', E15.5, 'PS(3) = ', E15.5)
      DVTR03 = (PS(1) - SINV1) * (PS(2) - SINV1) * (PS(3) - SINV1)

      THETA = (1.0D0/3.0D0) * ACOS(2.5980762D0 * DVTR03 / (DVTR02**3))
C     WRITE(*, 1000) THETA
1000  FORMAT('THETA = ', E15.5)
      IF(THETA .GT. 1.046324D0) THETA = 1.046324D0
      IF(THETA .LE. 0.8726646D-3) THETA = 0.8726646D-3
      AA = PROPS(3) * PROPS(5) * (SINV1 - DVTR02 / DSQRT(3.0D0) *
     1     ( COS(THETA) + DSQRT(3.0D0) * SIN(THETA)))
     2     + PROPS(4) * (PROPS(5)**2)
      FAILUR = DVTR02*(DSQRT(3.0D0)*COS(THETA)+SIN(THETA)) - DSQRT(AA)
C     WRITE (*, 100) AA, DVTR02, DVTR03, FAILUR, THETA
100   FORMAT('AA = ', E15.5, 'DVTR02 = ', E15.5, 'DVTR03 = ', E15.5,
     1     'FAILURE = ' E15.5, 'THETA = ', E15.5)
      RETURN
      END


C     SUBROUTINE HOEKBR
C     CALCULATE STRESS STATE DUE TO PLASTIC STRAINING

      SUBROUTINE HOEKBR(TPSTRS, PROPS, NTENS, NPROPS, DEPSP, CONSTI)

      IMPLICIT REAL*8(A-H, O-Z)
      DIMENSION PS(3), TPSTRS(6), PROPS(NPROPS), DVT(6)
      DIMENSION CONSTI(6,6), DEPSP(6)

      CALL SINV( TPSTRS, SINV1, SINV2)

C     CALCULATE HYDROSTATIC STRESS (I-1), SQRT OF J-2, J-3
      HYDROS = 3.0D0 * SINV1
      DVTR02 = SINV2 / DSQRT(3.0D0)

      CALL SPRINC(TPSTRS, PS, 1)
      DVTR03 = (PS(1) - SINV1) * (PS(2) - SINV1) * (PS(3) - SINV1)
      DO 10 II=1,3
        DVT(II) = TPSTRS(II) - SINV1
        DVT(II+3) = TPSTRS(II+3)
10    CONTINUE

C     WRITE(*, 90) SINV1, DVTR02, DVTR03
90    FORMAT('SINV1 = ', E15.5, ' DVTR02 = ', E15.5, 'DVTR03 = ', E15.5)
```

```
C     WRITE(*, 100) (DVT(I), I=1,6)
100   FORMAT(6E13.5)
      THETA = (1.0D0/3.0D0) * ACOS(2.5980762D0 * DVTR03 / (DVTR02**3))
      IF(THETA .GT. 1.046324D0) THETA = 1.046324D0
      IF(THETA .LE. 0.8726646D-3) THETA = 0.8726646D-3
      AA = PROPS(3) * PROPS(5) * (SINV1 - DVTR02 / DSQRT(3.0D0) * (
     1     COS(THETA) + DSQRT(3.0D0) * SIN(THETA)))
     2     + PROPS(4) * (PROPS(5)**2)

C     WRITE(*, 500) PROPS(6)
500   FORMAT('PROPS(6) = ', F10.3)
      POIRAT = 3.0D0*PROPS(1) - 2.0D0*PROPS(2) / (2.0D0*PROPS(2) +
     1          6.0D0*PROPS(1))
      FACT = (1.0D0 + POIRAT) / (1.0D0 - 2.0D0*POIRAT)
      FACT2 = (2.0D0/3.0D0) * DVTR02*DVTR02
      B0 = -1.0D0 * PROPS(3) * PROPS(5) / (6.0D0 * DSQRT(AA))
      B1 = 0.5D0 / DVTR02 * (DSQRT(3.0D0) * COS(THETA) + SIN(THETA) +
     1     (COS(THETA) - DSQRT(3.0D0)*SIN(THETA)) / TAN(3.0D0*THETA) +
     2     0.28867513D0*PROPS(3)*PROPS(5)/DSQRT(AA) * ( COS(THETA) +
     3     DSQRT(3.0D0)*SIN(THETA) + (DSQRT(3.0D0) *COS(THETA) -
     4     SIN(THETA)) / TAN(3.0D0*THETA)))
      B2 = 0.5/SIN(3.0D0*THETA)/(DVTR02**2) * ( 3.0D0 * SIN(THETA) -
     1     DSQRT(3.0D0)*COS(THETA) - 0.5*PROPS(3)*PROPS(5)/DSQRT(AA) *
     2     ( DSQRT(3.0D0) *COS(THETA) - SIN(THETA)))

      RR = PROPS(6)*PROPS(5)*(SINV1-DVTR02)+PROPS(4)*PROPS(5)**2
C     WRITE(*,*) RR
      Q0 = -1.0D0*PROPS(6)*PROPS(5) / (6.0D0*DSQRT(RR))
      Q1 = (1.0D0 + PROPS(6)*PROPS(5) / (4.0D0*DSQRT(RR)) ) / DVTR02

C     FOR ASSOCIATIVE FLOW RULE

C      H = 2.0D0*PROPS(2) * ( 3.0D0*B0*B0 * FACT
C     1      + 2.0D0*B1*B1*DVTR02*DVTR02 + (2.0D0/3.0D0) *
C     2      B2*B2*(DVTR02**4) + 6.0D0*B1*B2*DVTR03)

C     FOR NON-ASSOCIATIVE FLOW RULE

      H = 2.0D0*PROPS(2) * ( 3.0D0*B0*Q0 * FACT
     1        + 2.0D0*B1*Q1*DVTR02*DVTR02 + 3.0D0*B2*Q1*DVTR03)


      HX = 2.0D0*PROPS(2) * (B0 * FACT + B1*DVT(1) + B2*(DVT(1)*DVT(1)
     1  + DVT(4)*DVT(4) + DVT(6)*DVT(6) - FACT2))
      HY = 2.0D0*PROPS(2) * (B0 * FACT + B1*DVT(2) + B2*(DVT(2)*DVT(2)
     1  + DVT(5)*DVT(5) + DVT(4)*DVT(4) - FACT2))
      HZ = 2.0D0*PROPS(2) * (B0 * FACT + B1*DVT(3) + B2*(DVT(3)*DVT(3)
     1  + DVT(6)*DVT(6) + DVT(5)*DVT(5) - FACT2))

      HXY = 2.0D0*PROPS(2) * (B1*DVT(4) + B2*(DVT(1)*DVT(4) + DVT(4)
     1    *DVT(2) + DVT(5)*DVT(6)))
      HYZ = 2.0D0*PROPS(2) * (B1*DVT(5) + B2*(DVT(4)*DVT(6) + DVT(2)
     1    *DVT(5) + DVT(5)*DVT(3)))
      HZX = 2.0D0*PROPS(2) * (B1*DVT(6) + B2*(DVT(6)*DVT(1) + DVT(5)
     1    *DVT(4) + DVT(3)*DVT(6)))
```

```
      HXST = 2.0D0*PROPS(2) *(Q0 * FACT + Q1*DVT(1))
      HYST = 2.0D0*PROPS(2) *(Q0 * FACT + Q1*DVT(2))
      HZST = 2.0D0*PROPS(2) *(Q0 * FACT + Q1*DVT(3))

      HXYST = 2.0D0*PROPS(2)*Q1*DVT(4)
      HYZST = 2.0D0*PROPS(2)*Q1*DVT(5)
      HZXST = 2.0D0*PROPS(2)*Q1*DVT(6)

      HIN = -1.0D0/H
C      WRITE(*, 5) Q0, Q1, H, HIN, HXST, HYST, HZST, HXYST,
C     1      HYZST, HZXST
5     FORMAT('Q0 = ', E15.5, ' Q1 = ', E15.5 /
     1        ' H = ', E15.5, ' HIN = ', E15.5, /' HXST = ', E15.5,
     4        ' HYST = ', E15.5,
     2        ' HZST = ', E15.5, / ' HXYST = ', E15.5, ' HYZST = ', E15.5,
     3        ' HZXST = ', E15.5)

      TERM1 = PROPS(1) + 4.0D0/3.0D0 * PROPS(2)
      TERM2 = PROPS(1) - 2.0D0/3.0D0 * PROPS(2)

      CONSTI(1,1) = TERM1 + HIN*HX*HXST
      CONSTI(1,2) = TERM2 + HIN*HXST*HY
      CONSTI(1,3) = TERM2 + HIN*HXST*HZ
      CONSTI(1,4) = HIN*HXST*HXY
      CONSTI(1,5) = HIN*HXST*HYZ
      CONSTI(1,6) = HIN*HXST*HZX

      CONSTI(2,1) = TERM2 + HIN*HYST*HX
      CONSTI(2,2) = TERM1 + HIN*HY*HYST
      CONSTI(2,3) = TERM2 + HIN*HYST*HZ
      CONSTI(2,4) = HIN*HYST*HXY
      CONSTI(2,5) = HIN*HYST*HYZ
      CONSTI(2,6) = HIN*HYST*HZX

      CONSTI(3,1) = TERM2 + HIN*HZST*HX
      CONSTI(3,2) = TERM2 + HIN*HZST*HY
      CONSTI(3,3) = TERM1 + HIN*HZ*HZST
      CONSTI(3,4) = HIN*HZST*HXY
      CONSTI(3,5) = HIN*HZST*HYZ
      CONSTI(3,6) = HIN*HZST*HZX

      CONSTI(4,1) = HIN*HXYST*HX
      CONSTI(4,2) = HIN*HXYST*HY
      CONSTI(4,3) = HIN*HXYST*HZ
      CONSTI(4,4) = PROPS(2) + HIN*HXY*HXYST
      CONSTI(4,5) = HIN*HXYST*HYZ
      CONSTI(4,6) = HIN*HXYST*HZX

      CONSTI(5,1) = HIN*HYZST*HX
      CONSTI(5,2) = HIN*HYZST*HY
      CONSTI(5,3) = HIN*HYZST*HZ
      CONSTI(5,4) = HIN*HYZST*HXY
      CONSTI(5,5) = PROPS(2) + HIN*HYZ*HYZST
      CONSTI(5,6) = HIN*HYZST*HZX

      CONSTI(6,1) = HIN*HZXST*HX
```

```
      CONSTI(6,2) = HIN*HZXST*HY
      CONSTI(6,3) = HIN*HZXST*HZ
      CONSTI(6,4) = HIN*HZXST*HXY
      CONSTI(6,5) = HIN*HZXST*HYZ
      CONSTI(6,6) = PROPS(2) + HIN*HZX*HZXST

C     WRITE(*,*) CONSTI(2,2)
C      DO 11 I=1,6
C        WRITE(*, 12) (CONSTI(I,J), J=1,6)
11    CONTINUE
12    FORMAT(6E13.5)

C     UPDATE STRESS TENSOR

      DO 30 J=1,6
        DO 20 I=1,6
          TPSTRS(J) = TPSTRS(J) + CONSTI(J,I)*DEPSP(I)
20      CONTINUE
30    CONTINUE
      RETURN
      END


C     CALCULATE DERIVATIVE OF FAILURE SURFACE W.R.T. STRESS TENSOR
C       TO CALCULATE RATIO
C     RETURN DFST(6) - THE DERIVATIVES

      SUBROUTINE DERSTR(ST, PROPS, NTENS, NPROPS, DFST)

      IMPLICIT REAL*8(A-H, O-Z)
      DIMENSION PS(3), ST(6), PROPS(NPROPS), DVT(6)
      DIMENSION CONSTI(6,6), DEPSP(6), DFST(6)

      CALL SINV( ST, SINV1, SINV2)

C     CALCULATE HYDROSTATIC STRESS (I-1), SQRT OF J-2, J-3
      HYDROS = 3.0D0 * SINV1
      DVTRO2 = SINV2 / DSQRT(3.0D0)

      CALL SPRINC(ST, PS, 1)
      DVTRO3 = (PS(1) - SINV1) * (PS(2) - SINV1) * (PS(3) - SINV1)
      DO 10 II=1,3
        DVT(II) = ST(II) - SINV1
        DVT(II+3) = ST(II+3)
10    CONTINUE

C     WRITE(*, 90) SINV1, DVTRO2, DVTRO3
90    FORMAT('SINV1 = ', E15.5, ' DVTRO2 = ', E15.5, 'DVTRO3 = ', E15.5)
C     WRITE(*, 100) (DVT(I), I=1,6)
100   FORMAT(6E13.5)
      THETA = (1.0D0/3.0D0) * ACOS(2.5980762D0 * DVTRO3 / (DVTRO2**3))
      IF(THETA .LE. 8.726D-3) THETA = 0.01D0
      IF(THETA .GT. 1.038D0) THETA = 1.03D0
      AA = PROPS(3) * PROPS(5) * (SINV1 - DVTRO2 / DSQRT(3.0D0) * (
     1     COS(THETA) + DSQRT(3.0D0) * SIN(THETA)))
     2     + PROPS(4) * (PROPS(5)**2)
```

```
      FACT2 = (2.0D0/3.0D0) * DVTR02*DVTR02
      B0 = -1.0D0 * PROPS(3) * PROPS(5) / (6.0D0 * DSQRT(AA))
      B1 = 0.5D0 / DVTR02 * (DSQRT(3.0D0) * COS(THETA) + SIN(THETA) +
     1     (COS(THETA) - DSQRT(3.0D0)*SIN(THETA)) / TAN(3.0D0*THETA) +
     2     0.28867513D0*PROPS(3)*PROPS(5)/DSQRT(AA) * ( COS(THETA) +
     3     DSQRT(3.0D0)*SIN(THETA) + (DSQRT(3.0D0) *COS(THETA) -
     4     SIN(THETA)) / TAN(3.0D0*THETA)))
      B2 = 0.5/SIN(3.0D0*THETA)/(DVTR02**2) * ( 3.0D0 * SIN(THETA) -
     1     DSQRT(3.0D0)*COS(THETA) - 0.5*PROPS(3)*PROPS(5)/DSQRT(AA) *
     2     ( DSQRT(3.0D0) *COS(THETA) - SIN(THETA)))
      DFST(1) = B0 + B1*DVT(1) + B2*(DVT(1)*DVT(1)
     1  + DVT(4)*DVT(4) + DVT(6)*DVT(6) - FACT2)
      DFST(2) = B0 + B1*DVT(2) + B2*(DVT(2)*DVT(2)
     1  + DVT(5)*DVT(5) + DVT(4)*DVT(4) - FACT2)
      DFST(3) = B0 + B1*DVT(3) + B2*(DVT(3)*DVT(3)
     1  + DVT(6)*DVT(6) + DVT(5)*DVT(5) - FACT2)

      DFST(4) = B1*DVT(4) + B2*(DVT(1)*DVT(4) + DVT(4)
     1    *DVT(2) + DVT(5)*DVT(6))
      DFST(5) = B1*DVT(5) + B2*(DVT(4)*DVT(6) + DVT(2)
     1    *DVT(5) + DVT(5)*DVT(3))
      DFST(6) = B1*DVT(6) + B2*(DVT(6)*DVT(1) + DVT(5)
     1    *DVT(4) + DVT(3)*DVT(6))

      RETURN
      END
```

B.2 Sample Input Data File for ABAQUS

```
**
** Circular tunnel initial stress ratio of 1.00
**
*HEADING, UNSYMM
Elasto-plastic (Hoek-Brown) Analysis of Circular Tunnel, NON-ASSOCIATIVE FLOW
RULE
**DATA CHECK
*PREPRINT, ECHO=NO, MODEL=NO, HISTORY=NO
**
** Model Data
** ==========
**
*NODE
101,0,0
1701,0,0
103,1,0
1703,0,1
121,10,0
1721,0,10
**
*NGEN, NSET=CENTER
101,1701,100
*NGEN, NSET=LINING, LINE=C
103,1703,100,101
*NGEN, NSET=FAR, LINE=C
121,1721,100,101
*NFILL
CENTER,LINING,2
*NFILL, BIAS=0.75, TWOSTEP
LINING,FAR,18
**
*NSET, NSET=LEFT, GENERATE
1701,1721,1
*NSET, NSET=BOTTOM, GENERATE
101,121,1
*NSET, NSET=PRINT, GENERATE
103,121
1703,1721
*NSET, NSET=NHIST
103,1703
**
*ELEMENT, TYPE=CPE8
101,101,103,303,301,102,203,302,201
*ELGEN, ELSET=ALL
101,10,2,1,8,200,100
**
*ELSET, ELSET=TUNNEL, GENERATE
101,801,100
*ELSET, ELSET=HOST, GENERATE
102,110
202,210
302,310
402,410
502,510
```

```
602,610
702,710
802,810
*ELSET, ELSET=PRINT, GENERATE
102,110
802,810
*ELSET, ELSET=ELHIST
102,402,802
**
*BOUNDARY
LEFT,1
BOTTOM,2
FAR,1,2
**
*SOLID SECTION, ELSET=ALL, MATERIAL=ROCK
*MATERIAL, NAME=ROCK
*USER MATERIAL, CONSTANTS=6, UNSYMM
6666.67, 4000, 7, 1, 8.6, 0.0
*DEPVAR
1
*USER SUBROUTINE, INPUT=15
**
*INITIAL CONDITIONS, TYPE=STRESS(GEOSTATIC)
ALL,-15.0,1.0,-15.0,0.0,1.00,1.00
**
*RESTART, WRITE, FREQUENCY=5
**
** History data
** ============
**
*STEP
Geostatic initialization.
*GEOSTATIC, PTOL=0.10
*EL PRINT, ELSET=PRINT, SUMMARY=NO, FREQUENCY=1
S11,S22,S33,S12,E11,E22,E33,E12
*NODE PRINT, NSET=PRINT, SUMMARY=NO, FREQUENCY=1
COORD, U
*END STEP
**
**===*STEP, CYCLE=10, INC=150, SUBMAX
*STEP, INC=150, CYCLE=10
Excavate the tunnel.
*STATIC, PTOL=0.05
0.02,1.0, ,0.02
*MODEL CHANGE, REMOVE
TUNNEL,
*EL PRINT, ELSET=HOST, POSITION=AVERAGED AT NODES, SUMMARY=NO, FREQUENCY=100
COORD,S11,S22,S33,S12
*NODE PRINT, NSET=PRINT, SUMMARY=NO, FREQUENCY=100
COORD, U
*EL PRINT, ELSET=HOST, FREQUENCY=100, SUMMARY=NO
COORD,PRIN1,PRIN2,PRIN3,SDV1
*EL FILE, ELSET=ELHIST, FREQUENCY=1
S
*END STEP
** End of file.
```